UNIVERSITY OF SOUTHAMPTON

FACULTY OF MEDICINE

Cancer Science Unit

The biological role of the TNF super family ligand TL1A and its receptor DR3

by

John Robert Ferdinand

MBiochem (Hons)

Thesis for the degree of Doctor of Philosophy

September 2015

UNIVERSITY OF SOUTHAMPTON

ABSTRACT

FACULTY OF MEDICINE

CANCER SCIENCE UNIT

Doctor of Philosophy

THE BIOLOGICAL ROLE OF THE TNF SUPER FAMILY LIGAND TL1A AND ITS RECEPTOR DR3

By John Robert Ferdinand

Members of the Tumor Necrosis Factor superfamily of cytokines are an important source of costimulatory signalling required for the proper activation of T cells. One such receptor-ligand pair is Death receptor 3 (DR3) and its ligand TNF-like ligand 1A (TL1A). Genetic variants in TL1A are associated with inflammatory bowel disease and TL1A-DR3 interactions are required for full pathology in murine models of asthma, multiple sclerosis and colitis, with DR3 on T cells thought to play a major role in promoting immunopathology. Tumor Necrosis Factor superfamily cytokines, including TL1A, are synthesised as type II transmembrane proteins, some of which are subsequently cleaved to yield a soluble form in the serum. We have investigated the biological function of transmembrane versus soluble TL1A in mice using a mutant that prevents cleavage of TL1A from the plasma membrane. Overexpression of either full length or membrane restricted TL1A promoted an IL-13 driven small intestinal pathology which appeared earlier in mice where soluble TL1A was present. We hypothesise that this may be due to cell-type specific effects of the different forms of TL1A. In these same mice we identified increased total IgA in the serum, and went on to demonstrate that DR3 deficient mice have a defect in IgA in response to immunisation and TL1A can promote IgA class switching *in vivo*. Lastly we assessed the role of DR3 in lupus-like murine models. Here we found lack of DR3 was protective for the development of kidney disease. Overall we have shown that different forms of TL1A can have differing functions and that TL1A is important for components of both the humoral and cellular immune response.

Table of Contents

Abstract i

Table of Contents ii

List of Figures ix

List of Tables xi

Author's Declaration xii

Acknowledgements xiii

Abbreviations xiv

Chapter 1. Introduction 1

1.1. Cells of the immune system 2

1.1.1. T cells 2

1.1.2. B cells 6

1.1.3. Innate lymphoid cells 7

1.2. The Tumour Necrosis Factor Receptor and Ligand super family: members and signalling 9

1.2.1. TNFRSF sub-families 10

1.2.2. Control of signalling 12

1.2.3. Spatial temporal regulation and role of the TNFSF throughout the immune system 12

1.2.4. NF-κB signalling pathway 14

1.2.5. AP1 signalling pathway 15

1.3. Death Receptor 3 16

1.4. TNF-like Ligand 1A 19

1.5. Decoy Receptor 3 21

1.6. Non TNF superfamily ligands for DR3 21

1.7. DR3/TL1A signalling and the immune response 22

1.7.1. Downstream signalling pathways 22

1.7.2. Costimulation of T cells 23

1.7.3. ILC costimulation 24

1.7.4. Modulation of B cells 24

1.7.5. Myeloid cell signalling 25

1.8. DR3/TL1A in murine models and human health and disease 25

1.8.1. Crohn's Disease and Colitis 26

1.8.2. Rheumatoid Arthritis 27
1.8.3. Asthma 29
1.8.4. Myelin oligodendrocyte glycoprotein induced experimental autoimmune encephalomyelitis 30
1.8.5. TL1A association with other diseases and immunological models 31
1.8.6. TL1A transgenic mice 32

Chapter 2. Aims of the project 34

Chapter 3. Methods 35

3.1. Reagents 35
3.1.1. Cell culture media 35
3.1.2. Buffers 35
3.1.3. Antibodies 36
3.1.4. Oligonucleotides 37
3.1.5. Molecular enzymes 38
3.2. Molecular biology 39
3.2.1. Polymerase chain reaction 39
3.2.2. Agarose gel electrophoresis 39
3.2.3. DNA cleanup 40
3.2.4. Sewing PCR 40
3.2.5. Topo cloning 40
3.2.6. Restriction Digestion 40
3.2.7. Dephosphorylation 40
3.2.8. T4 ligase 41
3.2.9. Bacterial transformation 41
3.2.10. Plasmid purification – mini and maxi prep 41
3.2.11. Sequencing 41
3.3. Production of key plasmids 42
3.3.1. TL1A and TL1A Δ 69-93 peYFP-C1 42
3.3.2. TL1A and TL1A Δ 69-93 pIMP71 42
3.3.3. CD2 TL1A Δ 69-93 42
3.4. Production of cell lines 42
3.4.1. Cell culture 42
3.4.2. Cell counting 43
3.4.3. Transfection 43
3.4.4. Retroviral transduction 43
3.5. Production of soluble TL1A 44

3.5.1. CHOK-1 cell culture 44
3.5.2. Purification 44
3.5.3. SDS PAGE 45
3.5.4. Endotoxin Testing 45
3.6. Flow cytometry 45
3.6.1. Biotinylation 45
3.6.2. Cell staining 45
3.6.3. Live/Dead staining 46
3.6.4. Staining mouse blood 46
3.6.5. Intracellular staining 46
3.6.6. Flow based counting of cells 46
3.6.7. Flow cytometry analysis 47
3.7. In Vitro Assays 47
3.7.1. Splenocyte preparation 47
3.7.2. Bone marrow preparation 47
3.7.3. Kidney cell extraction 47
3.7.4. BMDC production 48
3.7.5. BMDC assay for sTL1A production 48
3.7.6. Magnetic separation 48
3.7.7. T cell enrichment 48
3.7.8. T cell activation 48
3.7.9. MMP inhibition assay 48
3.7.10. siRNA mediated knockdowns 49
3.7.11. B cell IgA class switching 49
3.7.12. Proliferation assay 49
3.8. Immunofluorescence 49
3.8.1. Freezing Tissue 49
3.8.2. Cutting sections 50
3.8.3. Staining sections 50
3.9. Histochemistry 50
3.9.1. Tissue Fixation 50
3.9.2. Processing 50
3.10. Image capture 50
3.11. Image processing and analysis 51
3.11.1. Image processing 51
3.11.2. Goblet cell scoring 51
3.11.3. Kidney pathology score 51

3.12. RNA extraction and reverse transcription 51
3.12.1. RNA extraction for low cell numbers 51
3.12.2. RNA extraction from tissues taken from retrotransgenic mice 52
3.12.3. RNA extraction from tissue from all remaining experiments 52
3.12.4. Reverse transcription of RNA from low cell number extraction 52
3.12.5. Reverse transcription from RNA from retrotransgenic mice 52
3.13. Quantitative PCR 52
3.13.1. qPCR from low cell numbers 53
3.13.2. qPCR from retrotransgenic mice 53
3.13.3. qPCR from all remaining experiments 53
3.14. RNASeq 54
3.14.1. RNA integrity analysis. 54
3.14.2. First and second strand synthesis 54
3.14.3. Library preparation and sequencing 54
3.15. Soluble Protein assays 55
3.15.1. Serum preparation 55
3.15.2. Sandwich ELISA 55
3.15.3. Commercial ELISA kits 56
3.15.4. Creatinine assay 56
3.15.5. Luminex 56
3.16. Mouse lines 57
3.16.1. C57bl/6 57
3.16.2. CD45.1 congenic mice 57
3.16.3. Mem and Mem Hi TL1A mice 57
3.16.4. Mem+Sol TL1A mice 57
3.16.5. DR3 KO mice 57
3.16.6. TL1A KO mice 57
3.16.7. TL1A and DR3 KO x VavBCL-2 58
3.16.8. DR3 conditional mouse 58
3.16.9. MMP9 KO mice 58
3.16.10. RAG KO mice 58
3.16.11. RAG GC KO mice 58
3.17. Genotyping 58
3.17.1. Genomic DNA extraction and genotyping PCR 58
3.17.2. Commercial genotyping kit 59
3.17.3. Genotyping PCR reaction conditions 59
3.17.4. Vav-BCL2 mice 60

3.18. *In vivo* protocols 60
3.18.1. Injections 60
3.18.2. Collection of blood from the tail vein 60
3.18.3. Collection of blood from the maxillary plexus 60
3.18.4. Euthanasia 61
3.18.5. Terminal cardiac bleed 61
3.18.6. Perfusion of organs 61
3.18.7. Whole body Irradiation 61
3.19. *In Vivo* experiments 62
3.19.1. Salmonella infection 62
3.19.2. Retrotransgenics 62
3.19.3. Airway resistance 63
3.19.4. Continual infusion of sTL1A via osmotic pump 64
3.19.5. Alum precipitation 65
3.19.6. T dependent immunisation 65
3.19.7. T Independent NP Immunisation 65
3.19.8. RAG transfer models 65
3.19.9. Chronic GVHD 66
3.20. Bioinformatics 66
3.20.1. RNASeq analysis 66
3.20.2. Heatmap generation 66
3.20.3. Gene ontology analysis 67
3.20.4. Cleavage site prediction 67
3.21. Statistical analysis 67

Chapter 4. Investigating expression patterns and potential differential roles of membrane restricted and soluble TL1A 68

4.1. Introduction 68
4.2. Results 71
4.2.1. Assays for the detection of membrane and soluble TL1A 71
4.2.2. In vitro TL1A detection and function 73
4.2.3. In silico prediction of TL1A cleaving protease 75
4.2.4. TL1A is cleaved in vitro by ADAM17 but not MMP9 76
4.2.5. In vivo soluble TL1A detection 78
4.2.6. Higher order TL1A complexes do not affect T cell costimulation 78
4.2.7. Production of a membrane restricted form of TL1A 80

4.2.8. Retrotransgenic overexpression of membrane restricted TL1A promotes pathology 81
4.2.9. Production of expression matched TL1A transgenic lines....84
4.2.10. TL1A from Mem+Sol T cells is cleaved by a metalloprotease other than MMP9 86
4.2.11. Phenotype of different TL1A transgenic strains....87
4.2.12. Chronic delivery of sTL1A promotes intestinal pathology....101
4.3. Discussion 103

Chapter 5. The result of signals conferred through excessive TL1A production and the potential cell types involved.... 111

5.1. Introduction....111
5.2. Results....113
5.2.1. Production of a TL1A overexpressing mouse which lacks DR3 on T cells. 113
5.2.2. The effect of the lack of T cell DR3 on the phenotype of TL1A transgenic mice. 115
5.2.3. Role played by TL1A mediated T cell responses upon transfer into RAG or RAG GC KO mice....118
5.2.4. Identification of differentially expressed genes conserved across multiple tissues as a result of constitutive TL1A expression 122
5.3. Discussion 126

Chapter 6. DR3 is required on B cells for optimal class switching to IgA 130

6.1. Introduction....130
6.1.1. T dependent B cell response....130
6.1.2. T independent B cell response 131
6.1.3. B cell phenotypes are induced in response to TL1A 132
6.1.4. IgA in health and disease 132
6.2. Results....134
6.2.1. T dependent immunisation of DR3 KO mice 134
6.2.2. DR3 KO mice do not have a global defect in IgA 135
6.2.3. Defect in IgA is not due to DR3 expression on T cells 135
6.2.4. T independent immunisation of DR3 KO. 136
6.2.5. TL1A is a potential novel IgA switch factor in vitro 139
6.3. Discussion 140

Chapter 7. The role of DR3 in chronic autoimmunity 142
7.1. Introduction.....142
7.2. Results.....144
7.2.1. Vav-Bcl-2 x Mem+Sol TL1A transgenic mice 144
7.2.2. DR3 KO x Vav-Bcl2 mice 146
7.2.3. Parent into F1 model of lupus.....150
7.3. Discussion 157
Chapter 8. General discussion 161
8.1. General comments 161
8.2. Concluding remarks.....166
Appendix I – TL1A transgenic RNASeq analysis graphs..... 167
Appendix II – TL1A transgenic lung RNASeq differential expression analysis..... 172
Appendix III – TL1A transgenic lung RNASeq gene ontology analysis 176
References..... 185

List of Figures

Figure 1-1 – CD4+ T helper subsets 4
Figure 1-2 – The Tumour Necrosis Factor Receptor Super Family (TNFRSF) 10
Figure 1-3 – Overview of the NF-κB pathway 15
Figure 1-4 – Comparative predicted protein structure of the extracellular domains of DR3 and TNFR1 16
Figure 1-5 – Murine DR3 splice variants 18
Figure 1-6 – TL1A gene structure 21
Figure 3-1 Correct intubation of a mouse for analysis of airway resistance 64
Figure 3-2 – Mouse with osmotic pump 65
Figure 4-1 - Luminex based assay for detection of mouse sTL1A 72
Figure 4-2 - Membrane and soluble expression of TL1A in vitro 74
Figure 4-3 - Matrix metalloprotease mediated cleavage of TL1A 77
Figure 4-4 - TL1A expression in response to Salmonella-OVA 78
Figure 4-5 - In vitro stimulation with sTL1A 79
Figure 4-6 - Design and production of full length and uncleavable TL1A constructs 80
Figure 4-7 - Production of TL1A retrotransgenic mice 82
Figure 4-8 - Phenotypic analysis of intestine 83
Figure 4-9 - Phenotypic analysis of lungs 84
Figure 4-10 - Matching TL1A transgenic lines 85
Figure 4-11 - Transgenic TL1A cleavage from T cells 86
Figure 4-12 - Phenotypic analysis of TL1A transgenic T cell responses 87
Figure 4-13 - Phenotypic analysis of TL1A transgenic B cell responses 88
Figure 4-14 - Serum cytokines in TL1A transgenic mice 90
Figure 4-15 - TL1A transgenic mice develop spontaneous small bowel pathology 92
Figure 4-16 - Mild lung pathology in TL1A transgenic mice 94
Figure 4-17 - Methacholine sensitivity of TL1A transgenic mice 95
Figure 4-18 - Lung transcriptional profile in TL1A transgenic mice 96
Figure 4-19 - RNASeq analysis of TL1A transgenic lungs 97
Figure 4-20 - Down regulated genes in TL1A transgenic lungs 98
Figure 2-21 - Up regulated genes in TL1A transgenic lungs 99
Figure 4-22 - Continuous administration of sTL1A promotes small bowel pathology 101
Figure 5-1 - Parent TL1A transgenic line for crossing to T cell conditional DR3 KO 113
Figure 5-2 - T cell conditional DR3 KO 114
Figure 5-3 - Direct Effect of TL1A on T cells 115
Figure 5-4 - Role of T cell DR3 signaling on the B cells response 116
Figure 5-5 - T cell DR3 is not required for small intestinal pathology 117
Figure 5-6 - T cell DR3 expression is required for aberrant lung transcriptional profile 118
Figure 5-7 - TL1A transgenic or WT T cell reconstitution of lympho-deficient mice 119

Figure 5-8 - Lung pathology in response to reconstitution with Transgenic T cells 120
Figure 5-9 - Morbidity and mortality response to reconstitution with transgenic T cells 121
Figure 5-10 - Colon pathology in response to reconstitution of RAG GC with transgenic T cells 122
Figure 5-11 - Comparison of transcriptional profile of Mem+Sol TL1A Transgenic lungs and ileum 123
Figure 6-1 - T cell dependent NP immunisation of DR3 KO mice 134
Figure 6-2 - DR3 KO mice have no defect in total IgA 135
Figure 6-3 - T cell dependent NP immunisation of T cell specific DR3 KO mice 136
Figure 6-4 - Type 1 T independent NP immunisation of total DR3 KO mice 137
Figure 6-5 - Type 2 T independent NP immunisation of total DR3 KO mice 138
Figure 6-6 - TL1A induces IgA class switching in vitro 139
Figure 7-1 – Splenic components of Mem+Sol TL1A x Vav-BCL2 144
Figure 7-2 - CD4 T cell subsets in the spleen of Mem+Sol TL1A x Vav-BCL2 145
Figure 7-3 - B cell compartment in the spleen of Mem+Sol TL1A x Vav-BCL2 145
Figure 7-4 - Splenic composition in DR3KO x Vav-Bcl2 146
Figure 7-5 - Immunoglobulin serum composition in DR3KO x Vav-Bcl2 147
Figure 7-6 - Kidney pathology in DR3KO x Vav-Bcl2 148
Figure 7-7 - Glomerular immune deposition in DR3KO x Vav-Bcl2 149
Figure 7-8 - Development of chronic graft vs host disease in the parent into F1 model 150
Figure 7-9 - Splenic phenotype of mice with chronic graft versus host disease 151
Figure 7-10 - Splenic T helper cell compartment in mice with chronic graft versus host disease 152
Figure 7-11 - T cell exhaustion in mice with chronic graft versus host disease 153
Figure 7-12 - Splenic B cell compartment in mice with chronic graft versus host disease 153
Figure 7-13 - Kidney pathology in response to chronic graft versus host disease 154
Figure 7-14 - Glomerular immune deposition 155
Figure 7-15 - Cellular composition of the kidney in response to chronic graft vs host disease 156
Figure I-1 - QC plots for RNASeq analysis of TL1A transgenic lungs 167
Figure I-2 - QC plots for RNASeq analysis of TL1A transgenic lungs 168
Figure I-3 - QC plots for RNASeq analysis of TL1A Mem+Sol transgenic Ileum 169
Figure I-4 - QC plots for RNASeq analysis of TL1A Mem+Sol transgenic Ileum 170
Figure I-5 - RNASeq analysis of TL1A Mem+Sol transgenic Ileum 171

List of Tables

Table 1-1 – Expression of DR3 throughout the immune and non-immune systems 17
Table 1-2 – Expression of TL1A throughout the immune and non-immune systems 20
Table 1-3 – Effect of the DR3/TL1A pathway on murine models 25
Table 3-1 – Cell culture media 35
Table 3-2 – Non-commercial buffers 35
Table 3-3 – Primary Antibodies 36
Table 3-4 – Secondary antibodies and reagents 37
Table 3-5 – Oligonucleotides 37
Table 3-6 – Molecular biology enzymes 38
Table 3-7 – Agarose percentages 39
Table 3-8 – qPCR probes 53
Table 3-9 – ELISA setup 56
Table 3-10 – PCR conditions for genotyping of mouse strains 59
Table 3-11 – Maximum volumes for injections 60
Table 4-1 – In silico prediction of protease specificity for TL1A 75
Table 4-2 – Differentially regulated genes in transgenic lungs 100
Table 4-3 – Summary of TL1A induced in vivo phenotypes 110
Table 5-1 - Genes that are down regulated in both lung and ileum samples from Mem+Sol TL1A transgenic mice compared to WT 123
Table 5-2 - Genes that are up regulated in both lung and ileum samples from Mem+Sol TL1A transgenic mice compared to WT 124
Table 5-3 - Expression pattern of differentially expressed genes from combined lung and ileum comparison across different TL1A transgenic mice within the lung only 124
Table II-1 – Differentially regulated genes in TL1A transgenic lungs as defined by groups of common expression 172
Table III-1 – Gene ontology analysis of decreased lung transcripts in all TL1A transgenic lines compared to WT mice 176
Table III-2 – Gene ontology analysis of decreased lung transcripts in Mem+Sol TL1A transgenic mice and not in Mem or Mem Hi compared to WT mice 177
Table III-3 – Gene ontology analysis of decreased lung transcripts in Mem and Mem Hi TL1A transgenic mice and not in Mem+Sol Hi compared to WT mice 178
Table III-4 – Gene ontology analysis of increased lung transcripts in all TL1A transgenic lines compared to WT mice 178
Table III-5 – Gene ontology analysis of increased lung transcripts in Mem+Sol TL1A transgenic mice and not in Mem or Mem Hi compared to WT mice 181
Table III-6 – Gene ontology analysis of increased lung transcripts in Mem+Sol TL1A transgenic mice and not in Mem or Mem Hi compared to WT mice 181

Author's Declaration

I, John Robert Ferdinand, declare that this thesis and the work presented in it are my own and has been generated by me, as the result of my own original research.

The biological role of the TNF super family ligand TL1A and its receptor DR3

I confirm that:

This work was done wholly or mainly while in candidature for a research degree at this University.

Where any part of this thesis has previously been submitted for a degree or any other qualification at this University or any other institution, this has been clearly stated.

Where I have consulted the published work of others, this is always clearly attributed.

Where I have quoted from the work of others, the source is always given. With the exception of such quotations, this thesis is entirely my own work.

I have acknowledged all main sources of help.

Where the thesis is based on work done by myself jointly with others, I have made clear exactly what was done by others and what I have contributed myself.

None of this work has been published before submission.

Signed: ……

Date: ……

Acknowledgements

I wish to extend my thanks to my two supervisors Prof. Aymen Al-Shamkhani and Dr. Richard Siegel for their ideas and mentorship over the last 4 years. I also wish to thank them for all their help with the organisation and overcoming the logistical nightmares surrounding a PhD split across the two sides of the pond.

I am eternally grateful to the Wellcome trust-NIH program and the NIAMS intramural program for financial support.

I could not have completed this thesis without the great support I have received from all members both past and present in the Siegel and Al-Shamkhani labs.

This work would not have been possible without the amazing support I received from the Biomedical Research Unit at the University of Southampton and the NIAMS Laboratory Animal Care and Use Section. Thank you for all your help and training and for putting up with my less than straightforward experiments.

Thanks must also go to the NIAMS next generation sequencing core faculty for technical assistance and training.

A special thanks to Harvey, Ruth and Arianne for keeping me (vaguely) sane and supplied with gin!

Finally I wish to thank Mandy for her love, support and lemon cakes. I couldn't have done it without you.

Abbreviations

AIA	Antigen induced arthritis
ANA	Anti nuclear antibodies
APC	Antigen presenting cells
BCR	B cell receptor
BMDC	Bone marrow derived DCs
CD	Crohn's disease
CIA	Collagen induced arthritis
CLP	Common lymphoid progenitor
CRD	Cysteine rich domains
cGVHD	Chronic graft versus host disease
CTLA4	Cytotoxic T lymphocytes associated protein 4
DC	Dendritic cells
DcR3	Decoy receptor 3
DR3	Death Receptor 3
dsDNA	Double stranded DNA
DSS	Dextran sodium sulphate
EAE	Experimental autoimmune encephalomyelitis
FADD	Fas associated protein
FasL	Fas ligand
GC	Germinal center
GWAS	Genome wide association studies
HBD	Heparin binding domain
IC	Immune complex
IFN	Interferon
Ig	Immunoglobulin
IL	Interleukin
ILC	Innate lymphoid cell
ITAM	Immunoreceptor tyrosine based activation motif
KO	Knock out
LT	Lymphotoxin
MHC	Major Histocompatibility Complex
MMP	Matrix metalloprotease
MOG	Myelin oligodendrocyte glycoprotein
NK	Natural Killer
NP	4-hydroxy-3-nitrophenylacetyl
OVA	Ovalbumin
PI3K	Phosphoinositide 3-kinanse
PLAD	Pre-ligand association domains
RA	Rheumatoid Arthritis
RAG	Recombinase activating gene
SLE	Systemic Lupus Erythematous
SNP	Single nucleotide polymorphisms
ssDNA	Single stranded DNA
sTL1A	Soluble TL1A

Tconv	Conventional T cells
TCR	T cell receptor
Td	T dependent
Tfh	T follicular helper cells
Th	T helper
THD	TNF- homology domain
Ti	T independent
TIMP	Tissue inhibitor of metalloprotease
TL1A	TNF like ligand 1a
TNBS	2,4,6-trinitrobenzenesulfonic acid
TNF	Tumuor Necrosis factor
TNFRSF	TNF receptor super family
TNFSF	TNF super family
TRADD	TNFR-associated death domain
TRAF	TNFR-associated factors
Tregs	Regulatory T cells
WT	Wild Type

Chapter 1. Introduction

The immune system is vital to the protection of the host from a whole range of pathogens. This vital role of the immune system is demonstrated by the catastrophic effects of immunodeficiency diseases such as infection with Human Immunodeficiency virus (HIV). In HIV infected individuals T cell mediated immunity is destroyed, making the patient more vulnerable to pathogenic organisms and the initial infection may lead to development of acquired immune deficiency syndrome (AIDS). In the end these individuals may fall victim to opportunistic infections that in a healthy individual would be controlled through the coordinated activity of the immune system.

Immunity can also have pathogenic consequences such as in autoimmune diseases where an inappropriate immunological response is mounted against the host. A central goal of immunological research is understanding how cytokines and immune cell signalling pathways differentially regulate appropriate versus inappropriate responses. Advances in this area have resulted in the development of therapeutic agents which block cytokine signalling pathways effectively treating multiple autoimmune and inflammatory diseases without significantly compromising the host immune system.

Depending upon the type of pathogen involved the response mounted by the immune system is different; further different cells are involved at different stages in the immune response. The immune system can be divided into innate and adaptive immune cells which mediate distinct types of response. Innate immunity involves the recognition of generic features of pathogens through pattern recognition receptors leading to the activation of effector cells that respond in a generic manner. The second arm of the immune system is the adaptive immune system that includes B cells and T cells. Each of these cells recognise specific antigenic epitopes from a specific pathogen and act against them.

This project focuses on the role of Tumour necrosis factor (TNF)-like Ligand 1a (TL1A) and Death receptor 3 (DR3) throughout the immune system.

1.1. Cells of the immune system

Through the course of this project multiple cell types within the immune system have been examined as either downstream targets or mediators of TL1A/DR3 signalling. Here follows a brief description of these cell types.

1.1.1. T cells

T cells can broadly be divided into two main groups based on expression of the co-receptors CD4 and CD8. CD4+ T cells are the T helper (Th) lineage and provide help in the form of cytokines to CD8+ T cells as well as other immune cells including B cells. Upon activation of CD4+ T cells through encounter with antigen/Major histocompatibility complex (MHC) class II (MHC II) complexes on professional antigen presenting cells (APCs) and exogenous cytokines they are able to differentiate into further subsets as defined by their cytokine profile and role within the immune system (Figure 1-1). CD8+ T cells are the cytotoxic T cells. These cells target and destroy cells which display foreign antigens upon their MHC I be they derived from virus, intracellular pathogens or altered self proteins such as in the case of cancers.

Production of common lymphoid progenitor (CLP) cells occurs in the bone marrow from haematopoietic stem cells[1]. These cells migrate to the thymus where they undergo maturation and selection into a mature T cell before egress into the peripheral blood system. However for this egress to take place several checkpoints have to be passed successfully, an achievement which many of the initial thymic immigrants fail to complete.

Initial synthesis of the pre-T cell receptor (TCR) occurs following rearrangement of the TCR genes by the recombinase activation genes (RAG). At this point the cells lose their reliance on Notch and Interleukin (IL)-7 signalling conferred by thymic epithelial stromal cells[2]. Upon development of a successfully rearranged β chain the immature T cell, referred to as a double negative T cell, commences proliferation thus passing the first checkpoint, β selection. After this initial checkpoint the cells progress to the double positive stage in T cell development. At this step the T cell expresses both co-receptors CD4 and CD8. Positive selection occurs if T cells are able to interact with a MHC class I or II molecule on thymic epithelial cells. T cells which are unable to interact successfully at this stage, die by neglect. These MHC molecules present peptides for recognition via the TCR to the T cells. Dependent upon the class of MHC bound the double positive T cell looses expression of one of

its co-receptors, becoming a single positive cell and thus committing it to either the CD4+ or CD8+ lineage. CD4+ T cells interact with antigens presented upon MHC II and CD8+ T cells with antigens on a MHC I. At either the double or single positive stage the immature T cell is also susceptible to negative selection via interaction with thymic epithelial cells that express MHC containing self antigen. Here T cells bearing TCRs which strongly recognise self, either through high affinity or avidity, are clonally deleted. Further cells which show an intermediate affinity for self go on to become regulatory T cells (Tregs) and only cells which have mild interactions are able to go on to become mature conventional T cells (Tconv) and exit the thymus[3-5].

Activation of a T cell outside of the thymus is a multistep process requiring integration of a variety of signals. Initially an antigenic, or non-self, peptide is presented in complex with a MHC class I or II molecule on an APC. The specific antigen is recognised by a specific TCR clone which is complementary for the antigen MHC complex. Recognition of a TCR's cognate antigen induces cross linking of the TCR receptor. The TCR complex is composed of the α and β chains of the TCR (in the case of αβ T cells) in complex with CD3. As a result of TCR crosslinking CD3 undergoes a conformational change that exposes the immunoreceptor tyrosine based activation motifs (ITAMs) enabling phosphorylation at this location on the ζ chain of CD3 by the Src protein tyrosine kinase Lck which is associated with the co-receptors CD4 and CD8. Phosphorylation of the ITAM residues enables the binding of Zap70 to CD3, which promotes the downstream signalling cascade of T cell activation via phosphorylation of multiple signalling molecules. Two of the major targets of Zap70 phosphorylation are LAT and SLP-76 which serve as the centre for the generation of the proximal signalling complex which leads to the activation of the cell[6].

This initial interaction between a TCR and its cognate ligand, known as signal 1, is not enough to provide appropriate stimulation for T cell activation and further signalling events are required. These further signalling events are known as signal 2 or costimulatory signalling.

Costimulatory signals were traditionally thought to be between receptors present on the T cell and ligands present on the APC however ligands and receptors have been shown to be expressed on other cell types. Two families of proteins that are known to be involved in costimulation are the Immunoglobulin (Ig) super family and the TNF super family.

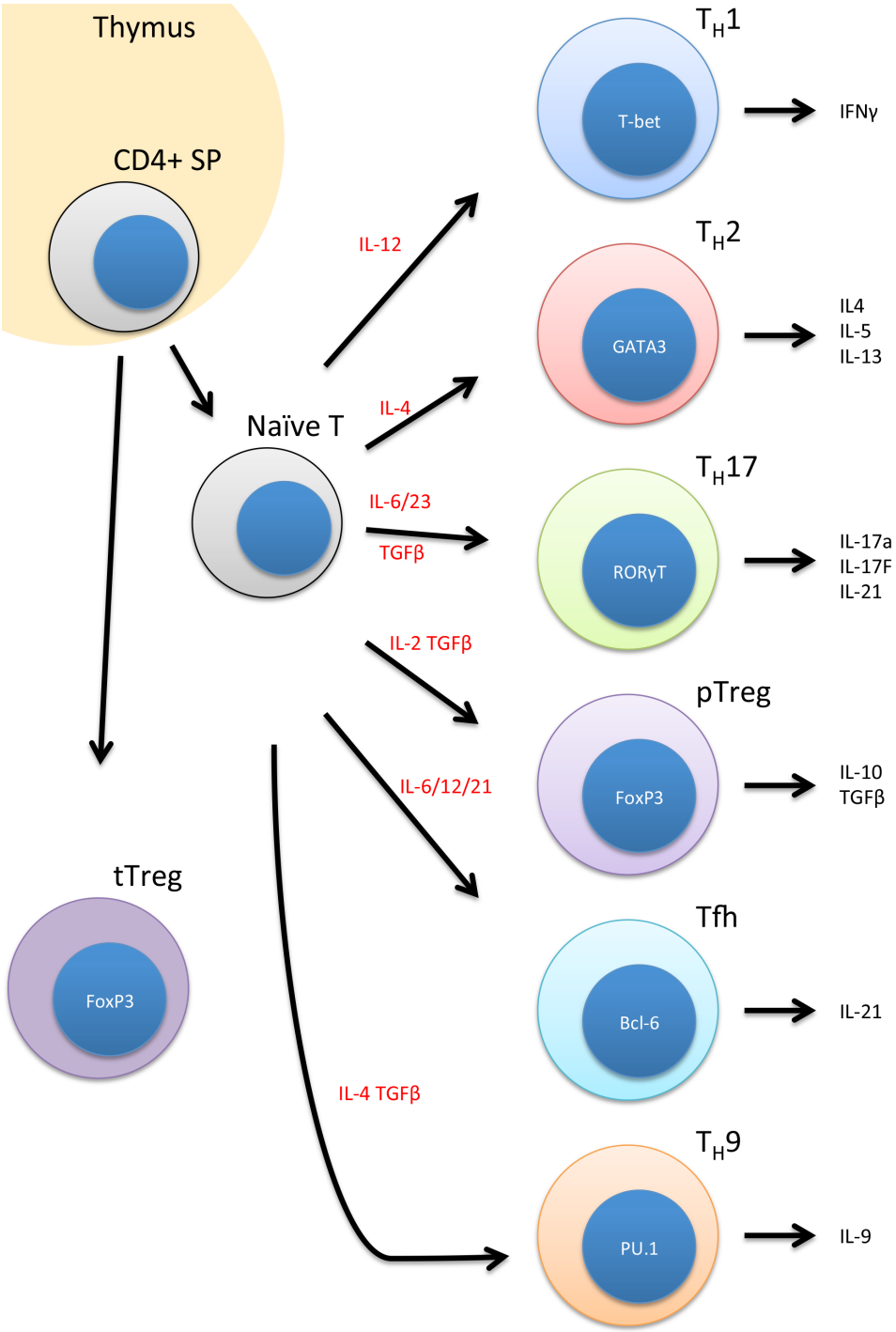

Figure 1-1 *– CD4+ T helper subsets. Upon maturation of the CD4+ single positive (SP) T helper cell in the thymus the cell exits into the immune system. When the T cell encounters its cognate MHC/Ligand complex on a professional antigen presenting cell the T helper cell activates and differentiates into one of the subsets of T helper cells within the figure. The induction of each subset has been found to be promoted by the cytokines in red and the cytokines which each cell subtype produces has been indicated after the cell. The master transcription factor has been indicated for each subset. Figure adapted from [7].*

CD28, an Ig super family member, is perhaps one of the best examples of a classical T cell costimulator and acts to enhance TCR mediated signalling. CD28 binds the ligands CD80 and CD86 that are highly expressed by APCs and has been shown to be highly important in many but not all T cell mediated responses[8]. A predominant mechanism by which CD28 mediates its effect is through the activation of phosphoinositide 3-kinanse (PI3K). The p85 regulatory subunit of PI3K is able to bind CD28 post ligation of its ligand, this then recruits the p110 catalytic subunit leading to activation of PI3K[9] which converts the membrane lipid phosphatidylinositol (3,4)-bisphosphate to phosphatidylinositol (3,4,5)-trisphosphate (PIP3). PIP3 can activate a number of kinases, including PDK1 which in turn promotes activation of Akt. Akt regulates many processes required for activation within the T cell including the NF-κB pathway via association with CARMA1[10].

In contrast to costimulatory receptors, coinhibitory receptors are also important for control of T cell responses. A classical example of a coinhibitory receptor is cytotoxic T lymphocytes associated protein 4 (CTLA4). The importance of this receptor in controlling the T cell response is exemplified by the CTLA4 knock out (KO) mouse which exhibits lymphoproliferation and fatal autoimmunity[11].

CTLA4 binds CD80 and CD86 in competition with CD28 however multiple models have arisen for its action as a coinhibitor of T cell activation. One proposed mechanism was through intracellular signalling mediated by its cytoplasmic tail. It was proposed that CTLA4 can modulate the phosphorylation of CD3ζ chain[12] or interfere with Zap70 activation thus reducing time spent as APC-T cell conjugates[13], however others have found this not to be the case[14]. Further, as a transcriptional based approach demonstrated, blocking of CTLA4 *in vitro* had very minimal effects on CD3 stimulated T cells suggesting that it is not a key means for downstream signal transduction[15]. A second model proposes that CTLA4 is able to promote ligand down regulation thus reducing the availability for stimulation via CD28. It was found that *in vitro* culture of dendritic cells (DC) with either Treg or Tconv CD4+ T cells from DO11.10 mice was able to specifically down regulate CD80 and CD86 in the presence of TCR stimulation via Ovalbumin (OVA). Further this was dependent on CTLA4 expression and the effect was greater when mediated through Tregs, which is most likely due to their increased expression of CTLA4[16]. A second group has gone further and proposed that the down regulation of CD80 and CD86 occurs by a process of trans-endocytosis where the T cell actively captures and takes up the ligands and degrades them thus limiting signalling via CD28[17].

However the debate on the proposed mechanism of action for CTLA4 turns out, it is clear that CTLA4 acts as a coinhibitor of T cell activation through acting as an antagonist for the costimulator CD28.

1.1.2. B cells

B cells are the antibody secreting cells of the immune system. These cells are capable of recognising and responding to unprocessed antigen and mounting a specific antibody mediated response which can either neutralise the invasive pathogen or highlight it for destruction through phagocytosis or activation of the complement system.

B cells are differentiated from the CLP in the bone marrow from embryonic day 17.5 in the mouse. Prior to this they are differentiated in the yolk sac and subsequently the foetal liver. In the bone marrow early B cell progenitors, termed pro-pre B cells are found associated with CXCL12 positive mesenchymal stromal cells, as the B cells start to mature and become pre B cells they move close to IL-7 positive cells[18]. It is at this point that rearrangement of the heavy chain for production of the B cell receptor (BCR) starts to take place and the cells transition to become pre-BI cells. Upon withdrawal of IL-7 the pre-BI cells differentiate and undergo V_H to D_HJ_H rearrangements on one allele of the Ig heavy chain utilising the recombination activating genes (RAG 1 and 2) and becoming pre-BII cells. At this point a functional Ig heavy chain can be produced from one in three successful rearrangements and can be trafficked to the membrane as a μ heavy chain forming a pre-BCR with a surrogate light chain. This event causes allelic exclusion of the other heavy chain allele thus preventing the cell from expressing two different heavy chains[19]. Only pre-BII cells which are capable of forming a pre-BCR are able to proliferate, cells which are not die through apoptosis[20]. Once the pre-BII cells start to proliferate, signalling via the pre-BCR causes down regulation of the surrogate light chain which in turn limits the proliferative potential of these cells eventually causing them to exit the cell cycle[21]. Concurrent with cell cycle arrest the RAG genes are re-expressed and the light chains of the Ig locus are rearranged to form a mature BCR. If a productive pairing of the light and heavy chain is achieved and the BCR is not autoreactive then RAG expression is turned off and the immature B cell exits the bone marrow as a result of S1P and migrates to the spleen[22]. If a BCR is produced but is autoreactive then RAG stays on and rearrangement continues with the second allele[23]. Once in the spleen the immature B cell is screened for autoreactivity again and matures into a naïve B cell which is capable of antigen recognition. Upon

activation in the spleen or secondary lymphoid organs AID is switched on which promotes class switching of the conserved region of the heavy chain leading to expression of different antibody isotypes. At the same time the germinal centre (GC) reaction occurs. This enables production of high affinity antibody secreting plasma cells and memory B cells through the help of T follicular helper cells. This will be discussed at length in later chapters.

Signalling via the BCR in many ways is similar to the TCR in that through antigen recognition a signalling cascade is initiated within the cells that brings about multiple transcriptional changes. Further as well as signalling via the BCR directly there is also a role for costimulation.

Signals conferred by the BCR can be split into two types; antigen independent and antigen dependent. The antigen independent signal promotes cell survival on mature B cells and it has been demonstrated that lack of a functional BCR caused B cells to undergo premature apoptosis[24]. In contrast antigen dependent signals promote activation of the B cell and differentiation into memory and plasma B cells.

The BCR complex is composed of the membrane bound Ig, which is responsible for antigen recognition, and the associated CD79a/b heterodimer which promotes downstream signalling via phosphorylation of the ITAM domains within its cytoplasmic tail by LYN. Once phosphorylated the CD79a/b heterodimer acts as staging point for assembly of the BCR signalling complex initiated by the binding of SYK. SYK leads to the downstream activation of PLCγ2 and LYN dependent phosphorylation of CD19 promoted activation of the PI3K pathway thus leading to the promotion of multiple pathways promoting B cell activation and differentiation[25].

Costimulation of B cells occurs via the TNFRSF member CD40. CD40 ligand (CD154) is expressed by activated Th cells and can function to boost activation via the BCR and inhibiting apoptosis. Signalling via CD40 causes an increase in SYK dependent signalling pathway activity via increasing the levels of phosphorylated SYK within the B cell in a synergistic manner[26].

1.1.3. Innate lymphoid cells

Innate lymphoid cells (ILCs) are a relatively newly defined family of innate cells that have been shown to play important roles within the immune system. Multiple members of this family were discovered over several decades starting with the discovery of the Natural killer (NK) cells[27], however they were recently grouped into

a family and divided into subsets based on their cytokine and transcription factor profile[28].

ILCs are located at barrier surfaces throughout the body including the skin, intestine and the lungs. Here they respond to inducer cytokines and microbial signals by production of further cytokines which control and aid the immune response as well as promoting wound repair. As a family, ILCs are identified as cells which are negative for all usual lineage markers of T, B and myeloid cells however express the common gamma chain and Thy1[29].

The family of ILCs are all differentiated from the CLP in the bone marrow[30] and are separated into three main classes[28].

Group 1 ILCs (ILC1) are induced to produce cytokines including Interferon-γ (IFN-γ) and TNF by IL-12 and IL-15 and include classical NK cells. All members of this group express the transcription factor T-bet[30, 31]. ILC1s have been shown to be a major source of responder cytokines in response to infection of mice with the intracellular pathogen *Toxoplasma gondii.* Further, transfer of ILC1s into mice that lack all lymphoid cells (RAG2-/- Il2rg-/-) significantly reduced the titre of pathogens in the liver by day 6 post infection[30].

Group 2 ILCs (ILC2s) constitutively express GATA3 and respond to IL-25 and IL-33. Once activated the ILC2s produce IL-4, IL-5 and IL-13[32-34]. Through infection with *Nippostrongylus brasiliensis* ILC2s have been shown to have a role in response to extracellular parasite infection. ILC2s were greatly increased in the draining lymph node 5 days post infection and to such a level that they were the most abundant IL-13+ cell type measured. Transfer of ILC2s was able to restore the defect in worm clearance seen in IL-17br -/- mice which have reduced numbers of ILCs[33]. This role of ILC2s in defence against extracellular parasites is performed through the action of IL-13 promoting mucus production and smooth muscle contraction to aid in expulsion of the worms[35].

Group 3 ILCs (ILC3s) are RORγT+ cells and include lymphoid tissue inducer (LTi) cells. ILC3s respond to IL-1β, IL-6 and IL-23 and express IL-17 and IL-22[36-38]. ILC3s act to mediate inflammatory responses at mucosal surfaces. Within 6 days of infection of mice with *Citrobacter rodentium* ILC3 numbers greatly increase in the intestinal epithelium and express IL-22 which is required for host defence[38]. IL-22 promotes the expression of the Reg family microbial proteins (RegIIIβ and RegIIIγ)

by colonic epithelial cells, which is required for survival of *Citrobacter rodentium* infection[39].

1.2. The Tumour Necrosis Factor Receptor and Ligand super family: members and signalling

The TNF super family (Figure 1-2) is composed of 19 ligands (TNFSF) and 28 receptors (TNFRSF) in the mouse and 29 in humans. The range of receptors and ligands are expressed across a multitude of cell types throughout multiple different systems. The family is named after the archetypal ligand TNF which binds to either TNF receptor 1 or 2 (TNFR1, TNFR2) and has been shown to be involved in many aspects of the immune system. Therapeutic blockade of TNF interaction with its receptors has proved to be successful in autoimmune diseases such as Rheumatoid Arthritis[40].

The receptors in this family are mostly expressed as type I membrane proteins, some members, such as Decoy receptor 3 (DcR3) are secreted and can act as decoy receptors [41]. A type I membrane protein is composed of a single transmembrane domain with its N terminus on the cytoplasmic side and a signal peptide. A type II transmembrane protein has a single transmembrane domain containing a signal anchor with the C terminus on the cytoplasmic side. These receptors contain multiple extracellular cysteine rich domains (CRD) consisting of repeats of 6 cysteines forming 3 disulphide bridges[42]. The corresponding ligands are type II membrane proteins some of which, for example TL1A[43], can be cleaved to form soluble ligands. The extracellular domain of the ligands contains a TNF homology domain which shows 20-30% sequence identity between the members of the family and is responsible for receptor binding[42]. In the membrane the receptor exists as either monomers or pre-assembled into multimers via the pre-ligand association domain (PLAD) found in some members of the family[44]. Further pre-association of Fas has been shown to be required for correct function[45]. The ligands for the family are associated into trimers; when they engage with their receptor they promote the formation of larger receptor oligomers which are thought to induce signalling[46, 47].

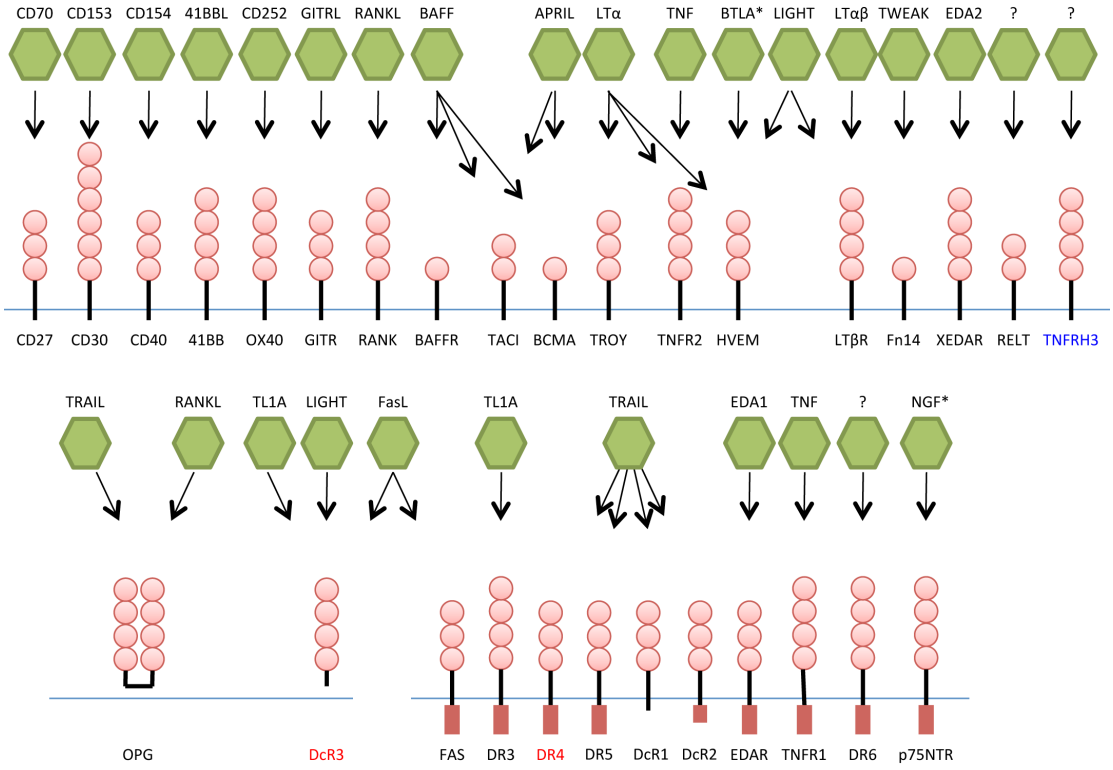

Figure 1-2 *– The Tumour Necrosis Factor Receptor Super Family (TNFRSF). The TNFRSF is composed of 19 ligands (green hexagons) and 28 receptors in the mouse or 29 in humans. These proteins are expressed on a variety of cell types across multiple different systems. The receptors are either membrane (blue line) bound or soluble and are characterised by the presence of multiple cysteine rich domains (pink circles). Some of the members of this family have an intracellular death domain (red rectangles). Names of proteins found in both the human and mouse are in black, those found only in the mouse are in blue and those only in humans in red. Non TNF family members are indicated with *. ? Indicates unknown ligands for orphan receptors. Adapted from [48-52].*

1.2.1. TNFRSF sub-families

TNF family receptors can be sub divided further based upon their mechanism for signalling. One of the groups, which includes members such as CD27[53] and CD40[54], signals via TNFR-associated factors (TRAFs) which bind to the TRAF-interacting motif (TIM) on the cytoplasmic tail of the receptors. With the exception of TRAF1, which only contains 1 zinc finger domain[55], all other TRAF family members contain 5-7 N terminal zinc finger domains and a RING domain[56]. Whilst the N terminal domain of TRAFs is highly conserved the C terminal region is less so; this is the region responsible for binding to the TIM. Ligation and subsequent trimerisation

of the TNF super family receptors results in recruitment of the TRAFs [57, 58]. TRAFs bind and oligomerise to form higher order complexes resulting in NF-κB activation. TRAF-TRAF association is promoted by RING domains and zinc finger motifs found in the N terminus[59, 60]. Once oligomerised TRAFS can induce ubiquitination of RIP1, cIAPs and TAB2 through action as an E3-ubiquitin ligase. This enables recruitment and activation of the IKK complex and MAPK thus promoting downstream signalling[61, 62].

A second group of receptors are those that signal via an intracellular death domain. These can be further divided into ones that promote death signalling, such as Fas, and those that are pro survival, such as DR3. Interaction of Fas with its cognate ligand, FasL, results in oligomerisation of the receptor and recruitment of the Fas associated protein with death domain (FADD). Recruitment of the adaptor protein FADD occurs via homotypic interaction between death domains in FADD and in Fas. This subsequently induces recruitment of procaspase 8 and 10 to the receptor complex via their death interaction domains. This is referred to as the death inducing signalling complex (DISC)[63]. Once assembled into the DISC the procaspase autocatalytically cleaves resulting in activation and induction of apoptosis[64]. In contrast DR3 does not induce apoptosis under physiological conditions despite the presence of a death domain. This is due to the binding of the adaptor protein TNFR-associated death domain (TRADD). TRADD contains both a death domain and a TRAF binding domain enabling it to act as an intermediary binding partner between the death domain of DR3 and TRAFs thus bypassing death signalling and instead promoting pro-survival pathways such as the NF-κB pathway[58]. Various signalling pathways will be discussed later in this chapter.

The final group of TNFSF receptors are the decoy receptors. These receptors lack a functional intracellular signalling domain however, are still able to bind TNFSF ligands. There are several of these in the family. Some, such as DcR3[65], are soluble proteins whereas others, such as DcR1[66] and DcR2[67] are membrane bound however their intracellular signalling domains are either absent or truncated and non-functional. As a result of their lack of a signalling domain these receptors occupy TNFSF ligands through binding but prevent their canonical signalling. There are however reports of these receptors inducing alternative signalling pathways[68].

1.2.2. Control of signalling

Signalling by the TNFSF can be controlled in a number of ways. Decoy receptors, as discussed above, are one means by which the bioavailability of a ligand can be controlled. Alternatively the ligand may be cleaved from the surface of a cell. The matrix metalloproteinase ADAM17, also known as TNF converting enzyme (TACE), was originally identified as the enzyme responsible for cleavage of membrane bound TNF from the surface of cells[69]. Several groups have demonstrated that the membrane bound and soluble forms of TNF have different functions thereby cleavage of the ligand may act as a means of control[70, 71]. This topic will be discussed at greater length in chapter 4.

1.2.3. Spatial temporal regulation and role of the TNFSF throughout the immune system

The TNFRSF members can be spatially and temporally separated with different receptors either upregulated or induced in response to stimuli at different stages of an immune response. It is this, along with the non-overlapping function of the family, which defines them as a super family rather than a gene family[72].

T cells constitutively express the TNFRSF member CD27 at a low level which, upon TCR engagement is upregulated within 24 hours. In contrast OX40 is not expressed by the naïve T cell and is induced upon activation requiring both TCR and CD28 stimulation[73]. Through examination of the function of T cells lacking these receptors it is possible to hypothesise the point at which they act in a normal immune response. CD27 KO cells are able to proliferate normally *ex vivo* however their ability for long term survival and memory generation is diminished[74] suggesting activation is not affected in the first few days following stimulation but that CD27 is required for long term survival. Further studies with a CD19 promoter driven CD70 (the ligand for CD27) transgenic mouse demonstrated CD27 driven proliferation of CD4+ and CD8+ effector T cells and an increase in memory populations[75]. CD27 signalling has also been demonstrated to be required for protection of activated CD8+ T cells from TRAIL mediated activation induced cell death[76]. In contrast OX40 acts later in the response as OX40 KO cells do not show any defect in activation however apoptosis is increased by day 12. This was demonstrated to be due to a later OX40 mediated maintenance of anti-apoptotic proteins Bcl-2 and Bcl-XL which are initially induced via CD28 signalling[73].

Fas, as discussed above, is an apoptosis inducing member of the TNFRSF. Fas is relatively ubiquitously expressed throughout the body and its ligand is mainly expressed by activated T cells and NK cells[77]. The critical role of Fas within the immune system is highlighted by the human autoimmune disease ALPS (autoimmune lymphoproliferative syndrome) and the Lpr mouse model of lupus nephritis. ALPS is characterised by abnormal lymphocyte survival resulting in non-malignant chronic splenomegaly, lymphadenopathy and expanded double negative T cells in the periphery[78]. Over 70% of patients with ALPS have a mutation in the Fas gene or another gene in the downstream signalling pathway[79]. The murine equivalent, as exemplified by the Lpr mouse, has many of the same symptoms and is caused by an insertion mutation in intron 2 of the Fas gene which causes premature termination of transcription[80]. It is believed that both these diseases are due to an impairment in clonal deletion of autoreactive T and B cells due to the lack of action of Fas. Another proposed role for Fas is in the maintenance of sites of immune privilege. In sites, such as the eye, introduction of antigens is tolerated without a normal immune response being mounted. Based on viral infection experiments in Gld mice, which lack FasL, it was proposed that immune privileged sites are maintained via Fas mediated apoptosis. These sites have a high level of FasL which induces Fas dependent apoptosis of any Fas expressing lymphocytes that enter thus protecting the site from inflammation mediated damage and maintaining immune privilege[81].

Lymphotoxin (LT) is an atypical member of the TNFSF in that it can exist in both a homo- and hetero-trimer. LTα exists as a soluble homotrimer and is secreted by activated lymphocytes, resting B cells, myeloid cells, ILC3s and non- haematopoietic lineage cells[82, 83]. It is able to bind to TNFR and HVEM however the affinity for the receptor HVEM is low[84]. LTβ can also exist as a homo-trimer however is membrane restricted. More often though it is found in a hetero-trimeric complex of either LTα1β2 or LTα2β1 and has been shown to be expressed by activated T cells, B cells, ILC3s and NK cells[83, 85]. Complexes involving LTβ signal via the LTβ receptor[86]. The LTβ receptor is expressed on mast cells[87], stromal cells in lymphoid tissue and monocytes[88] but not lymphocytes[89]. Blocking of this pathway leads to inhibition of the GC reaction[90], prevention of development of collagen induced arthritis(CIA)[91] as well as lack of development of Peyer's patches and lymph nodes[92] and severely attenuated basal and responsive IgA levels[93]. The role of LT in lymph node organogenesis is carried out by LTi cells, part of the ILC3 group of innate cells[94]. In these cells the expression of LT is induced through RANK, another member of the TNFRSF, and maintained through IL-7[95]. LT derived

from ILC3s also has a role in IgA responses in the gut. LTα promotes T dependent (Td) IgA responses through regulation of T cell homing whereas LTα1β2 promotes T independent (Ti) IgA through modulating iNOS expression in CD11c+ DCs[83]. Overall this shows the key role that the LT pathway plays in the innate and adaptive immune response including humoral immunity.

CD40 is another member of the TNFRSF which has wide ranging effects across the immune system. CD40 is expressed on activated T cells, B cells and DCs and is also expressed at a lower level on monocytes, platelets and several types of epithelial cells[82]. CD154, the ligand for CD40, is expressed by activated CD4+ T cells[96], B cells[97], activated DCs[98] and activated platelets[99]. CD40/CD154 have several different roles throughout the immune system. A major role for this pair is the costimulation and proliferation of B cells during the GC reaction. Stimulation via soluble CD154 *in vitro* was shown to promote B cell growth and differentiation[100] and ectopic expression of CD154 driven by the V_H promoter led to spontaneous lupus like disease within a year on a C57bl/6 background[101]. The importance of CD40 signalling in the GC response is demonstrated by the disease X-linked hyper IgM syndrome. This disease is caused by a lack of expression or a loss of function of CD154 and presents as a hypo-IgG and IgA, hyper-IgM and a lack of GC formation thus highlighting the essential role of CD40 in class switching of antibodies[102]. A second role of CD40 in the immune system is the licensing of APCs such as DCs. It was found early on that CD40 agonistic antibodies could replace the need for CD4+ T cell help in some CD8+ driven immune responses[103]. Further, CD40 activation of a DC via CD40 resulted in increased MHC expression and an increase in the expression of the costimulatory ligands CD80 and CD86 thus increasing the stimulatory capacity of that DC for T cell activation[104].

1.2.4. NF-κB signalling pathway

A major signalling pathway activated directly as a result of TNFRSF signalling is the NF-κB pathway (Figure 1-3). This pathway is responsible for expression of a host of genes which promote cell survival and immune effector responses. Activation of the NF-κB pathway first requires the activation of IKKα/β NEMO complex (NF-κB essential modulator; IKKγ)[105]. This occurs either through direct polyubiquitination by TRAF6 [106] or by cIAP1/2 following recruitment by TRAF2[107]. NEMO facilitates the activation of IKKα/β either by inducing a conformational change or promoting trans-autophosphorylation[108]. Once active, IKKα/β phosphorylates two serine residues on IκB which acts as an inhibitor and binds the NF-κB dimer and

occludes its nuclear localisation signal[109, 110]. Phosphorylated IκB is targeted for degradation in the proteasome and the free NF-κB can translocate to the nucleus where it binds to specific regulatory sequences in the promoters of genes resulting in the expression of a specific transcriptional profile[111, 112].

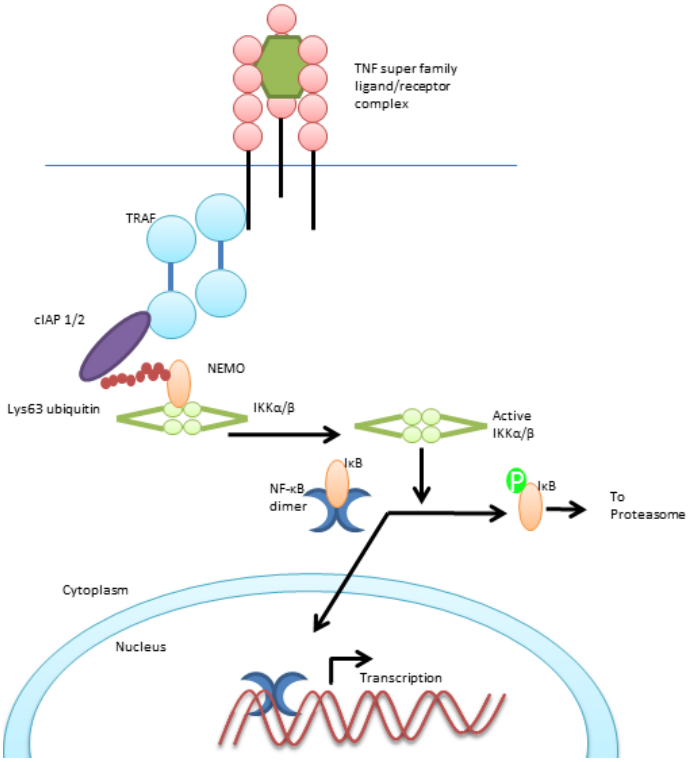

Figure 1-3 *– Overview of the NF-κB pathway. Members of the TNFRSF are able to activate the NF-κB pathway as a result of ligation of the receptor by an appropriate ligand. Activation results in translocation of the NF-κB dimer to the nucleus where it binds to specific regions in the promoter of genes and promotes a pro-inflammatory phenotype (Adapted from [113]).*

1.2.5. AP1 signalling pathway

A second major signalling pathway in TNFRSF signalling is the activation of activating protein 1 (AP1). AP1 is a transcription factor which is activated through the mitogen activated protein kinase (MAPK) pathways and has binding sites in the promoter region of many genes involved in immunological responses[114]. The AP1 complex is composed of hetero- or homo-dimers of Fos (Fos-B, c-Fos, Fra-1 and Fra-2), Jun (Jun-B, c-Jun,and Jun-D) and the activating transcription factor (ATF-1 and ATF-2) families[115, 116] which, when activated, act as transcription factors. Following signalling via the TNFRSF, the binding of TRAFs promotes activation of various MAPK pathways. For TRAF2 binding in response to TNFα stimulation c-Jun

N-terminal kinases (JNK)[117] are activated via interaction with multiple MAPK3 including ASK1[118] and MEKK1[119]. JNK subsequently promotes the activation of AP1[120].

1.3. Death Receptor 3

DR3, also known as TNFRSF25, LARD (Lymphocyte-associated receptor of death), WSL-1, TRAMP (TNF receptor-related apoptosis mediating protein) and APO-3, was initially cloned by multiple groups due to its sequence homology with TNFR1[121-125]. It is a type I membrane protein and is composed of three to four CRD, a transmembrane domain and an intracellular death domain.

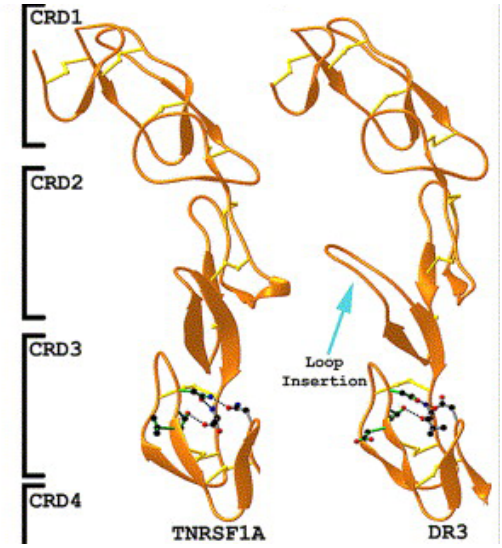

Figure 1-4 *– Comparative predicted protein structure of the extracellular domains of DR3 and TNFR1. Using the crystal structure of the extracellular domain of TNFR1 (left) the structure of the extracellular domain of DR3 was predicted (right). The major difference is the addition of a loop region in CRD II that has been indicated. Adapted from [126].*

DR3 is the member of the TNFRSF that shows the highest homology to the archetypal protein of the family TNFR1. 30% sequence identity and 44% similarity is apparent between the extracellular domain of TNFR1 and DR3 in humans[126]. Though the crystal structure of DR3 has not been solved comparative modelling has predicted a highly homologous structure between DR3 and TNFR1. The CRDs of TNFR1 and DR3 are believed to be structurally conserved. They are predicted to be aligned along a highly twisted ladder composed of disulphide bonds, forming a β-sheet dominated topology. The ligand-receptor structure is proposed to consist of three ligands interacting with three receptor molecules with a conserved binding site

between CRD II and the C terminal end of CRD III. The major structural difference between DR3 and TNFR1 is believed to be in the insertion of a loop region in CRD II (Figure 1-4)[126-128].

Cell type/ Organ	Comments	Reference
IgM$^+$ B cells	Increased upon activation with anti-IgM	[129]
B220$^-$ CD138$^-$IgM$^-$ Plasma cells	15 days post BTIIC/CFA immunization	[130]
CD4$^+$ T cells	Increases post activation. Th17 and Th9 show greater expression than Th0/1/2	[131-133]
CD8$^+$ T cells	Transient increase post activation.	[132, 134]
CD161$^+$ CD4/8$^+$ T cells	Subpopulation of DR3 $^+$ which increases with low IL-12/IL-18 stimulation	[135]
FoxP3$^+$ CD4$^+$ T cells	*Ex vivo* Treg, FoxP3-GFP reporter mouse: of CD4$^+$, GFP$^+$ and GFP$^-$ express similar levels *ex vivo* iTreg. Comparable to Th17	[136, 137] [131, 133]
NK cells / ILC1	*Ex vivo,* Lower than CD4$^+$ T cells from mesenteric lymph nodes Subpopulation of DR3+ among NK/ ILC1 cells NK1.1$^+$ CD3$^-$ Lin$^-$ NK1.1$^+$	[138, 139] [140]
NKT cells	*Ex vivo* *NK1.1+ TCRβ+* *NK1.1+ CD3+*	 [132] [138]
ILC2	*Ex vivo,* comparable to CD4$^+$ T cells from mesenteric lymph nodes Lin$^-$ NK1.1$^-$KLRG1$^+$ Mouse: Lin$^-$Sca1$^+$CD127$^+$ST2$^+$ Human: Lin$^-$CRTH2$^+$CD161$^+$CD127$^+$	[140] [141]
ILC3	*Ex vivo,* comparable to CD4$^+$ T cells from mesenteric lymph nodes	[140]
Monocyte-derived macrophages	M-CSF cultured	[142]
CD11c $^+$ cells	Subpopulation of DR3+ cells directly *ex vivo*	[138]
Kidney tubular epithelial cells	Normal human kidney and increased in Ischemic allographs	[143]
Glomerular endothelial cells	Ischemic allographs. Not in healthy tissue.	[143]
Brain neuronal linage cells	Neurons within hippocampal and cortical regions	[144]

Table 1-1 *– Expression of DR3 throughout the immune and non-immune systems. Expression patterns of DR3 along with the cell types and conditions under which they have been observed. Where expression among multiple cell types has been shown within one publication comparisons have been made and where different cell markers have been used by different groups these have also been noted[145].*

TNFR1 is expressed upon the majority of cell types however the expression of DR3 is more restricted (Table 1-1)[146, 147]. DR3 has been shown to be expressed on CD4+ T cells, activated CD8+ T cells, IgM+ B cells, ILCs and macrophages[129, 132, 138, 140, 142, 148]. This more restricted expression pattern of DR3 suggests that it

may have a specific non-redundant role in the immune system. DR3 has also been found to be expressed outside the immune system in diseased kidney endothelial cells and neuronal cells[144, 149].

DR3 is encoded by 10 exons present on chromosome 4E1 in mice and is found in its syntenic location on human chromosome 1p36.2[127]. Up to 13 alternatively spliced forms of DR3 have been shown to be present at the mRNA level in humans[121, 122, 150], of which 3 have been demonstrated to be present in mice[127](Figure 1-5). Variant I of murine DR3 is the full length isoform containing four CRD; however DR3 can also be alternatively spliced to produce variant II which lacks exon 6 or variant III which lacks exons 5 and 6. As a result of a frame shift due to the absence of exon 6, variant II encodes a predicted soluble version of DR3 which is lacking the second half of CRD IV, the transmembrane domain and the death domain. The loss of exon 5 along with exon 6 corrects this frame shift thus causing variant III to be a membrane bound splice variant which is lacking CRD IV[127]. The relative expression level of these variants has been shown to be varied dependent upon the cellular context. Naïve CD8+ T cells and Th17 cells show a 1:1 ratio of variants I and III whereas activated CD8+ T cells show a greater relative expression of variant I than III. In contrast natural and induced Treg cells show greater relative expression of variant III compared to variant I[131, 132].

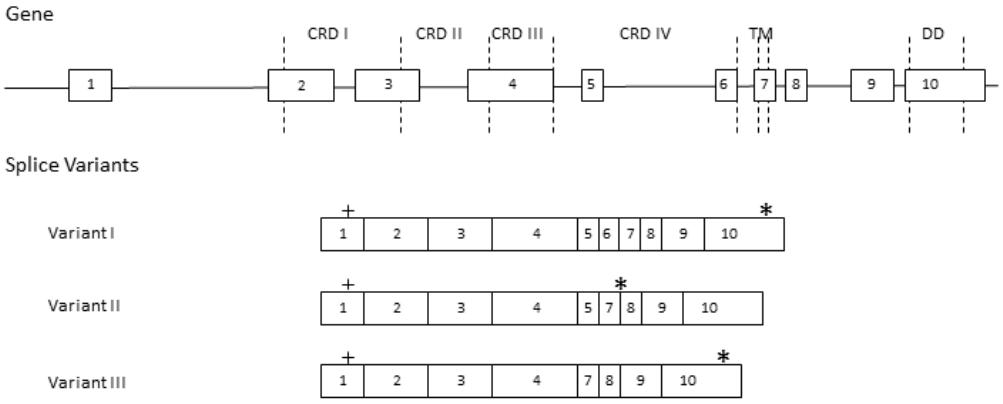

Figure 1-5 *– Murine DR3 splice variants. The gene for DR3 is composed of 10 exons which can be alternatively spliced to produce 3 splice variants. Variant I and III produce membrane bound receptors and variant II is a predicted soluble form. The domains have been indicated on the gene, + and * indicate start and stop codons respectively. Adapted from [132].*

1.4. TNF-like Ligand 1A

Original work identified TWEAK/APO3L as the ligand for DR3[151] however later work indicated that this was not the ligand for DR3 and instead TNF-like ligand 1A (TL1A, TNFSF15) was identified as the true ligand. TL1A was identified through searching an expressed sequence tag (EST) database using a BLAST algorithm for TNF-like molecules. Initially a shorter transcript was cloned from the gene encoding TL1A called TL1 or VEGI. It was found to inhibit angiogenesis and induce apoptosis of endothelial cells however prevailing opinion is that this was either a cloning artefact or not the main transcript of the *TNFSF15* gene[152, 153].

TL1A is a type II membrane protein with a predicted hydrophobic transmembrane domain proximal to the N terminus [43]. The extracellular domain contains globular TNF-homology domain (THD) composed of a homotrimeric arrangement of β-sheet jellyroll folds. This structural arrangement is highly conserved among the TNF ligand family members and to a greater extent than the primary sequence would indicate. The crystal structure of TL1A demonstrated that the ligand forms homotrimers through electrostatic interactions via the THD which is indicative of the TNF ligand family[154]. To date the crystal structure of TL1A in complex with DR3 has not been solved but this has been modelled as discussed above[126].

TL1A is highly conserved between species with 63.7% and 66.1% sequence homology of mouse and rat TL1A respectively compared to humans[43]. TL1A has also been shown to have a role in chicken immunology however signalling via TL1A appears to have a role closer to TNF in humans (TNF has not been identified in chickens) and signals via TNFR2 and DcR3. Further phylogenetic analysis of TNFSF members showed chicken TL1A is more closely related to mammalian TL1A and TNF than other members of the chicken TNFSF[155, 156].

Chromosomal mapping has identified the location of human TL1A to be on 9q32 and is composed of 4 exons, which do not appear to be alternatively spliced[43]. The gene for TL1A contains NF-κB and AP-1 regulatory sites which have both enhancer and suppressor functions however NF-κB blockade inhibits TL1A expression *ex vivo[157]*.

Expression of TL1A (Table 1-2) is highly controlled and is often inducible. TL1A has been shown to be expressed on endothelial cells [43] and induced in response to Fcγ receptor cross linking and LPS mediated TLR signalling on monocytes and DC. Further, TCR stimulation induces TL1A expression on T cells [158, 159]. TL1A

expression has also been shown by immunofluorescence on macrophages following infection with *Salmonella* and to be highly expressed at the mRNA level from a newly defined subset of CX3CR1+ mononuclear phagocytes in the gut[160, 161].

Cell type/ Organ	Comments	Reference
T cells	Upregulated on activation via the TCR on both CD4+ and CD8+ T cells *in vitro*	[138, 159]
F4/80+ Macrophages	In response to Chronic infection with *Salmonella enterica serovar Typhimurium*	[160]
Monocytes	Upregulation upon stimulation with immune complex and TLR ligands	[158, 162]
Dendritic cells	Upregulation upon stimulation with immune complex and TLR ligands	[158, 159, 162]
CX3CR1+ mononuclear phagocytes	High mRNA expression in cells isolated from murine colon	[161]
HUVEC cells	Highly expressed and inducible in response to IL-1α and PMA stimulation	[43]
Kidney vascular endothelial cells	mRNA and protein detected	[149]
Kidney tubular epithelial cells	Protein but no mRNA in allograft rejection	[149]
Murine Brain	mRNA detected	[144]
IBD patient colon biopsies	Protein detected via histological staining. mRNA upregulated in active sections	[163]
Synovial tissue and fluid	RF+ Rheumatoid arthritis patients	[164]

Table 1-2 *– Expression of TL1A throughout the immune and non-immune systems. Expression patterns of TL1A and the conditions under which they were observed[145].*

Similar to many other TNF family members TL1A can be cleaved by an as yet unidentified matrix metalloprotease (MMP). Recently Hedl *et al* claimed identification of ADAM17 as a protease which cleaves TL1A however their data only suggests the possibility of TL1A being directly cleaved by ADAM17 among several other enzymes. As such identification of the protease responsible still remains an unanswered question[142]. Overexpression of human TL1A in 293T cells yields a soluble protein into culture supernatant which is cleaved at leu72[43]. Soluble TL1A has also been detected in the cell culture supernatant of *ex vivo* stimulated DCs and monocytes but does not appear to be cleaved from the surface of T cells[158, 165]. The cleavage site of human TL1A has been mapped through the production of deletion mutants([165], F. Meylan and I. Malm unpublished observations, Figure 1-6). These data indicated that to prevent cleavage of TL1A from the surface of 293T or HEK293 cells a large region close to the transmembrane region has to be deleted implying the possibility of involvement of multiple proteases.

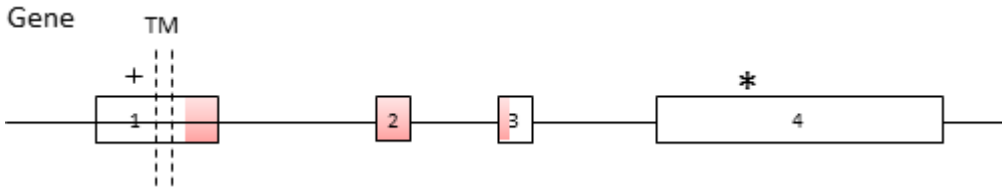

Figure 1-6 *– TL1A gene structure. TL1A is a type II transmembrane protein and is composed of 4 exons. The transmembrane domain (TM), Start codon (+) and stop codon (*) have been marked. The red shaded area indicates the putative TL1A cleavage site in human TL1A ([165], F. Meylan and I. Malm unpublished observations).*

1.5. Decoy Receptor 3

DcR3, also called TR6 and TNFRSF6B, is a secreted protein which has been shown to bind TL1A[43] along with LIGHT[65] and FasL[151]; a homologue of which has not been found in mice[68]. The gene for DcR3 is found on chromosome 20q13.3 and is expressed in a variety of human tissues[118]. DcR3 consists of four N terminal CRDs and a heparin binding domain (HBD) at the C terminus. Interaction of the various ligands with the decoy receptor occurs through interaction of CRD2 with the conserved backbone of the ligands thus enabling interaction with multiple targets[166]. The HBD enables interaction of DcR3 with heparin sulphate proteoglycans present upon the surface of many cell types. Through crosslinking of these glycans on DCs, DcR3 has been shown to induce apoptosis via a PKC-γ signalling cascade[68]. Upregulation of DcR3 has been observed in various cancers and expression level has been linked to cancer progression and survival[118, 151, 167].

1.6. Non TNF superfamily ligands for DR3

Along with TL1A recent work has highlighted non-TNF superfamily members as ligands for DR3. Progranulin, along with a man made derivative Atsttrin, has been demonstrated to bind to DR3. Further Atsttrin has been demonstrated to inhibit TL1A driven gene expression in THP-1 cells and also protect mice from development of DSS induced colitis[168]. Interestingly Progranulin also binds to TNFR1 and TNFR2, though with a higher affinity for TNFR2[169, 170]. DR3 was also demonstrated to bind to E-selectin in a pull down from tumour cell line lysates and DR3 antagonistic antibodies reduced the attachment of HT-29 and LoVo cells to E-selectin. Binding of

DR3 via E-selectin was also able to activate ERK which was also reduced with anti-DR3 treatment[171].

1.7. DR3/TL1A signalling and the immune response

1.7.1. Downstream signalling pathways

During the initial cloning of DR3 it was noted that overexpression in 293T cells promoted apoptosis of the cell in a caspase 8 dependent manner. This finding was expected due to the presence of the death domain after which DR3 was named. As a result this led to the initial idea that DR3 may be implicated in control of the host T cells through promotion of apoptosis in a similar fashion to that of Fas[121-125]. However the apoptotic role of DR3 has not been seen to be a major one *in vivo* with only one known example where DR3 deficient mice appear to have a minor defect in negative selection of auto reactive T cells in the thymus[127]. Further, the method for the activation of caspase 8 mediated apoptosis is debated as there are mixed reports on the capability of DR3 to bind FADD via its death domain as assessed by either GST pulldown or yeast 2 hybrid screens[122, 124].

Early studies on overexpression of DR3 also identified the activation of the NF-κB pathway. It was found that in the presence of an apoptotic inhibitor the NF-κB pathway was upregulated which, in the context of T cells, indicates increased activation status. The activation of the NF-κB pathway was shown to be due to binding of TRADD to the intracellular death domain of DR3 enabling recruitment of downstream adaptor proteins such as TRAF2[122, 124, 125]. This finding was confirmed in TRADD KO mice, which were unable to induce proliferation as a result of costimulation with TL1A or recruit TRAF2 or RIP to DR3 to form a signalling complex[172].

The identification of the ligand for DR3, TL1A, enabled the investigation of the apoptotic versus NF-κB signalling in DR3 stimulation. Using a naturally DR3 expressing human erythroleukaemic cell line, TF-1, it was shown that the stimulation of DR3 with TL1A only resulted in recruitment of FADD, caspase activation and subsequent apoptosis when the NF-κB pathway or protein synthesis was inhibited. This suggests that the default response to DR3 signalling is not apoptosis. It was found that in TF-1 cells activation of the NF-κB pathway resulted in the upregulation of cellular inhibitor of apoptosis 2 (cIAP2) which protected the cell via pro-survival signalling[58, 173].

1.7.2. Costimulation of T cells

TL1A has been demonstrated to act as a costimulator of T cells *in vitro*. Under sub-optimal TCR stimulation exogenous TL1A increased the proliferation of both CD4+ and CD8+ T cells as well as the secretion of IL-2 and IFN-γ (only CD4+ T cells). Further, TL1A costimulation resulted in an upregulation of CD25 (IL-2Rα) and CD122 (IL-2Rβ) thus increasing the capacity of the T cells to respond to IL-2 stimulation. Whilst DR3 KO T cells did not show a defect in proliferation in response to CD3 stimulation alone, stimulation of antigen specific OTII DR3 KO T cells with antigen loaded APCs proliferated less and produced less IL-2 and IL-4 compared to their wild type (WT) counterparts[148, 159]. TL1A has been shown to increase the effector function of CD8+ T cells through the enhanced cytotoxic T cell mediated eradication of a TL1A expressing tumour[148].

DR3 is expressed on Tregs [136, 137] and has been implicated in their development. *In vitro* TL1A appears to have a negative effect on iTreg generation as demonstrated by a reduction of differentiation of naïve T cells in response to TGF-β[133, 174]. However TL1A was able to boost proliferation of Tregs *in vitro* when stimulated via CD3 and CD28[175]. It was found that Treg numbers increased in mice following administration of either soluble recombinant TL1A or the agonistic DR3 antibody 4C12 in an IL2 dependent manner[137, 176]. Also these *in vivo* generated Tregs had an attenuated suppressive *ex vivo* function which could be further overcome through exogenous TL1A in the cell culture media[177]. An expansion in the number of Tregs is also observed in mice where TL1A is constitutively expressed[174, 175].

DR3 signalling has also been implicated in development of Th17 cells. It has been shown that DR3 KO naïve CD4+ T cells have the capacity to differentiate into Th17 (as well as Th1 and Th2) cells using cytokines [159] however when stimuli from TL1A KO DCs are used, Th17 differentiation is reduced[131]. Exogenous TL1A has also been shown to attenuate the differentiation into Th17. In contrast once a naïve T cell has differentiated into a Th17 cell exogenous TL1A may act to reduce the levels of IL-17a secreted in the presence of TCR stimulation, however in the absence of TCR stimulation the Th17 phenotype is maintained[178]. Further, T cells taken from the spleen of mice which overexpress TL1A secrete increased levels of IL-17a compared to WT[174, 175]. It appears that the effect of TL1A on Th17 cell function and differentiation is a complex one however as TL1A KO mice show attenuated effects of Myelin oligodendrocyte glycoprotein induced experimental autoimmune

encephalomyelitis (MOG-EAE) (Th1 and Th17 dependent model, discussed further below); the lack of TL1A appears to be detrimental to overall function[131].

Recent work has highlighted a role for TL1A in the induction of Th9 cells. This is a relatively newly defined subset of Th cells that secrete IL-9 and express the master transcription factor PU.1[179]. As has been mentioned above it was found that addition of TL1A to iTreg differentiation conditions resulted in a reduction in FoxP3+ cells however there was a concurrent increase in a population of IL-9+ FoxP3- cells. Further the addition of TL1A to previously defined conditions for the *in vitro* differentiation to Th9[180] resulted in a 6 to 10 fold increase in the production of IL-9+ cells in an IL-2/STAT5 dependent manner. Whilst this highlights TL1A as a potential differentiation factor for Th9 cells its should be noted that, as in all other subsets, DR3 KO cells are still able to differentiate into Th9 cells albeit without the added costimulatory effect conferred by TL1A[133].

1.7.3. ILC costimulation

TL1A has also been shown to have a costimulatory effect on ILCs. Both transgenic expression and treatment of mice with TL1A has demonstrated the potential for production of ILC2 cytokines IL-5 and IL-13. Further purified ILC2s can be costimulated to produce these cytokines through TL1A acting synergistically with IL-25 and IL-33 in both the mouse[140, 141] and human[141]. TL1A can also costimulate IL-22 production by both mouse and human ILC3 acting synergistically with IL-23 and IL-1β[161, 181]. An effect of costimulation with TL1A was the upregulation of CD25 thus making the TL1A treated ILC3 more sensitive to IL-2 mediated proliferation[181]. In the case of the gut it was shown that a potential major source of the TL1A for this costimulation comes from CX3CR1+ mononuclear phagocytes. These cells express significantly higher levels of TL1A mRNA compared to other cells isolated from the intestinal lamina propria and were shown to promote cytokine production in a co-culture system dependent on DR3 expression on human ILC3[161].

1.7.4. Modulation of B cells

The role of DR3 signalling on B cells has not been investigated in any great depth to date however TL1A has been implicated in the inhibition of proliferation of B cells *in vitro*. It was found that human B cells which were cultured in the presence of TL1A showed reduced proliferation in response to anti-IgM and IL-2 stimulation. Further DR3 induction did not have any detrimental effect on survival[129]

1.7.5. Myeloid cell signalling

Whilst multiple cell types within the myeloid lineage express TL1A (Table 1-2), less express DR3 (Table 1-1). In monocyte-derived macrophages NOD2 signalling, in response to muramyl dipeptide, is enhanced via TL1A and IL1-β[142]. Further macrophage differentiation to foam cells and uptake of oxidised low-density lipoprotein is promoted in response to TL1A[182].

1.8. DR3/TL1A in murine models and human health and disease

The role of DR3/TL1A signalling has been studied in several animal models (Table 1-3) and has also been shown to play a role in the pathogenesis of several human diseases.

Pathology			
Model	Intervention	Phenotype	Reference
Experimental autoimmune encephalomyelitis	DR3 KO TL1A KO	Reduced severity and cellular infiltration	[159] [131]
Ovalbumin lung hypersensitivity	DR3 KO Antagonistic anti-TL1A (prophylactic and treatment)	Reduced severity and cellular infiltration	[133, 159] [138]
Papain induced allergic lung disease	DR3 KO	Reduced severity and cellular infiltration	[133, 140]
TNBS induced colitis	Antagonistic anti-TL1A, DR3-FC, anti DR3 Fab (prophylactic)	Reduced pathology and mortality	[174]
DSS induced colitis	DR3 KO Antagonistic anti-TL1A (prophylactic)	Reduced weight loss	[174] [183]
Antigen induced arthritis	DR3 KO	Reduced joint pathology	[184, 185]
Collagen induced arthritis	TL1A KO Antagonistic anti-TL1A (prophylactic)	Reduced pathology	[130] [185]
Host Defence			
Model	Intervention	Phenotype	Reference
Salmonella infection	DR3 KO	Reduced clearance of bacteria	[160]
MCMV and Vaccinia virus infection	DR3 KO	Increased viral titres, increased morbidity and mortality	[132]

Table 1-3 *– Effect of the DR3/TL1A pathway on murine models. Models where an effect was found through manipulation of the DR3/TL1A pathway either by genetic*

ablation or pharmaceutical intervention. Models are divided into effects on chronic pathology or host defence[145].

1.8.1. Crohn's Disease and Colitis

TL1A and DR3 play a prominent role in intestinal homeostasis and deregulation of their signalling results in gross changes in intestinal pathology and human disease.

Early genome wide association studies (GWAS) linked single nucleotide polymorphisms (SNP) in TL1A to an increased susceptibility to Crohn's disease (CD)[186, 187]. CD, a type of inflammatory bowel disease, is a genetically complex disease which is thought to arise from aberrant responses to intestinal flora. It is a disease which often presents between the ages of 20 and 30 and is characterised by chronic inflammation most often focused on the terminal ileum and the colon however it can be found on any portion of the gastrointestinal tract[188, 189].

The initial GWAS which found the association between CD and TL1A in a Japanese cohort, later confirmed it with 2 UK cohorts[186]. Further associations were found between CD and TL1A within a European cohort[190]. An inverse association of the risk verses protective allele was reported in an Ashkenazi Jewish cohort[187] however this has not been able to be replicated[191, 192].

SNPs in TL1A have been grouped into two risk haplotypes for the development of CD with high and low risk groups. Further, examination of biopsies from CD patients showed an increase in TL1A at the protein and mRNA level in inflamed tissue which correlated with an increase in IFN-γ[163] in one study and elevated levels of IL-17a in another[193]. Increased levels of TL1A in the serum of CD patients have also been found however did not correlate with levels of systemic IL-17a[193]. Signalling by other members of the TNFSF has also been linked to the development of CD with aberrant signalling by TNF a contributing factor. TNF blockade via a chimeric anti-TNF antibody has proved to be an effective treatment[188].

The role of TL1A and DR3 signalling has also been examined in several models of murine CD. Both TL1A and DR3 were found to be increased in $TNF^{\Delta ARE}$ mice and SAMP1/YitFc mice. These two models share many similarities with human CD and thus are accepted as good disease models[194, 195]. DR3 was found to be increased in an age dependent manner in the inflamed ileums of these mice and TL1A expression was also upregulated on CD11c+ DCs[196].

Using the dextran sodium sulphate (DSS) colitis model the role of TL1A and DR3 in CD has been further explored. As per other CD models an increase in expression of both TL1A and DR3 was observed in the colon of DSS treated mice. Upon restimulation of the CD4+ cells from the mesenteric lymph nodes and the lamina propria, exogenous TL1A boosted IL-17a and IFN-γ production. This effect of TL1A was synergistic with IL-23 and IL-12 thus implicating the role of TL1A in differentiation to Th17 or Th1 cells dependent upon other cytokines. Lastly it was shown that administration of a TL1A blocking antibody reduced the severity of colitis when administered with DSS and that if TL1A blockade therapy was delayed until establishment of the disease then recovery was improved[183]. Mice were also protected in the 2,4,6-trinitrobenzenesulfonic acid (TNBS) colitis model when treated prophylactically with TL1A/DR3 blocking reagents[174].

As stated previously CD is thought to occur due to aberrant response to commensal bacteria and it appears that TL1A also has a role. Recently TL1A was shown to be induced in response to various bacterial pathogens including gram positive and negative bacteria as well as anaerobes and aerobes. The induction of TL1A expression is dependent upon TLR 1, 2, 4, 6 and 9 signalling resulting in downstream activation of the p38 MAPK and NF-κB pathway and TL1A expression. As a result of the bacteria induced TL1A expression, differentiation into Th1 and Th17 cells is supported promoting CD pathology[162, 183].

1.8.2. Rheumatoid Arthritis

Rheumatoid Arthritis (RA) is a chronic inflammatory disease that is focused around the synovium resulting in the destruction of bone and cartilage. This autoimmune disease is characterised by the presence of chronically activated Th1 cells, increased serum rheumatoid factor (RF, anti-FC autoantibodies) and immune complex (IC) formation. Complement activation is induced by IC thus damaging the surrounding tissue and perpetuating the proinflammatory environment[197].

RA has multiple genetic factors and it was noted in one study that 78% of RA patients had a whole gene duplication event of DR3 compared with 39% in healthy controls where a second copy of DR3 was found 200kb upstream[198]. Subsequent GWAS however have failed to find an association between DR3 and RA.

Expression of TL1A on macrophages has been observed in RF+ RA patients at points of inflammation and IC containing serum from these patients was a strong inducer of TL1A on peripheral blood mononuclear cells (PBMCs) from a healthy

donor[164]. TL1A is detectable in the serum and synovial fluid of RA patients; the highest levels of which are found in RF+ patients although it is elevated above healthy control in RF- groups[199, 200]. Further high levels of serum TL1A have been found to correlate with increased RF and levels of anticyclic citrullinated peptide antibodies[201, 202]. An effective treatment for RA is adalimumab which is a blocking α-TNF mAb, one effect of which is to reduce the serum concentration of TL1A[201].

Given that TL1A in the serum decreases on treatment[201] and that serum and synovial TL1A levels correlate[200] these data suggests that serum TL1A has the potential to be a prognostic marker for RA.

The role of DR3 and TL1A has been studied in both antigen (methylated bovine serum albumin, mBSA) and CIA (AIA and CIA respectively) models. In AIA DR3 KO mice showed a reduction in the severity of disease (as measured by the arthritis index, AI) following the peak of the response compared to WT controls[185]. Further the decrease that was observed in cartilage damage was due to a reduction in the CXCL1 mediated recruitment of neutrophils to the joint[184]. AIA and CIA were further exacerbated by the administration of TL1A [185, 199]. TL1A blocking antibody (Tan2-2) reduced disease severity of both AIA and CIA. In both of these models the absence of TL1A did not affect macrophage accumulation at the joint however TL1A was found to promote osteoclastogenesis *in vitro[185]*. The generation of osteoclasts, which are responsible for bone disassembly and resorption, in response to TL1A may suggest a method by which TL1A acts in RA. Interestingly other TNFSF members have been implicated in this process[203].

Administration of TL1A in the CIA model highlighted a possible role for TL1A in B cell help. These mice had enlarged and more numerous GCs and increased anti-collagen antibody titres. Both in CIA and human CD anti-collagen antibodies are pathogenic[199, 204].

IC promotion of TL1A in RA suggests a feedback loop leading to exacerbation of disease. Overall this implicates the role of TL1A as an inflammatory agent in mouse models of RA and suggests TL1A may be a useful therapeutic target in humans despite the lack of a genetic link[185].

1.8.3. Asthma

The OVA induced lung hypersensitivity model is an established mouse model of human allergic asthma that is dependent upon Th2 and NKT cells. In this model mice are primed systemically with OVA and a suitable adjuvant and disease is induced with local administration of OVA to the lungs[205, 206]. NKT cells showed a high level of DR3 expression and costimulation *in vitro* with an anti-DR3 agonistic antibody (4C12) in the presence of OCH-glycosphingolipid (a derivative of α-Galactosyceramide) resulted in an increase in IL-13, and to a lesser extent IL-4, production. This was matched by an increase in the number of IL-13+ NKT cells[138].

To study the lack of DR3/TL1A signalling *in vivo* a TL1A antagonistic blocking antibody (L4G6), dominant negative DR3-CD2 mice[138] and DR3 KO mice[159] have been used. In all cases the severity of the disease was reduced as demonstrated by a decrease in cellular infiltrate, reduced mucus production and a reduction in IL-13 and IL-5[138, 159]. However comparable to the control, levels of IFN-γ and IL-10 were not affected[159]. Impressively, administration of L4G6 4 hours before examination of the lungs at the peak lung inflammation (day 3 post airway challenge) led to a ~50% reduction in eosinophil infiltrate highlighting the potential use of TL1A blockade as a therapy[138].

However DR3 costimulation with 4C12 also protected the mice from development of lung inflammation. Mice were given repeated injections of 4C12 prior to lung stimulation with OVA. 3 days post-stimulation a lack of eosinophilia in the lungs was observed along with an increase in the proportion of CD4+FOXP3+ Tregs of the CD4+ T cells (55% in the group treated with 4C12 compared to 22% in the group treated with an isotype control)[137]. This apparent paradox in the role of the DR3/TL1A signalling can be explained by the preferential binding of 4C12 to Tregs over conventional cells[136]. Further in mice which constitutively express TL1A (discussed in detail later) an increase in IL-13 is observed[174, 175].

As previous work has shown that mice which lack NKT cells are resistant to developing lung hypersensitivity in this model[206] either WT or dominant negative DR3 NKT cells were transferred into Jα18 KO mice (Lack NKT cells); only the mice which received WT NKT cells developed the disease. The mice which received cells lacking in functional DR3 showed a reduction in IL-13 and IL-5 in the lungs as well as decreased TL1A mRNA (suggests a positive feedback loop for the production of TL1A) and decreased eosinophil presence. In asthma IL-13 and IL-5 are major

drivers of eosinophilia and the lack of DR3/TL1A signalling appears to be required for the secretion of these cytokines by NK cells[138].

In this model Th2 cells appear to have a normal systemic function however trafficking to the lungs is decreased. In DR3 KO OVA challenged mice Th2 cytokines are reduced in the lungs however restimulation of splenic cells showed comparable levels of IL-5 and IL-13 between DR3 KO and WT. Further DR3 KO mice were able to produce normal levels of anti-OVA IgG1 and IgE. To assess the role of DR3 on trafficking DR3 KO or WT OT2 cells were differentiated into Th2 cells and adoptively transferred into mice that subsequently received an OVA challenge to the lung. There was a reduction in the number of these cells in the lungs however naïve DR3 KO OT2 cells were able to traffic as well as WT.

More recent work has examined the role of DR3 on ILC2 and Th9 cells in murine asthma models. The expansion of both Th9 and ILC2 cells was reduced in the absence of DR3 signalling in the OVA and papain induced murine lung models[133, 140, 141]. Further the transfer of OVA specific DR3 KO Th9 cells resulted in reduced pathology in the OVA asthma model demonstrating the role of these cells in development of pathology[133].

1.8.4. Myelin oligodendrocyte glycoprotein induced experimental autoimmune encephalomyelitis

MOG-EAE is an inducible murine model of human multiple sclerosis. The model is dependent upon Th1 and Th17 responses and is induced by immunisation on day 0 and 2 with MOG 35-55 peptide in CFA with pertussis toxin. Disease activity starts around day 12 and peaks by day 17. Progression of the model is based on a clinical scoring system from 0 to 5 where 1 is initial signs of creeping paralysis through to 4 which is near complete paralysis and 5 is death. Typically the model peaks with an average score of 3.5[131].

The MOG-EAE model has been used by two separate groups to investigate the role of DR3/TL1A signalling in an inflammatory autoimmune setting. One group used DR3 KO[159] mice whereas the other group used TL1A KO[131] mice however their findings are unsurprisingly similar. In both cases the onset of disease occurred at the same point as WT controls however the severity of the disease was greatly attenuated. Further this difference was found to be due to a decrease in inflammation in the spinal cord and was linked with a decrease in the number of T cells at the point of inflammation[131, 159]. This defect was not due to an increase in apoptosis[131]

and was not due to a proliferation defect as T cells taken from the draining lymph nodes proliferated normally when restimulated with MOG peptide *ex vivo*[159]. IL-17 and IFN-γ mRNA showed a decrease in the spinal cord however this was a result of the reduction in the number of T cells rather than a decrease in production[131, 159].

The results from these studies mimics the data from the asthma models and imply that TL1A is required for optimal costimulation of the T cells, the lack of which results in a decrease in the number of pathogenic cells able to migrate into the inflammatory site.

1.8.5. TL1A association with other diseases and immunological models

The roles of TL1A and DR3 have been associated with several other human disease and murine models. Below is a brief description of these findings.

A potential role for TL1A in host defence has been implicated by the association of TL1A via GWAS with leprosy in a Chinese population[207, 208] but not in Vietnamese[209], Indian or West African[210]. This also makes TL1A one of several genes which have been linked to both leprosy and CD[209].

TL1A is upregulated in the serum of patients with primary biliary cirrhosis with both early and late stage disease. However TL1A only decreases on treatment in the early stage group[211]. TL1A protein expression was also observed at multiple sites throughout the liver[211] and has been associated via GWAS for susceptibility[212].

Using a hen egg lysozyme transgenic ocular inflammation model the role of TL1A on Th9 cells was assessed. T cells that were differentiated to Th9 with the presence of TL1A promoted worse pathology as did intra-ocular injection of TL1A. Systemic injection of a TL1A blocking antibody (5G4.6) significantly decreased pathology[145].

As the pathology observed in the ileum of TL1A transgenic mice (see below[174, 175]) resembles that of a parasitic infection two groups studied the role of DR3 on the clearance of the parasite *Nippostrongylus brasiliensis*. One group showed a defect in clearance of the parasite[141] whereas the other group found no defect[140]. However the two groups used different protocols whereby the group which found a difference gave oral antibiotics for 5 days following infection. This suggests that if DR3 does indeed have an effect it may be host microbiome dependent or bacteria given with the worms during the infection may be responsible

for stimulation of TL1A/DR3 signalling in a manner which further promotes parasite clearance.

1.8.6. TL1A transgenic mice

As an increase in TL1A expression has been reported in the pathogenesis of CD (see above) several groups independently produced TL1A transgenic mice that constitutively expressed TL1A either on T cells or APCs. Two of the groups used the CD11c cassette to express TL1A [174, 175] with the third using a c-fms promoter[213] to target a greater proportion of the myeloid compartment. To target the T cells one group used the CD2 cassette[174] and a second group used the Lck CD2 promoter[213]. The phenotype observed in all of these mice showed similar effects the magnitude of which was mediated by relative TL1A expression with the CD2/TL1A mice being the most extreme[174].

Constitutive expression of TL1A resulted in an increase in the number of T cells in the spleen and the mesenteric lymph nodes[174, 175, 213]. Of these T cells there was an increase in the number of cells showing an activated phenotype defined by high CD69 and CD44 expression and low CD69L expression. The activated phenotype was lost when the CD2/TL1A mice were crossed to an OT2 mouse on a RAG KO background. The resultant TCR restriction prevents the activation of T cells by environmental antigens and the loss of the activated profile demonstrated the need for TCR signalling for TL1A to have a stimulatory effect. The phenotype of these mice was ablated when the CD2/TL1A mouse was crossed to a DR3 KO confirming that DR3 is the primary receptor for TL1A in mice[174].

As an increase in TL1A expression has been linked with intestinal pathology[163], the small and large intestines of the various mouse strains were examined. The colon appeared physiologically normal with only one group reporting an increase in histological fibrosis in the colonic mucosa and submucosa[213]. However the effect of TL1A on the small intestine was greatly pronounced with much of the phenotype confined to the ileum. The various mice developed age dependent goblet and panenth cell hyperplasia, lengthening of the small intestine, thickening of the intestinal muscularis, lengthening and blunting of the villi, increase in lymphocyte infiltrate into the laminar propria, lymphocyte and mast cell infiltrate into the muscularis and weight loss (due to intestinal issues) compared to littermate controls[174, 175, 213]. Whilst crossing these mice to a TCR restricted background reduced the intestinal phenotype the CD2/TL1AxOT2 mice displayed increased

intestinal pathology compared to littermate controls suggesting that TL1A has a non T cell target[174].

The cytokine expression profile of the small intestine and the mesenteric lymph nodes was examined. mRNAs for IL-13 and IL-17 were increased in the mesenteric lymph nodes however IL-4 and IFN-γ were not affected; in the ileum only IL-13 was significantly elevated[175]. Blocking IL-13, and not IL-17, using antibody therapy along with crossing to an IL-13 receptor KO resulted in loss of the phenotype indicating that the TL1A drives intestinal pathology in an IL-13 dependent manner [140, 174, 177]. To rule out potential IL-13 sources the CD2/TL1A transgenic mice were crossed to the Jα18 KO and CD1d KO mouse strains to delete iNKTs and all NKTs respectively[140]. Neither of these crosses nor crossing to a TCR transgenic[174] resulted in a loss of pathology thus ruling these out as sources. Further antibiotic treatment, as microbiota can influence gut cytokine profiles[214], increased the pathology[140]. As a result it was concluded that the IL-13 mediated phenotype in these mice was most likely dependent on stimulation of ILC2s by TL1A.

Chapter 2. Aims of the project

To date TL1A has been demonstrated to be a potent costimulator of T cells via DR3 in both normal and inflammatory environments. It has been shown to be involved in pathogenic human disease and presents a potential therapeutic target. However much still remains to be elucidated regarding the function of this ligand and receptor pair. To this end the following potential roles of TL1A are being investigated and reported herein.

- Is there a difference in function between the membrane bound and the cleaved form of TL1A?
- Are there functional differences as a result of chronic TL1A stimulation of different cell types and what is the interplay between them?
- What is the role of TL1A and DR3 in the help provided to B cells via CD4+ T cells?
- Do TL1A and DR3 play a role in the development of chronic autoimmunity?

Chapter 3. Methods

The following chapter contains all the methods used within this thesis. As the project was split between two different institutions some sections have two different methods. Where this has occurred the experiments to which they refer have been indicated.

3.1. Reagents

3.1.1. Cell culture media

The composition of all cell culture media is given below. All Media and constituents was made by Life technologies except MSX (Sigma) and FCS (Atlanta biologicals).

Media	Components	Cells
Complete DMEM	DMEM, 10%FCS, 2%GP, 1%P/S,	293T, Phenoix, NIH3T3
Complete RPMI	RPMI 1640, 10%FCS, 2%GP, 1%P/S, 52µM 2-ME	T cells, BMDC
Complete GMEMs	GMEMs, 10%dFCS, 1%P/S, 25µM MSX	Cho-K1
Bone Marrow Media	DMEM, 20% FCS, 50ng/ml IL-3, 50ng/ml IL-6, 50ng/ml mSCF, 2%GP	Bone marrow cells for transduction

Table 3-1 *– Cell culture media. Table gives the composition of the different cell culture media and the type of cells they are used for. All percentages are v/v.*

3.1.2. Buffers

All buffers were prepared in distilled water. All chemicals were purchased from sigma apart from the kappa extraction buffer (Kapa Biosystems).

Name	Reagents
Bicarbonate buffer	15mM Na_2CO_3, 35mM $NaHCO_3$
Citrate buffer	100mM $C_6H_8O_7$
DNA Isolation buffer	50mM Tris pH8.9, 12.5mM $MgCl_2$, 0.5% (*v/v*) Tween-20
EasySep buffer	PBS, 2% (*v/v*) FCS, 1mM EDTA
Kapa extraction buffer	1x Kapa Express extract buffer, 1U/50µl kapa extract enzyme
MACS buffer	PBS pH7.2, 0.5% (*w/v*) BSA, 2mM EDTA
PBS	120mM NaCl, 24mM Na_2HPO_4, 9mM KH_2PO_4
Phosphate Buffer	200mM Na_2HPO_4
PSB	160mM Tris, 6.4M urea, 0.08% *(w/v)* Bromophenol Blue
Red cell lysis buffer	92mM NH_4CL_2, 1mM $KHCO_3$
TBE	90mM Tris, 90mM Boric acid, 2mM EDTA
TE	0.1mM EDTA, 10mM Tris
Stock Tris	200mM Tris, 1M NaCl, 10mM EDTA

Table 3-2 *– Non-commercial buffers. All buffers which were made in house. RO water was used as the solvent for all of these buffers.*

3.1.3. Antibodies

Primary antibodies, which were used for a range of applications, are listed below. All targets are mouse unless otherwise stated.

Target	Clone/Reference	Application	Manufacturer	Final Dilution
B220	RA3-6B2	Immunochemistry	BD Bioscience	1/200
Bcl2 (Human)	Bcl2/100	Flow cytometry	eBioscience	1/100
C3	CL7503F	Immunofluorescence	Cedarlane	1/10
CD4	GK1.5	Flow cytometry	eBioscience/Tonbo bioscience	1/200-1/500
Rat CD4	OX68	In vitro, Protein purification	University of Southampton	5µg/ml
CD8	53-6.7	Flow cytometry	eBioscience/Tonbo bioscience	1/200-1/500
CD11b	M1/70	Flow cytometry	eBioscience	1/200
CD11c	N418	Flow cytometry	Serotec eBioscience	1/10 1/200-1/500
CD16/32	2.4G2	Flow cytometry	University of Southampton	25µg/ml
CD19	6D5	Flow cytometry	Serotec	1/10
CD19	1D3	Flow cytometry	eBioscience/Tonbo bioscience	1/200-1/500
CD25	PC61.5	Flow cytometry	eBioscience	1/200
CD28	37-51	In vitro	University of Southampton	5-10µg/ml
CD3	1452C11	In vitro	University of Southampton	0.1-10µg/ml
CD3	1452C11	Flow cytometry	eBioscience	1/100
CD40	1c10	In Vitro	eBioscience	1ng/ml
CD40L	MR1	Flow cytometry	eBioscience	1/200
CD44	IM7	Flow cytometry	eBioscience	1/100-1/500
CD45	30-F11	Flow cytometry	eBioscience	1/200-1/500
CD45.1	A20	Flow cytometry	eBioscience	1/200
CD45.2	104	Flow cytometry	eBioscience	1/200
CD62L	MEL-14	Flow cytometry	eBioscience	1/100-1/500
CD138	281-2	Flow cytometry	BD Bioscience	1/500
CXCR5	2G8	Flow cytometry	BD Bioscience	1/200
CXCR5	SPRCL5	Flow cytometry	eBioscience	1/200
F4/80	A3-1	Flow cytometry	Serotec	1/10
FoxP3	FJK-16s	Flow cytometry	eBioscience	1/100
GC B cells	PNA	Flow cytometry, Immunochemistry	Vector Laboratories	1/200
GL-7	GL-7	Flow cytometry	eBioscience	1/200
ICOS	7E.17G9	Flow cytometry	eBioscience	1/2000
IFN-γ	XMG1.2	Flow cytometry	eBioscience	1/100
IFN-γ	HB170	ELISA	University of Southampton	4µg/ml
IgA	1040-2	Flow cytometry	Southern Biotech	1/500
IgA	1040-05	ELISA	Southern Biotech	1/4000-1/12000
IgD	11-26c	Flow cytometry	eBioscience	1/100
IgG	1037-01	ELISA	Southern Biotech	0.2µg/ml
IgG	Poly4053	Immunofluorescence	Biolegend	1/25
IgG1	1070-05	ELISA	Southern Biotech	1/4000-1/15000
IgG2b	1090-05	ELISA	Southern Biotech	1/4000-1/15000
IgG2c	1079-05	ELISA	Southern Biotech	1/4000-1/15000
IgM	eb121-15F9	Flow cytometry	eBioscience	1/200-1/500
IgM	1020-05	ELISA	Southern Biotech	1/4000-1/15000

Kb	AF6-88.5.5.3	Flow cytometry	eBioscience	1/200-1/500
Kd	SF1-1.1.1	Flow cytometry	eBioscience	1/200-1/500
Lag3	C9B7W	Flow cytometry	eBioscience	1/200
Ly6C	AL-21	Flow cytometry	BD Bioscience	1/200
Ly6G	1A8	Flow cytometry	BD Bioscience	1/200
NK1.1	PK136	Flow cytometry	eBioscience	1/200
PD1	J43	Flow cytometry	eBioscience	1/200
TL1A	Tan2-2	Flow cytometry, Luminex	University of Southampton	Flow Cytometery 10µg/ml Luminex 2µg/ml
TL1A	5G4.6	Luminex	NIH/NIAMS/BioXcell	8.5µg/5x10^5 beads

Table 3-3 *– Primary Antibodies. All primary antibodies used for the range of applications described. For antibodies from Southern Biotech the second column refers to the catalogue number as many of these are polyclonal.*

The following secondary antibodies were used when primary antibodies were not appropriately labelled for detection.

Target/reagent	Conjugate	Application	Manufacturer	Final Dilution
Streptavidin	APC, FITC, PE, PE-Cy7	Flow cytometry	eBioscience	1/100
Streptavidin	AF488	Immunochemistry	Molecular Probes	1/500
Streptavidin	HRP	ELISA	Jackson	1/1000
Rat IgG	aAF568	Immunochemistry	Molecular probes	1/1000

Table 3-4 *– Secondary antibodies and reagents.*

3.1.4. Oligonucleotides

All oligonucleotides used for PCR and sequencing were manufactured by Life Technologies or integrated DNA technologies.

Name	Sequence	Description
TL1A exon 1 F	TTC GGA GAA GGA GTC CCA GTG GAA G	Forward primer mouse TL1A exon 1
TL1A exon 3 F	CAC AGC AAG TTA TTA AGA AAC AAA CCC CAG CAC CA	Forward primer mouse TL1A exon 3
TL1A exon 4 R	CCC GTT CTT GGT GAA GGC CAT C	Reverse primer in mouse TL1A exon 4
F EcoR1 Afe1 Kozak HA TL1A	ATA TGA ATT CAG CGC TGC CAC CAT GTA CCC ATA CGA TGT TCC AGA TTA CGC TAT GGC AGA GGA GCT GGG GTT GGG	Forward primer for cloning mouse TL1A into CD2 vector
R EcoR1 Kpn1 STOP TL1A	TAT AGA ATT CGG TAC CTT ATA GCA AGA AAG CTC CAA	Reverse primer for cloning mouse TL1A into CD2 vector
Kpn1 TL1A	ATG CGG TAC CAT GGC AGA GGA GCT GGG GTT	Forward primer for cloning TL1A into peYFP-c1
BamH1 TL1A	TAT AGG ATC CTT CTA GAC AGA AAG CTC CAA	Reverse primer for cloning TL1A into peYFP-c1
TL1A forward sewing	CGG GTC CCC GGA GGC AAG CCG AGA GCA CAC CT	Forward sewing primer for TL1AΔ69-93
TL1A reverse sewing	TCT CGG CTT GCC TCC GGG GAC CCG GAG CTG GC	Reverse sewing primer for TL1AΔ69-93

F Not1 Bgl2 TL1A	ATA TGC GGC CGC AGA TCT GCC ACC ATG GCA GAG GAG CTG GGG TT	Forward primer for cloning TL1A into pmp71 and pMIG-R1
R Sal1 Xho1 TL1A	ATA TGT CGA CCT CGA GTT ATA GCA AGA AAG CTC CAA AGA AAG TTT TAT CTT	Reverse primer for cloning TL1A into pmp71 and pMIG-R1
DR3 F8	TCT CCT GTC ATC TCA CCT TGC	DR3 KO genotyping primer
DR3 4F	AGA AGG AGA AAG TCA GTA GGA CCG	DR3 KO genotyping primer
DR3 2R	GAA AGG ATG AAA CTT GCC CTG TTG G	DR3 KO genotyping primer
TL1A KO 1	GTA AGT TGG CTT AGC AGA AGC TAG	TL1A KO genotyping primer
TL1A KO 2	TGA TGT GGC ATG CAC ACA TGT AAC	TL1A KO genotyping primer
TL1A KO 3	TGC TAA AGC GCA TGC TCC AGA CTG	TL1A KO genotyping primer
Ires Rev	CCT CAC ATT GCC AA AGA CG	Reverse sequencing primer for constructs containing a IRES
Seq TL1A F1	CAG GAG CAA AGC CTG CCT GG	Forward TL1A sequencing primer 1
Seq TL1A F2	CAC ATT CCG AGG GAC CAC AT	Forward TL1A sequencing primer 2
Seq TL1A R1	GTT CCC AGT GTA GAG CAG AG	Reverse TL1A sequencing primer 1
Cre F	GCT AAG GAT GAC TCT GGT CA	CD4 cre forward primer
Cre R	CTA ATC GCC ATC TTC CAG CA	CD4 cre reverse primer
Beta globin F	CCA ATC TGC TCA CAC AGG ATA GAG AG	Beta globin control genotyping primer
Beta globin R	CCT TGA GGC TGT CCA AGT GAT TCA GGC	Beta globin control genotyping primer
MMP9 KO 1	CTG AAT GAA CTG CAG GAC GA	MMP9 KO genotyping primer
MMP9 KO 2	ATA CTT TCT CGG CAG GAG CA	MMP9 KO genotyping primer
MMP9 KO 3	GTG GGA CCA TCA TAA CAT CAC A	MMP9 KO genotyping primer
MMP9 KO 4	CTC GCG GCA AGT CTT CAG AGT A	MMP9 KO genotyping primer
3431-31	CAG CCT GAA AGC CAC TAT TAC CTG G	DR3 flox forward primer
3431-32	GTG GTG CAC ACT ACA TAC TGG AAG C	DR3 flox reverse primer

Table 3-5 *– Oligonucleotides. Table contains a list of all the primers used for PCR within this project. The primers used for genotyping are indicated.*

3.1.5. Molecular enzymes

All enzymes were manufactured by Promega.

Restriction enzyme	Activity	Target sequence
Not1	Restriction endonuclease	GCGGCCGC
Sal1	Restriction endonuclease	GTCGAC
Afe1	Restriction endonuclease	AGCGCT
EcoR1	Restriction endonuclease	GAATTC
BamH1	Restriction endonuclease	GGATCC
Bgl2	Restriction endonuclease	AGATCT
Xho1	Restriction endonuclease	CTCGAG
Kpn1	Restriction endonuclease	GGTACC
TSAP	DNA 5' phosphatase	
T4	DNA ligase	

Table 3-6 *– Molecular biology enzymes. A list of all the enzymes used for molecular biology for the construction of novel plasmids.*

3.2. Molecular biology

3.2.1. Polymerase chain reaction

The polymerase chain reaction (PCR) was used for the amplification of specific DNA sequences for cloning or analytical purposes. Reactions were carried out with either Taq (Promega) or Pfu (Promega) for analytical or cloning purposes respectively as per manufacturer's instructions in provided buffers. The exact program of amplification was dependent upon the oligonucleotide primers used and the target. Below is a general programme for PCR where X is ~5°C lower than the lowest melting temperature of primer set (calculated using OligoEvaluator, Sigma-Aldrich) and Y is the number of cycles (Typically 25-40 dependent upon the abundance of the target sequence). Both X and Y were optimised for each reaction experimentally.

94°C	5 min	
94°C	1 min	
X°C	1 min	Y cycles total
72°C	2 min	
72°C	10 min	
4°C	∞	

3.2.2. Agarose gel electrophoresis

Agarose (Life Technologies) was heated in a microwave in an appropriate volume of buffer TBE until dissolved. Ethidium bromide (Fluka) or GreenGlo (Denvile Scientific) was added to the dissolved agarose to a final concentration of $5x10^{-5}$%*(v/v)* and the gel cast in an appropriate size gel tank. The table shows the concentration of agarose used for gels dependent upon the resolution required.

Size of DNA products to resolve (Kb)	Agarose %*(w/v)*
Only one band expected	1
>5	0.8
1-5	1
0.5-1	1.5
<0.5	2

Table 3-7 *– Agarose percentages. Table gives the present of agarose used to enable resolution of the indicated band of DNA.*

Samples were mixed with loading dye (Fermantas) if required and loaded into the gel along with a suitable ladder (100bp or 1Kb O'gene ruler, Fermantas). Gels were run at 80-120V until the low molecular weight marker had migrated sufficiently down the gel. Gels were imaged using a UV transluminator (Gel doc, Bio-rad).

3.2.3. DNA cleanup

DNA was required to be cleaned up following extraction from a gel or enzymatic reaction. Purification of DNA was carried out using a Quiax II gel purification kit (Qiagen) using spin columns as per manufacturer's instructions with the final product re-suspended in sterile distilled water.

3.2.4. Sewing PCR

A sewing PCR was performed to join two PCR products. The protocol was the same as for a standard PCR however regions were incorporated into the primers such that the two individual products contained complementary sequences at the ends that were to be joined. The two separate PCR products were subsequently used as templates and combined with suitable 3' and 5' primers to amplify the whole joined product.

3.2.5. Topo cloning

PCR products were cloned into TOPO blunt (Life Technologies) as per the manufacturer's protocol.

3.2.6. Restriction Digestion

DNA was digested using appropriate restriction enzymes in the recommended buffer. The reaction mix contained target DNA, restriction enzyme (5U/restriction site/µg of target DNA, Promega), reaction buffer (final dilution to 1x, Promega) and sterile distilled water to a suitable dilution to ensure the restriction enzyme did not exceed 10% of the total volume. The reaction was mixed and incubated at 37°C for 1-2 hours. Successful digestion was confirmed by agarose gel electrophoresis and the resulting DNA was either purified from the gel or from the reaction mix directly.

3.2.7. Dephosphorylation

For ligation reactions where the vector was cut with only one restriction enzyme the vector was dephosphorylated to prevent re-ligation of the vector; Thermostable shrimp alkaline phosphatase (TSAP, Promega) was used for this purpose as per manufacturer's instructions.

3.2.8. T4 ligase

Ligation of inserts and vector was carried out using T4 ligase (Promega) as per the manufacturer's protocol using 100ng of vector with a 3:1 insert:vector molar ratio. Reaction was carried out for 3 hours at 16°C.

3.2.9. Bacterial transformation

One shot Top10 chemically competent cells (Invitrogen) were transformed with 1µl of ligated plasmid as per the manufacturer's protocol. At the same time a separate vile of bacteria was transformed with non-ligated plasmid as a control. 50-100µl of transformed bacteria were plated on a LB-Agar plate containing an appropriate antibiotic. A ligation was considered a success if the ligated plate had significantly more colonies than the non-ligated plasmid control.

3.2.10. Plasmid purification – mini and maxi prep

A single colony was picked and grown in 5ml (mini prep) or 200ml (maxi prep) of LB medium containing an appropriate antibiotic overnight. Bacterial cultures were centrifuged and plasmid DNA was purified using either a mini or maxi prep kit (Qiagen) as per the manufacturer's instructions.

3.2.11. Sequencing

For sequencing of constructs dideoxynucleotide sequencing using Big-Dye reaction mix (Life technologies) was carried out. Reactions contained 2µl 5x sequencing buffer, 2µl Big-Dye reaction mix, 1µl of an appropriate primer (Table 3-5), 0.5µg of target DNA and sterile distilled water to a final volume of 10µl. Reactions were carried out in a thermocycler on a program of 25 repeats of 94°C for 10 seconds, 50°C for 5 seconds and 60°C for 4 minutes. Following completion of the reaction samples were precipitated. 2µl of 3M NaAc and 48µl of 100% *(v/v)* ETOH were added to the sequencing reaction which was centrifuged at maximum speed in pre cooled 4°C centrifuge for 30 minutes. The supernatant was removed and replaced with 180µl of 70% *(v/v)* ETOH and the sample centrifuged for a further 10 minutes. The supernatant was removed and the sample was air dried at 37°C before 10µl of formamide was added. Samples were denatured at 95°C for 5 minutes and loaded into an automated sequencer (Applied Biosystems 3130 XL genetic analyser).

3.3. Production of key plasmids

Several key plasmids were produced for this project. The names of primers mentioned below refer to the table.

3.3.1. TL1A and TL1A Δ 69-93 peYFP-C1

For production of TL1A pEYFP-C1 TL1A was PCR amplified from TL1A pCDNA3 (Kind gift from Dr. J Mongkolsapaya, MRC, Oxford, UK) using Kpn1 TL1A and BamH1 TL1A and cloned into topo blunt. To produce TL1A Δ 69-93 pEYFP-C1 TL1A was initially amplified as two fragments from TL1A pCDNA3 using Kpn1 TL1A and TL1A reverse sewing and BamH1 TL1A and TL1A forward sewing. 1µl of each of these reactions after clean up was subsequently used in a sewing PCR with Kpn1 TL1A and BamH1 TL1A and cloned into topo blunt to yield the plasmid TL1A Δ 69-93 topo blunt. Both plasmids were sequenced at this stage. pEYFP-c1 and the two topo blunt plasmids were digested with Kpn1 and BamH1 and ligated together to yield TL1A pEYFP-C1 and TL1A Δ 69-93 pEYFP-C1.

3.3.2. TL1A and TL1A Δ 69-93 pIMP71

TL1A and TL1A Δ 69-93 were amplified from TL1A pEYFP-C1 and TL1A Δ 69-93 pEYFP-C1 using primers F Not1 Bgl2 TL1A and R Sal1 Xho1 TL1A and cloned into Topo Blunt. The vector and the inserts were cut with Not1 and Sal1 and ligated.

3.3.3. CD2 TL1A Δ 69-93

TL1A Δ 69-93 was amplified from TL1A pEYFP-C1 and TL1A Δ 69-93 pEYFP-C1 using primers F EcoR1 Afe1 Kozak HA TL1A and R EcoR1 Kpn1 STOP TL1A and cloned into topo blunt. Both TL1A Δ 69-93 topo and the CD2 vector were cut with EcoR1 and the cut vector dephosphorylated with TSAP. After ligation the plasmid was transformed into top10 cells, purified and vectors with the correct direction were identified by digestion with Kpn1.

3.4. Production of cell lines

3.4.1. Cell culture

Several different cell lines were used to enable the study of different forms of TL1A along with the binding kinetics of antibodies. Cells were regularly passaged to

prevent the cells becoming confluent. Suspension cells were passaged by dilution with a regular change of tissue culture flasks to prevent selection for adherent cells.

Adherent cells were passaged by removing media and washing in PBS to remove any remaining media. Cells were incubated with Trypsin EDTA (Life Technologies) for 3-5 minutes until cells had detached from the tissue culture plastic. Cells were centrifuged at 800xg for 5 minutes, re-suspended and diluted into a new tissue culture flask.

3.4.2. Cell counting

When viability was not required cells were counted using a coulter counter (Beckman coulter). 5-20µl of cells were added to a counting vile and diluted in 10ml of coulter buffer. If a primary sample was being counted then 5 drops of zappoglobin II lytic reagent (Beckman coulter) was added to lyse red blood cells. The diluted cells were subsequently loaded into the coulter counter and a cell count made. To insure accurate readings cells were diluted to maintain a count of no greater than $5x10^6$/ml.

If a viable cell count was required 15µl of cells was mixed with 15µl of Trypan blue (Sigma) and pipetted under a cover slip on a haemocytometer. Cells in two of the large counting squares were counted. To calculate the cell concentration the average count per square was multiplied by 2 (dilution factor) then by $1x10^4$ to give cells/ml in the original solution. If more than 100 cells were counted per counting square the cells were diluted before counting again to ensure accuracy.

3.4.3. Transfection

Cells were transfected with effectine (Qiagen) as per the manufacturer's protocol.

3.4.4. Retroviral transduction

$0.4x10^5$ Phoenix Eco cells (Retroviral packaging cell line) were plated in a well of a 6 well plate and left for three days to grow until they reached ~60% confluency. The media was removed and the cells were transfected with 0.4ug of pCL-Eco and 1ug of the retroviral plasmid containing the protein to be expressed per well with effectine (Quiagen) as per the manufacturer's protocol. After 23 hours, before the virus was secreted, the media on the phoenix eco cells was changed. 48 hours post transduction the phoenix cell media, which should contain retrovirus secreted by the cells, was removed. As all the plasmids used contained GFP successful transfection

of the phoenix cells was confirmed by expression of GFP under an appropriate fluorescence microscope.

The retroviral containing media was filtered through a 0.22µm filter and polybrene (Sigma) added to 4µg/ml final concentration. As a positive control of transduction NIH3T3 cells were plated 24 hours previous to retroviral containing media collection at $3x10^5$ cells in a well of a 6 well plate. If the target cells to be transduced for experiments were adherent then they were plated at the same time as the NIH3T3 cells, if they were suspension cells they were plated on the day of transduction.

To increase the efficiency of transduction the target cells were spin transduced. The media on the target cells was removed and replaced with the retroviral containing media. The plates were subsequently centrifuged at 800xg for 90minutes at 32°C after which they were placed back in the incubator. 24 hours post spin transduction the media was refreshed and 48 hours post transduction the cells were analysed for expression of the protein of interest by flow cytometry.

3.5. Production of soluble TL1A

Soluble TL1A (sTL1A) was produced in house from cells previously transfected by Dr J. Baker with a construct produced by Dr T. Sleboida (pEE14-sTL1A-CD4) containing the extracellular domain of TL1A tagged with domains 3 and 4 of rat CD4[148].

3.5.1. CHOK-1 cell culture

Cho-K1-sTL1A-CD4 cells were grown in GMEMs supplemented with 25µM methionine sulfoximine (MSX, Sigma). Once the cells had bulked up they were transferred into 10 layer flasks after which the media was changed every 10 to 14 days without passage and the supernatant stored at -20˚C.

3.5.2. Purification

Collected media from Cho-K1-TL1A cells was centrifuged at 6000xg for 15 minutes and filtered to remove cell debris. An OX68 conjugated Sepharose 4B column was washed with 10 column volumes 1 in 7 tris and the supernatant added and left to run at 4°C (approximately 0.5-0.75ml/min). The column was washed as before and eluted with 0.1M Glycine.HCl. Once the flow through attained a pH of <6 30ml of run through was collected into a container containing 3ml 2M Tris.HCl (pH 8) to neutralise. The collected supernatant was concentrated by ultra-filtration, dialysed

against PBS and quantified by absorbance at 280nm. The extinction coefficient of sTL1A at 280nm is 0.95 abs/mg/cm.

3.5.3. SDS PAGE

SDS-PAGE was used to examine the efficiency of purification. 20µg of sTL1A was diluted into 30µl 2xPSB +/- 1µl 1M DTT and heated at 95˚C for 5 minutes. The samples were loaded onto a 4-12% bis-tris gel (Life Technologies) and run at 100-140V against a ladder of known molecular weight. The gel was removed and fixed (25% Isopropanol/ 10% Acetic acid) for 10minutes, washed and stained for 1 hour with coomassie blue (0.06% coomassie blue/ 5% Acetic acid) and de-stained (10% acetic acid) overnight. Gels were subsequently imaged using a gel doc (bio-rad).

3.5.4. Endotoxin Testing

Contamination of protein preparations with endotoxin was tested using an Endosafe PTS (Charles River). This is a portable automated system which runs a chromogenic limulus amebocyte lysate. To determine endotoxin contamination in Protein preparations samples were diluted 1/50 in endotoxin free water and loaded into a PTS cartridge (Charles River) and placed in the Endosafe PTS. After an automated incubation time the Endosafe PTS gives the contamination with endotoxin as EU/ml of solution where 1EU is equal to 100pg of endotoxin. Protein preparations were only used if the final level of endotoxin was less than 10EU/mg of protein.

3.6. Flow cytometry

3.6.1. Biotinylation

In house produced antibodies that were required for flow cytometry (or other assays) to be biotinylated were covalently coupled to biotin using EZ-link sulfo-NHS-biotin (Thermo scientific) as per manufacturer's instructions. For less than 0.5mg of protein a 50 fold molar excess of biotin was used and for greater than 0.5mg a 20 fold molar excess.

3.6.2. Cell staining

100µl Prepared cells were aliquot into 5ml FACS tubes (BD) after re-suspension in 0.2% BSA *(w/v)* in PBS. Depending upon the size of the population of interest within prepared cells the number of cells aliquoted was adjusted. If the target cells were rich in FC receptors these were blocked by pre-incubation of the samples with 2.4G2

at 25µg/ml. Cells were stained with the primary antibody at the indicated concentration for 30 minutes at 4°C or room temperature and washed by dilution to 5ml in 0.2% BSA *(w/v)* in PBS and centrifugation at 800xg for 5 min. If the primary antibody was not conjugated to a fluorochrome then a secondary antibody or fluorochrome conjugated secondary was added and incubated as before.

3.6.3. Live/Dead staining

To enable distinction of live from dead cells a viable stain may be used. Cells were washed and re-suspended in HBSS (life technologies) containing 1/1000 Ghost Dye (Tonbo Biosciences). Primary surface staining antibodies were added at the same time in HBSS. Samples were incubated and washed as before.

3.6.4. Staining mouse blood

For staining of mouse blood 25-50µl of blood was diluted in 50µl of 0.2% BSA *(w/v)* in PBS containing the appropriate antibodies. Samples were incubated as above after which samples were lysed with 3ml of red cell lysis buffer, centrifuged at 800xg for 5 min then washed as above. Any subsequent staining was carried out as for other types of cells.

3.6.5. Intracellular staining

Following surface staining cells were washed and fixed using the FoxP3 fix perm buffer (ebioscience) for 20 minutes to 18 hours at 4°C. Cells were washed in perm buffer (ebioscience) and stained with required intracellular antibodies in perm buffer. Cells were washed twice with perm buffer and analysed using a flow cytometer. If the cells expressed GFP the intensity was greatly reduced by fixation of the cells.

3.6.6. Flow based counting of cells

For some experiments absolute numbers of cells were required. In this case $1x10^4$ CountBright absolute counting beads (Life technologies) were added to the sample at the start. When analysis was carried out at least $1x10^3$ beads were collected and the number of cells back calculated.

3.6.7. Flow cytometry analysis

Samples for flow cytometry analysis were run on a Canto II flow cytometer (BD) or a FACS Verse (BD) using an appropriate gating strategy and analysed using either BD FACSDiva, FloJo or FCS express.

3.7. In Vitro Assays

3.7.1. Splenocyte preparation

Spleens were taken from euthanized mice *perimortum* and placed in ice cold PBS. Tissue was subsequently homogenised by mashing through a 100µm cell strainer (Fisher). The homogenate was re-suspended in 25ml PBS and centrifuged at 800xg for 5 minutes. The cell pellet was re-suspended in 5ml red blood cell lysis buffer and immediately centrifuged as before. The cell pellet was re-suspended in 25ml PBS and any detritus removed then centrifuged as before. The sample was counted and temporarily stored at 4°C for subsequent use.

3.7.2. Bone marrow preparation

Bone marrow was prepared from the Femur and Tibia from the hind limbs of mice. The bones were dissected whole from mice, briefly immersed in 70% *(v/v)* ETOH, placed in sterile PBS and stored at 4°C until processing. The bones were cut at each end and the bone marrow flushed from the bones with complete media using a 25 gauge needle. The bone marrow was collected in a 50ml universal tube after passing through a 100µm cell strainer. The sample was re-suspended in 5ml red blood cell lysis buffer and immediately centrifuged as before. The cell pellet was re-suspended in 25ml PBS centrifuged as before. The sample was counted and temporarily stored at 4°C for subsequent use.

3.7.3. Kidney cell extraction

Post perfusion of the mouse with PBS the kidney was excised and placed into ice cold PBS until processing. The kidney was placed into a 70µm filter (Fisher) in 10ml of RPMI supplemented with 20mM Hepes (Life Technologies), 2.25 mg liberase TL (Roche) and 1mg DNAse I (Roche). The kidney was minced into 1mm long pieces and incubated at 37°C for 20 minutes after which the remaining tissue was pressed through the filter and the filtrate, now containing the cells, collected. 20ml of complete RPMI was added to the filtrate and the samples subsequently processed for down stream analysis.

3.7.4. BMDC production

Bone marrow was re-suspended at $2x10^5$ cells/ml in complete RPMI supplemented with 20ng/ml GM-CSF (PeproTech) to a maximum volume of 60ml and plated in a tissue culture T175 flask. At day 4 media was topped up with half the original volume of complete RPMI supplemented with 20ng/ml GM-CSF. On day 7-8 the cells were harvested by gently washing the surface of the flask and taking the supernatant. Successful production of Bone marrow derived DCs (BMDCs) was confirmed by expression of CD11c by flow cytometry.

3.7.5. BMDC assay for sTL1A production

$0.5x10^6$ BMDC were washed and plated in 1 ml in a 48 well plate with 100ng LPS (Enzo) and 20ng/ml GM-CSF. Cells and supernatant were collected up to 72 hours post plating.

3.7.6. Magnetic separation

T and B cells were negatively selected using MACS (Miltenyi Biotec) or easysep Kits (Stem cell technologies) as per manufacturer's instructions. Following T cell selection purity of selected population was assessed by flow cytometry.

3.7.7. T cell enrichment

T cells were enriched using mouse CD4 or CD8 T cell negative selection kit (Cedarlane). This kit enriched the required population however some APCs remained. T cell enrichment was carried out as per manufacturer's instructions.

3.7.8. T cell activation

$0.2x10^6$ purified T cells were activated with plate bound αCD3 (coated in bicarbonate buffer or PBS overnight at 4°C, 5μg/ml) and soluble αCD28 (10μg/ml) in T cell media in one well of a 48 well plate. Plates were incubated at 37°C and samples were taken at regular intervals for assays.

3.7.9. MMP inhibition assay

GM6001 (Millipore) was used to inhibit MMP function. It was added to the media at a concentration and for a time detailed in the individual experiment.

3.7.10. siRNA mediated knockdowns

For knock down of Adam17 a pool of 4 siRNA (OnTarget plus smart pool, Darmacon) or an appropriate non-targeting control pool was used. 8 days post culture of BMDC (as described above) $2.5x10^5$ cells were transfected with 60pmol of siRNA using the mouse DC nucleofector kit (Amaxa) as per manufacturer's instructions. After 8-10 hours media was replaced on the cells with complete RPMI plus 20ng/ml GM-CSF (PeproTech) and 100ng/ml LPS (Enzo). Cells were harvested for mRNA and supernatant collected 24 hours later.

3.7.11. B cell IgA class switching

B cells were purified from the spleens of naïve mice and $1x10^5$ cells plated in 1ml in a 48 well plate with a selection of anti CD40 (1ng/ml), IL-4 (2.5ng/ml), TGFβ (1ng/ml) and TL1A (100ng/ml) for 3 days. Class switching to IgA was assessed by flow cytometry.

3.7.12. Proliferation assay

Splenocytes were enriched for CD4 or CD8 T cells and $2x10^5$ cells were plated per well in a 96 well U bottomed plate with either stimulatory antibodies or target cells in 200µl. After the indicated period of time 100µl of the cell supernatant was removed for quantification of IFN-γ content by ELISA. 1µCi of 3H-thymidine was added per well and the cells were culture overnight. Cells were subsequently harvested using an automated Filtermate harvester (PerkinElmer) onto a UniFilter glass fibre plate (PerkinElmer). The plates were dried and the incorporation of ^{3}H-thymidine was measured by liquid scintillation counting using a TopCount Microplate Scintillation counter (PerkinElmer).

3.8. Immunofluorescence

3.8.1. Freezing Tissue

For frozen tissue sections tissue was frozen in optimal cutting temperature (OCT, VWR) compound. Moulds were produced out of foil and filled with OCT. *Perrimortum,* tissue was placed in the OCT in the moulds which were placed into a petri dish containing iso-pentane on top of dry ice. Once the samples had frozen they were transferred to -80°C for storage until cutting. To produce frozen lung sections, after perfusion, the lungs were filled with OCT via the trachea prior to removal from the mouse.

3.8.2. Cutting sections

Sections of frozen tissue were cut on a cryostat (Leica) at a thickness of 10μm and attached to a super-frost plus slide (Fisher). Tissue sections were left to dry for 30 minutes to 48 hours.

3.8.3. Staining sections

All steps were carried out at room temperature. Sections were fixed in dry acetone for 10 minutes and air-dried. Sections were marked using a barrier pen (Immedge Pen) and washed three times with PBS. Sections were blocked using 5% *(v/v)* normal serum from the host of the secondary antibody for 30 minutes. Primary antibody was added at the concentration indicated for 1.5-2 hours. Sections were washed as before and the secondary antibody was added for 45 minutes. Sections were washed again and counter stained with DAPI (Life technologies) for 20 minutes, briefly washed and cover slips mounted using Vectasheild Hardset or mounted with prolong gold mountant with DAPI (Life technologies) omitting the previous DAPI staining step.

3.9. Histochemistry

Tissue was collected from mice as indicated and placed in fixative.

3.9.1. Tissue Fixation

Tissue samples were taken *perimortum* and immersed in 10% neutral buffered formalin for at least 24 hours before subsequent processing. Care was taken to ensure samples were no more than 5mm thick in at least one dimension, the volume of formalin was at least 10 times the volume of the tissue and the tissue was completely immersed in the formalin.

3.9.2. Processing

Further processing was carried out at the histochemistry research unit, University of Southampton, UK or Histoserve, MD, USA. Samples were embedded in paraffin, cut and stained with either H and E or PAS as indicated in the appropriate figure legend.

3.10. Image capture

Stained slides were imaged on a CKX41 (Olympus) or a BZ9000 (Keyence) microscope at an appropriate magnification.

3.11. Image processing and analysis

3.11.1. Image processing

Post capture of the image minimal processing was performed. For H and E and PAS stained sections the background white balance was corrected using photoshop (Adobe). Scale bars were added using FIJI after calibration using an image with a bar of known length taken on the same microscope and same magnification as the image to be processed.

3.11.2. Goblet cell scoring

Numbers of goblet cell per villi were counted using the Cell counter plugin for FIJI. Goblet cells were enumerated on at least 3 full in plane villi per section. Goblet cells were counted as large pink/purple cells on the luminal surface of an villi above the crypt in an PAS stained section.

3.11.3. Kidney pathology score

The scoring of kidney pathology in the VavBCl-2 x Mem+Sol TL1A mice was carried out by a trained veterinary pathologist in the Department of Veterinary Medicine, NIH.

3.12. RNA extraction and reverse transcription

Different methods were used dependent upon where the experiment was carried out and the cell number.

3.12.1. RNA extraction for low cell numbers

For extraction of low numbers of cell (eg post siRNA knock down) a trizol based RNA extraction system was used. Briefly, cells were pelleted by centrifugation and re-suspended in 1ml trizol (Life technologies). 200µl of chloroform (Mallinckrodt) was added, vortexed and centrifuged at 8600xg for 15 min at 4°C. The top aqueous layer was removed and an equal volume of isopropanol and 2ul of glycoblue (Life technologies) added. The sample was mixed and left to precipitate at -20°C for 10 minutes. The sample was centrifuged at 13000xg for 10 min at 4°C. The pellet washed with 1ml 75% ice cold EtOH, centrifuged at 6800xg for 5 min and left to air dry. The pellet was re-suspended in 10µl RNase free H_2O and the RNA was quantified using a Nanodrop spectrophotometer and stored at -80°C until required.

3.12.2. RNA extraction from tissues taken from retrotransgenic mice

For RNA extraction from tissues the tissue was homogenised using a pellet pestle motor (Sigma) and the cells homogenised by centrifugation through a QIAshredder (13000xg, 2 minutes). The RNA was purified using a Purelink RNA mini kit (life technologies) according to manufacturer's instructions. The RNA was quantified using a nanodrop spectrophotometer and stored at -80°C until required.

3.12.3. RNA extraction from tissue from all remaining experiments

For RNA extraction from tissues the tissue was homogenised using 2.38 mm metal bead tubes (Mo Bio) in a precellys 24 (Bertin) submurged in Lysis buffer (Life technologies). The sample was mixed with 70% EtOH and centrifuged at 3800xg for 3 min and subsequently the RNA was purified using a Purelink RNA mini kit (Life technologies) according to manufacturer's instructions. The RNA was quantified using a Nanodrop spectrophotometer and stored at -80°C until required.

3.12.4. Reverse transcription of RNA from low cell number extraction

7µl of RNA was reverse transcribed to cDNA using the VILO kit (Life technologies) as per manufacturer's instructions. The cDNA was used for subsequent qPCR reactions or stored at -20°C until required.

3.12.5. Reverse transcription from RNA from retrotransgenic mice

100ng-1µg of RNA was reverse transcribed to cDNA using superscript III kit (Life technologies) using the manufacturer's protocol. Random hexamers were used as the primer.

3.13. Quantitative PCR

Quantitative PCR (qPCR) was used to measure the relative expression of mRNA in RNA isolates following reverse transcription to cDNA. The Taqman probes below (ABI) were used for amplification of transcripts. Data was analysed using the ΔCT method[215].

Gene	Probe reference
HPRT	Mm00446968_m1
IL17-a	Mm00439619_m1
IFN-γ	Mm00801778_m1
IL-13	Mm00434204_m1
Col6a1	Mm00487160_m1
IL-4	Mm00445259_m1
IL-9	Mm00434305_m1
IL-5	Mm00439646_m1
Adam17	Mm00456428_m1
TNFSF15	Mm00770030_m1
Custom TNFSF15 for transgenic line comparison	AI70MVX

Table 3-8 *– qPCR probes. Table lists the reference numbers for all taqman probes used for qPCR. The custom probe was designed by life technologies to recognise the cDNA for TL1A Δ69-93*

3.13.1. qPCR from low cell numbers

cDNA was analysed using Taqman Gene expression master mix (Life Technologies) as per manufacturer's instructions with 0.2-0.5 ul of cDNA per well. Samples were run on a C1000 Thermal cycler (Bio-rad) with a Bio-rad CFX96 real time system or a C1000 Touch Thermal cycler (Bio-rad) with a Bio-rad CFX384 real time system for 45-50 cycles.

3.13.2. qPCR from retrotransgenic mice

cDNA was analysed using Platinum quantitative PCR supermix-UDG (Invitrogen) as per manufacturer's recommendations. Reactions were carried out in a 20µl volume using a C1000 Thermal cycler (Bio-rad) with a Bio-rad CFX96 real time system for 45 cycles.

3.13.3. qPCR from all remaining experiments

qPCR reactions were carried out directly from RNA using the iTaq universal probes one step kit (Bio-Rad). Brefily 10-500ng of RNA was combined with 0.4µl iTaq, 10µl Master mix and 1ul of an appropriate taqman probe. The volume as made up to 20ul with RNase free water and run on the protocol below for 45-50 cycles on a C1000 Thermal cycler (Bio-rad) with a Bio-rad CFX96 real time system or a C1000 Touch Thermal cycler (Bio-rad) with a Bio-rad CFX384 real time system for 45-50 cycles.

3.14. RNASeq

3.14.1. RNA integrity analysis.

After Purification of RNA from the post-caval lobe of a TL1A transgenic or WT mouse as described above RNA quality was assessed using a 2200 TapeStation (Agilent Technologies). A RNA integrity number (RIN) of greater than 7.5 was considered to be of great enough quality to continue.

3.14.2. First and second strand synthesis

mRNA was purified from the RNA pool using a NEBNext Poly (A) mRNA Magnetic isolation Module (New England Biolabs) from an initial 1µg of RNA as per manufacturer's instructions. The sample was eluted from these beads into the buffer from the NEBNext RNA first strand synthesis module (New England Biolabs), which was subsequently used for first strand synthesis. NEBNext second strand synthesis module (New England Biolabs) was subsequently used for second strand synthesis following manufacturer's instructions. Double stranded cDNA was purified using Agencourt AMPure XP Beads and quantified using Quant-it pico-green double stranded DNA (dsDNA) assay (Life technologies)

3.14.3. Library preparation and sequencing

An Ovation SP ultralow library system (Nugen) was used in conjunction with a Mondrian SP work station (Nugen) for automation of the end repair, adaptor ligation and subsequent purification of a suitable library for multiplexing for next-gen sequencing. 10ng of ds-cDNA per sample was used for creation of the library and the automation was carried out as per manufacturer's recommendation. Once the library had been produced it was amplified for 15 cycles as recommended. The samples were then quantified using Quant-it pico-green dsDNA assay as before and diluted to 2nM and mixed in groups of 4-6 samples (now identifiable by the adapter barcode). The samples were subsequently denatured with 0.1M NaOH for 5 minutes and 10pmol of the samples with 4% PhiX (Illumina, control) were loaded onto a HiSeq 2000 (Illumina) for sequencing.

3.15. Soluble Protein assays

3.15.1. Serum preparation

Whole blood was left at 4°C in a 1.5ml epindorff until it had clotted. Sample was spun at 16000xg in a microfuge for 2 minutes and the supernatant removed.

Alternatively serum separator tubes (Sarstedt) were used. Blood was collected directly into these tubes which containing a clotting agent. Tubes were spun at 3800xg for 3 minutes and the serum removed from above the gel layer. Serum was stored at -80°C until required.

3.15.2. Sandwich ELISA

Plates (Nunc Maxisorb) were coated with capture antibody or antigen in bicarbonate buffer overnight then blocked with 350µl PBS with 1% *(v/v)* BSA for 2 hours. Plates were washed 3 times in PBS with 0.05% *(v/v)* Tween-20 using a 405TS plate washer (BioTek) and incubated with the sample or appropriate standards in PBS with 1% *(v/v)* BSA for 1 hour. Plates were washed as before and incubated secondary antibody at an appropriate dilution in PBS with 1% *(v/v)* BSA for 1 hour. Plates were washed as before and if the secondary was not conjugated to Horseradish peroxidase (HRP) were incubated with an appropriate HRP conjugate. Plates were washed as before and detected using 100µl TMB substrate (Biolegend). The reaction was stopped using 100µl 2N H_2SO_4 and the plate absorbance read at 450nm using an Epoch (BioTek) or Synagy H1M (BioTek).

Combinations of capture antigen and detection method are indicated below.

Analyte	Coating	Secondary	Detection
NP	NP(4/28)-BSA (4µg/ml)	GtαmIgG1-HRP 1:4000 GtαmIgG2b-HRP 1:4000 GtαmIgG2c-HRP 1:4000 GtαmIgA-HRP 1:4000 GtαmIgM-HRP 1:4000 GtαmIgE-HRP 1:4000	N/A
Total IgG	GtαmIgG (0.2 µg/ml)	GtαmIgG1-HRP 1:15000 GtαmIgG2b-HRP 1:15000 GtαmIgG2c-HRP 1:15000	N/A
Total IgA	GtαmIgA (0.2 µg/ml)	GtαmIgA-HRP 1:12000	N/A
Total IgE	GtαmIgE (0.2 µg/ml)	GtαmIgE-HRP 1:12000	N/A
Anti dsDNA	Calf intestinal DNA (1µg/ml)	GtαmIgG1-HRP 1:4000 GtαmIgG2b-HRP 1:4000 GtαmIgG2c-HRP 1:4000	N/A
IFN-γ	HB170 (4µg/ml)	αmIFN-γ-Biotin 1:500	Streptavidin HRP 1:1000

Table 3-9 *– ELISA setup. Table gives the concentration of antibodies used for non-commercial ELISA assays.*

3.15.3. Commercial ELISA kits

Where the levels of either anti nuclear antibodies (ANA) or anti dsDNA have been given in AU/ml Kits from Alpha diagnostic have been used. Mouse serum was diluted in sample buffer to 1/100 for ANA and 1/500 for anti dsDNA. EILISAs were performed according to manufacturer's instructions.

For albumin levels in murine urine samples were diluted to 1/4000 in sample buffer and analysed using the mouse albumin ELISA kit (Alpha diagnostics) according to manufacturer's instructions.

3.15.4. Creatinine assay

To measure creatinine in murine urine a creatinine parameter assay kit (R and D) was used. Samples were diluted 1/50 and the assay carried out according to manufacturer's instructions.

3.15.5. Luminex

Anti TL1A luminex assays were carried out using a combination of 5G4.6 conjugated beads and biotinylated Tan2-2. 5G4.6 (Anti mouse TL1A mAB) was conjugated to Region 27 Bio-plex Xmap luminex beads (biorad) as per the manufacturer's protocol. Buffers were supplied by Biorad and the assay followed their protocol using $2.5x10^3$ beads per well and 1-4µg/ml of biotinylated Tan2-2. Recombinant mouse TL1A (R and D) was used for the standard curve.

Cytokine content of the serum was assessed using the Group 1 23-plex mouse panel (Biorad) and the TGF panel (Biorad) according to manufacturer's instructions.

Assays were read on a Bio-plex 200, a luminex 100 or a magpix following a standard operating protocol for the individual machine.

3.16. Mouse lines

3.16.1. C57bl/6

All mice unless otherwise stated were on the C57bl/6 background. At the University of Southampton WT mice were maintained as a colony originally from Jackson Labs. At the NIH WT mice were purchased from Taconic.

3.16.2. CD45.1 congenic mice

CD45.1 WT congenic C57bl/6 mice were purchased from Taconic.

3.16.3. Mem and Mem Hi TL1A mice

The Mem and Mem Hi TL1A mouse lines were produced by the NCI transgenic core facility. The CD2 TL1A Δ 69-93 plasmid was cut with Sal1 and Not1 for injection. From multiple founders ones of the required expression level were selected and maintained as a homozygous line.

3.16.4. Mem+Sol TL1A mice

Apart from the experiments involving VavBcl-2 all Mem+Sol TL1A mice were from founder R6 of the CD2 TL1A mouse strain at the NIH[177]. The remainder were from a colony at the University of Southampton which was generated separately.

3.16.5. DR3 KO mice

DR3 KO mice were maintained as a colony at the NIH and the University of Southampton. The mice were originally produced by E. Wang[216].

3.16.6. TL1A KO mice

TL1A KO mice were maintained as a colony at the University of Southampton and were originally from Biogen.

3.16.7. TL1A and DR3 KO x VavBCL-2

Mem+Sol TL1A mice and DR3KO from the University of Southampton were crossed to the VavBCL-2 mouse strain also housed at the University of Southampton.

3.16.8. DR3 conditional mouse

DR3 flox mice were produced by ozgene. LoxP sites were added into intron 1 and intron 6. These mice were subsequently crossed to a CD4 Cre (Jackson, stock number 017336).

3.16.9. MMP9 KO mice

MMP9 KO mice were obtained from Jackson labs (Stock number 007084).

3.16.10. RAG KO mice

RAG 1 KO mice (Stock number 002216) and RAG 2 KO (Stock number 008449) mice were purchased from Jackson labs.

3.16.11. RAG GC KO mice

RAG GC (Gamma chain) KO mice were maintained as a colony at the NIH. These mice were on the RAG 2 KO background.

3.17. Genotyping

3.17.1. Genomic DNA extraction and genotyping PCR

For genotyping in the UK ear punches or tail tips were collected from mice to be genotyped and immersed in 100µl DNA isolation buffer supplemented with Proteinase K (0.5mg/ml, Sigma). Samples were incubated at 55°C over night. The following day the samples were centrifuged at 16000xg for 5 minutes and the supernatant, which contains genomic DNA, removed and stored at -20°C until analysis.

To extract genomic DNA cells were lysed in buffer RLT (Qiagen) and processed through a QIAshredder (Qiagen) as per manufacturer's instructions. The lysate was loaded onto a RNeasy column (Qiagen) and processed for RNA extraction as per manufacturer's instructions. After elution of RNA with 50µl of water the column was incubated with 50µl 8mM NaOH at 55°C for 7 minutes and spun at 5000xg for 5 minutes. The genomic DNA is contained in the elute. Purity and concentration was

confirmed by absorption at 260 and 280nm. Genotyping was carried out using the protocol for the commercial genotyping kit (Section 3.17.2).

For genotyping 1µl of genomic DNA was added to a master mix which contained 1.25µl dNTP (10mM stock, Promega), 0.5µl of each genotyping primer (100µM), 10µl 5x GoTaq buffer(Promega), 1µl of Go Taq polymerase (Promega) and PCR grade water to 50µl total volume. PCR was carried out as in section 3.17.3.

3.17.2. Commercial genotyping kit

For genotyping at the NIH the standard Kappa mouse genotyping kit (Kapa Biosystems) was used. Ear punches or tail tips were collected from mice to be genotyped. The tissue was suspended in 100µl Kapa extraction buffer and incubated at 75°C for 10 minutes then 95°C for 5 minutes. For the PCR 4µl of the supernatant from the extraction was added to 10ul 2x Kapa 2G Fast HS genotyping mix, 0.1µl of each genotyping primer (100µM) and PCR grade water to 20µl final volume. PCR was carried out as below.

3.17.3. Genotyping PCR reaction conditions

PCRs were carried out for genotyping following the general program below according to the specific conditions in the table.

Mouse strain	Genotyping Primers	Annealing temperature (°C)	Number of cycles	Size of products (bp)
Mem TL1A Mem+Sol TL1A	TL1A seq F1 and R1 Beta globin F and R	55 (65,-2)	35 (5)	TL1A-188 Beta globin-500
DR3 KO	DR3 F8 DR3 4F DR3 2R	60 (65, -1)	35 (5)	WT-250 KO-800
MMP9 KO	MMP9KO 1,2,3,4	66	36	WT-277 KO-172
Conditional DR3 - Flox	3431-31 3431-32	60	35	WT-311 Flox-438
CD4 Cre	Cre F and R Beta globin F and R	60	35	Cre-250 Beta globin-500
TL1A KO	TL1A KO 1,2 and 3	54	40	WT-569bp KO-381bp

Table 3-10 *– PCR conditions for genotyping of mouse strains. If the PCR involved a touch down the initial temperature, delta temperature per cycle and number of touchdown cycles are given in brackets.*

3.17.4. Vav-BCL2 mice

Vav-BCL2 mice were screened from blood by flow cytometry. 20µl of blood was collected and was stained for CD4 using the standard staining method for blood as described above. The blood cells were subsequently fixed and permeablised as previously described and stained for intracellular human BCL-2.

3.18. *In vivo* protocols

All *in vivo* experiments which were carried out in the UK were in accordance with Home office and University of Southampton Faculty of Medicine ethics committee approval and under an appropriate project and personal licence. All *in vivo* experiments carried out in the USA were approved by the NIAMS animal care and use committee (ACUC), were listed on animal study protocol AO14-01-01 and in agreement with ARAC guidelines.

3.18.1. Injections

Injections were carried out by a fully trained and competent person who held a Home Office licence (UK) or was named on an animal study protocol (USA). Maximum Injection volumes have been stated below.

Route	Volume (µl)
Intra-peritoneal	300
Intra-venous	200
Sub-cutaneous	200
Intra-derminal	50

Table 3-11 *– Maximum volumes for injections.*

3.18.2. Collection of blood from the tail vein

The mouse warmed under a heat lamp, placed in a restraint and the vein nicked using number 15 scalpel blade. The blood was collected into a heparinized tube (Sarstedt) if whole blood was required or a serum separator tube (Sarstedt) if serum was required. The wound was closed using Vetbond tissue adhesive (3M).

3.18.3. Collection of blood from the maxillary plexus

To collect blood from the maxillary plexus the mouse was restrained and the area punctured with a 4.5mm lancet. 20-50µl of blood could then be collected into an appropriate tube.

3.18.4. Euthanasia

Mice were euthanized by approved methods as defined by the Home Office or ACUC and ARAC unless a terminal procedure had been carried out.

3.18.5. Terminal cardiac bleed

Mice were anesthetised using gaseous isoflurane (3-5% isoflurane vaporised with O_2 at a flow rate of 0.5-1L^3/min), 100-200mg/kg pentobarbitone given IP or a mix of 100-200mg/kg ketamine and 15-30mg/kg xylzine. Mice were considered sufficiently anesthetised if they did not respond to a pain stimulus to their footpad. Blood was collected via cardiac puncture before being euthanised by an approved method. Alternatively blood was collected from the descending aorta within the abdominal cavity.

3.18.6. Perfusion of organs

Lungs and kidneys were perfused for histology, RNA and cell extraction. Mice were anesthetised as for terminal cardiac bleeds and pinned to a dissection board. The thoracic and abdominal cavity was opened and the heart exposed. For lung perfusion the descending aorta was severed and PBS injected into the right ventricle using a 23G butterfly needle (Jelco) at approximately 5ml/minute until clear liquid ran from the incision site and the lungs appeared white. For kidney perfusion the heart was injected into the left ventricle and the right atrium was perforated, the mouse was then perfused as for lungs.

3.18.7. Whole body Irradiation

7 days prior to whole body irradiation the drinking water was replaced with acid water (Tap water adjusted to pH 2.5). On the morning of irradiation mice were sedated via IP injection with 1in10 Hypnorm and subsequently irradiated with an appropriate dose. For bone marrow reconstitutions mice were subjected to 2 doses of 5.5Gry separated by 24 hours as this was found to reduce treatment associated complications. Mice were allowed to regain full consciousness before any subsequent injection. For two weeks post irradiation mice were kept on acid water supplemented with 0.25%*(w/v)* Baytrol. After this time the mice were placed back on regular tap water.

3.19. *In Vivo* experiments

3.19.1. Salmonella infection

Mice were infected with ~0.5x10^6 Salmonella and the response in the spleen and blood followed. *Salmonella Typhimurium* which had been genetically modified to express OVA on the surface was used for infection.

Bacteria from a frozen stock were streaked on a LB agar plate supplemented with ampicillin and grown overnight at 37°C. A single colony was picked and grown overnight in a 37°C shaking incubator in 10ml of LB media supplemented with ampicillin. In the morning the optical density (OD) was measured at 600nm. An OD of 0.8 was required as this ensured the bacteria were in the log phase of growth. If the OD was greater than 0.8 the sample was diluted 1 in 10.

1ml of bacterial culture with an OD of 0.8 was centrifuged at 6000xg for 5 minutes at 4°C, the pellet re-suspended in PBS and centrifuged as before. The sample was subsequently washed a further time and re-suspended in 1ml of PBS. The final bacterial solution was diluted 1 in 200. This resulted in ~2.5x10^6 Salmonella per ml of which 200µl were injected IP into a mouse.

3.19.2. Retrotransgenics

Retrotransgenics is a method for the retroviral transduction of murine bone marrow and subsequent reconstitution of a lethally irradiated mouse to result in expression of the protein of interest within the mouse's hematopoietic system. For production of the virus see section above on retroviral transduction and see section above on whole body irradiation for preparation of lethally irradiated mice. All days are given relative to bone marrow transfer.

Day -7 donor mice were given 150mg/kg 5-fluorouracil (Sigma). This depletes the bone marrow in the donor mouse to encourage proliferation as retrovirus can only transduce actively proliferating bone marrow[217]. On Day -4 the donor mice were culled and the bone marrow taken and processed as indicated above. The donor bone marrow was re-suspended in bone marrow media supplemented with IL-3, IL-5 and mouse stem cell factor (mSCF, all at 50ng/ml, the cytokines were maintained in all further tissue culture stages for the bone marrow, New England Biolabs) to further encourage proliferation and cultured at 37°C. On Day -2 the media was removed from the bone marrow and it was spin transduced using virus-containing supernatant

supplemented with 2µg/ml of polybrene. The bone marrow was spin transduced twice with fresh retroviral containing media approximately 7 hours apart. The media was changed on the bone marrow on day -1 and on day 0 GFP expression was assessed on the total bone marrow cells. A minimum of 7% GFP was required for successful retrotransgenic production. 1-4x10^6 total bone marrow cells were injected per mouse IV. The number of cells injected did not seem to affect the success or the retrotransgenic production however the time taken for the mouse to reconstitute was proportional to the number of total bone marrow cells injected.

A blood sample was collected 6-10 weeks post transfer of bone marrow to check for reconstitution and GFP expression in the hematopoietic subsets.

3.19.3. Airway resistance

To assess lung hypersensitivity airway resistance was measured following challenge with Acetyl-β-methycholine chloride post intubation.

The mouse was anaesthetised with 100mg/kg ketamine and 10mg/kg xylzine IP and given a second dose after 20-30 minutes. Once a sufficient level of anaesthesia had been achieved a 5mm midline cervical incision was made in the skin from the larynx to the top of the sternum and the skin opened. The subcutaneous fat and the infrahyoid muscles were then removed to visualise the trachea. A silk 2-0-suture thread was placed under the trachea and move down proximal to the top of the sternum. A small incision was made in the top of the trachea between and parallel with the cartilage rings in the top surface only with a razor blade and a 19G blunt needle inserted and the suture tied around to form an airtight seal (Fig 3-1). The mouse was placed on FlexiVent (Scireq) with module 1 installed that had been calibrated to the blunt needle used and the mouse's weight. A default ventilation pattern was started and the mouse observed for correct inflation of both lungs. A mechanical scan program was subsequently indicated to ensure the mouse was anaesthetised sufficiently so as to not resist the mechanical inflation. If necessary a half dose of anaesthesia was administered at this point. Once the mouse was ready the challenge was started. Acetyl-β-methycholine chloride (in PBS) was added to the nebuliser in increasing concentrations from PBS alone to 100mg/ml. At each dose 12 recordings of resistance were taken and the mean from this used for analysis. Care was taken to ensure the mouse remained alive and free from distress throughout the procedure.

Figure 3-1 *Correct intubation of a mouse for analysis of airway resistance.*

3.19.4. Continual infusion of sTL1A via osmotic pump

As a model for increased sTL1A abundance mice were fitted with osmotic pumps (Alzet 2006 osmotic pumps). The pumps delivered 500ng of sTL1A in PBS (0.16µl/hr) for 6 weeks. The osmotic pumps were filled prior to surgery according to manufacturer's instructions. Sterile surgical technique was observed throughout the procedure with all instruments autoclaved before each session. The backs of the mice were shaved and the mice were given 0.1mg/kg Buprenorphine IP in PBS. Mice were anaesthetised using gaseous isoflurane (3% isoflurane vaporised with O_2 at a flow rate of 0.6L^3/min) in a tank and subsequently transferred to a nose cone for surgery. The surgical site was scrubbed with provodone iodine solution and 75% EtOH. A 5-7mm dermal incision was made in the back of the mouse perpendicular to the spinal column approximately 1 cm forward of the base of the tail. A pocket was created using round ended surgical scissors to separate the skin from the back of the mouse and the osmotic pump inserted so the flow regulator was furthest from the incision site. The wound was closed with 9mm surgical staples (MikRon Precision inc) and the mouse was returned to its home cage and monitored until it recovered. The pump was checked daily for 7 days and care taken to ensure it remained mobile. After 7 days the staples were removed. Figure 3-2 shows a mouse with a pump 3 weeks after surgery.

Figure 3-2 *– Mouse with osmotic pump. Mouse 3 weeks post implantation of an osmotic pump subcutaneously. The pump was originally placed on the back of the mouse however it was found that over time it would migrate down to the side of the animal.*

3.19.5. Alum precipitation

For alum precipitation the antigen was diluted in PBS and mixed 1:1 with alum. The mixture was incubated rotating at room temperature for 30-45 minutes before injecting into a mouse. Typically a total of 100µl was injected subcutaneously into a mouse.

3.19.6. T dependent immunisation

Mice were immunised on day 0 with 10µg of 4-hydroxy-3-nitrophenylacetyl (NP)-16 conjugated to OVA prepared in alum as described above. Mice were boosted on day 48 with 10ug NP-16-OVAL in PBS given IP.

3.19.7. T Independent NP Immunisation

Mice were immunised on day 0 and boosted day 48 with 10ug of NP-0.15-LPS or NP-49-ACEM-FICOLL given IP with PBS.

3.19.8. RAG transfer models

To study the effect of reconstitution of a mouse with T cells from either a WT, TL1A transgenic or DR3 KO mouse, cells were injected IV into RAG KO mice.

To study the effect of TL1A on different cell types $4x10^5$ purified CD4+ WT or TL1A transgenic T cells were transferred into either RAG 2 KO or RAG 2 GC KO mice. After 8 weeks the phenotype of the mice was assessed.

To investigate if CD4+ DR3 KO T cells had an altered rate of homeostatic proliferation compared to WT $5x10^5$ cells were transferred into WT RAG 1 KO mice.

3.19.9. Chronic GVHD

To induce a lupus like disease a parent into F1 chronic graft versus host disease (cGVHD) model was used. $1.5\text{-}2x10^7$ purified CD4+ T cells from either a WT or DR3 KO mouse were transferred into the F1 progeny from a cross of C57bl/6 and DBA/2 mice. Expansion of the graft in the blood was followed every 14 days and the engraftment in internal organs assessed after 12 weeks.

3.20. Bioinformatics

3.20.1. RNASeq analysis

Sequencing run data, in the form of a BCL file, was obtained upon completion of the run. This was demultiplexed and converted to a FASTQ file with CASAVA (Illumina) using the NIAMS cluster. The data was transferred to the Biowulf high performance computational cluster. The sequencing files were aligned using TopHat splice junction mapper within the short read aligner Bowtie2[218] against the mm10 USSC mouse genome on the 21st July 2015. The samples were sorted using samtools [219] and the features counted and a table produced using Rsubread [220] within R. At this point the counts table was transferred to a local computer for further analysis using R running within R studio. For differential analysis DESeq was used [221]. For comparison of the ileum samples the differential expression between transgenic and WT samples was calculated using a negative binomial distribution model. As the lung RNASeq data came from two independent runs a generalised liner model was used. For plotting of QC graphs and data plots the following packages within R were used: DESeq, VennDiagram, RcolorBrewer and gplots. All packages are publicly available for download from the CRAN and Bioconductor servers.

3.20.2. Heatmap generation

For the RNASeq data and the 23plex cytokine panel heatmap.2 was used for plotting the heatmaps. The packages RcolorBrewer and gplots were used for plotting the data and adjusting the colour of the graph.

3.20.3. Gene ontology analysis

Gene ontology analysis was carried out using the Gene Ontology enRIchment anaLysis and visuaLizAtion tool (GOrilla)[222] was used to perform gene ontology analysis. The database was accessed on the 29th July 2015.

3.20.4. Cleavage site prediction

Prediction of the cleavage site and MMP responsible for said cleavage of TL1A was predicted using the PROtease Specificity Prediction servER[223] (PROSPER).

3.21. Statistical analysis

Statistical analysis was performed using Graphpad prism 6 and R. The statistical test used is detailed in the figure legends.

Chapter 4. Investigating expression patterns and potential differential roles of membrane restricted and soluble TL1A

4.1. Introduction

TL1A is a type II membrane protein that is expressed on the surface of cells. Like other members of the TNFSF, membrane bound TL1A can be proteolytically cleaved to produce a 20kDa soluble form[43]. At present the identity of the specific protease is unknown but it most likely belongs to the matrix metalloproteinase family[165]. Both soluble recombinant[148, 178] and membrane bound TL1A[165] have been shown to be capable of induction of signalling however the physiological relevance has not been investigated.

The existence and differing functions of soluble and membrane bound ligands is a common feature of the TNFSF. Both membrane bound and soluble forms of TNF are active; however not equally[70]. TNF binds the receptors TNFR1 and TNFR2 and membrane bound TNF can signal via TNFR2 with a higher efficiency than soluble[224]. Through deletion of the cleavage site a membrane restricted TNF only mouse was produced[71, 225]. To assess defects in function of membrane restricted TNF, knock in mice were compared to TNF KO mice which are known to be susceptible to *Listeria monocytogenes,* protected from LPS induced endotoxic shock and have defects in the formation of primary B cell follicles[226]. The membrane restricted TNF mouse was unable to mount an effective response against *Listeria monocytogenes*[71] and was protected in the MOG-EAE model[71, 225]. The membrane restricted TNF mouse was also protected from lethal LPS induced endotoxic shock completely at a dose of 1μg, which is 100% lethal within 8 hours in a WT mouse when sensitised with 20mg D-galactosamine. At both this dose, and 100μg of LPS, TNF KO mice were protected, however the membrane restricted mouse had a 60% survival rate after 53 hours at the higher dose suggesting this response is mostly but not totally dependent on soluble TNF[225]. The membrane bound TNF mostly repaired the defect in lymphoid organ structure and the GC response observed in the TNF KO. Further the membrane restricted TNF fully repaired defects in steady state chemokine gene expression in the spleen[225]. It should be noted that these studies came from two different membrane-restricting mutations and some differences are observed between these strains. In particular

the strain made by Alexopoulou *et al*[71] often behaved more like a TNF KO than the strain made by Ruuls *et al*[225, 227]. Overall these data highlight potential differences in the signalling pathways of membrane and soluble TNF. Whilst the membrane restricted TNF mice were able to repair defects in lymphoid homeostasis they were unable to the repair defects in response to pathogens suggesting that soluble TNF is more important for this role.

Fas ligand (FasL) is also produced as a membrane bound form and subsequently cleaved[228]. To study the function of both forms of FasL, membrane restricted and soluble only forms of FasL mice were produced. The soluble only FasL mouse displayed a slightly more severe phenotype than the non-functional FasL mutant, the Gld/Gld mouse. The soluble only FasL mouse presented with splenomegaly and lymphadenopathy and accumulation of CD3+ B220+ cells. These mice also exhibited worse hyperglobulinemia than the Gld/Gld mice and succumbed to lethal autoimmunity at an earlier age. Further, T cells from the soluble only FasL mouse were unable to kill target cells via Fas however T cells which expressed membrane restricted FasL were fully functional and able to kill marginally better than WT cells. There were no reported signs of autoimmunity in the membrane restricted FasL mice[229]. A separate study by Hohlmaum *et al* assessed the role of membrane and soluble FasL on a lymphoma cell line through the expression of a membrane restricted or soluble form. When given via IP injection the membrane restricted form promoted an inflammatory environment with an increase in neutrophil extravasation into the peritoneum. When the tumour was given subcutaneously it was rejected and if mixed with the WT tumour it exerted a bystander effect promoting rejection. The lymphoma which expressed soluble FasL was unable to promote an inflammatory response in the peritoneum or promote tumour rejection. However it was found that when mixed with the membrane restricted tumour the soluble FasL inhibited the proinflammatory effect of membrane FasL[230]. These data suggest that for normal function membrane bound FasL is the active form and the soluble FasL may have a pathogenic signalling role as indicated by the increased severity of autoimmunity in soluble only FasL mice compared to a non-functional mutant.

These data highlight the contrasting roles of membrane and soluble ligands in the TNFSF with TNF proving to be more active when soluble whereas FasL demonstrates the inverse, possibly acting as a decoy. Understanding these differences is key in designing therapeutics to target these pathways, particularly if one wishes to target a pathological role of a ligand whilst preserving a homeostatically important one.

Given these dramatic differences in the biological function of TNF and FasL dependent on their state, we investigated the biological function of membrane and soluble TL1A. To this end we developed assays for the detection of membrane and soluble TL1A in the mouse and examined expression patterns of both forms *in vitro* and *in vivo*. To further study the potential differential roles of membrane and soluble TL1A *in vivo* we generated retrotransgenic and subsequently transgenic mice expressing a membrane restricted or full length TL1A and examined the phenotype conferred in multiple organs. We also assessed the role of soluble TL1A in chronic administration via an osmotic pump.

4.2. Results

4.2.1. Assays for the detection of membrane and soluble TL1A

Assays were required to facilitate the measurement of membrane and soluble TL1A. Levels of membrane TL1A was measured using the rat anti mouse TL1A (Tan 2-2), which has been previously described[185]. Tan 2-2 was biotinylated and used for flow cytometry in conjunction with a fluorophore tagged streptavidin as described in the methods.

To measure the concentration of sTL1A a Luminex based assay was developed. As a pair of antibodies Tan 2-2 and 5G4.6 were tested for compatibility. To check for competition between the antibodies, cells which had been previously transfected with TL1A were stained with increasing concentrations of unlabelled Tan 2-2 (Figure 4-1 A) or 5G4.6 (Figure 4-1 B) followed by addition of the remaining antibody, which had been biotinylated, at a fixed concentration. Binding of the second antibody was detected using a fluorophore tagged streptavidin. As Figures 4-1 A and B show there was no reduction in the staining observed indicating that Tan 2-2 and 5G4.6 bind to separate epitopes and as such are a potential antibody pair suitable for use in a Luminex assay.

Luminex custom beads were conjugated to 5G4.6 and used to capture sTL1A. These were incubated with serial dilutions of sTL1A. Biotinylated Tan 2-2 in conjunction with streptavidin PE was used to detect sTL1A bound to the beads. To test the assay standard curves were run using both 5000 and 2500 beads per well (Figure 4-1 C and D respectively). 2500 beads per well gave a marginal increase in sensitivity at the low range with a detection threshold of 7.8125pg/ml.

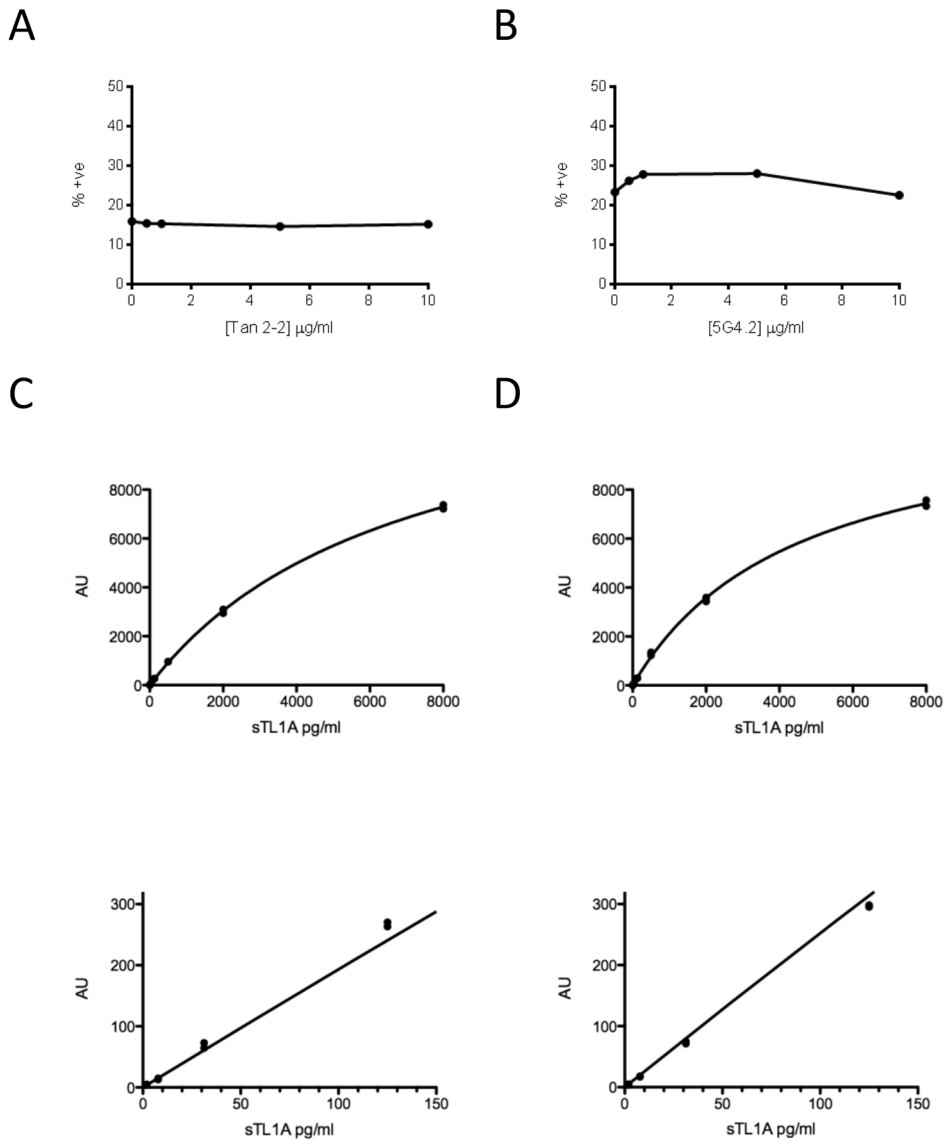

Figure 4-1 *- Luminex based assay for detection of mouse sTL1A. To determine the suitability of the anti mouse TL1A antibodies, Tan2-2 and 5G4.6, as a pair for detection of sTL1A, unlabelled Tan 2-2 (**A**) or 5G4.6 (**B**) was incubated with TL1A transfected 293T cells at the concentrations indicated. The reciprocal biotinylated antibody was added at 10µg/ml and binding measured using a fluorophore tagged streptavidin. **C** and **D** – Custom Luminex beads were conjugated to 5G4.6 and used to detect serial dilutions of sTL1A in conjunction with biotinylated Tan 2-2 at 2µg/ml. Either 5000 (**C**) or 2500 (**D**) of 5G4.6 conjugated beads were used per well. The top panel in C and D shows the full standard curve and the bottom panel highlights the low concentrations.*

4.2.2. In vitro TL1A detection and function

Once methods for the detection of soluble and membrane bound TL1A had been optimised, the expression of TL1A by murine T cells and BMDCs was examined (Figure 4-2). T cells were activated with anti-CD3 and anti-CD28 and BMDCs were activated with LPS. By 24 hours both CD4+ and CD8+ T cells showed up regulation of membrane TL1A with a greater expression on CD8+ T cells. Maximal T cell expression of membrane TL1A was observed by 48 hours however no sTL1A was present in the media. BMDCs constitutively expressed membrane TL1A and high levels of sTL1A was found in the media with an increase induced by 24 hours of LPS stimulation compared to media alone.

As no sTL1A was present after culture of T cells in isolation a co-culture system was employed to attempt to see if TL1A could be cleaved from the surface of T cells. Given that BMDCs are capable of cleaving TL1A to produce a soluble form we hypothesised that co-culture with T cells may result in trans cleavage of T cell TL1A. To ensure that any soluble TL1A detected would be from the T cells rather than the BMDCs we planned to use BMDCs produced from TL1A KO mice, however due to the strategy used to make the mouse[131] a non-functional portion of TL1A was secreted by the BMDCs in response to LPS. Whilst this was not functionally relevant it was however recognised by the Luminex assay (Data not shown). Alternatively, as we found 293T cells were able to cleave murine TL1A (See section 4.2.7) T cells were activated in the presence of 293T cells. sTL1A was not detected in the cell culture media after 48 hours.

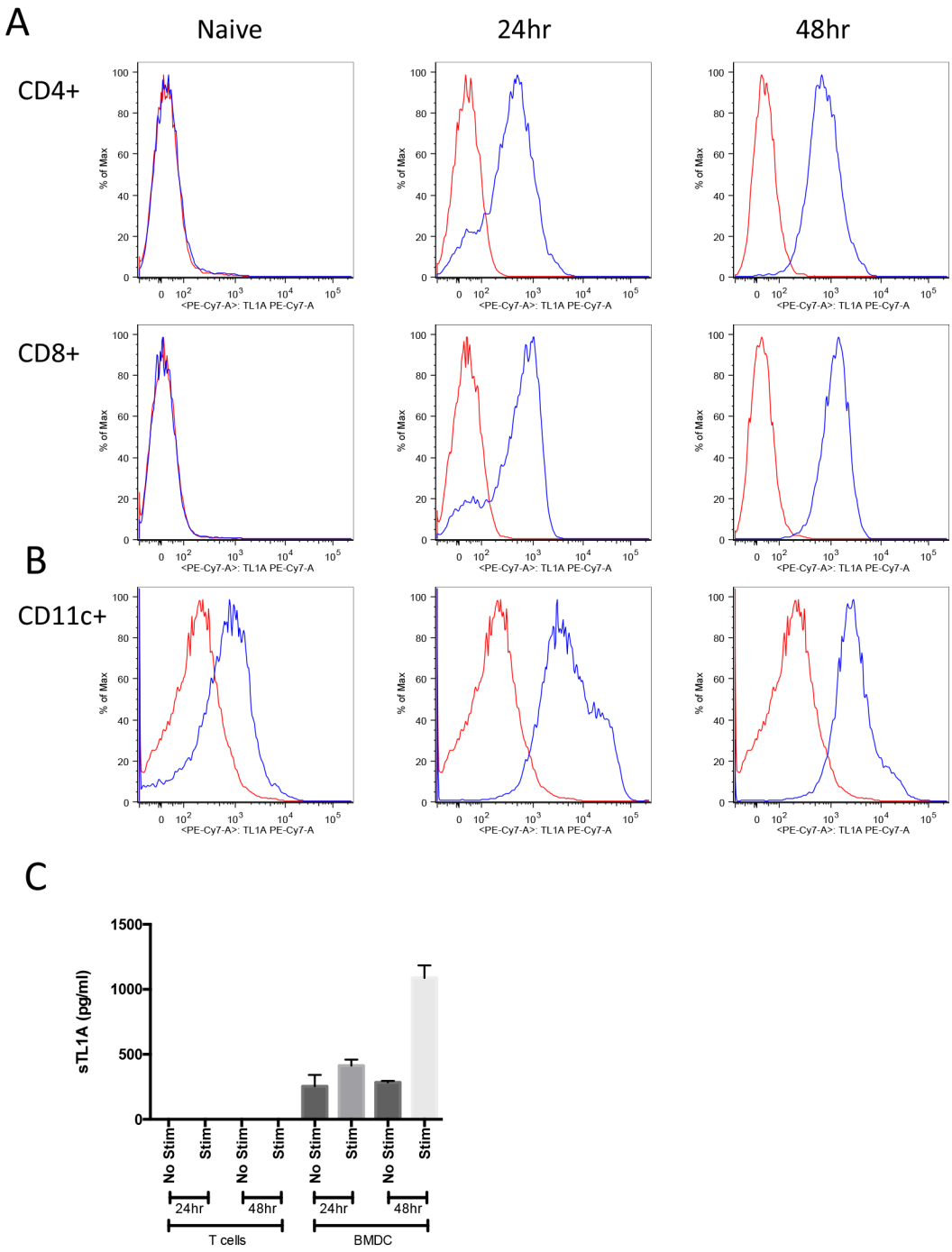

Figure 4-2 *- Membrane and soluble expression of TL1A in vitro.* ***A*** *– Total T cells were purified using an easysep T cell enrichment kit, 0.2x10^6 were plated in 0.5ml of complete RPMI and cultured for the indicated period of time with plate bound anti CD3 (5µg/ml) and soluble anti CD28 (10µg/ml). Cells were stained with either MC39-16 (Red – Isotype control) or Tan 2-2 (Blue).* ***B*** *– BMDCs were harvested 8 days after culture of bone marrow cells with 20ng/ml GM-CSF. 0.5x10^6 cells were plated in 1ml of complete RPMI supplemented with 20ng/ml GM-CSF and activated for the indicated period of time with 100ng LPS. Cells were stained as for A.* ***C*** *- Supernatant*

from A and B was collected at 24 and 48 hours and sTL1A production was analysed by Luminex. T cells cultured either as above (Stim) or with IL-7 (10ng/ml, no stim) or BMDCs as above (stim) or with GM-CSF alone (no stim) for indicated period of time.

4.2.3. In silico prediction of TL1A cleaving protease

Whilst the cleavage site of human TL1A is known[43, 165], the protease responsible for the cleavage remains to be identified. Prior to commencement of functional studies, all possible metalloprotease cleavage sites in the extracellular domain of murine TL1A were predicted *in silico* using PROSPER[223]. Within the extracellular domain only MMP3 and MMP9 were predicted to cleave TL1A, however when the search was narrowed down to the complementary region to the known cleavage site in human TL1A (amino acid 69-93 in mouse TL1A, see section 4.2.7), only MMP9 was predicted to cleave mouse TL1A appropriately. It should be noted that the authors of PROSPER give the F-score (measure of accuracy) of MMP3 and MMP9 prediction to be 45.5% and 43.4% suggesting that these may not be correctly identified sites and should be assessed experimentally. This problem with prediction of MMP cleavage sites is due to the presence of exosites, which are common in the MMP family and enable binding of potential substrates at regions distinct from the active site and therefore not cleaved[223].

Position	Segment	Protease	Notes
73	KDCM▮LRAI	MMP9	Within predicted cleavage site
76	MLRA▮ITEE	MMP9	Within predicted cleavage site, homologous to human cleavage site[43]
88	SPQQ▮VYSP	MMP9	Within predicted cleavage site
126	HDLG▮MAFT	MMP9	Exon 4
132	FTKN▮GMKY	MMP9	Exon 4
141	NKSL▮VIPE	MMP9	Exon 4
153	FIYS▮QITF	MMP3/9	Exon 4
182	ITMV▮ITKV	MMP9	Exon 4
228	GDRL▮MVNV	MMP9	Exon 4
236	SDIS▮LVDY	MMP9	Exon 4
250	FFGA▮FLL	MMP3	Exon 4
252	GAFL▮L	MMP9	Exon 4

Table 4-1 *– In silico prediction of protease specificity for TL1A. The extracellular domain of murine TL1A was analysed using PROSPER for protease cleavage sites. The position indicates the N terminal amino acid number of the predicted soluble product. The red box indicates the position of cleavage within the cleavage site.*

4.2.4. TL1A is cleaved in vitro by ADAM17 but not MMP9

As the Luminex based assay cannot distinguish between cleaved and vesicular bound TL1A, BMDCs were treated for 48 hours with increasing concentrations of the MMP inhibitor GM6001[231] either with GM-CSF alone (untreated) or with the addition of LPS (treated). In both the treated and untreated group there was a decrease in the amount of sTL1A detectable in the cell culture supernatant, however this decline was greatest in the treated group (Figure 4-3A) and occurred with minimal effect on cell viability (Figure 4-3B). As this indicated a MMP was indeed responsible for TL1A cleavage from BMDCs and the *in silico* prediction had implicated MMP9 in cleavage, this was tested. BMDCs were produced from MMP9 KO mice and stimulated for up to 48 hours with LPS as before. The MMP9 KO cells were as viable as the WT cells, however no defect was found in production of TL1A into the cell culture supernatant (Figure 4-3C). Given TNF is cleaved by ADAM17 and its cleavage is also inhibited by GM6001[231], ADAM17 was knocked down using siRNA in BMDCs which were subsequently activated with LPS. In this preliminary experiment levels of sTL1A were reduced (Figure 4-3D) suggesting it is one possible protease for the cleavage of TL1A, however this needs further experimentation to confirm.

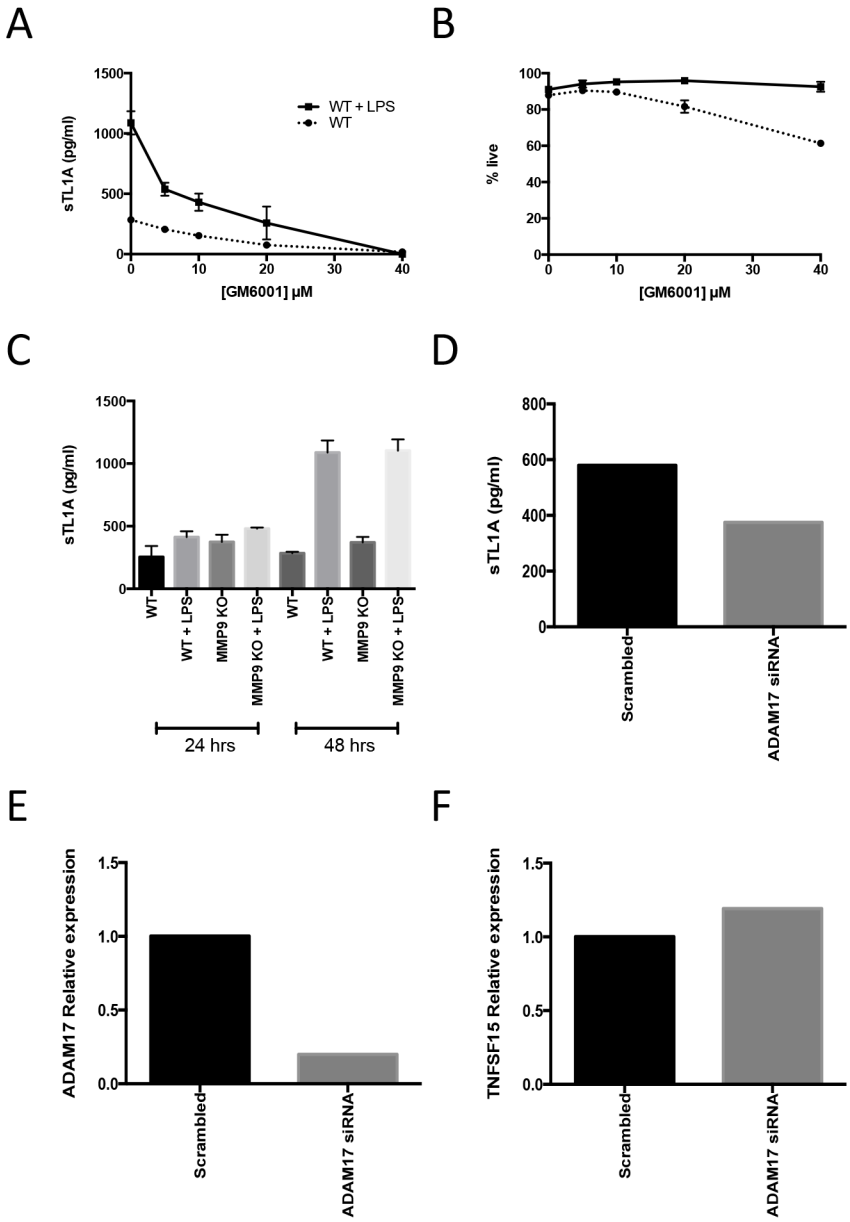

Figure 4-3 *- Matrix metalloprotease mediated cleavage of TL1A.* ***A*** *and* ***B*** *– BMDCs were cultured +/- 100ng/ml LPS with increasing concentrations of GM6001 as indicated. After 48 hours sTL1A production in the supernatant (****A****) and cell viability (****B****) was measured.* ***C*** *– BMDCs were derived from either WT or MMP9 KO mice and cultured +/- 100ng/ml LPS as indicated and sTL1A in the supernatant measured.* ***D-F*** *– BMDCs were transfected with either a non targeting (scrambled) siRNA pool or a pool against ADAM17. 14 hours after transfection cell culture media was refreshed and supplemented with 100ng/ml LPS. Supernatant was removed after a further 24 hours and sTL1A levels measured (****D****). Knock down and continued expression of TL1A was assessed by qPCR (****E-F****).* ***A-C*** *are representative of 3 independent experiments, error bars represent SD.* ***D-F*** *is from a single experiment.*

4.2.5. In vivo soluble TL1A detection

To study the expression patterns of membrane and soluble TL1A *in vivo,* infection with *Salmonella Typhimurium* was used as it had been previously shown to induce TL1A mRNA and protein on F4/80+ cells by immunochemistry[160]. The infection can be followed by the induction of splenomegaly (Figure 4-4A). The strain of bacteria used expresses OVA which enabled the activation of transferred OT2 cells (Figure 4-4B). Membrane TL1A expression was observed on the transferred OT2 cells (Figure 4-4C) as well as endogenous CD4+, CD8+ and F4/80+ cells (Figure 4-4D and E). sTL1A was detected from 4 days post infection at a low level in the serum (Figure 4-4F).

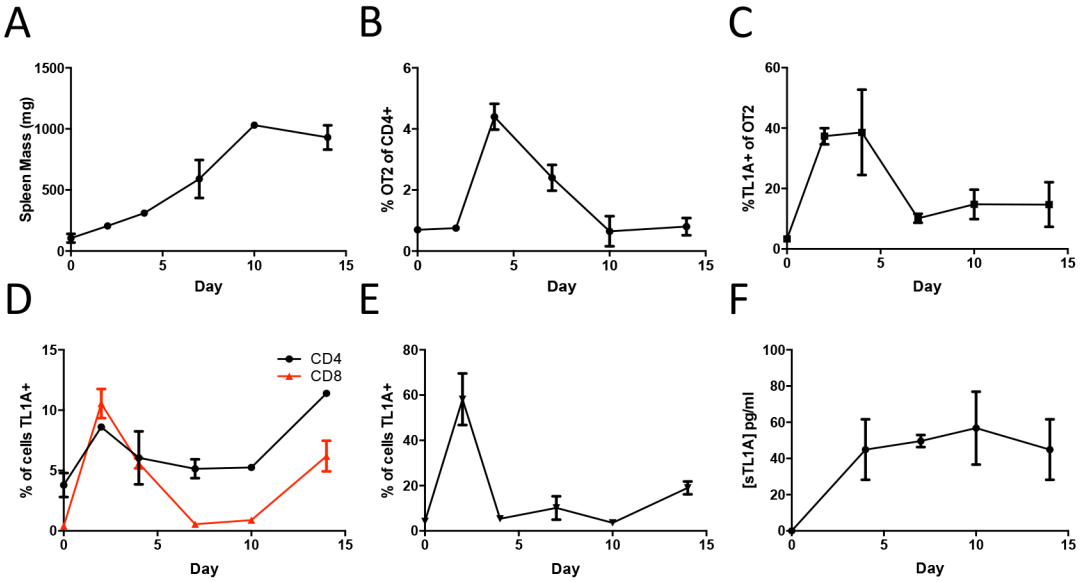

Figure 4-4 *- TL1A expression in response to Salmonella-OVA. Mice were given 0.5x10^6 Salmonella-OVA one day after transfer of 1x10^6 OTII cells. Spleens were taken at the time points indicated and weighed (**A**) and the fraction of OT2 cells present within the CD4 population was measured (**B**). Expression of TL1A was measured by flow cytometery using Tan2-2 and the fraction of TL1A positive cells per population of OTII (**C**), endogenous CD4+ and CD8+ T cells (**D**, black and red respectively) and F4/80+ macrophages (**E**) was plotted. Serum was taken at the same time points and levels of sTL1A were measured (**F**). N=2/time point. Error bars inticate the SEM. Data is from a single experiment.*

4.2.6. Higher order TL1A complexes do not affect T cell costimulation

Previously a recombinant form of sTL1A had been produced which comprised of the extracellular domain of TL1A fused to domains 3 and 4 of rat CD4[134] enabling the *in vitro* study of the effect of sTL1A. To assess the oligomeric state of TL1A its native

molecular mass was assessed by size exclusion chromatography on a Superdex 200 10/300 column. The protein eluted as one major peak which ran slightly larger than IgG and a minor peak which ran slightly above the Fab fragment of IgG. The larger peak corresponds to a trimeric form of the ligand and the smaller peak to monomers. Using OX68 (anti-rat CD4 domains 3+4 mAb) we were able to show cross-linking of the sTL1A protein to produce higher order multimers (Figure 4-5A). We used the cross-linked form of TL1A to model membrane bound forms where a higher concentration of TL1A is focused at a single point. Using serial dilutions of either form to costimulate CD4+ T cells in the presence of suboptimal TCR stimulation, we measured the effect of TL1A on T cell proliferation and IFN-γ production (Figure 4-5B). Cross-linking of sTL1A had no effect on the costimulation of the T cells.

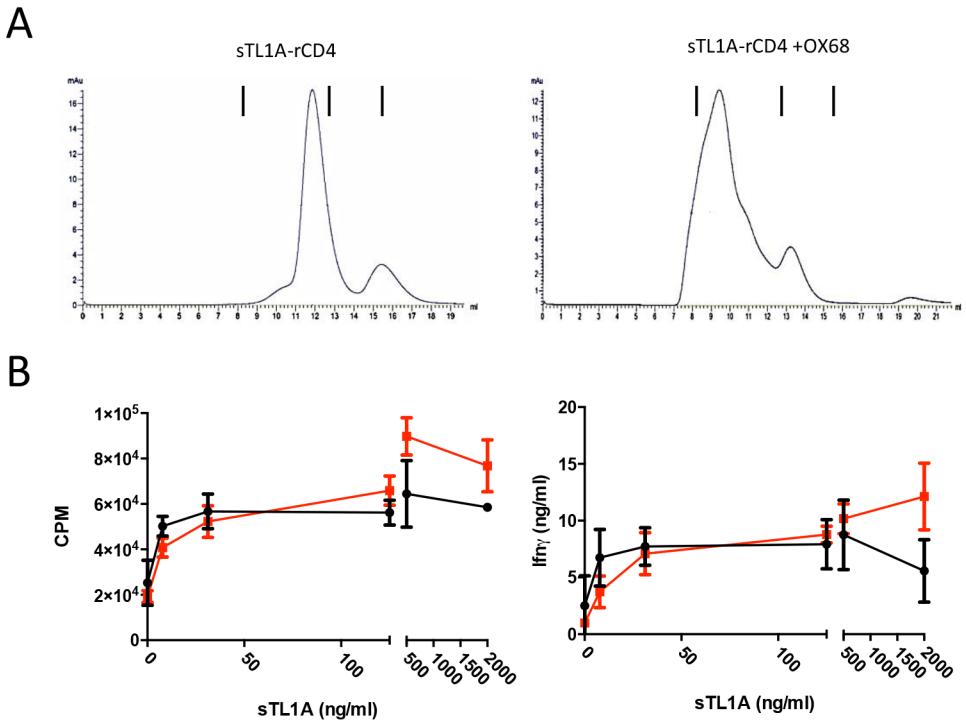

Figure 4-5 *- In vitro stimulation with sTL1A.* ***A*** *sTL1A was produced from the media of ChoK1 transfected as previously described[134]. Either TL1A (left panel) or TL1A +OX68 (1:3 molar ratio, right panel) was run on a Superdex 200 10/300 column. The positions of standard peaks are indicated by black bars. From left to right IgM, whole IgG and IgG Fab.* ***B*** *Splenocytes from a C57BL/6 mouse were enriched to ~80% CD4+ cells. 2x10^5 total cells were plated per well and stimulated with 0.1µg/ml soluble anti-CD3 (1452C11) with the concentrations of sTL1A indicated either with crosslinking (5µg/ml OX68, red) or without (black). After 48hrs half the supernatant was taken and levels of IFN-γ were measured (right panel). Supernatant was partially replaced with fresh media containing tritiated thymidine, incubated overnight and*

incorporation measured as counts per minute (CPM) the following day (left panel). Error bars indicate the SEM. Data representative of 2 independent experiments.

4.2.7. Production of a membrane restricted form of TL1A

As detectable levels of both membrane and soluble TL1A had been found both *in vitro* and *in vivo* the next step was to examine the biological function of these alternative forms. To achieve this a membrane restricted mutant of TL1A was required.

Unpublished data from F. Meylan and I. Malm along with published data from the laboratory of S. Targen [165] mapped the region in human TL1A which, if deleted, produced a membrane restricted form. We identified the homologous region in mouse TL1A (Figure 4-6A), amino acids 69 to 93, and produced a construct with that region removed; TL1A Δ69-93.

Transfection of 293T cells with full length TL1A yielded a modest surface expression and ~12.5ng/ml of sTL1A into the culture supernatant. Removal of amino acids 69 to 93 resulted in an increase in surface TL1A expression and reduced the detected sTL1A to ~75pg/ml. This indicated the requirement for amino acids 69-93 in the cleavage of mouse TL1A (Figure 4-6B and C).

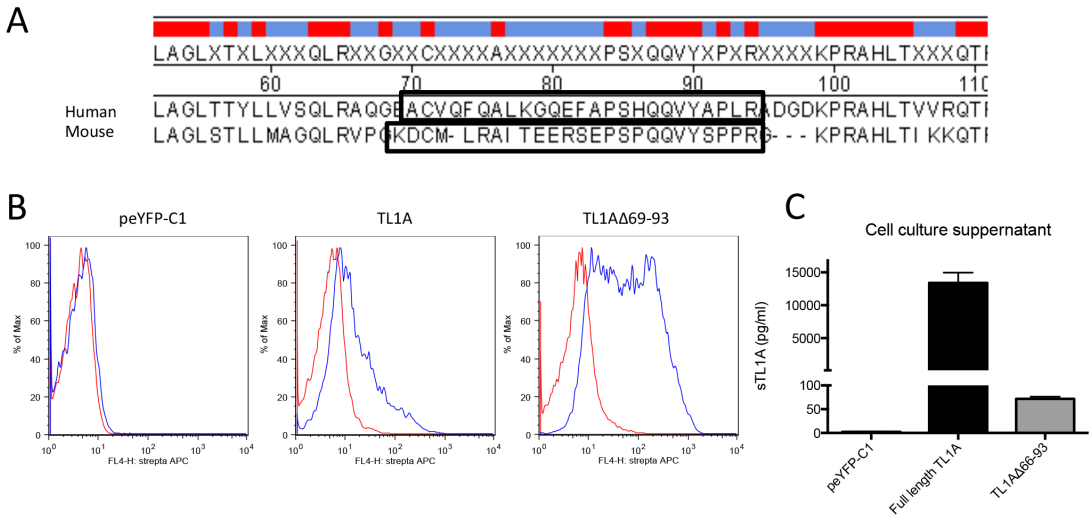

Figure 4-6 *- Design and production of full length and uncleavable TL1A constructs.* ***A*** *Alignment of human and mouse TL1A. The amino acids which when deleted have previously be shown to inhibit cleavage of human TL1A, are indicated and the corresponding region (amino acids 69-93) in mouse TL1A was removed.* ***B*** *Either full length TL1A or TL1AΔ69-93 was cloned into pEYFP-C1 and transfected into 293T cells. Expression of surface TL1A was detected by flow cytometry using Tan 2-2*

(blue) compared to an isotype control (red) on YFP positive cells. ***C*** *The concentration of sTL1A in the media from the transfectants (****B****) was measured using a sTL1A Luminex assay 72hrs post transduction. Error bars are SD of technical replicates, n=2.*

4.2.8. Retrotransgenic overexpression of membrane restricted TL1A promotes pathology

To study the effect of TL1A cleavage *in vivo* we used a retrotransgenic approach to overexpress either TL1A or TL1AΔ69-93 in all compartments of the haematopoietic lineage in a mouse. The empty vector, pMP71 was used as a control[232].

Mice were culled 24 weeks post transfer of transduced bone marrow cells and the spleen, ileum and lung were examined. The vector used for transduction of murine bone marrow contained an IRES GFP thus enabling the tracking of positively transduced cells and the levels of reconstruction of transduced cells within a mouse. The initial transduction of the bone marrow was relatively low (8-14%, Figure 4-7A) however this translated to a much higher proportion of positively expressing differentiated cells. All 3 vectors showed a range of reconstruction efficiency within each group however the groups were comparable to one another (Figure 4-7B). Membrane TL1A expression was examined on different subsets and in all cases TL1AΔ69-93 showed increased surface expression compared to full length TL1A and pMP71. Transduction with full length TL1A did not demonstrate a significant increase in surface TL1A expression over empty vector controls (Figure 4-7C). Levels of sTL1A in the serum were measured. Full length TL1A showed up to a 10 fold increase compared to TL1AΔ69-93 when comparing mice with a similar splenic GFP expression. A strong positive correlation was observed between splenic GFP expression and serum sTL1A (Figure 4-7D, R^2 = 0.9287 and 0.6658 for full length TL1A and TL1AΔ69-93 respectively).

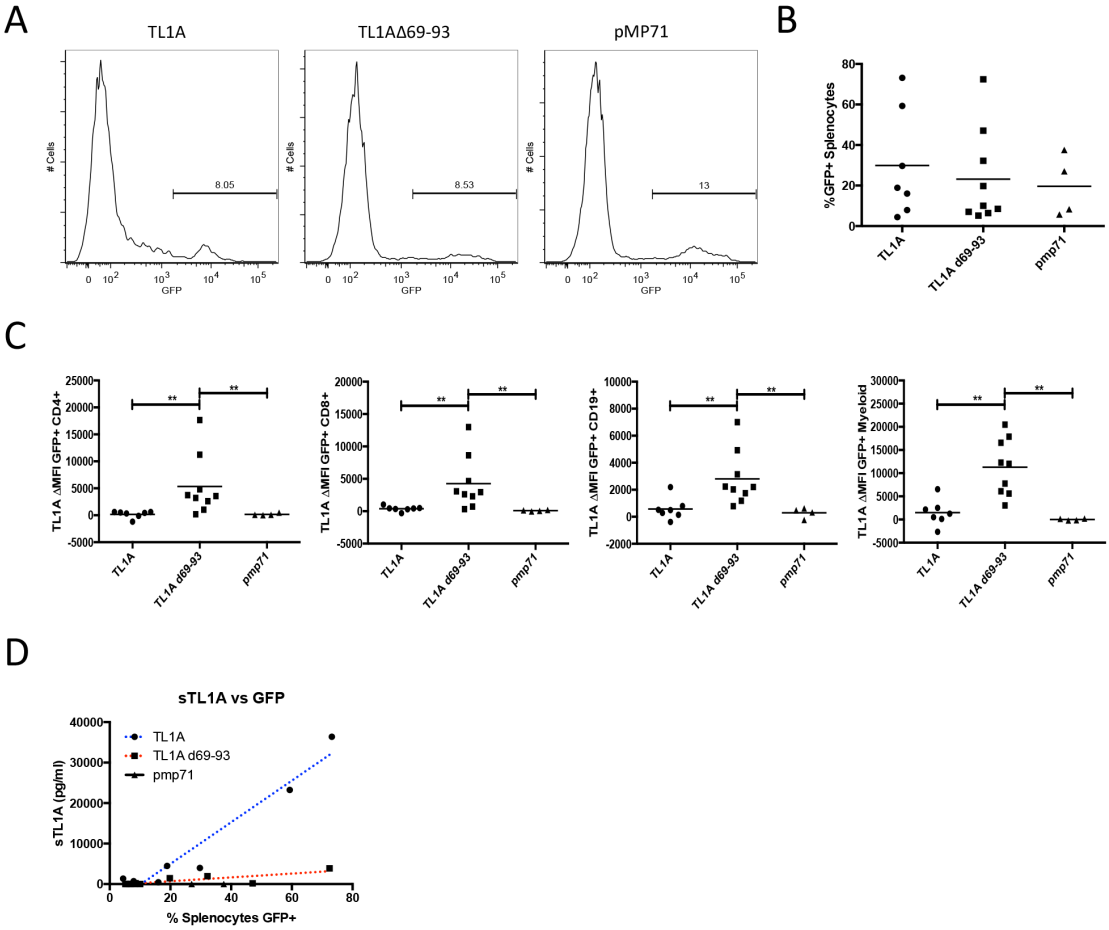

Figure 4-7 *- Production of TL1A retrotransgenic mice. For production of TL1A retrotransgenic mice either full length TL1A or TL1AΔ69-93 was cloned into the pMP71 vector and used to transduce bone marrow prior to transfer into lethally irradiated mice.* ***A*** *Prior to injection transduction efficiency of bone marrow was measured. 24 weeks post transfer of transduced bone marrow mice were sacrificed and the GFP expression measured by flow cytometry within the splenocytes (**B**). The surface expression of TL1A was measured on the indicated subsets within the spleen (**C**) and the level of TL1A within the serum of the mice (**D**). ** indicates 0.01>P>0.001 using the Mann-Whitney U test.*

Previous work established the phenotype of TL1A overexpression in a transgenic system [174, 175], as such we initially decided to focus our efforts on the ileum. By 24 weeks post transduction TL1AΔ69-93 mice showed a significant reduction in weight compared to control retrotransgenics (Figure 4-8A). The weight loss is consistent with intestinal complications. The length of the intestines, measured from the pyloric sphincter to the end of the colon, was increased by 14% and the average number of goblet cells per villi was increased by 72% compared to empty vector control mice (Figure 4-8B and C). Paneth cell hyperplasia, goblet cell hyperplasia,

thickening of the muscularis and lymphoid cell infiltrate into the lamina propria was also observed in TL1AΔ69-93 (Figure 4-8D) compared to controls. There was no obvious phenotype in the ileum histology in the full length TL1A retrotransgenic. qPCR analysis showed an increase in IL-13 in the TL1AΔ69-93 (Figure 4-8E) and a non-significant trend towards an increase in IFN-γ in the full length TL1A. IL-17a showed no change.

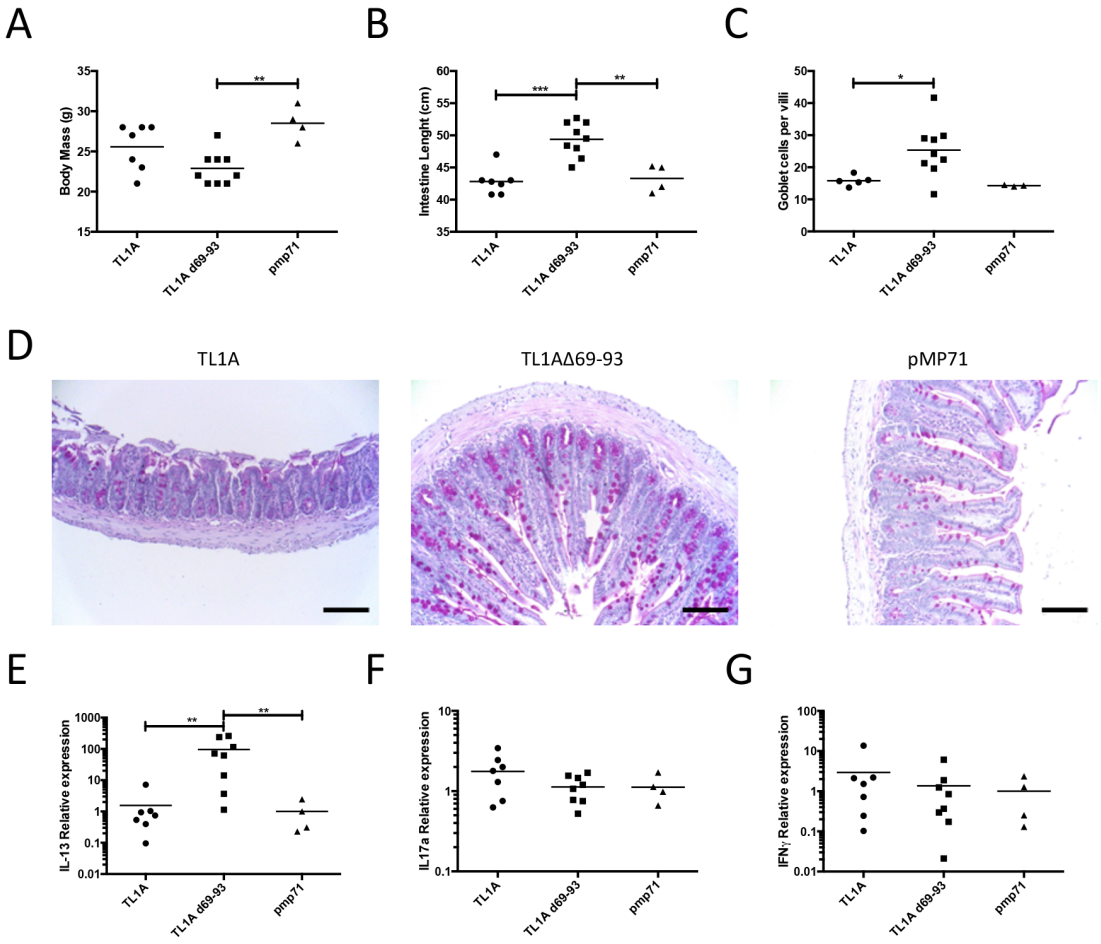

Figure 4-8 *- Phenotypic analysis of intestine. 24 weeks post transfer of transduced bone marrow the mice were culled and weighed (**A**) and the complete length of both the small and large intestines were measured (**B**). Sections of the terminal ileum were taken and PAS stained (**D**, Scale bars are equal to 100μm) and the number of goblet cells per villi were counted (**C**). A minimum of 4 in plane villi were counted per mouse. qPCR was performed on the terminal ileum for Il-13 (**E**), Il-17a (**F**) and IFN-γ (**G**). * indicates 0.05>P>0.01, ** 0.01>P>0.001 and *** 0.001>P>0.0001 using the Mann-Whitney U test.*

Earlier work on transgenic TL1A overexpression did not examine the lungs however, as lack of DR3/TL1A signalling has been shown to decrease the severity of asthma models [138, 159], we examined the lungs for the presence of an inflammatory phenotype. H and E stained sections from the lungs showed perivascular and peribronchiolar infiltrates composed of approximately 90% lymphoid cells with a small number of plasma cells and histocytes in TL1AΔ69-93 retrotransgenic mice (Figure 4-9A). Some of the mice also showed diffuse inflammation in the interstitial space. The histology from full length TL1A and empty vector control mice was physiologically normal. Cytokine mRNA expression was examined by qPCR in the lungs and both IL-13 and IL-17a (Figure 4-9B and C) were elevated in TL1AΔ69-93 mice above full length TL1A and empty vector controls, IFN-γ was not affected (Figure 4-9D). In full length TL1A mice IL-17 was significantly elevated above empty vector controls confirming the presence of a phenotype.

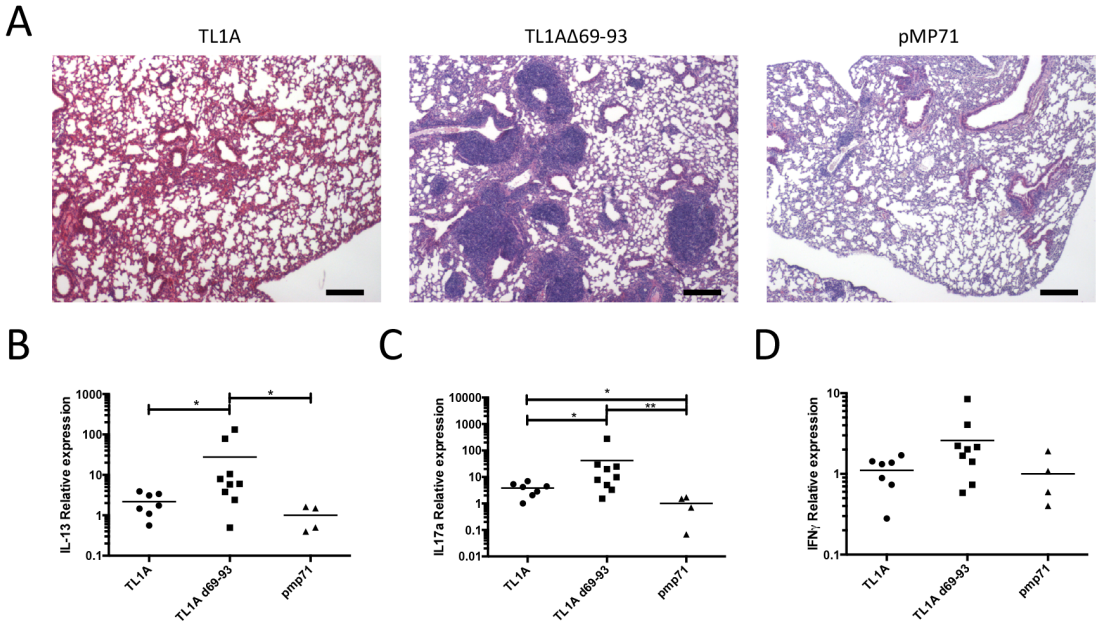

Figure 4-9 *- Phenotypic analysis of lungs. Lungs were taken 24 weeks post transfer of transduced bone marrow and H and E stained (**A**, scale bars are equal to 250μm). qPCR was performed on the lungs for Il-13 (**B**), Il-17a (**C**) and IFN-γ (**D**) * indicates 0.05>P>0.01 and ** 0.01>P>0.001 using the Mann-Whitney U test.*

4.2.9. Production of expression matched TL1A transgenic lines

To further study potential roles of membrane bound TL1A, multiple membrane restricted TL1A founder lines were created at the NCI (NIH, USA) transgenic facility. The mice were produced using a vector which contained a CD2 promoter and the

TL1AΔ69-93 mutation. For comparison to a TL1A transgenic which expressed WT TL1A, line R6 from Meylan *et al* was used[174]. It was found that even though T cells appear incapable of cleaving TL1A in WT mice, when the TL1A was overexpressed it was cleaved into the serum (Figure 4-10C) and so line R6 was renamed Mem+Sol. Of the multiple founder lines generated of the mutant TL1A lines two were chosen to be taken forward for analysis; Mem and Mem Hi. Using a custom Taqman probe which would detect both transgenic and WT TL1A, lines were matched based on mRNA in naïve CD4+ T cells as well as surface expression via flow cytometry. Mem Hi had the same level of TL1A mRNA expression as Mem+Sol but showed much higher levels of surface expression whereas Mem had a lower level TL1A mRNA but the same level of surface expression (Figure 4-10 A and B). The disparity between mRNA and surface was due to cleavage of TL1A which was detected only in the Mem+Sol line(Figure 4-10C). As such the Mem+Sol and Mem lines can be thought to be matched for surface expression of TL1A and the Mem+Sol and Mem Hi can be matched for the potential to produce the same level of total TL1A regardless of state. This may not be exact as the relative half lives of the two forms of TL1A have not been investigated.

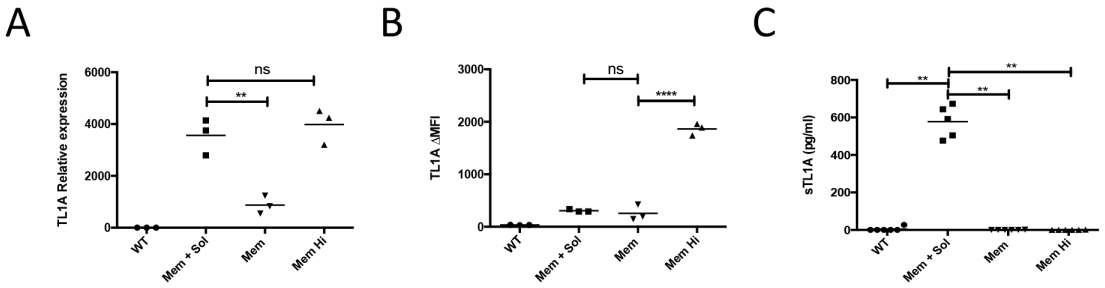

Figure 4-10 *- Matching TL1A transgenic lines. Novel TL1A transgenic lines were produced which carried the TL1AΔ69-93 transgene under a CD2 promoter (Mem and Mem Hi) and compared to WT mice and the previously published CD2 TL1A transgenic strain (Mem+Sol)* ***A*** *and* ***B*** *– Naïve T cells were enriched from spleens taken from WT, Mem+Sol, Mem or Mem Hi mice using a Easysep mouse naïve CD4+ T cell isolation kit. Levels of TL1A mRNA was measured by q-PCR (****A****) using a custom probe against TNFSF15 designed by Life Technologies and the relative expression compared to WT. The membrane expression of TL1A was compared by staining with either anti TL1A (Tan 2-2) or an isotype control (MC 39-16) and the difference in the geometric mean plotted (****B****).* ***C*** *– Serum was taken from 12 week old mice and the level of sTL1A was measured using a custom Luminex assay. Data was analysed pairwise using the students two tailed T test (****A*** *and* ***B****) or the Mann-Whitney U test (****C****), ** 0.01>P>0.001 , **** = P<0.00001, ns = p>0.5.*

4.2.10. TL1A from Mem+Sol T cells is cleaved by a metalloprotease other than MMP9

T cells are unable to cleave WT TL1A however the Mem+Sol mouse has high levels of TL1A in the serum. To demonstrate that this sTL1A is a result of cleavage and not due to spontaneous release from the surface of cells transgenic T cells were cultured for 48 hours either in the presence of IL-7 or activated with anti CD3 and anti CD28. After 48 hours the levels of sTL1A was assessed in the cell culture media. It was found sTL1A increased upon activation and that GM6001 could reduce the levels of sTL1A by up to 50% without decreasing the viability of the cells (Figure 4-11 A and B). Further this activity is not dependent upon MMP9 as levels of sTL1A in the serum of 6 week old mice was not affected when crossed to the MMP9 KO mouse(Figure 4-11C).

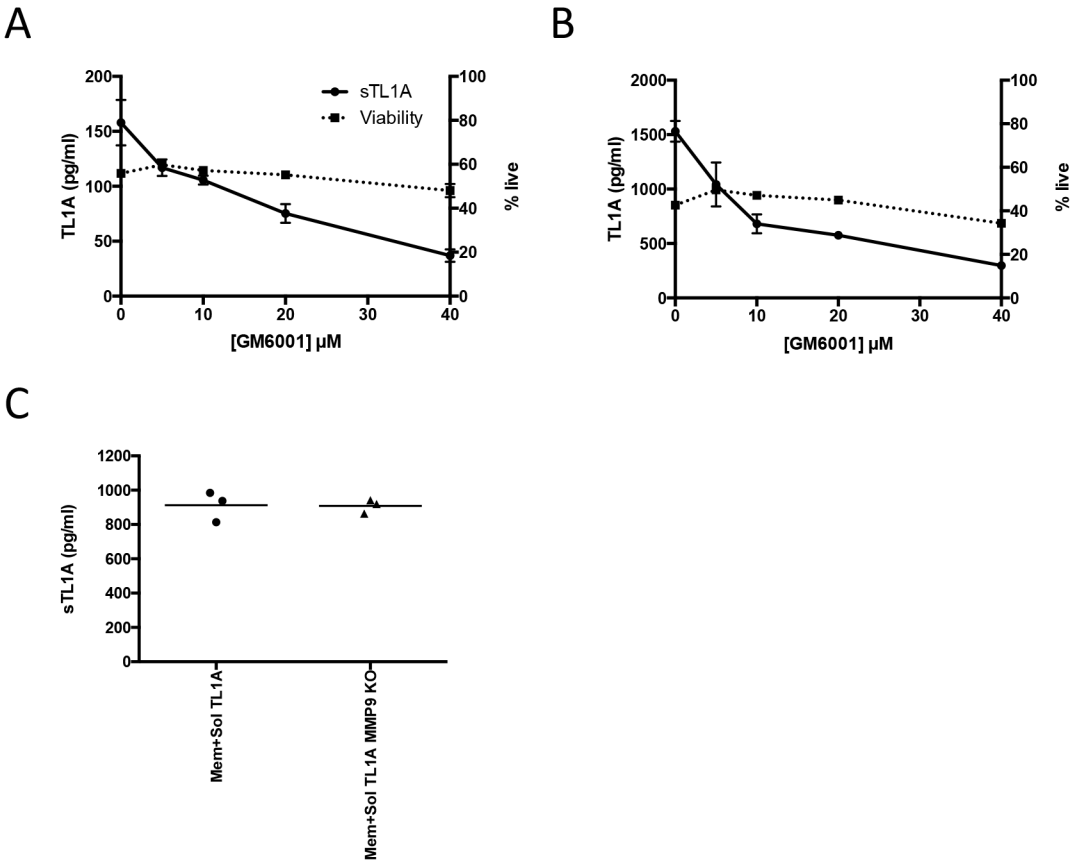

Figure 4-11 *- Transgenic TL1A cleavage from T cells. Purified transgenic T cells from Mem + Sol TL1A mice were cultured for 48 hours in the presence of IL-7 (**A**) or anti CD3/28 (**B**) with the indicated concentration of GM6001. The level of sTL1A in the cell supernatant was measured by Luminex and the cell viability by flow cytometry. Data is representative of 2 independent experiments.* ***C*** *Mem+Sol TL1A*

mice were crossed to the MMP9 KO mouse. Serum was taken at 6 weeks of age and the level of sTL1A measured by Luminex.

4.2.11. Phenotype of different TL1A transgenic strains

The phenotype of TL1A transgenic mice was assessed in multiple organs in 12 week old mice. The various transgenic strains showed no splenomegaly and no profound defects in lymphocyte subtypes (Figure 4-12 A-C). All transgenic mice showed an expansion in Tregs and a non-significant trend towards an increase in T follicular helper cells (Tfh) as a fraction of CD4+ cells (Figure 4-12 D and E). Further T cell activation status, as measured by proportion of CD44hi CD62l low cells was increased in all transgenic lines for Teff (CD4+ FoxP3-) and Treg (CD4+ FoxP3+). However only Mem+Sol and Mem Hi showed an increased for CD8+ cells (Figure 4-12F) suggesting higher total levels of TL1A are required for CD8+ T cell costimulation.

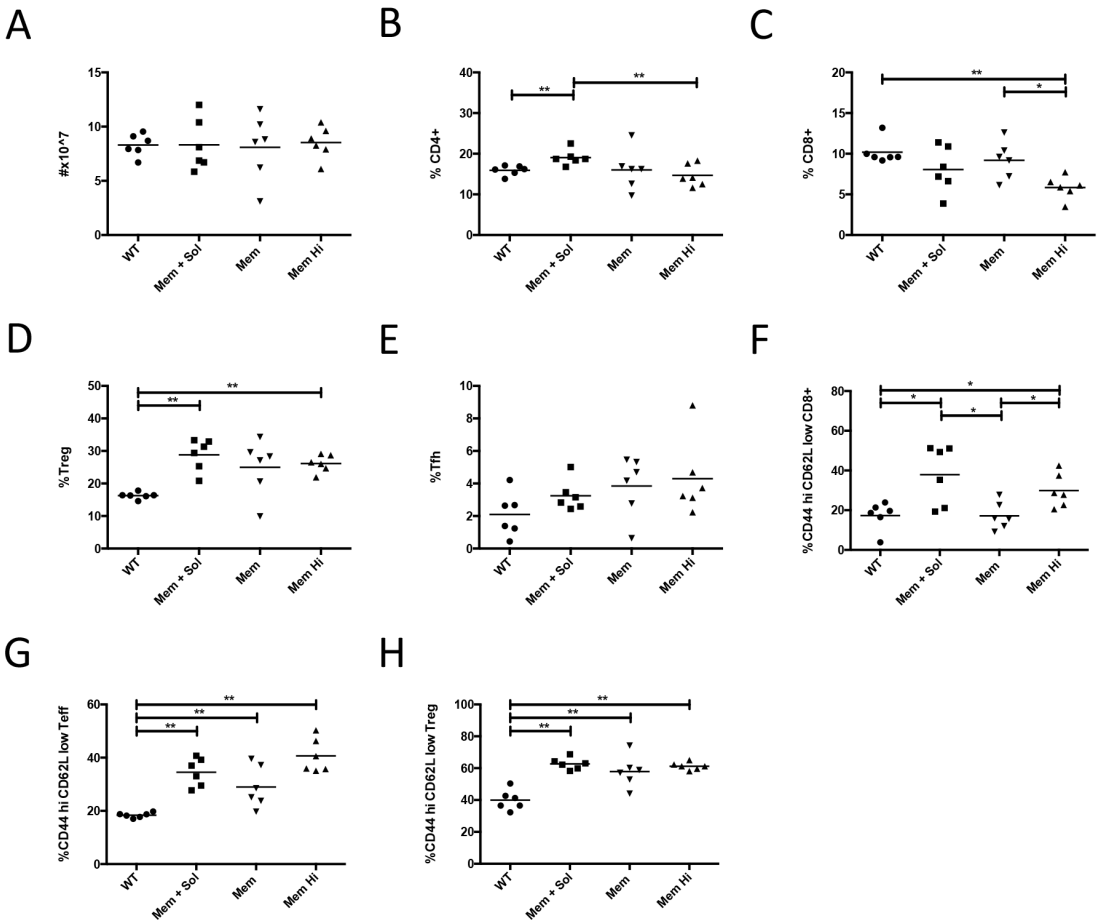

Figure 4-12 *- Phenotypic analysis of TL1A transgenic T cell responses. At 12 weeks of age spleens were taken from all transgenic strains, the cells counted (**A**) and populations analysed by flow cytometry. Samples were stained for CD4 (**B**, fraction of total), CD8 (**C**, fraction of total), Tregs (**D**, CD4+ FoxP3+, fraction of CD4+), Tfh (**E**,*

*CD4+ CD40L+ ICOS+ PD1+ CXCR5+, fraction of CD4+) and the activation status of CD8+, CD4+Teff (FOXP3-) and Treg cell populations (**F-H** respectively) * indicates 0.05>P>0.01 and ** 0.01>P>0.001 using the Mann-Whitney U test.*

The cellular component of the B cell compartment showed increased levels of GC B cells and a trend towards increased class switched (IgM- IgD-) B cells as a proportion of total B cells (Figure 4-13 B and C). There was a mild trend towards increased total IgG, especially IgG2b, in the serum however there were profound increases in total IgA and IgE across all strains compared to WT with maximal levels in Mem+Sol mice (Figure 4-13 G and H). Mem+Sol mice were also the only strain to show increased levels of ANA (Figure 4-13 I) with an incidence of 50% by 12 weeks of age.

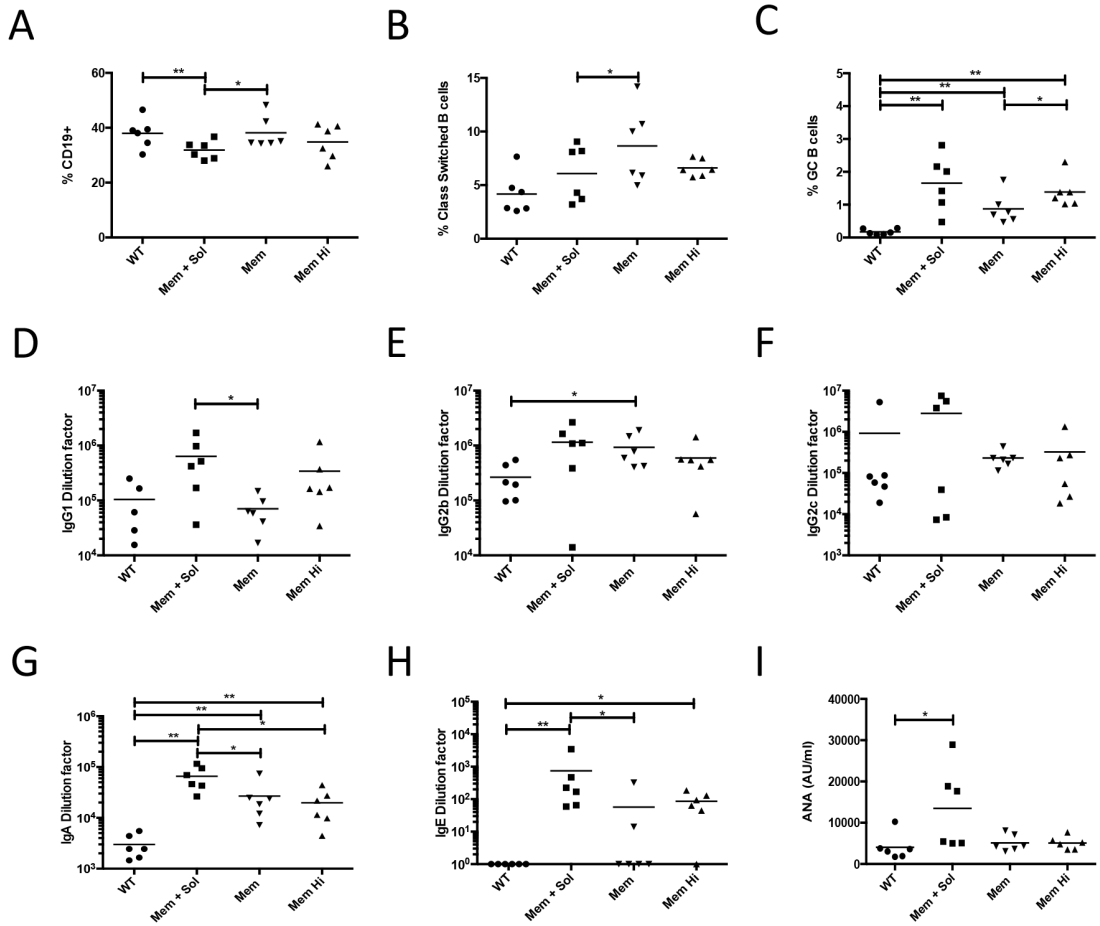

***Figure 4-13** - Phenotypic analysis of TL1A transgenic B cell responses. **A-C** – B cell composition of the spleen from 12 week old mice was assessed by flow cytometry. Cells were stained for B cells (**A**, CD19+, fraction of total) and subsequently for class switched B cell (**B**, IgM- IgD-) and GC B Cells (**C**, GL7+ PNA+) as a fraction of B cells. Serum was collected at the same time and analysed for levels of IgG1 (**D**), IgG2b (**E**), IgG2c (**F**), IgA (**G**) and IgE (**H**) as well as for the presence of anti-nuclear*

*antibodies (**I**, all isotypes). * indicates 0.05>P>0.01 and ** 0.01>P>0.001 using the Mann-Whitney U test.*

The composition of cytokines in the serum of the transgenic mice was assessed. Cytokines were measured using the Bioplex pro mouse 23-plex assay (Figure 4-14 A, Biorad) and the Bioplex pro TGF-β 3 plex assay (Figure 4-14 E-G, Biorad). Of the multiple cytokines measured there were very few cytokines which were significantly different. IL-5 was slightly increased in the transgenic mice with a trend towards dependence on total TL1A (Figure 4-14 B). Despite TL1A being known to be an enhancer of IL-13[174, 175] there was no effect on systemic levels (Figure 4-14 C). Further a group of group of cytokines showed significant down regulation in the Mem+Sol line only; Eotaxin, G-CSF, GM-CSF and KC (Figure 4-14 D-G).

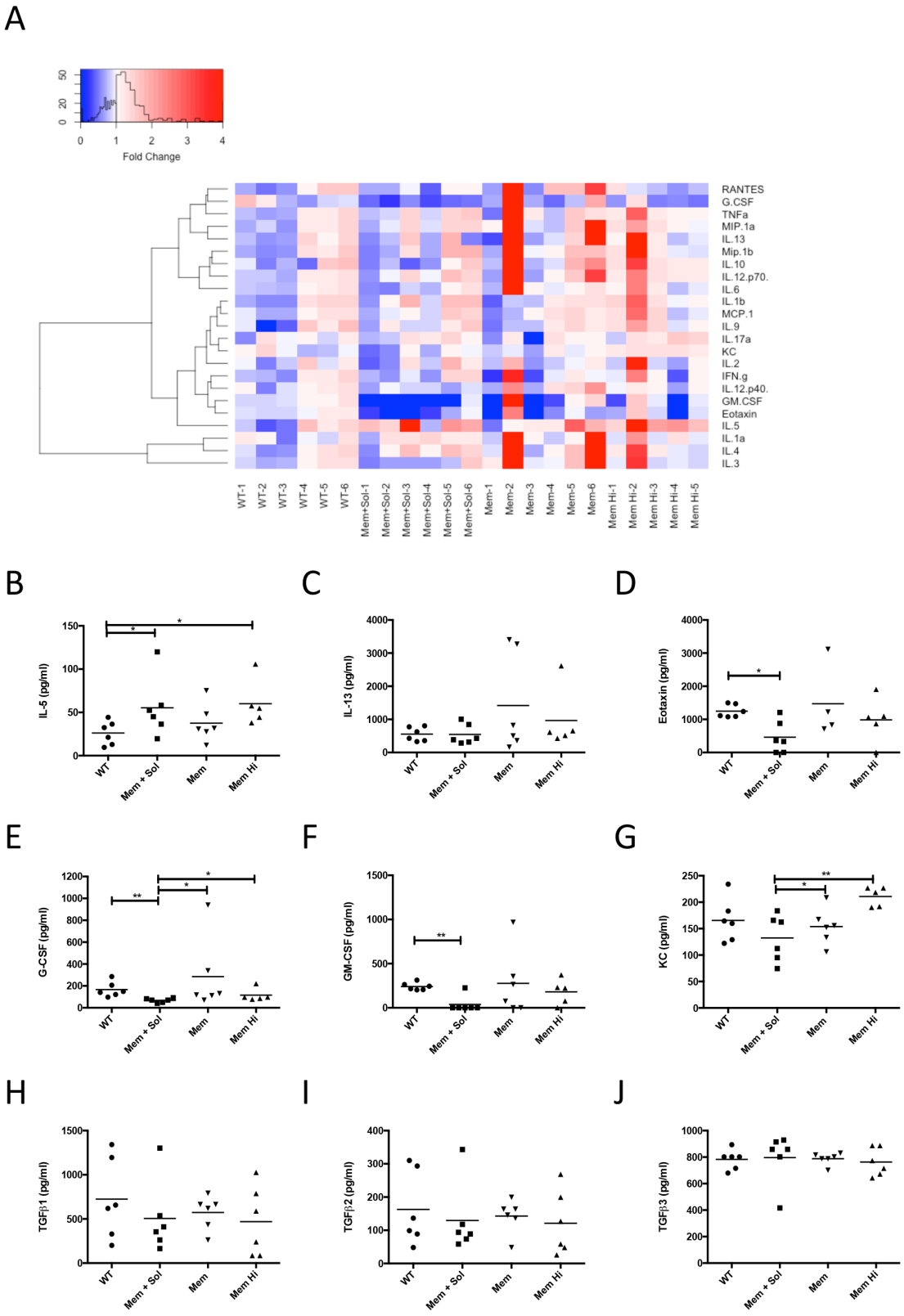

Figure 4-14 *- Serum cytokines in TL1A transgenic mice. Serum was collected from 12 week old mice and analysed using a Luminex based assay.* ***A*** *– Relative abundance of all cytokines measured using the Bio-plex pro 23-plex assay. Each column represents an individual mouse and are grouped according to genotype, the cytokines are given in rows and are hierarchically clustered.* ***B-G*** *cytokines of interest*

*or which show significant differences from **A** have been plotted. **H-I** A separate Luminex based panel was run on serum samples for the 3 isoforms of TGF-β. * indicates 0.05>P>0.01 and ** 0.01>P>0.001 using the Mann-Whitney U test.*

Given the previously described phenotype in the ileum for TL1A transgenics[174, 175, 213], the effect of the membrane restricted phenotype within the gut was assessed. Sections of the terminal ileum were taken at 6, 12 and 18 weeks and both the length of the small bowel and the goblet cells per villi reported (Figure 4-15 A-D). It was found that whilst all transgenic mice developed goblet cell hyperplasia as well as an increased length of the small bowel, that development of this phenotype was significantly reduced in the mice that did not express both membrane and soluble TL1A. Further the examination of levels of key cytokine transcripts in the terminal ileum further demonstrated differences between membrane restricted strains and Mem+Sol mice (Figure 4-15 E-J). All transgenic strains showed a 40-50 fold increase in IL-13 mRNA at week 12 whereas only the Mem+Sol mouse showed an increase in IL-4 and a trend towards a decrease in IL-17a. In contrast, the membrane restricted form had the greatest increase in IL-9 in both Mem and Mem Hi suggesting this was a feature of membrane restricted TL1A transgenics. Col6a1, which is dependent on IL-13 signalling[233] is also upregulated in all transgenic strains and reflects the total level of TL1A.

A

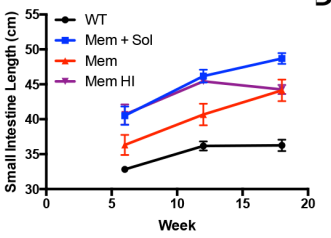

B

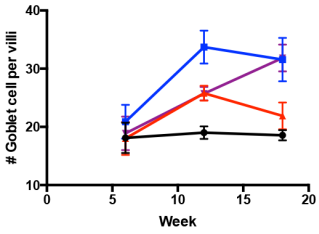

C

Comparison	Goblet cells per villi	Intestine Length
WT vs Mem+Sol	0.0001	< 0.0001
WT vs Mem	0.0222	0.0001
WT vs Hi Mem	< 0.0001	< 0.0001
Mem+Sol vs Mem	0.0151	0.0001
Mem+Sol vs Hi Mem	[+]0.1952	[+]0.067
Mem vs Hi Mem	0.0503	0.0025

D

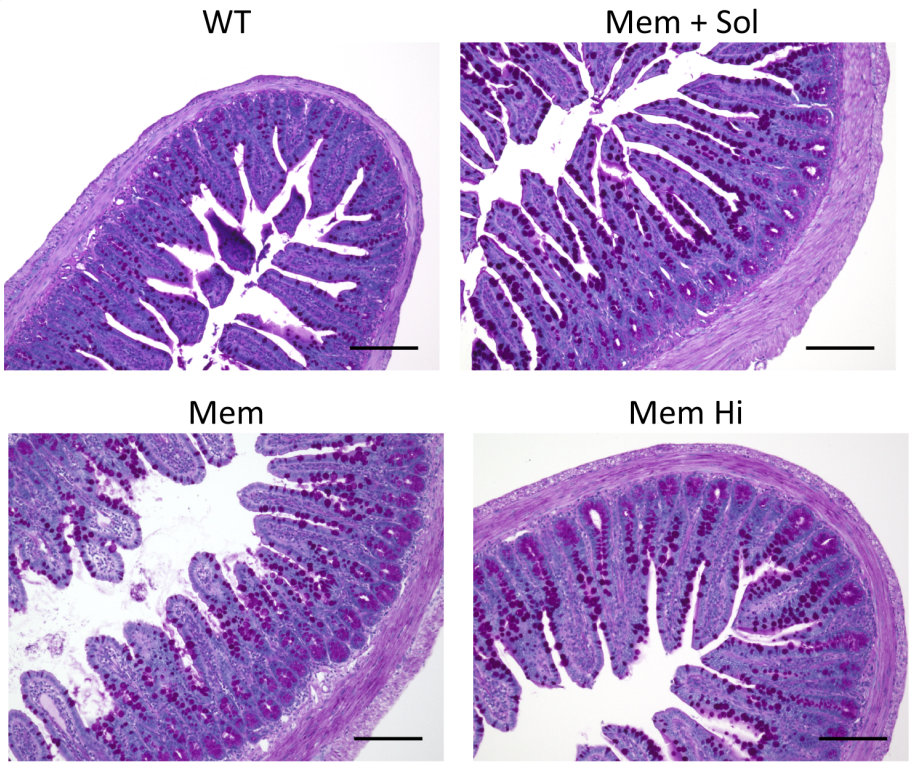

E

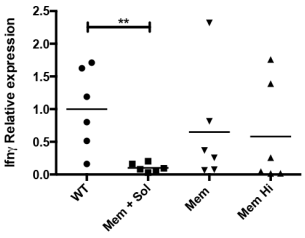

F

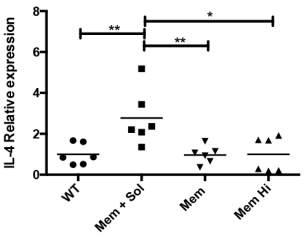

G

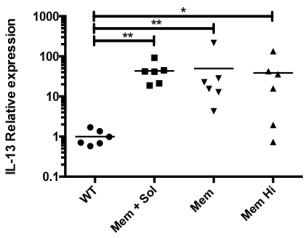

H

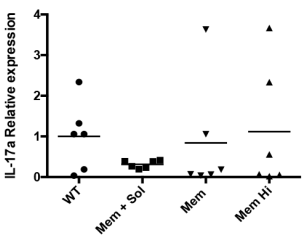

I

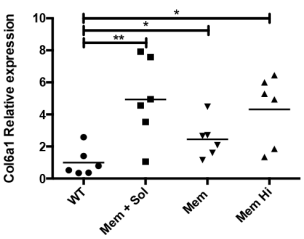

J

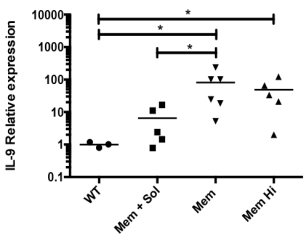

Figure 4-15 *- TL1A transgenic mice develop spontaneous small bowel pathology.* ***A-D*** *The small bowel was taken and measured (**A**). Sections were taken from the terminal ileum at 6, 12 and 18 weeks of age and stained with PAS. The mean number of goblet cells per villi was calculated with at least 3 full size in-plane villi counted per section in 3-6 mice per genotype per time point (**B**). Statistical analysis was carried out for **A** and **B** using a two way ANOVA for genotype and the P values for each pairwise comparison reported in the table, + indicates P>0.05 (**C**). Examples of the pathology observed in 12 week old mice are shown in **D**. Scale bars are equal to 150μm.* ***E-J*** *Small sections of the terminal ileum (excluding payers patches) were taken, RNA extracted and processed for qPCR to measure the indicated genes. Expression is relative to WT littermates. * indicates 0.05>P>0.01 and ** 0.01>P>0.001 using the Mann-Whitney U test.*

As the membrane restricted retrotransgenic TL1A mouse displayed overt lung pathology this was assessed at 6, 12 and 18 weeks in the transgenic system. The membrane restricted mice only developed mild perivascular and peribronchular aggregates which worsened with age. There was occasional small lymphoid aggregates also observed in the WT and Mem+Sol mice but at a lower frequency and smaller in size (Figure 4-16).

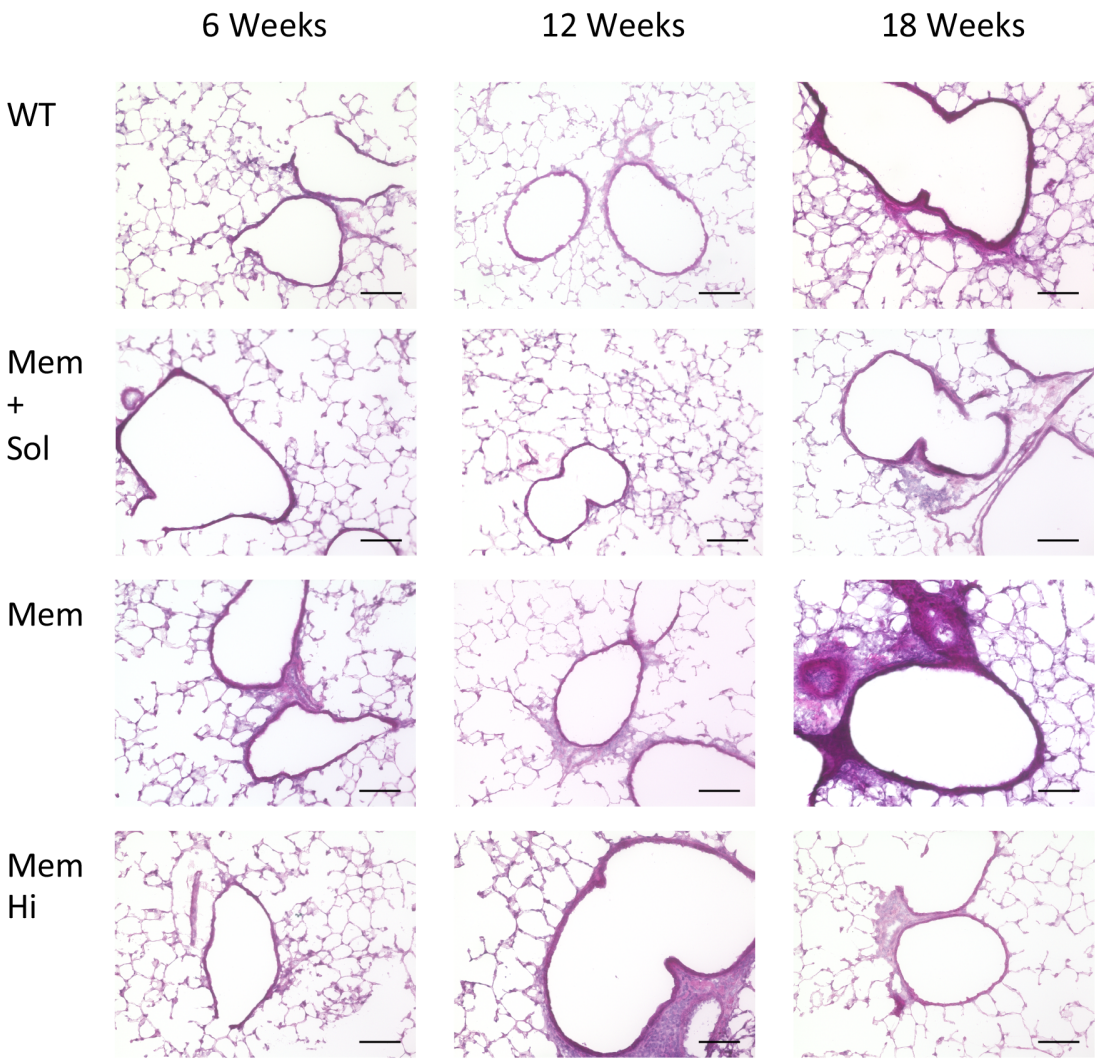

Figure 4-16 *- Mild lung pathology in TL1A transgenic mice. Lungs were taken from transgenic mice at 6, 12 and 18 weeks and frozen sections were processed for H and E staining. Images are representative of 4+ mice per group. Scale bar represents 100μm.*

To assess if the mild pathology observed in the lung was functionally relevant the mice were submitted to a methacholine challenge at 12 weeks of age. Methacholine induces smooth muscle contraction in the airway when breathed in. Challenge with methacholine is used in humans and mice as a test for airway hyper-responsiveness in asthma[234]. Only the Mem+Sol strain was found to have a significant increase in airway resistance in response to methacholine compared to WT mice (Figure 4-17 A). Further this increase was heterogeneous within the strain.

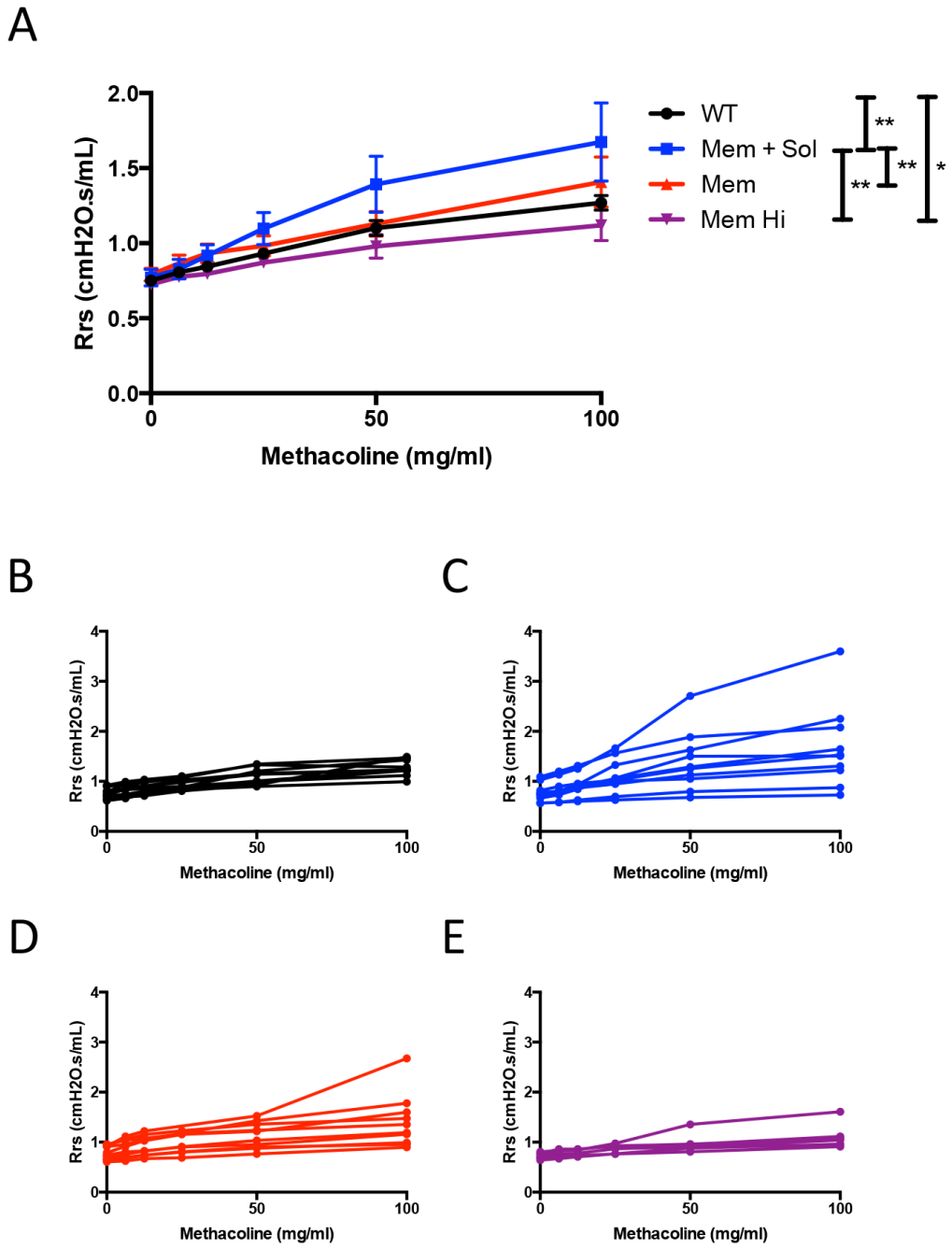

Figure 4-17 *- Methacholine sensitivity of TL1A transgenic mice.* ***A*** *Airway resistance was measured in response to methacholine challenge on 12 week old intubated TL1A transgenic or WT control mice.* ***B-E*** *– Individual mice from* ***A*** *separated by genotype. Data is combined from 3 independent experiments. Error bars represent SEM. * indicates 0.05>P>0.01 and ** 0.01>P>0.001 using two way ANOVA for genotype.*

The postcaval lobe was removed from the lungs of 12 week old mice and used for qPCR analysis of key genes (Figure 4-18). There was a minimal effect of TL1A on IFN-γ and IL-4 however IL-13, IL-17 and to a lesser extent IL-5 were upregulated

with Mem being the highest expression. This suggests a certain level of TL1A is required for this expression however if the level is either too high or too low then this phenotype is lost. Col6a1 was upregulated and, as for the ileum, reflected the total level of TL1A within the animal. The IL-9 expression pattern also matched the ileum where membrane restricted transgenic mice were able to promote its expression but not when sTL1A was present in addition to membrane bound (Figure 4-18 F).

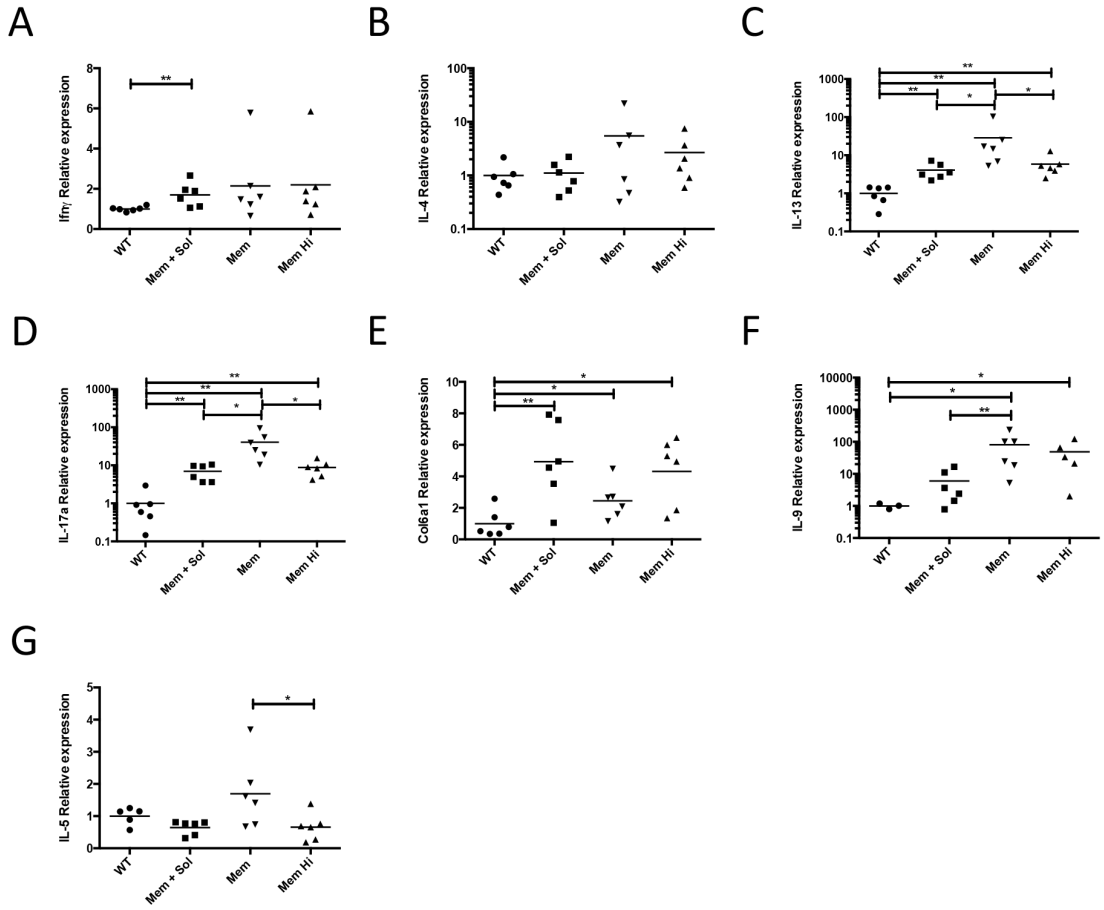

Figure 4-18 *- Lung transcriptional profile in TL1A transgenic mice.* ***A-G*** *RNA was extracted from the postcaval lobe from 12 week old transgenic and qPCR was performed for expression analysis of the indicated transcripts. Expression is relative to WT littermates. * indicates 0.05>P>0.01 and ** 0.01>P>0.001 using the Mann-Whitney U test.*

As the qPCR data for the lungs indicated that there may be some differences between the transgenic strains that can be attributed to the presence of only membrane TL1A, an RNASeq based analysis was performed on the RNA extracted from the lungs. The data from the sequencing was of a good quality and showed clustering by genotype in principle component 1 in a principal component analysis (See Appendix I for clustering and quality control graphs). Each transgenic line was

compared to WT and gene lists generated for genes that were either up or down regulated and had an adjusted p value of less than 0.05. These gene lists were then compared between the different transgenic strains to highlight genes which may be dependent on either membrane restricted TL1A or the addition of soluble TL1A (Figure 4-19). For down regulated genes there were 37 genes which were common to all strains (Figure 4-20 A), 114 genes that were shared by both membrane restricted strains (Figure 4-20 C) and 108 genes which were uniquely down regulated in the Mem+Sol transgenic (Figure 4-20 B). For upregulated genes there were 117 genes which were common to all strains (Figure 4-21 A), 10 genes that were shared by both membrane restricted strains (Figure 4-21 C) and 38 genes which were uniquely down regulated in the Mem+Sol transgenic (Figure 4-21 B). Gene ontology analysis for all 6 sets of genes is given in Appendix III. The top 40 genes for significant changes in magnitude of expression are given below (Table 4-2). The full gene lists are given in appendix II.

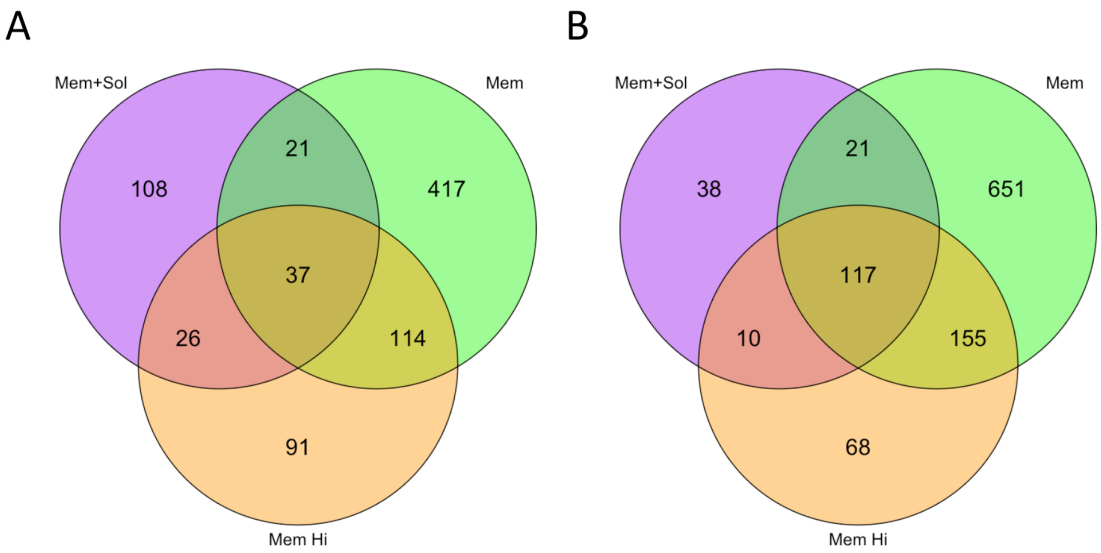

Figure 4-19 *- RNASeq analysis of TL1A transgenic lungs. RNA was extracted from the postcaval lobe of 12 week old transgenic and WT mice prepared for and sequenced on a HiSeq (Ilumina). Differential expression was calculated with DESeq using a generalised linear model comparing each transgenic line to WT in a pairwise manner. Genes were considered to be significantly differentially expressed which had an adjusted P value <0.05 using the Benjamini-Hochberg method. The number of genes that were either down regulated (A) or up regulated (B) compared to WT are indicated for each transgenic line.*

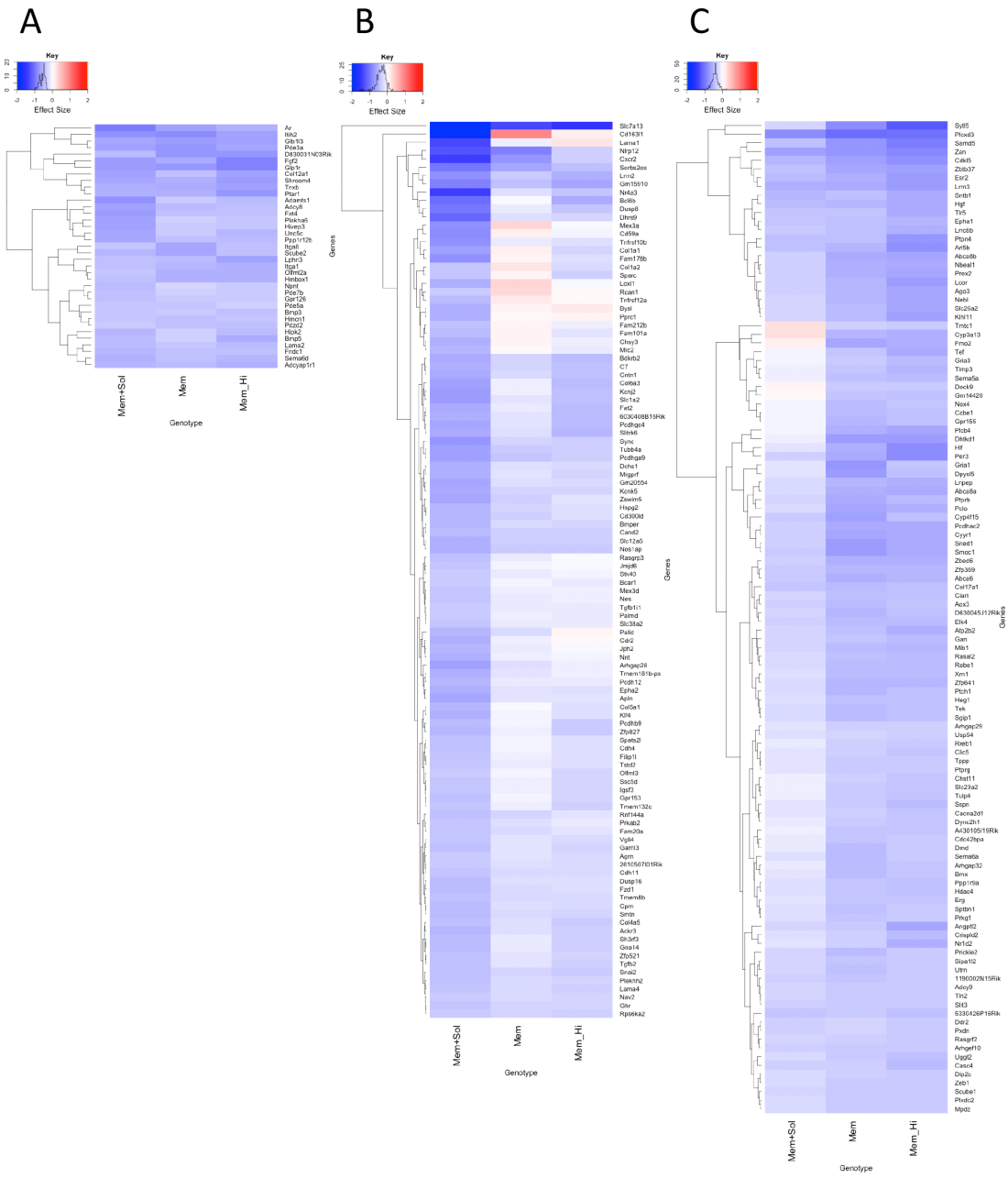

Figure 4-20 *- Down regulated genes in TL1A transgenic lungs. Heat maps of down regulated genes in TL1A transgenic mouse lungs compared to WT mice which have an adjusted P value of <0.05 in either all lines (**A**), Mem+Sol only (**B**) or Mem and Mem Hi but not Mem+Sol (**C**). Genes have been hierarchically clustered.*

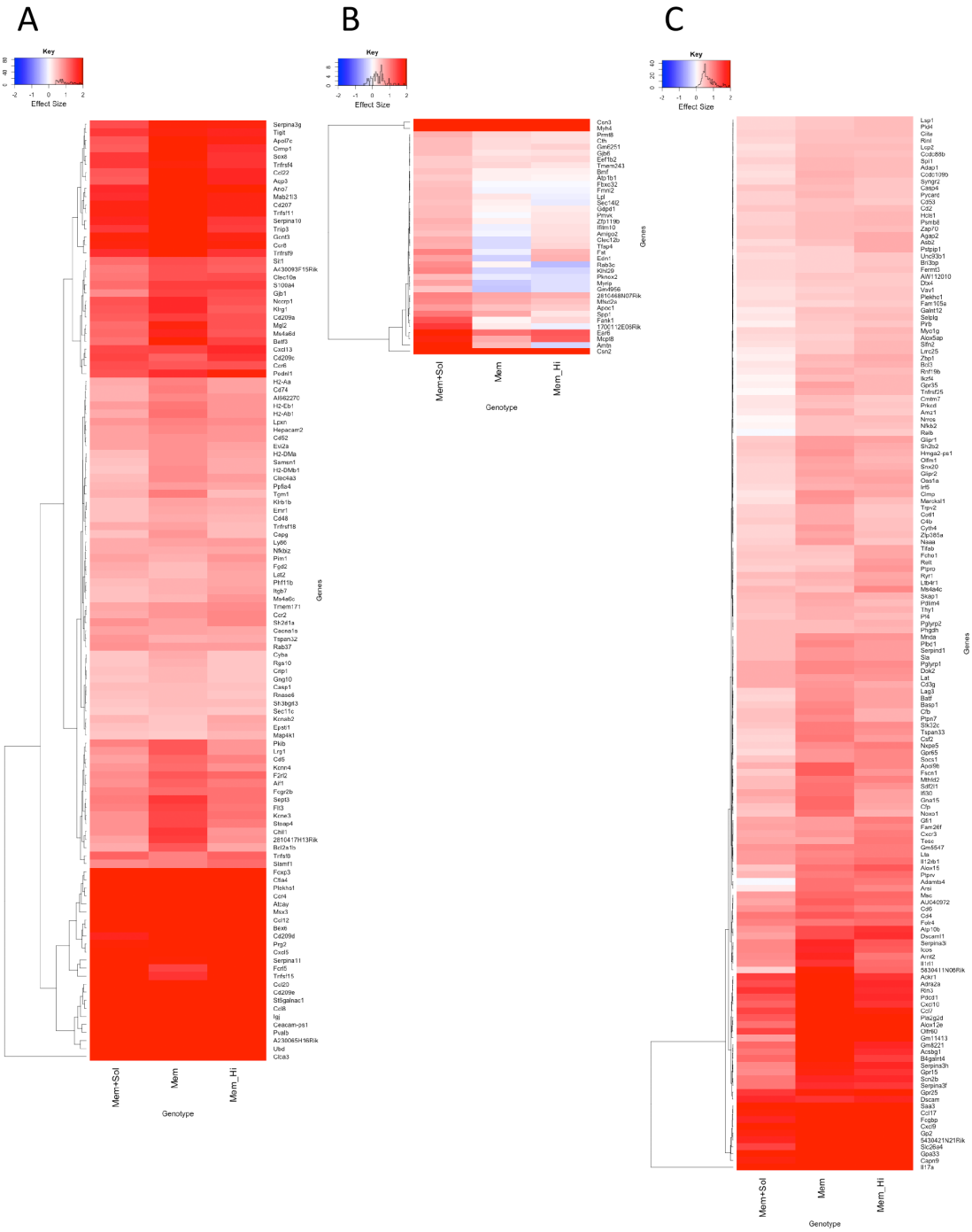

Figure 2-21 *- Up regulated genes in TL1A transgenic lungs. Heat maps of up regulated genes in TL1A transgenic mouse lungs compared to WT mice which have an adjusted P value of <0.05 in either all lines (**A**), Mem+Sol only (**B**) or Mem and Mem Hi but not Mem+Sol (**C**). Genes have been hierarchically clustered.*

Decreased			Increased		
All	Mem+sol only	Mem and Mem Hi only	All	Mem+sol only	Mem and Mem Hi only
Glp1r	Slc7a13	Plcxd3	Clca3	Csn3	Il17a
Itih2	Cd163l1	Sytl5	A230065H16Rik	Myh4	Capn9
Fgf2	Nr4a3	Samd5	Ubd	Csn2	Gpa33
Ar	Cxcr2	Zan	Ceacam-ps1	Amtn	Slc26a4
Pde3a	Lama1	Cdkl5	Pvalb	Ear6	Saa3
Glb1l3	Nlrp12	Per3	Ccl20	Mcpt8	Fcgbp
D830031N03Rik	Dhrs9	Dhtkd1	Cd209e	1700112E06Rik	Ccl17
Shroom4	Bcl6b	Hlf	Igj	Fank1	Cxcl9
Ptar1	Dusp8	Smoc1	St6galnac1	Spp1	Gp2
Tnxb	Sorbs2os	Arl5b	Ccl8	Klhl29	5430421N21Rik
Col12a1	Gm15910	Sned1	Msx3	2810468N07Rik	Olfr60
Adamts1	Cd59a	Lrrn3	Foxp3	Fst	Ccl7
Fat4	Tnfrsf10b	Zbtb37	Atcay	Mfsd2a	Gm11413
Lphn3	Fam178b	Esr2	Ctla4	Rab3c	Alox12e
Adcy8	Mex3a	Cyyr1	Plekhs1	Apoc1	Pla2g2d
Scube2	Lrrn2	Lcor	Ccr4	Edn1	Pdcd1
Hmbox1	Sync	Pclo	Prg2	Myrip	Gpr25
Adcyap1r1	Slc1a2	Pcdhac2	Cxcl5	Clec12b	Rln3
Ppp1r12b	Kcnj2	Abca8b	Ccl12	Zfp119b	Cxcl10
Unc5c	Tubb4a	Ptpn4	Tnfsf15	Prmt8	Adra2a
Sema6d	Pcdhga9	Fmo2	Serpina11	Tfap4	Gm8221
Itga1	Arhgap28	Plcb4	Bex6	Ifitm10	Serpina3h
Olfml2a	Col1a1	Prex2	Cd209d	Cth	Acsbg1
Itga8	Col6a3	Dpysl5	Gcnt3	Pmvk	Ackr1
Hivep3	Gm20554	Klhl11	Ccr8	Lpl	B4galnt4
Fndc1	Pcdhgc4	Nbeal1	Ano7	Gdpd1	Gpr15
Bmp5	Apln	Nebl	Tnfrsf9	Fmnl2	Scn2b
Lama2	Zswim5	Slc26a2	Mab21l3	Gjb6	Dscam
Plekha6	Bdkrb2	Gria1	Cd207	Pknox2	Serpina3f
Hipk2	Slitrk6	Ago3	Serpina10	Gm6251	5830411N06Rik
Pdzd2	Kcnk5	Abca8a	Tnfsf11	Bmf	Serpina3i
Hmcn1	Cntn1	Hgf	Fcrl5	Fbxo32	Dscaml1
Bmp3	Fat2	Zbed6	Tnip3	Amigo2	Icos
Gpr126	6030408B16Rik	Cyp3a13	Ccl22	Sec14l2	Atp10b
Npnt	Pprc1	Cyp4f15	Aqp3	Gm4956	Arnt2
Pde5a	Nos1ap	Ptprb	Sox8	Atp1b1	Il1rl1
Pde7b	Loxl1	Abca6	Apol7c	Tmem243	Cd4
	Epha2	Lnpep	Serpina3g	Eef1b2	AU040972
	Bysl	Sntb1	Tigit		Alox15
	Tmem181b-ps	Tlr5	Tnfrsf4		Msc

Table 4-2 *– Differentially regulated genes in transgenic lungs. Top 40 genes for the subsets indicated ordered by descending magnitude of differential expression for either up or down regulated genes.*

4.2.12. Chronic delivery of sTL1A promotes intestinal pathology

To study the role of chronic sTL1A exposure a preliminarily experiment was carried out where mice were implanted subcutaneously with osmotic pumps which were set to secrete 500ng of recombinant sTL1A per day for 6 weeks. After 6 weeks the lungs, spleen and ileum were assessed for presence of a phenotype. In contrast to the transgenic mice no effect was observed on T cell activation status or Treg numbers within the spleen (Figure 4-22 A and B). In the ileum, goblet cell hyperplasia and a small significant increase in the length of the gut were observed, along with decreased IFN-γ and increased IL-13 mRNA (Figure 4-22 C-F). However no effect was observed in the lungs (Figure 4-22 G and H). There was also a small non-significant increase in total IgA in the serum (Figure 4-22 I). The same cell populations in the spleen and the same cytokines in the lung as for the analysis of the TL1A transgenic mice were carried out, however much of the negative data has been omitted for brevity.

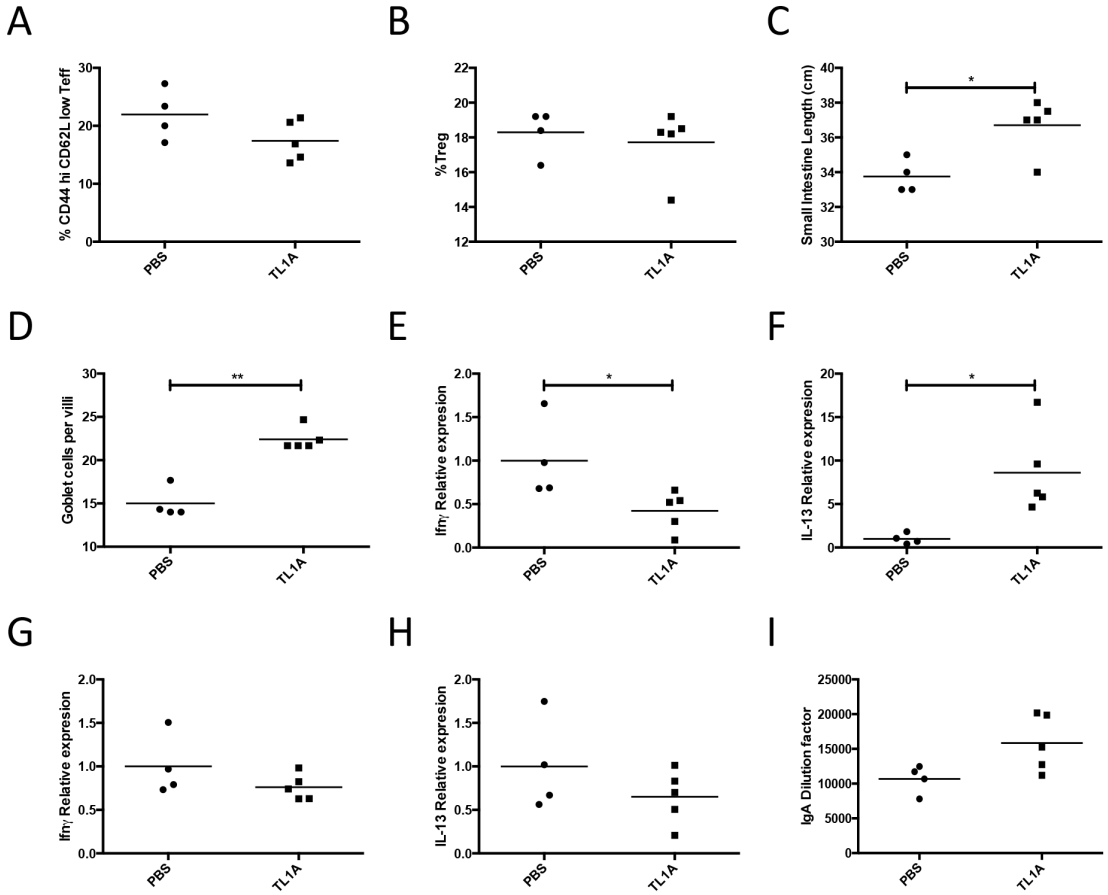

Figure 4-22 *- Continuous administration of sTL1A promotes small bowel pathology. Osmotic pumps were implanted subcutaneously on the back of a mouse for 6 weeks and set to deliver 500ng of TL1A per day or PBS alone at a rate of 0.15 µl per hour.* ***A*** *and* ***B*** *Spleens were taken and analysed by flow cytometry for activation status of Teff (****A****, CD4+, FoxP3-) and fraction of Tregs out of total CD4+ (****B****). The small bowel was taken and measured (****C****).* ***D*** *Sections were taken from the terminal ileum and stained with PAS. The mean number of goblet cells per villi was calculated with at least 3 full size in-plane villi counted per section.* ***E-H*** *- Small sections of the terminal ileum (****E*** *and* ***F****, excluding Peyer's patches) and the postcaval lobe (****G*** *and* ***H****) were taken, RNA extracted and processed for qPCR to measure the indicated genes. Expression is relative to PBS treated group.* ***I*** *– Serum was taken and total levels of IgA measured. * indicates 0.05>P>0.01 and ** 0.01>P>0.001 using the Mann-Whitney U test. Data is from a single experiment.*

4.3. Discussion

As soluble and membrane bound forms of other TNF superfamily ligands have been shown to be functionally distinct we decided to explore this phenomenon with respect to TL1A[71, 229].

We have demonstrated that we can detect expression of membrane bound TL1A using Tan 2-2 in flow cytometry and developed a sensitive Luminex based assay for the detection of sTL1A from cell culture supernatant and serum.

We showed membrane TL1A is upregulated upon *in vitro* stimulation of T cells by 24 hours with maximal expression by 48 hours however we were unable to detect the presence of sTL1A in the cell culture supernatant in isolation and also in a co-culture system with 293T cells. These data are consistent with previous publications which claim TL1A is not cleaved from the surface of WT T cells *in vitro*[164]. Interestingly TL1A was found in serum from Mem+Sol TL1A transgenic mice and in isolated T cell *in vitro* cultures. Further production of sTL1A was inhibited *in vitro* with the metalloprotease inhibitor GM6001 and was increased in response to TCR stimulation. This indicates that T cells have the capacity to cleave TL1A from T cells both in isolation and *in vivo*. As overexpression was required for TL1A cleavage this suggests a degree of disregulation of TL1A homeostasis is required. One possibility is that TL1A may exist in a complex in WT T cells that protects it from cleavage. However overexpression may result in the presence of TL1A outside of this hypothetical complex due to lack of overexpression of other members of this complex thus rendering it susceptible to cleavage.

Expression of both membrane and soluble TL1A was detected on BMDCs and LPS stimulation increased the levels of both. This was surprising as TL1A mRNA is upregulated on DCs in response to LPS[159] and we would not have expected to find such high constitutive expression of membrane bound TL1A on BMDCs. The expression of TL1A may be due to activation during the production of the BMDCs rather than the LPS stimuli. The cleavage of TL1A from BMDCs was also inhibited with GM6001 however the effect of the inhibition was most pronounced with 5μM of inhibitor with LPS stimulation. This implies that a protease that has the capacity to cleave TL1A is upregulated upon activation via TLR4. As LPS is also known to increase TL1A expression[159] there may be a link between TL1A expression and expression of its protease suggesting that DCs may be a major source of predominantly sTL1A.

To study expression of membrane and soluble forms of TL1A *in vivo* we utilised infection of C57BL/6 mice with *Salmonella typhimurium.* Previous work had demonstrated an increase in splenic TL1A mRNA and expression of TL1A protein on F4/80+ cells by immunochemistry in response to infection. It was also shown that DR3/TL1A signalling was required for optimal clearance of infection[160]. The mice developed splenomegaly indicating infection and expression of membrane TL1A was observed on T cells (CD4+ and CD8+) and on macrophages (F4/80+). Membrane TL1A on all cells peaked between days 2 and 4 followed by a rapid decline in expression and then a second increase in expression on day 14. These kinetics followed the observed expression of TL1A mRNA previously reported [160]. Soluble TL1A was detected from day 4 post infection and it remained at a steady level of expression. The steady level of expression implies two possibilities. Either sTL1A has a reasonably long half-life in the serum thus the drop in expression observed on the different cellular subsets examined was not long enough to observe a subsequent drop in sTL1A or a cell other than the ones assayed produces sTL1A.

The ultimate aim of our investigations was to determine if either membrane bound or soluble TL1A differed in function. To assess this TL1A was cross linked using an antibody against a N terminal tag on the protein to mimic a membrane bound form of TL1A however this did not highlight any difference in the ability of TL1A to costimulate T cells.

Previous unpublished work by F. Meylan and I. Malm, along with published work from the laboratory of S. Targan[165], highlighted the region of human TL1A required to prevent cleavage from the surface of cells. We identified the homologous region in mouse TL1A as amino acids 69 to 93 and removed it through PCR (TL1AΔ69-93). Initially we expressed the two forms of TL1A in 293T cells and showed that the membrane restricted form yielded very little TL1A in the cell culture supernatant and had a high surface expression compared to the full length form.

A recent publication by Hedl *et al*[142] claimed ADAM17 was able to cleave TL1A however they did not directly prove this. They demonstrated that TL1A cleavage from human monocyte derived macrophages was inhibited by the metalloprotease inhibitor TAPI-1 and by the actions of tissue inhibitor of metalloprotease (TIMP) 3 but not TIMP 1 or 2[142]. Whilst this does indeed suggest ADAM17 as being able to cleave TL1A it is by no means certain as the TIMPs and TAPI-1 are promiscuous in their inhibition. To investigate potential proteases responsible for the cleavage of TL1A protease cleavage sites were predicted *in silico* using PROSPER[223]. This

identified MMP9 as being the only protease cleavage consensus sequence within the known cleavage site of murine TL1A. To test this, production of sTL1A from BMDCs from MMP9 KO mice was measured. It was found lack of MMP9 had no effect on the expression levels of sTL1A compared to WT BMDCs. Further upon crossing of the Mem+Sol TL1A transgenic to the MMP9 KO mouse there was no effect on serum TL1A suggesting that MMP9 either does not cleave TL1A or is redundant. It was shown however that siRNA mediated knock down of ADAM17 did reduce sTL1A produced from WT BMDCs showing that ADAM17 is at least one of the metalloproteinases responsible for cleaving TL1A.

Using the TL1A membrane restricted mutant initially a retrotransgenic and subsequently transgenic approach was taken to study the effect of different forms of the ligand *in vivo*.

The TL1A constructs were cloned into the retroviral vector pMP71 and used to transduce murine bone marrow prior to transfer into lethally irradiated hosts. All constructs were expressed in multiple members of the haematopoietic lineage in mice with equal efficiency between the groups. The expression patterns of membrane and soluble TL1A mimicked the pattern observed from transfection into 293T cells. The full length TL1A retrotransgenic expressed very little surface TL1A above the empty vector control but had high serum TL1A whereas the TL1AΔ69-93 showed high expression of membrane TL1A and a lower level of sTL1A. It should be noted that there was still a significant level of sTL1A in the serum of the membrane restricted form compared to controls. This may be due to the level of overexpression and the release of TL1A from dying cells or endogenous TL1A being upregulated in a positive feedback manner. The very low levels of surface expression in the full length TL1A retrotransgenic could be surprising given the high levels of membrane TL1A present on TL1A transgenic cells[174, 175] however in standard transgenic mice all the expression is confined to one cell and is promoted by an efficient promoter. In the retrotransgenic model expression is promoted by a viral promoter across a broad range of cells which may lead to a lower level of expression of which the majority is able to be cleaved. As a result of the expression levels the full length TL1A mouse can be considered a model of overexpression of soluble TL1A and the TL1AΔ69-93 mouse was a model of overexpression of membrane bound TL1A.

The phenotype of the two models of retrotransgenic mice was compared. The TL1AΔ69-93 retrotransgenic had severe pathology in the ileum, similar to a CD2/TL1A transgenic mouse[174]. However the full length TL1A expressing

retrotransgenic did not show a pathological phenotype compared to control mice and only had a non-significant trend towards increased of IFN-γ in the ileum. As DR3 and TL1A have been implicated in asthma models [138, 159] we examined the lungs for a phenotype in these mice. The TL1AΔ69-93 retrotransgenics showed leukocyte infiltration into the lungs, which was not present in the full length TL1A or control mice. Whilst the full length TL1A retrotransgenic mice did not show any inflammation they did have a significant up regulation of IL-17a mRNA above control suggesting that sTL1A was capable of inducing a mild Th17 mediated inflammatory phenotype in the lungs.

Following on from this membrane restricted TL1A transgenic mice were produced which carried the Δ69-93 mutation. These expressed TL1A under the CD2 promoter and were compared to the previously produced transgenic line R6[174] which was renamed Mem+Sol. The advantage of creating a transgenic line is it enabled us to choose and propagate lines which had a known level of expression with ease. Of the multiple founder lines of membrane restricted transgenic mouse lines two were taken forward and compared to the Mem+Sol line. Having these 3 lines allowed comparison of the addition of soluble on top of membrane TL1A (Mem+Sol versus Mem) but also controlled for total TL1A level regardless of state (Mem+Sol versus Mem Hi).

In the spleen levels of Tregs were increased across all three transgenic lines compared to WT suggesting a threshold level of TL1A for Treg expansion had been passed. Indications for this were also seen in the increase in activation status of CD4+ T cells whereas in CD8+ T cells increases in activation status reflected total TL1A levels. A similar effect of total TL1A levels was also observed in numbers of GC B cells. Whether this is a direct effect of a trend towards an increase in Tfh due to increased activation status or a direct effect of TL1A on the B cells remains to be determined.

The effect on increases in total IgA and IgE in all transgenic strains is interesting and has not been reported before. Further the effect on these increases seems to be dependent upon the addition of sTL1A. The increased IgE levels are most likely due to the increase in type 2 cytokines observed in these mice[235] however the role of TL1A in systemic IgA is relatively unknown. There was one publication by Kayamuro *et al*[236] which demonstrates an adjuvant effect of TL1A on mucosal IgA but not on systemic. Further, no mechanism was indicated for this.

An assessment of the serum cytokines in the transgenic mice did not show many differences. Despite the large increases in IL-13 mRNA transcripts in both the lungs and ileum there was no increase in serum IL-13. The Mem+Sol TL1A transgenic mouse did have significantly reduced levels of several cytokines including Eotaxin, G-CSF, GM-CSF and KC compared to WT and the other transgenic lines. These cytokines are all involved in myeloid cell development, function and chemotaxis[237-240]. The decrease in these cytokine levels could be either due to decreased production or increased uptake. Either way this seems to be an effect specifically mediated by the addition of soluble TL1A.

TL1A induced pathology was observed in all strains. In the ileum, both goblet cell hyperplasia and increased small intestinal length required soluble TL1A for maximal phenotypic expression despite an equal induction of IL-13 between the different lines. There was also a significant decrease in the expression of IFN-γ and trend in IL-17a and an increase in IL-4 only in the Mem+Sol line. The differences in IL-17a and IFN-γ contradict the expression patterns found in the original publication of this strain[174]. There are several reasons why this may be the case. Firstly in this study the age of the mice was tightly controlled and all mice were 12 weeks old +/-1 day whereas in the original study the mice were between 8 and 52 weeks old. Further there has most likely been a change in the microbiota of these mice as they have moved animal house twice and 4 years have past since the original study took place. Unlike the retrotransgenics none of the transgenic mice showed large infiltrates in the lungs. The infiltrates that were present were much smaller in size. This may be due to the production method of the retrotransgenics as the irradiation likely induced tissue damage that could have exacerbated the response. Also the retrotransgenics were left for 24 weeks to reconstitute whereas the transgenics were assessed at 12 weeks of age. As IL-13 and lung infiltrates are known to affect airway resistance and sensitivity the mice[234] were subjected to a methacholine challenge. There was a very minimal effect of increasing methacholine dose with the transgenics and only the Mem+Sol line showed increase hypersensitivity compared to WT. However this increase in hypersensitivity is very small when compared to the same procedure carried out in mice which have been subjected to either papain or OVA induced asthma, which at a dose of 100mg/ml methacholine have a mean resistance of 2.5 and 3 $cmH_2O.s/ml$[133] respectively compared to 1.5 in the Mem+Sol mice. Interestingly the Mem+Sol strain does not have the highest level of IL-13 or pathology. It does however have the highest levels of Col6a1 suggesting that these mice may have a mild lung fibrosis phenotype.

Initially the expression of key cytokines in the lung was measured by qPCR. For IL-13 and IL-17a the Mem line showed the greatest induction with both the Mem+Sol and Mem Hi showing induction to a lower degree. This suggests that lower and higher doses of TL1A may have differential effects within the lungs either through the promotion of different cell types or different cytokines from the same cells. Interestingly in both the lungs and ileum IL-9 induction was observed with maximal induction in the membrane restricted TL1A lines and to a much lesser extent in the line with both membrane and soluble suggesting that membrane promotes differentiation to IL-9 producing cells better than in the presence of soluble TL1A. This is of interest as Richard *et al* recently demonstrated a novel role for the TL1A/DR3 pathway in the differentiation of T cells into Th9 cells[145].

To further characterise the expression profile of the lungs the transcriptome was sequenced using RNASeq. The expression profile of each line was compared to WT mice and the genes which were significantly up or down regulated compared between the lines. The gene ontology analysis of the various sets of genes highlighted that the majority of down regulated genes are involved in regulation of cell processes whereas most of the upregulated genes are linked to immune cell types and immune processes. The increase in many immune related genes could be due to two main reasons. Either TL1A has had an effect on an immune cell which has caused it to express a particular gene or the changes in expression profile represent a change in the cellular make up of the lungs. Whilst it was possible to sort for genes which are significantly differentially expressed either in all lines, just Mem+Sol or just Mem and Mem Hi, genes which did not pass the criteria were usually non-significantly expressed in the same direction as the other. For example Csn3 was only significantly up regulated in Mem+Sol (adjusted P value <0.05) however it was also non-significantly upregulated in both membrane restricted lines. As such it would not be correct to say the Csn3 was only upregulated in the Mem+Sol line just that it was only highly significant in the one line. The value of this data therefore lies in assessing genes which are differentially regulated regardless of the source of TL1A. As such it will be discussed at greater length in the next Chapter.

To model a system of overabundance of sTL1A mice were implanted with osmotic pumps that secreted 500ng/day of sTL1A for 6 weeks. After this time the mouse was assessed for apparent phenotypes. No effects of the sTL1A treatment were found in the spleen or lung however pathology was observed in the small bowel. The mice displayed goblet cell hyperplasia, increased IL-13 and decreased IFN-γ in the ileum along with an increase in the total length of the small bowel. In this instance sTL1A

specifically drives a non T cell mediated bowel pathology[140]. In addition sTL1A promoted a non-significant trend in increased total IgA in the serum. The lack of increase in T cell activation status or Treg levels is interesting in these mice. This may either be due to an insufficient level of TL1A being reached in the mouse or a qualitative difference in the signaling conferred. Give that all other indications, in including *in vitro* T cell costimulation assays, are that soluble TL1A is capable of T cell costimulation this is likely a quantitative issue and may imply a difference in the threshold of TL1A stimulation required for different cell types.

Taken together these data indicate that both membrane bound and soluble TL1A are expressed both *in vitro* and *in vivo* and are capable of signaling. The *in vivo* data from the transgenic mice and osmotic pump experiments are summarised in Table 4-3. The data from the retrotransgenic suggest a minimal role for sTL1A however both the transgenic and osmotic pump experiments suggest a greater role especially in the promotion of small bowel pathology. This apparent disparity may be due to the expression patterns. In the retrotransgenic multiple cells of the haematopoietic lineage will be expressing TL1A, as a result this may have different local effects. Overall for T cell costimulatory effects and for the promotion of IL-9, possibly from Th9 cells[133], membrane restricted TL1A is required and this may be negatively impacted by sTL1A. This suggests that for control of T cell costimulation cleavage of TL1A may be a means of control of signalling. In contrast sTL1A promotes an increase in total IgA in the serum and increased gut pathology, possibly through costimulation of ILC2s[140]. It should be noted that the level of soluble TL1A achieved in the transgenic mice required for effects on T cells, but not ILCs, is considerably above the biological level observed in response to *Salmonella Typhimurium.* Whilst soluble TL1A may be active, membrane bound TL1A may be the major signalling source in a normal immune response and cleavage may be a means of control. Where soluble TL1A mediated signaling may come into its own is in instances where cell to cell interactions between TL1A and DR3 expressing cells are limited. These data do imply that in cases of abnormally high sTL1A, for example in the synovium of RA patients[199, 202], that signalling will most likely occur through multiple cell types and as such soluble TL1A may have a pathogenic effect.

Phenotype	Membrane only	Membrane + Soluble	Soluble only
T cell activation	Increased	Increased	No effect
Tregs	Increased	Increased	No effect
GC B cells	Increased	Increased	No effect[+]
Total Ig	Mild increased IgG2b Increased IgE Increased IgA	Mild increased IgG2b Increased IgE Increased IgA	Mild increase in IgA
Serum cytokines	No effect	Reduced Eotaxin, G-CSF, GM-CSF,KC	Not Tested
Ileum pathology	Severe but later onset	Severe	Present
Ileum cytokines	Increased IL-13, Col6a1 and IL-9	Decreased IFN-ϒ and IL-17a. Increased IL-4, IL-13 Col6a1. Mild IL-9 increase	Decreased IFN-ϒ Increased IL-13
Lung pathology	Mild perivascular and peribronchular aggregates	Increased Methacholine hypersensitivity	None
Lung Cytokines	Increased IL-13, IL-17a and IL-9	Increased IL-13 and IL-17a	None

Table 4-3 *– Summary of TL1A induced in vivo phenotypes. Summary of phenotypes for transgenic TL1A and osmotic pump experiments.* [+] *Indicates data not shown.*

Chapter 5. The result of signals conferred through excessive TL1A production and the potential cell types involved

5.1. Introduction

The previous chapter demonstrated potential differential roles of membrane bound and soluble TL1A through overexpression. This chapter attempts to address changes in down stream gene expression mediated by TL1A and to further shed light on the cell types responsible for these effects.

Constitutive expression of TL1A has been shown to result in a significant up regulation of IL-13 and demonstrated its responsibility for the induction of small intestinal pathology[174, 175]. Published work by Meylan *et al*[140, 174] investigated the cell responsible for the IL-13 mediated phenotype in CD2-TL1A transgenic mice. It was found that neither T cells, NK cells, NKT cells or mast cell but most likely ILC2 that mediated this effect.

As the previous chapter highlighted there are multiple phenotypes in TL1A transgenic mice in addition to the elevation in IL-13 however these have not been investigated to the same degree. As TL1A is a known T cell costimulator[159] it is not surprising that the T cells from TL1A transgenic mice show an activated phenotype. This was previously shown to be dependent upon TCR signalling[174] however it has not been investigated if it was a direct effect via DR3 on T cells or via another cell type.

The role of DR3 in B cell homeostasis and activation is a relatively under studied and is a new area of research in TL1A biology[129]. The previous chapter reported for the first time hyper IgA and IgE in the TL1A transgenic mice. This isotype switching and overexpression of total IgA and IgE may be dependent upon T cell derived TL1A interacting with DR3 on non-class switched B cells as part of the GC reaction. Alternatively as DR3 is expressed on T cells this phenotype could exist due to an increased activation state of the T cell, which in turn promotes the observed B cell phenotype.

Membrane bound TL1A was shown to strongly promote IL-9 mRNA in both the lungs and ileum. As TL1A has been shown to promote the differentiation to the Th9 lineage[133] and costimulate ILC2 [140, 141], both of which produce IL-9[179, 241], it would be of interest to determine the cell type responsible.

In this chapter we compared T cell and non T cell mediated effects of constitutive TL1A expression. To this end we crossed a membrane restricted TL1A transgenic to a LoxP flanked DR3 mouse in conjunction with CD4 Cre thus creating a T cell conditional DR3 KO. Further, we examined the role of ILCs through transfer of WT or TL1A transgenic T cells into RAG KO and RAG GC KO mice. RAG GC KO mice lack the common gamma chain in addition to RAG and as such ILCs are unable to develop. Lastly, through comparison of RNASeq data from the lungs, genes which are up or down regulated in response to chronic TL1A expression were discovered, revealing potentially novel roles of the TL1A signalling pathway.

5.2. Results

5.2.1. Production of a TL1A overexpressing mouse which lacks DR3 on T cells.

To study the differential role of TL1A signalling via DR3 on T cells versus other cells a mouse overexpressing membrane restricted TL1A on T cells was crossed with a T cell dependent DR3 conditional KO. For the cross, line G3 from CD2/TL1AΔ69-93 was used. This mouse expressed levels of TL1A mRNA and protein on naïve T cells (Figure 5-1) similar to the Mem Hi line (Figure 4-10).

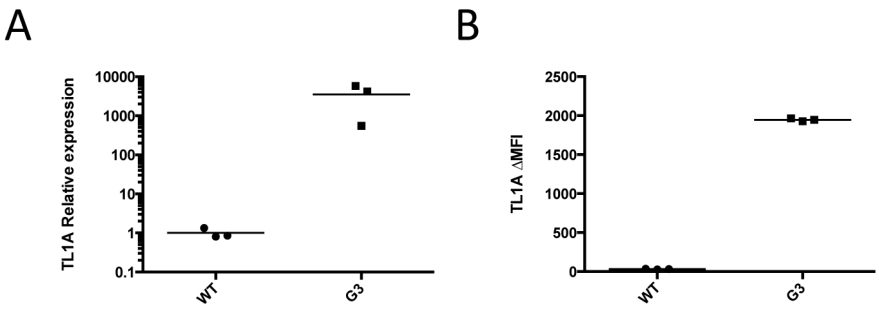

Figure 5-1 *- Parent TL1A transgenic line for crossing to T cell conditional DR3 KO. Transgenic line G3 was crossed to the DR3 $^{FL}/^{FL}$ CD4 Cre+/- to yield a mouse where direct effects of TL1A overexpression on T cells could be examined. G3 carries the TL1AΔ69-93 transgene under the CD2 promoter and at both the mRNA (**A**) and protein level (**B**) and is similar to the Mem Hi line on naïve CD4+ T cells.*

The conditional DR3 KO, to which G3 was crossed, has not been published before and was generated at Ozgene (Australia) by insertion of LoxP sites in introns 1 and 6. Upon induction of an appropriate Cre recombinase the functional domain of DR3 is deleted in a tissue specific manner[127]. This mouse was initially crossed to the CD4 Cre mouse enabling deletion of DR3 in both CD4+ and CD8+ T cells. The cell type specific KO of DR3 was examined in CD4+ T cells and CD19+ B cells. Cells were sorted from the spleen of mice homozygous for the LoxP flanked allele of DR3 and either heterozygous for CD4 Cre or negative. Genomic DNA was purified from these cells and DR3 amplified using primers for genotyping the conditional KO (primers 3431-31 and 3431-32). Amplification of the IL-2 gene was used as a loading control. Comparatively little amplification of DR3 was observed in CD4+ T cells which were positive for Cre compared to B cells from the same mouse and CD4+ T cells from a Cre negative mouse (Figure 5-2A). Expression of DR3 on the surface of CD4+ T cells and IgM+ IgD+ CD19+ B cells was measured by flow cytometry. DR3 protein

was found to be absent from only CD4+ T cells from the Cre positive mouse demonstrating this is a functional conditional KO of DR3 (Figure 5-2B).

A

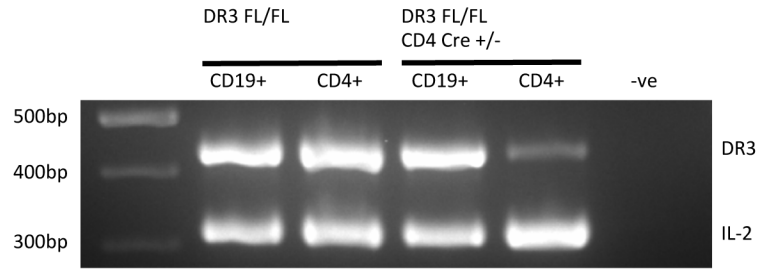

B

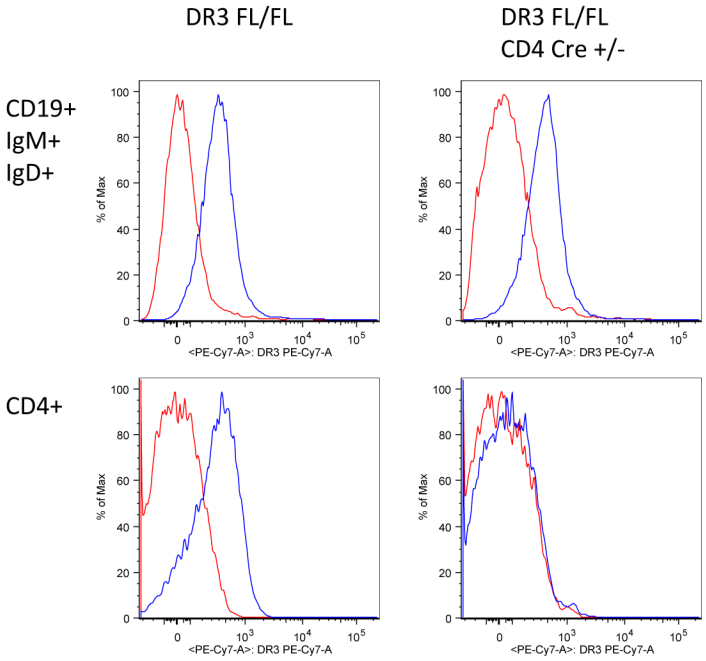

Figure 5-2 *- T cell conditional DR3 KO. LoxP sides were inserted into introns 1 and 6 of the gene encoding DR3 and the mice crossed to CD4-Cre to produce a T cell specific DR3 KO mouse.* ***A*** *– Genomic DNA was purified from flow sorted CD19+ or CD4+ cells from either a DR3 $^{FL/FL}$ or DR3 $^{FL/FL}$ CD4 cre +/- and a primer pair spanning the deletion site within DR3 was used. Primers for IL-2 were used as a loading control as indicated.* ***B*** *– Splenocytes from the mice in* ***A*** *were stained for DR3 on non-class switched B cells and CD4+ T cells as indicated. Cells were stained for DR3 (blue) or with an appropriate isotype control (red).*

5.2.2. The effect of the lack of T cell DR3 on the phenotype of TL1A transgenic mice.

After crossing the TL1AΔ69-93 with the CD4 conditional DR3 KO ($DR3^{FL/FL}$ CD4 $Cre^{+/-}$), mice were aged to 12 weeks and phenotyped in the same manner as the previous chapter. In unstimulated mice there were very few differences observed between $DR3^{FL/FL}$ CD4 $Cre^{+/-}$ and $DR3^{FL/FL}$ CD4 $Cre^{-/-}$. This is unsurprising given that no major immunological phenotypes were observed, at rest, in the total DR3 KO[216]. However lack of DR3 on the T cells did alter the phenotype observed in the TL1A transgenic mice.

DR3 on the T cells is required for the increase in the activation status (CD44hi CD62L low) observed within the T cell compartment (Figure 5-3A). Further DR3 is also required in the T cells for the increase in Tregs and Tfh cells (Figure 5-3B and C).

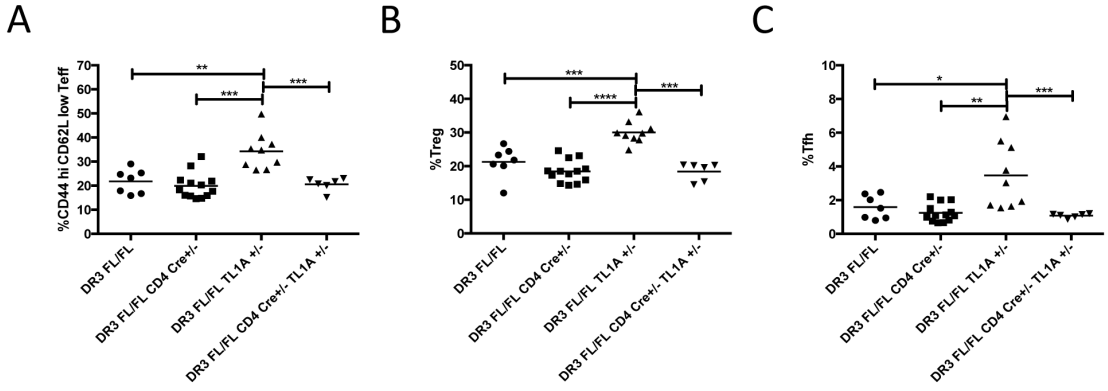

Figure 5-3 *- Direct Effect of TL1A on T cells. Spleens were taken from 12 week old mice and assessed for T cell activation (**A**, fraction of CD4+ FoxP3-), Treg (**B**, fraction of FoxP3+ of CD4+) and Tfh (**C**, CD4+ CD40L+ ICOS+ PD1+ CXCR5+ fraction of CD4+) composition. * indicates 0.05>P>0.01, ** 0.01>P>0.001, *** 0.001>P>0.0001 and **** P<0.0001 using the Mann-Whitney U test.*

The only major effect seen in the non-TL1A transgenic DR3 conditional KO mice was a reduction in fraction of GC B cells in the spleen. These cells were also increased in TL1A transgenic and were reduced back to lower levels when T cell DR3 was lacking in the presence of constitutive TL1A expression (Figure 5-4A). Interestingly, the hyper IgA that was observed in the TL1A transgenic was not significantly reduced in the TL1A transgenic conditional knockout however the hyper IgE was absent (Figure 5-4B and C).

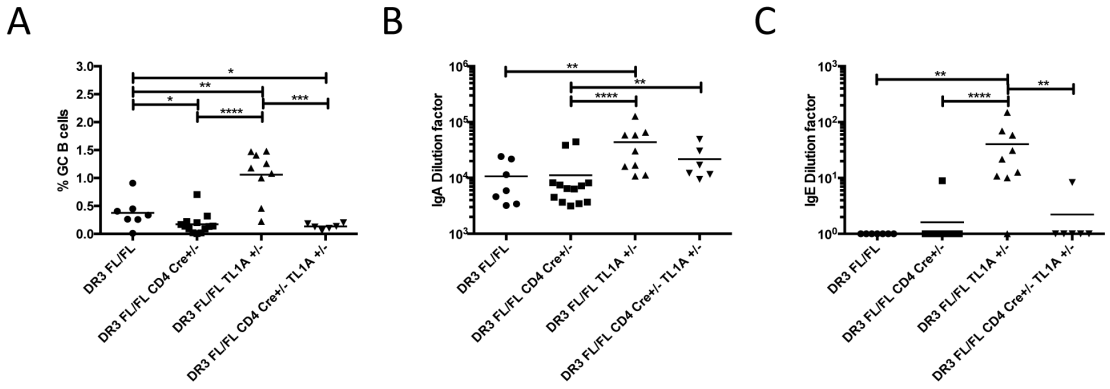

Figure 5-4 *- Role of T cell DR3 signaling on the B cells response.* ***A****- GC B cells (CD19+ GL7+ PNA+) abundance was assessed by flow cytometry in spleens taken from 12 week old mice as indicated.* ***B*** *and* ***C*** *– Serum was collected at the same time as in* ***A*** *and the total levels of IgA (****B****) and IgE (****C****) measured by ELISA. * indicates 0.05>P>0.01, ** 0.01>P>0.001, *** 0.001>P>0.0001 and **** P<0.0001 using the Mann-Whitney U test.*

As the small bowel is a major site of pathology in TL1A transgenic mice this was assessed for reliance on DR3 expression on T cells. The conditional KO TL1A transgenic mice still exhibited gross small intestinal pathology including goblet cell hyperplasia and an increase in the length of the small bowel (Figure 5-5A and B). Their cytokine profile was unaffected as well, with elevation of IL-13 and IL-9 present in the T cell conditional KO.

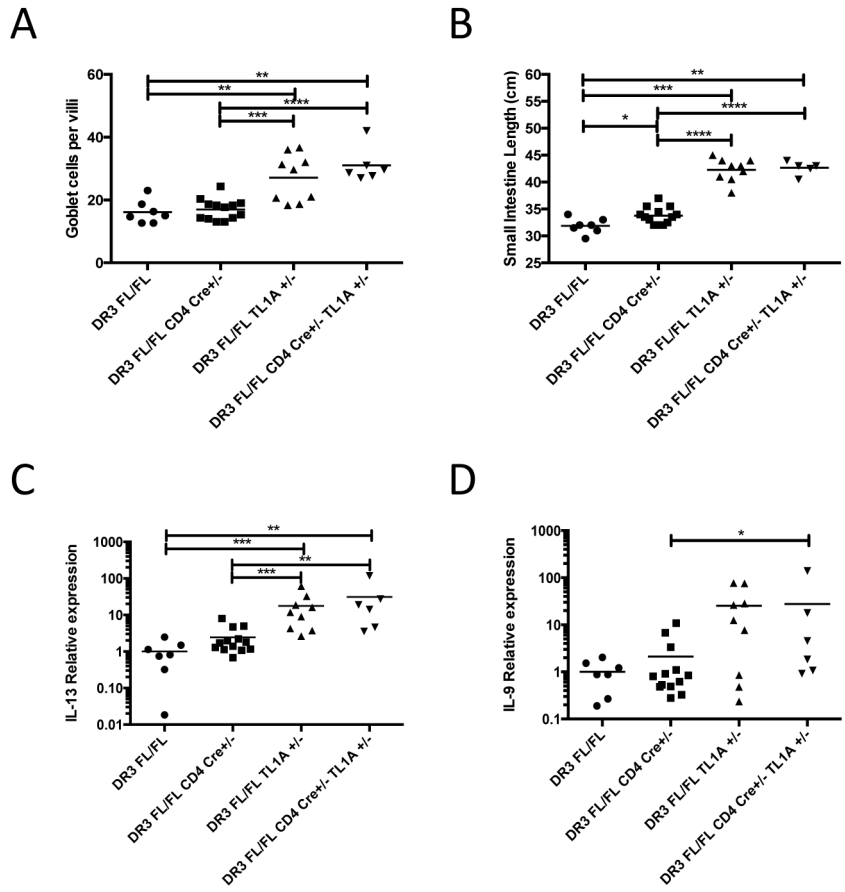

Figure 5-5 *- T cell DR3 is not required for small intestinal pathology. At 12 weeks of age the small bowel was taken and measured (**A**) and sections from the terminal ileum were stained with PAS. The mean number of goblet cells per villi was calculated with at least 3 full size in-plane villi counted per section in 3-6 mice per genotype (**B**). RNA was extracted from small sections of the terminal ileum (excluding Peyer's patches) and processed for qPCR to measure the indicated genes (**C** and **D**). Expression is relative to DR3 $^{FL/FL}$ littermates. * indicates 0.05>P>0.01, ** 0.01>P>0.001, *** 0.001>P>0.0001 and **** P<0.0001 using the Mann-Whitney U test.*

As we have previously shown a phenotype for the TL1A transgenic mice in the lungs (Chapter 4) we examined this compartment for dependence on T cell DR3. In contrast to the gut, the TL1A cytokine profile in the lungs is dependent upon DR3 on T cells. As a result of crossing to the T cell specific DR3 KO, levels of transcript of IL-13, IL-17a and IL-9 were reduced back to WT levels (Figure 5-6).

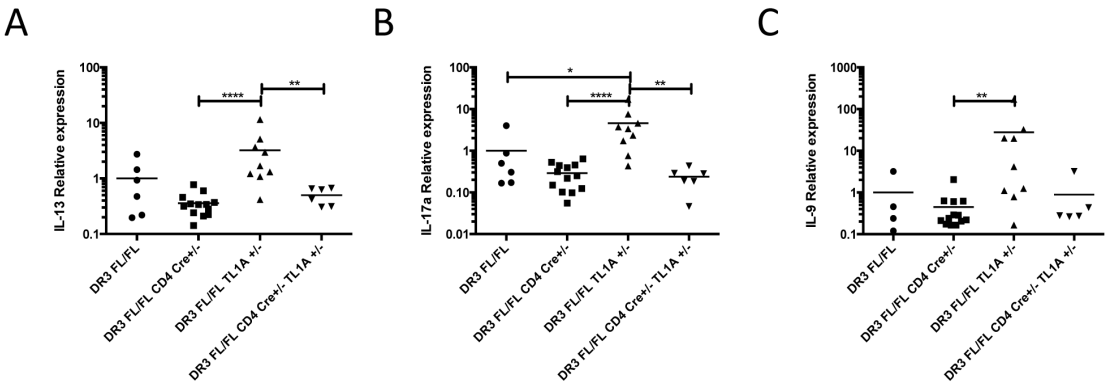

Figure 5-6 *- T cell DR3 expression is required for aberrant lung transcriptional profile.* ***A-C*** *- RNA was extracted from the post-caval lobe from 12 week old transgenic and qPCR was performed for expression analysis of the indicated cytokines. Expression is relative to DR3$^{FL/FL}$ littermates. * indicates 0.05>P>0.01, ** 0.01>P>0.001, *** 0.001>P>0.0001 and **** P<0.0001 using the Mann-Whitney U test.*

5.2.3. Role played by TL1A mediated T cell responses upon transfer into RAG or RAG GC KO mice.

As TL1A is overexpressed from birth in the transgenic there is a chance that the phenotype observed is a consequence of developmental defects. To overcome this a RAG transfer model was used where total CD4+ T cells (including Tregs) were transferred into RAG KO mice that were left to reconstitute for 8 weeks. To further examine if any observed phenotypes were due to cytokines released by T cells or other lymphoid lineages, transgenic T cells were also transferred into RAG GC KO mice. For the transfer WT, Mem or Mem+Sol sorted CD4+ sex matched T cells were used.

After 8 weeks the mice were culled. All groups successfully reconstituted the spleen and, in the RAG KO, transferred TL1A transgenic cells expanded more than WT cells (Figure 5-7a). Where Mem+Sol T cells were transferred there was a corresponding significant level of sTL1A present in the serum. When either transgenic line was transferred into RAG KO mice the ileum and lung phenotype recapitulated with an increase in IL-13 transcript in both organs and goblet cell hyperplasia in the ileum. However when transgenic T cells were transferred into RAG GC KO the gross pathology in the gut did not recapitulate this phenotype. Whilst there was a nonsignificant trend towards an increase in IL-13 in the ileum there was no increase in the lungs (Figure 5-7).

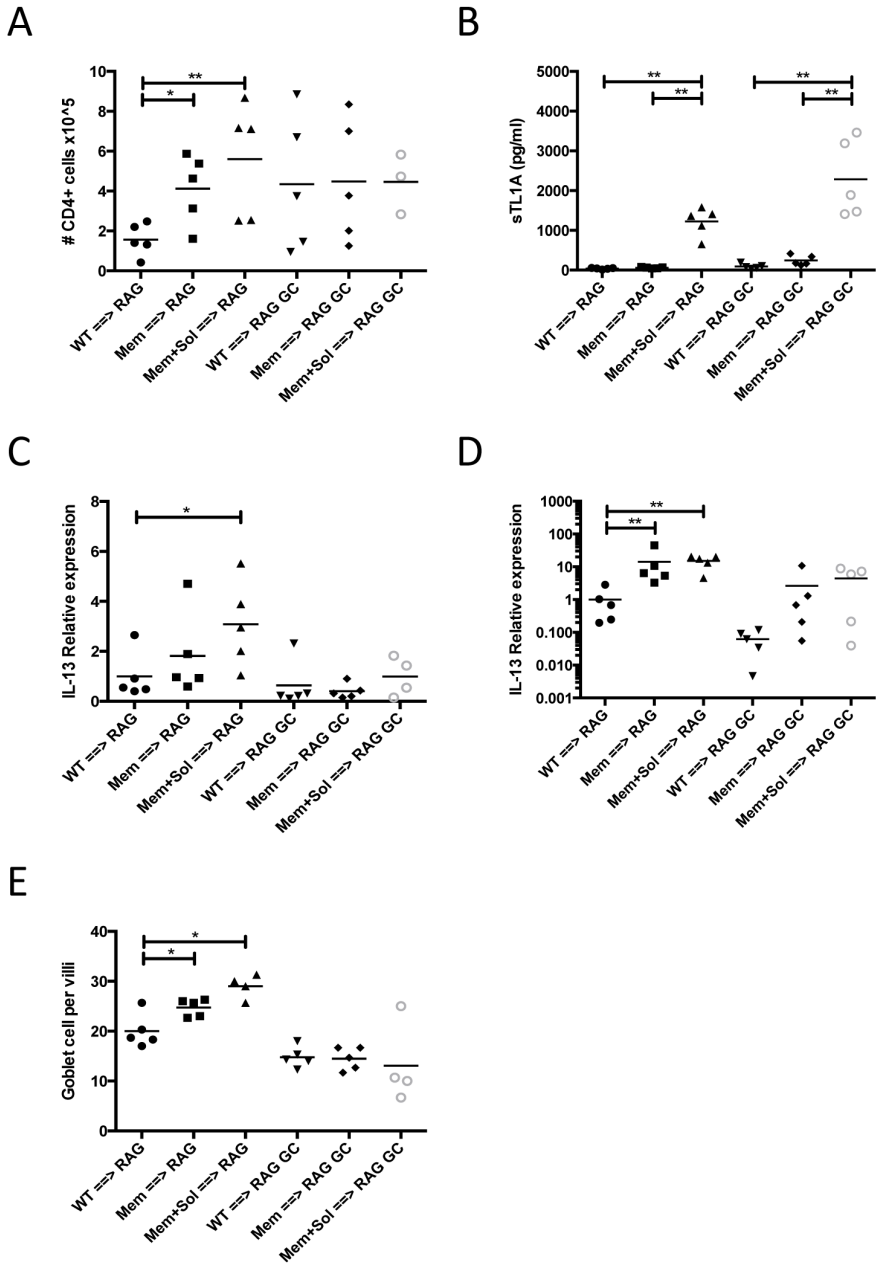

Figure 5-7 *- TL1A transgenic or WT T cell reconstitution of lympho-deficient mice. Either RAG 2 KO (RAG) or RAG 2 GC KO (RAG GC) mice were reconstituted with 4x10^5 CD4+ cells from WT, Mem or Mem+Sol TL1A transgenic mice for 8 weeks. After 8 weeks CD4+ T cell engraftment in the spleen was measured (**A**) along with sTL1A in the serum (**B**). RNA was isolated from the post-caval lobe (**C**) and the terminal ileum (**D**) and IL-13 mRNA levels measured by qPCR. The expression is relative to the RAG group which received WT cells. Sections were produced from the terminal ileum, stained with PAS and the number of goblet cells per villi enumerated with at least 3 full size in-plane villi counted per section (**E**). * indicates 0.05>P>0.01 and ** 0.01>P>0.001 using the Mann-Whitney U test. Data representative of two independent experiments.*

Histologically, transfer of CD4+ T cells into RAG KO mice promoted the formation of lymphoid infiltrates in the lungs in all groups. However the infiltrate was considerably increased upon transfer of transgenic T cells with Mem+Sol cells promoting worse pathology. In the RAG GC KO transfer the severity of pathology was greatly reduced however it was still present to an extent in the mice that received transgenic T cells (Figure 5-8).

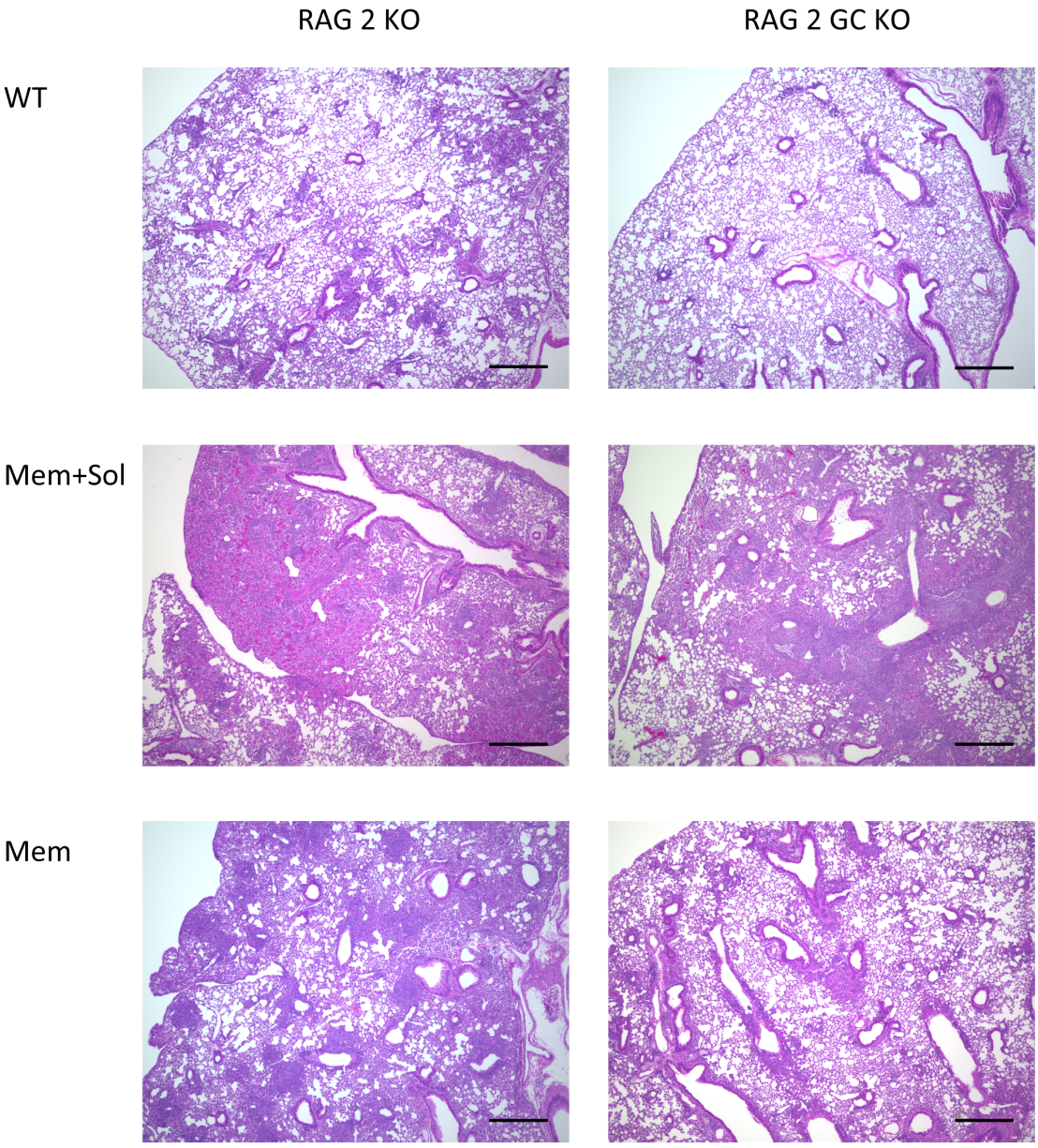

Figure 5-8 *- Lung pathology in response to reconstitution with Transgenic T cells. 8 weeks post reconstitution the lungs were taken, sectioned and stained with H and E. The samples are divided by column for recipient and row for donor. Images are representative of 5 mice per group in two independent experiments. Scale bars are equal to 500μm.*

As there was the potential for intestinal phenotypes in this transfer model the weight of the mice was followed throughout the course of the experiment. Given the intestinal phenotype of the RAG KO mice that received transgenic T cells it was surprising that these mice did not lose weight. However the RAG GC KO mice which received transgenic T cells did lose weight and as a result some had to be euthanized early in the experiment (Figure 5-9). This was surprising as these mice did not have a phenotype in the ileum (Figure 5-7).

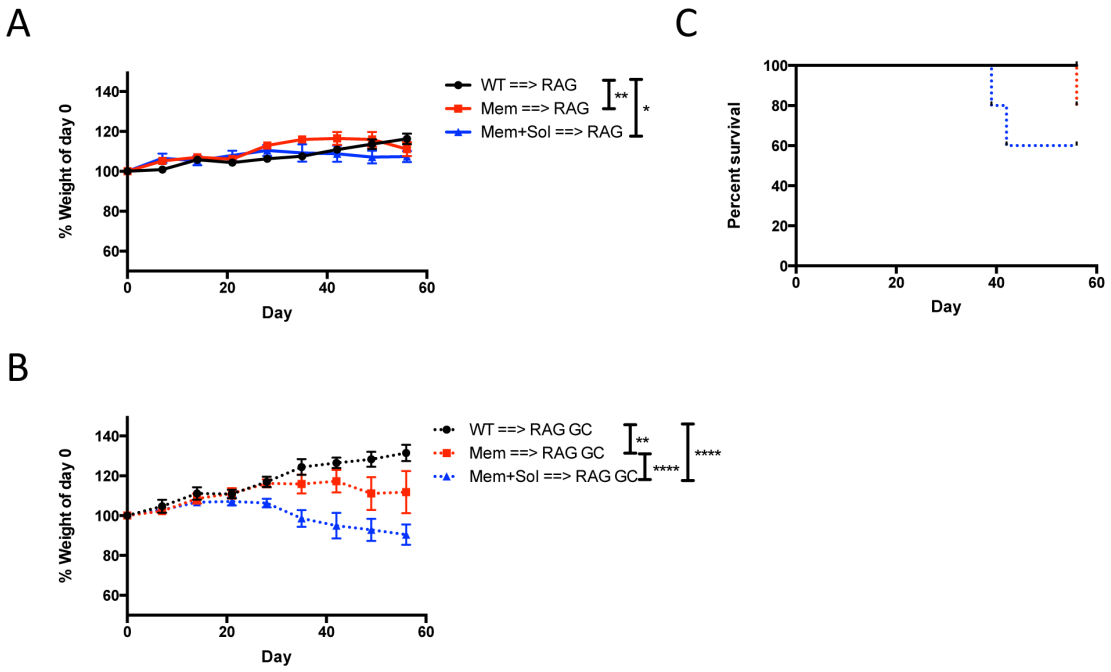

Figure 5-9 *- Morbidity and mortality response to reconstitution with transgenic T cells. The mass of the mice was followed over the course of the experiment (**A** and **B**), if a weight loss of 20% was observed the mice were euthanised and the survival plotted (**C**). * indicates 0.05>P>0.01, ** 0.01>P>0.001 and **** P< 0.0001 using two way ANOVA for genotype.*

In the course of the experiment some of the RAG GC KO mice which received transgenic cells developed loose and bloody stool. Upon necropsy it was also noted that the colon appeared inflamed and both the colon and the caecum were translucent (data not shown). Sections were taken from the colon and processed for H and E. It became apparent that the RAG GC KO mice which received transgenic CD4+ cells had developed colitis with oblation of the villi and massive lymphoid infiltrate (Figure 5-10).

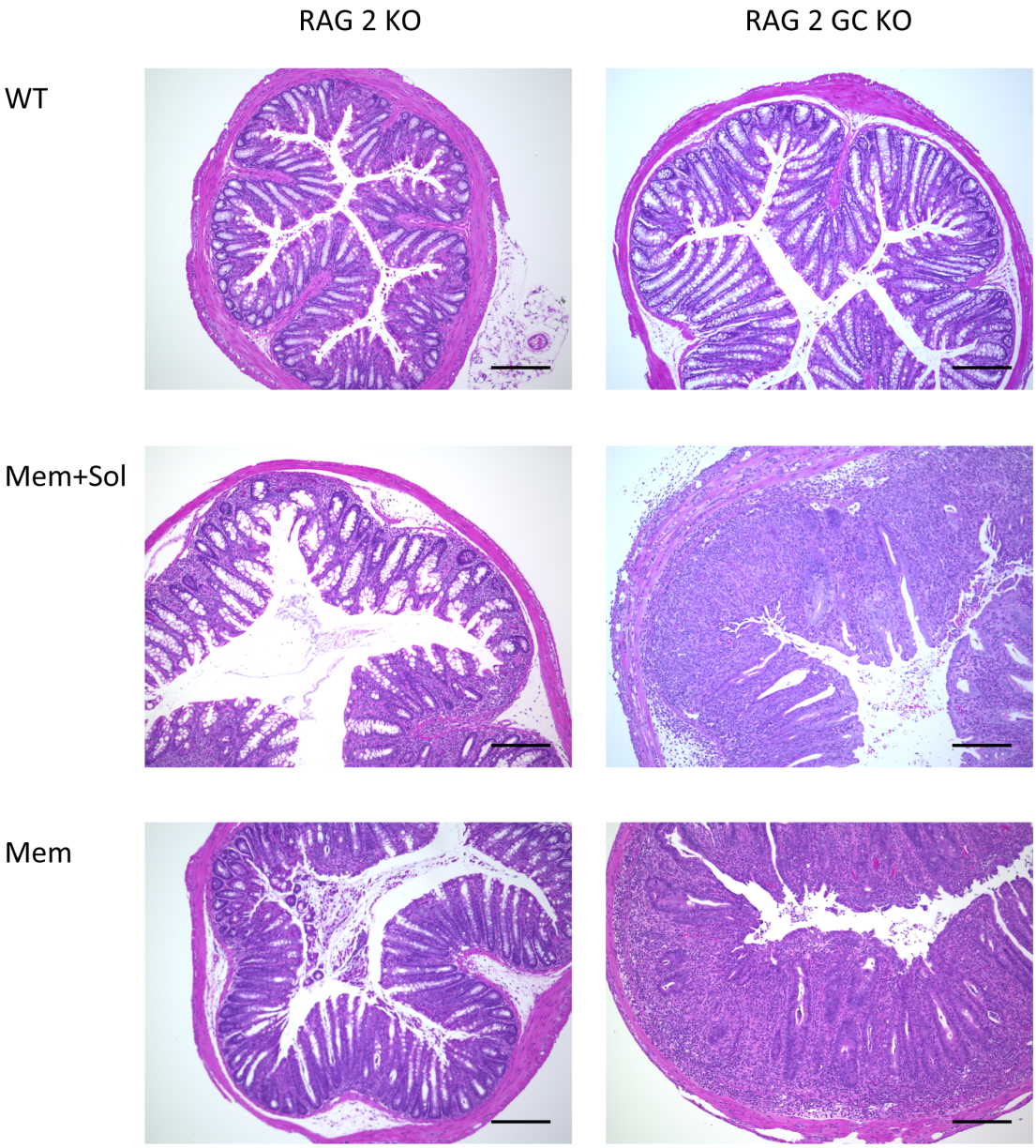

Figure 5-10 *- Colon pathology in response to reconstitution of RAG GC with transgenic T cells. 8 weeks post reconstruction the proximal colons were taken, sectioned and stained with H and E. The samples are divided by column for recipient and row for donor. Images are representative of 5 mice per group in two independent experiments. Scale bars are equal to 200μm.*

5.2.4. Identification of differentially expressed genes conserved across multiple tissues as a result of constitutive TL1A expression

Previously E. Hawley had sequenced the transcriptome of the ileum from 8 week old Mem+Sol and WT mice using RNASeq (unpublished data). To attempt to identify novel TL1A responsive genes, we reanalysed the ileum RNASeq data and compared

genes that were differentially expressed compared to WT mice sequenced at the same time both in this set of data and the lung RNASeq analysis from the previous chapter. The principal component analysis and quality control graphs are given in Appendix I. 3 genes were found to be significantly down regulated (Table 5-1) in both the lungs and ilea of Mem+Sol mice compared to WT and 6 genes were found to be up regulated (Table 5-2, Figure 5-11). The expression profile of the genes that were identified were also examined in the RNASeq analysis of the lungs of the Mem and Mem Hi transgenic lines, this is given in Table 5-3 however the full transcriptome of the ilea was not determined for these mouse lines.

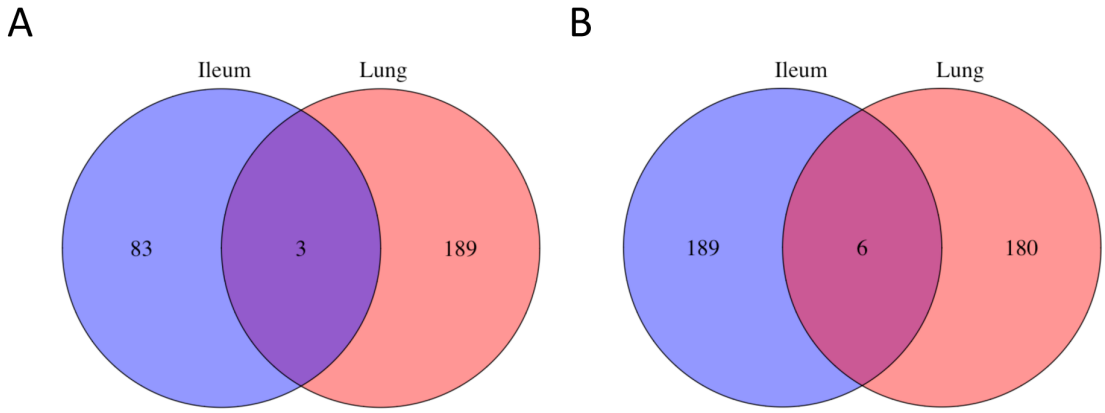

Figure 5-11 *- Comparison of transcriptional profile of Mem+Sol TL1A Transgenic lungs and ileum. RNA was isolated from the post-caval lobe (12 week old) and the ileum (8 Week old) of WT or Mem+Sol TL1A transgenic mice and prepared for and sequenced on a HiSeq (Ilumina). Differential expression between WT and transgenic mice in the ileum and lung was calculated with DESeq using a negative binomial distribution model and generalised linear model respectively. Genes were considered to be significantly differentially expressed which had a adjusted P value <0.05 using the Benjamini-Hochberg method. The number of genes that were either down regulated (**A**) or up regulated (**B**) compared to WT are indicated for each tissue. The RNA for the ileum samples was collected and prepared by E. Hawley.*

Gene	Notes
Itgad	Integrin alpha D, CD11d
Cd163L1	CD163 molecule-like 1
Col4a6	Collagen type IV alpha 6

Table 5-1 *- Genes that are down regulated in both lung and ileum samples from Mem+Sol TL1A transgenic mice compared to WT.*

Gene	Notes
Mgl2	Macrophage galactose N-acetyl-galactosamine specific lectin , CD301b
Samsn1	SAM domain SH3 domain and nuclear localisation signals 1
Tnfsf15	TL1A, Transgene present in strains
Mfsd2a	Major facilitator superfamily domain containing 2A
Csn2	Casein beta
Csn3	Casein kappa

Table 5-2 *- Genes that are up regulated in both lung and ileum samples from Mem+Sol TL1A transgenic mice compared to WT.*

Gene	Mem+Sol	Mem	Mem Hi
Itgad	Down	Down	-
Cd163L1	Down	-	-
Col4a6	Down	Down	-
Mgl2	Up	Up	Up
Samsn1	Up	Up	Up
Tnfsf15	Up	Up	Up
Mfsd2a	Up	-	-
Csn2	Up	-	-
Csn3	Up	-	-

Table 5-3 *- Expression pattern of differentially expressed genes from combined lung and ileum comparison across different TL1A transgenic mice within the lung only. Direction of expression is only indicated where adjusted P value <0.05.*

Here follows a brief description of these differentially expressed genes.

Itgad

The gene itgad encodes the integrin CD11d. This integrin is expressed at a basal level on all leukocytes and is upregulated in inflammatory environments[242]. Treatment with an antagonistic anti CD11d monoclonal antibody has been shown to promote wound healing in response to spinal cord injury in rats through a reduction in infiltration in inflammatory cells including neutrophils and macrophages[243, 244].

CD163L1

CD163L1 is expressed by IL-10 producing macrophages[245] and, according to Immgen, Gamma Delta T cells[246]. On *in vitro* differentiation of macrophages CD163L1 was induced by M-CSF and IL-10 and inhibited by TNF[245].

Col4a6

Col4a6 is a type IV collagen. Deletion mutations in Col4a6 have been associated with X linked Alport syndrome with associated diffuse leiomyomatosis[247].

Mgl2

Mgl2 transcript is, according to Immgen, highly expressed by thymic DCs, splenic plasmacytoid DCs and epidermal DCs[246]. Through specific transient deletion of Mgl2+ DC these APCs were demonstrated to play a role in Th2 cell mediated immunity[248].

Samsn1

Samsn1 is a member of the SLY family of cytoplasmic adapter proteins. It is expressed throughout most of the hematopoietic system and is also found, among other places, in the lung[249]. Samsn1 is up regulated in B cells as a result of IL-4, IgM cross-linking or CD40 signalling in a NF-κB dependent manner. Samsn1 KO mice show increased response to immunisation and B cell activation whereas ectopic expression of Samsn1 in B cells causes the opposite[250, 251]. Samsn1 is also highly expressed in ILC2s but not ILC1s or ILC3s and increased upon activation with IL-25 and IL-33 (G. Sciume, unpublished observations).

Mfsd2a

Mfsd2a is a lung associated tumour suppressor gene that is associated with lung cancer survival. It is down regulated in multiple lung cancer cell lines and ectopic expression decreases matrix attachment *in vitro* and tumorigenicity *in vivo*[252, 253]. Mfsd2a is also a transporter for the fatty acid DHA across the blood brain barrier[253] and maintains integrity of the barrier through the suppression of transcytosis[254].

Csn2 and Csn3

Csn2 and Csn3 are casein genes that make up major components of milk from multiple species[255]. These are the genes that showed the greatest differential expression in the ileum and in both the ileum and lungs are expressed at a very low level in WT mice and dramatically induced in TL1A transgenics.

5.3. Discussion

It was obvious from the initial description of TL1A transgenic mice [174, 175] as well as subsequent work by Meylan *et al*[140] that there was both a T cell and non T cell component to the phenotype observed. Through crossing TL1A transgenic mice to multiple immune cell lineage KO lines it was identified that the IL-13 phenotype in the ileum was most likely as a result of TL1A costimulation of ILC2s[140, 141]. However, as demonstrated in the previous chapter other phenotypes were observed both within and outside of the ileum.

Initially we tested a novel loxP flanked DR3 mouse line that we crossed to the CD4 cre mouse to create a T cell conditional DR3 KO mouse. We demonstrated that the specificity of the KO in T cells was near complete and specific. This mouse will be of great use in multiple future studies.

The conditional DR3 KO mouse was crossed to a membrane restricted TL1A transgenic and used for phenotyping studies at 12 weeks of age to determine the contribution of direct T cell DR3 signalling to the phenotype of the TL1A transgenic. These data demonstrated the T cell costimulatory effect as the increase in Treg numbers was a direct result of signalling via DR3 on the T cells. Further the increase in the number of GC B cells is also reduced. This suggests that rather than signalling from TL1A on the T cell interacting with DR3, which is expressed on non-class switched B cells[129], most likely the increase in activation status of T cells in the transgenic mice promotes switching to a Tfh cell fate which in turn promotes the GC reaction. Interestingly the hyper IgE is lost however the hyper IgA remains perhaps suggesting TL1A as a novel switch factor for IgA. This could be confirmed through crossing the TL1A transgenic mouse to a B cell conditional DR3 KO using CD19 cre.

The phenotype of these mice was examined in the ileum. Given previous data showing the independence of the IL-13 mediated phenotype from T cells [140] it is not surprising that the goblet cell hyperplasia, increase in small intestine length and levels of IL-13 are unchanged when DR3 is lacking from T cells. However the increase in IL-9 is unaffected. As recent data has shown IL-9 production from ILC2s we suggest that this is more the likely source rather than Th9 cells[241]. This is in contrast to the lungs where elevation in IL-13, IL-17a and IL-9 is all dependent upon T cell DR3. This suggests that the TL1A induced cytokine profile in the lungs is largely mediated by T cells.

To further assess T vs non T cell roles for TL1A signalling a transfer experiment was performed where WT or transgenic T cells (Mem or Mem+Sol) were transferred into either RAG KO mice or RAG GC KO mice. Whilst the RAG KO mice lack T and B cells the RAG GC KO also lack all other cells that rely on cytokine signalling via receptors that contain the common gamma chain for maturation. As a result RAG GC mice do not have any T cells, B cell or ILCs.

Transfer of either Mem or Mem+Sol CD4+ T cells into RAG KO mice recapitulated multiple aspects of the phenotype observed in the TL1A transgenic mice. There was an elevation of IL-13 mRNA in both the ileum and lungs and the mice exhibited goblet cell hyperplasia within the ileum. This not only shows the validity of the model for studying the role of TL1A on other cell types but also demonstrates for the first time that the phenotype observed in the TL1A transgenic mice is not developmental and can be initiated in an adult mouse.

When transgenic cells were transferred into RAG GC KO mice however no small intestinal pathology developed. This demonstrates nicely that the cell that responds to TL1A to induce pathology in the small intestine depend on the common gamma chain for development. There was no increase in IL-13 in the lungs after the transfer of transgenic T cells into the RAG GC KO however there was in the ileum. The basal level of IL-13 in the ileum of the RAG GC KO was an order of magnitude lower than the RAG KO however there was still a nonsignificant trend towards transgenic T cells promoting IL-13. As there is still this induction but no gross pathology it can be hypothesised that there is a component of T cell derived IL-13 however in this model the T cells alone were not able to produce enough to be pathogenic.

Following T cell transfer, lung pathology was observed in the recipient mice. The mice that received Mem+Sol had the worst pathology followed by those that received Mem CD4+ T cells. Further the transfers into the RAG GC KO mice showed an attenuated pathology compared to the RAG suggesting that the T cells were only able to expand to their full potential with the help of other cell types.

Unexpectedly the RAG GC KO, which received TL1A transgenic T cells, developed obliterative colitis. Those that received Mem+Sol had worse disease. The development of colitis in this model most likely occurred due to 3 reasons. Firstly, as has been reported before[174], Tregs from T cell specific TL1A transgenic mice show attenuated function, in part due to the ectopic expression of a known T cell costimulator, TL1A. In addition, a Treg suppression assay with a mix of DR3 KO effector T cells and DR3 sufficient Tregs demonstrated reduced functionality of Tregs

when sTL1A was added to the media indicating a Treg intrinsic attenuating effect[175]. As transfer of T cells without Tregs induces the T cell transfer model of colitis it is perhaps not surprising that some form was seen[256]. However why was it only seen in the transfer into RAG GC KO mice and not RAG KO mice? Signalling via the IL-23 receptor[257], and subsequent production of IL-22[258], are protective in the T cell transfer model of colitis. Given the costimulatory effect of TL1A on ILC3s for the production of IL-22[161, 181] we hypothesise that the pathogenic effect of TL1A transgenic Tregs is overcome in a RAG KO mouse due to the IL-22/23 pathway. Additionally early work on the T cell transfer model of colitis found that depletion of NK cells resulted in earlier onset and increased pathology of colitis[259]. More recent work demonstrated that depletion of NK cells resulted in increased production of pro-inflammatory cytokines including IL-17 and IFN-γ by lamina propria T cells and an earlier upregulation of activation markers on T cells from the mesenteric lymph node[260]. Together the effects of lacking NK cells promote increased pathology thereby implying a protective role for NK cells in this model. As both the NK and ILC3 dependent effects are lost upon transfer into RAG GC KO due to the lack of these cell types development of the observed phenotype may thus be able to occur.

The final section of this chapter attempts to identify novel TL1A responsive genes by identifying conserved differential expression in the lungs and the ileum using RNASeq. It is encouraging that relatively few genes fit the conservation criteria suggesting that these are true downstream effects of TL1A overexpression. The increased expression of TNFSF15 throughout all tissues and lines is a good positive control for the criteria used. Of the genes that were found several are very interesting and may indicate potential mechanisms for TL1As *in vivo* effects. The increased expression of Mgl2 along with its link to Th2 immunity[248] suggests a mechanism by which TL1A may result in the establishment of a type 2 immune environment through effects on APCs. Increased Samsn1 suggests a role for DR3 in B cell activation which is an area of TL1A biology that has been very understudied[129]. In addition an unpublished RNASeq analysis from the laboratory of J. J. O'Shea demonstrates the upregulation of this gene in ILC2s upon activation. Given the known effects of TL1A on ILC2s this may be a direct downstream effect of TL1A on this cell type[140]. Samsn1 was the only one of the identified genes that demonstrated a reasonable expression within any ILC subset (G. Sciume, unpublished observations). Finally the promotion of Csn2 and 3 is novel as, to the best of our knowledge, there is no reported role for these proteins outside of lactation. Further these genes were

increased in both male and female mice. As these data were derived from whole organ RNASeq it is not easy to tell if these are increased in expression due to increased numbers of particular cell types or increased production by a cell as a result of TL1A. Further work would have to be carried out to not only identify the cells responsible for these changes but also determine if this is a direct or secondary effect of TL1A overexpression. The fact that there are very few genes that are differentially regulated suggest that these may not be cell number effects. For example B cell markers such as CD19 are not included in this gene list. If they were then the increase in Samsn1 would be unsurprising. These data at least provide a starting point for investigation of novel effects of TL1A.

In conclusion these data suggest that in addition to the non T cell role in the production of IL-13[140, 174] multiple other effects of TL1A overexpression can be associated to different cell types. However, as was shown in the RAG transfer experiments, we must be careful in assigning one particular phenotype to one cell type as clearly other cells can participate, although they may not be the major source of a given cytokine. Further, as exemplified by IL-9, the cellular origin of a cytokine may differ dependent upon location.

Chapter 6. DR3 is required on B cells for optimal class switching to IgA

6.1. Introduction

Given the effect observed in previous chapters of TL1A over expression on B cell help we investigated the role of DR3/TL1A signalling in response to systemic immunisation.

Responses against many pathogens, both bacterial and viral, are mediated through the binding of antibodies to antigenic epitopes on the surface of the invader. Through binding the surface of pathogens antibodies are able to neutralise entry methods used by viruses to invade host cells as well as highlight bacterial pathogens for destruction through the action of complement or phagocytosis.

Antibodies are produced by activated plasma cells as a result of either a T dependent (Td) or T independent (Ti) reaction. The Td response involves T follicular helper (Tfh) cells, which are a subset of CD4+ T cells that aid the activation of B cells by promoting the GC reaction and long lived serological memory. In contrast Ti antigens promote B cell activation and antibody response in isolation of T cell help.

6.1.1. T dependent B cell response

Differentiation of naïve T cells into Tfh cells is initiated through priming by DCs [261, 262]. To enable Tfh cells to migrate from T cell zones to B cell zones in the spleen and secondary lymphoid organs, down regulation of CCR7 and PSGL-1 and up regulation of CXCR5 occurs. CCR7, the chemokine receptor for CCL19 and CCL21, enables circulating T cells to migrate into T cell zones through interaction with its ligands, which are expressed within the spleen and lymph nodes [263, 264]. PSGL-1 is also able to interact with CCL19 and CCL21 and is required for T cell zone homing [265, 266]. Inducible costimulator (ICOS) is highly up regulated upon differentiation into Tfh cells and is required for Tfh interaction with both DCs and B cells. Reduced initial and absent secondary GC formation have been observed in response to antigen challenge in ICOS KO mice demonstrating its vital function on Tfh cells[267]. Tfh cells also express PD-1 and CD154 and SAP which are required for effective B cell help [268-270].

The major transcriptional regulator for Tfh Cells is Bcl-6 and is essential for their function [271, 272]. Bcl-6 promotes the expression of CXCR5 and PD-1 and acts in

part through the repression of several micro RNAs. One such micro RNA is miR-17-92 which has been shown to negatively regulate CXCR5[272, 273].

Post encounter with antigen, Tfh cells migrate into B cell zones and provide help for B cell activation and differentiation. Ligation between CD40L on Tfh cells and CD40 on B cells promotes the GC reaction[274]. This is further promoted by IL-21 secreted by Tfh cells[275]. The interaction between Tfh cells and B cells is aided and prolonged through the action of the adaptor protein SAP that interacts with the SLAM family of adhesion molecules. The absence of this protein results in transient interactions between B cells and Tfh cells and attenuates the GC response[268].

A major component of the GC reaction is affinity maturation. This is a process through which somatic hyper mutation promotes the secretion of high affinity antibodies by B cells. One of the latest models for this process proposes that B cells capture antigen from follicular DCs via their BCR, which is subsequently internalised and presents the captured antigen on MHC II to a Tfh cell resulting in help for that B cell[276]. Recent work has shown that both proliferation and hypermutation are directly proportional to the amount of antigen presented to the Tfh by the B cell as a result of capture from follicular DCs[277]. As a high affinity BCR would be more successful in the capture and presentation of antigens to Tfh cells it would also receive more help thus promoting antibodies which, through mutation, encode a high affinity antibody. Evidence for this role of T cell help is that GC which have formed in the presence of T cell help are larger and show greater diversity in the library of antibody clones available[278]. The GC is composed of a dark and light zone. After initial activation of a B cell it migrates from the dark zone to the light. Here it engages with the Tfh and is helped. Once it has been helped it returns to the dark zone and undergoes clonal expansion[279]. During the GC reaction the B cell also undergoes class switch recombination resulting in isotype switching of the antibody.

6.1.2. T independent B cell response

The Ti response is promoted as a result of B cell activation via pattern recognition receptors (eg LPS with TLR4) or via crosslinking of the BCR (e.g. polysaccharide) with antigens that are unable to be processed for presentation upon a MHC II. These two types of response are referred to as Ti type 1 (Ti-1) and 2 (Ti-2) respectively. Specifically the two classes of Ti responses are defined on the ability of Btk KO mice to respond to antigen. Btk is a key kinase that is required for BCR signalling[280,

281]. In Btk KO, Ti-1 but not Ti-2 antigens are able to promote a response in a plaque forming assay[282].

Ti-1 responses result from recognition of an antigen via the BCR in combination with TLR signaling. In murine experiments this can be modeled by immunisation with the hapten NP conjugated to LPS. Induction of signaling via LPS can induce a polyclonal antibody response. However, depending on the BCR clone, it can also interact with the BCR thus promoting a more specific and robust response in addition to strong AID expression and an increased rate of class switch recombination[283].

Ti-2 responses are against BCR crosslinking antigens. An example would be the large polysaccharide antigens that contain vast arrays of antigenic epitope repeats. These allow for the binding of multiple BCRs simultaneously, promoting crosslinking and clustering of the receptor promoting downstream signaling, proliferation and secretion of Igs[284].

BAFF, a member of the TNFRSF, has previously been shown to promote Ti-2 responses. Mice in which BAFF signaling is interrupted have attenuated Ti-2 response[285] and BAFF overexpression promotes Ti-2[286]. Further, mice where iNOS has been knocked out show increased BAFF expression following Ti-2 immunisation and a concurrent increase in Ti-2 induced IgM titres[287].

6.1.3. B cell phenotypes are induced in response to TL1A

The role of TL1A on B cells is understudied with one *in vitro* paper demonstrating an effect on proliferation[129]. Soluble TL1A has also been found to act as a mucosal adjuvant. If given at the same time as an immunogen intranasally, TL1A, and to a lesser extent TNF, promoted increased titres of mucosal IgA[236]. In support of this we showed in previous chapters that TL1A transgenics exhibited hyper IgA and hyper IgE.

6.1.4. IgA in health and disease

IgA, whilst exhibiting a low level in the serum, is expressed at high levels in mucous membranes and accounts in mammals for around three quarters of daily secretion of all immunoglobulins[288]. The main effector site of IgA is in the gut. Here IgA coats pathogens preventing them from infecting the host but also, via the binding of IgA receptors, facilitates uptake and enhancement of antigen presentation[289].

The role of IgA is highlighted in patients with IgA deficiency and IgA KO mice. IgA deficiency presents at an incidence of approximately 1 in 600 however two thirds are non-symptomatic. Those that do suffer present with recurrent bacterial, protozoal and enteroviral infections and can also present with intestinal inflammatory disorders[289, 290]. In contrast IgA KO mice have a minimal phenotype with no susceptibility to influenza infection[291]. They do however show increased IgM secretions[292]. This compensatory mechanism may explain why so few IgA deficient patients present with symptoms.

IgA plays a role in the pathogenesis of glomerulonephritis. Deposition of IgA is the most common deposit found in patients with glomerulonephritis, of which 30-50% of IgA+ individuals go on to develop renal failure within 20 years of the initial biopsy[293].

Several members of the TNFSF have been shown to play a role in IgA production. Signalling via LT has been shown to be required for development of Peyer's patches and lymph nodes[92] and lack of signalling results in severely attenuated basal and responsive IgA levels[93]. In the gut LTα promotes Td IgA responses through regulation of T cell homing whereas LTα1β2 promotes Ti IgA through modulation of iNOS expression in CD11c+ DCs[83]. APRIL, another member of the TNFSF, also shows a role in IgA production. APRIL KO mice have reduced total serum IgA as well as a reduced antigen specific IgA in response to Td and Ti-1 but not Ti-2 antigens. In addition, exogenous APRIL was shown to promote IgA class switching *in vitro*[294].

In this chapter we assess the response of DR3 KO mice to both Td and Ti antigens *in vivo* using the model antigen NP conjugated to various carriers. We further assess the potential for exogenous TL1A in class switching. We demonstrate that DR3 is required on T cells and not on B cells for induction of IgA class switching and that TL1A may be a novel IgA switch factor.

6.2. Results

6.2.1. T dependent immunisation of DR3 KO mice

To assess the requirement of DR3 in response to immunisation, mice were immunised with alum precipitated NP-OVA on day 0 and boosted with NP-OVA on day 48. The levels of total and high affinity anti NP antibodies were measured by ELISA against NP-4-BSA and NP-29-BSA respectively on day 21 and day 56. DR3 KO mice had a significant defect in the IgG2b secondary response to NP. A strong defect was also observed in NP specific total IgA in the primary response and both total and high affinity in the secondary response (Figure 6-1).

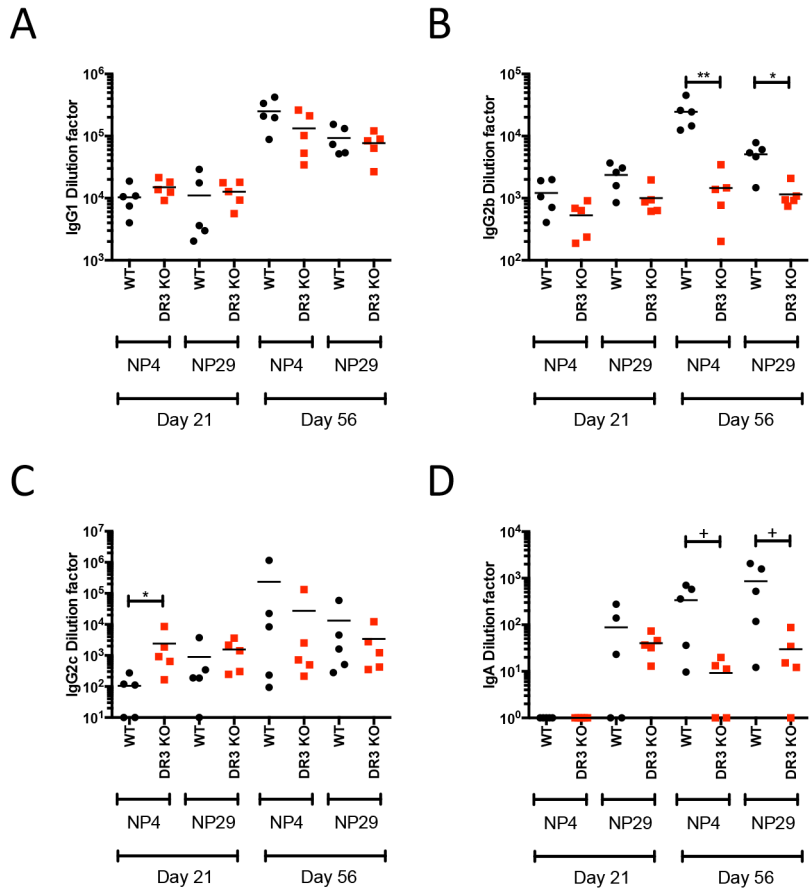

Figure 6-1 *- T cell dependent NP immunisation of DR3 KO mice. WT or DR3 KO mice were immunised subcutaneously on day 0 with 10ng of NP-16-OVA in alum and boosted with 10ng of NP-16-OVA in PBS on day 48. Serum was collected on day 21 and 56 and the level of total or high affinity NP specific antibodies measured by ELISA against either NP-4-BSA or NP-29-BSA respectively. Levels of NP specific IgG1 (**A**), IgG2b (**B**), IgG2c (**C**) and IgA (**D**) were measured. Dilution factor represents the fold dilution of each sample required to give an OD twice the*

*background. + indicates 0.065>P>0.05, * 0.05>P>0.01 and ** 0.01>P>0.001 using the Mann-Whitney U test. Data representative of at least 2 independent experiments.*

6.2.2. DR3 KO mice do not have a global defect in IgA

Defects in the production of a specific isotype of antibody can either be due to a global defect or due to a defect in the response to antigen. To address this the level of total IgA in the serum was measured in DR3 KO mice and age matched littermates. There was no defect found in total IgA (Figure 6-2).

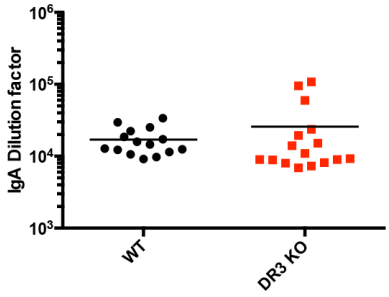

Figure 6-2 *- DR3 KO mice have no defect in total IgA. Serum was collected from WT and DR3 KO littermates between 10.5 and 13.5 weeks of age and total levels of IgA in the serum measured. Dilution factor represents the fold dilution of each sample required to give an OD twice the background. P=0.2003 using the Mann-Whitney U test. Experiment was carried out by A. C. Richard.*

6.2.3. Defect in IgA is not due to DR3 expression on T cells

As previous work has demonstrated DR3 expression both on CD4+ T cells[131] and B cells[129] the defect in IgG2b and IgA antigen specific responses could be conferred through lack of DR3 on either cell subset or both. To assess this the CD4 conditional DR3 KO was immunised as before with NP-OVA. There was still a mild defect in IgG2b responses (Figure 6-3B) however there was no longer a defect in IgA responses (Figure 6-3D).

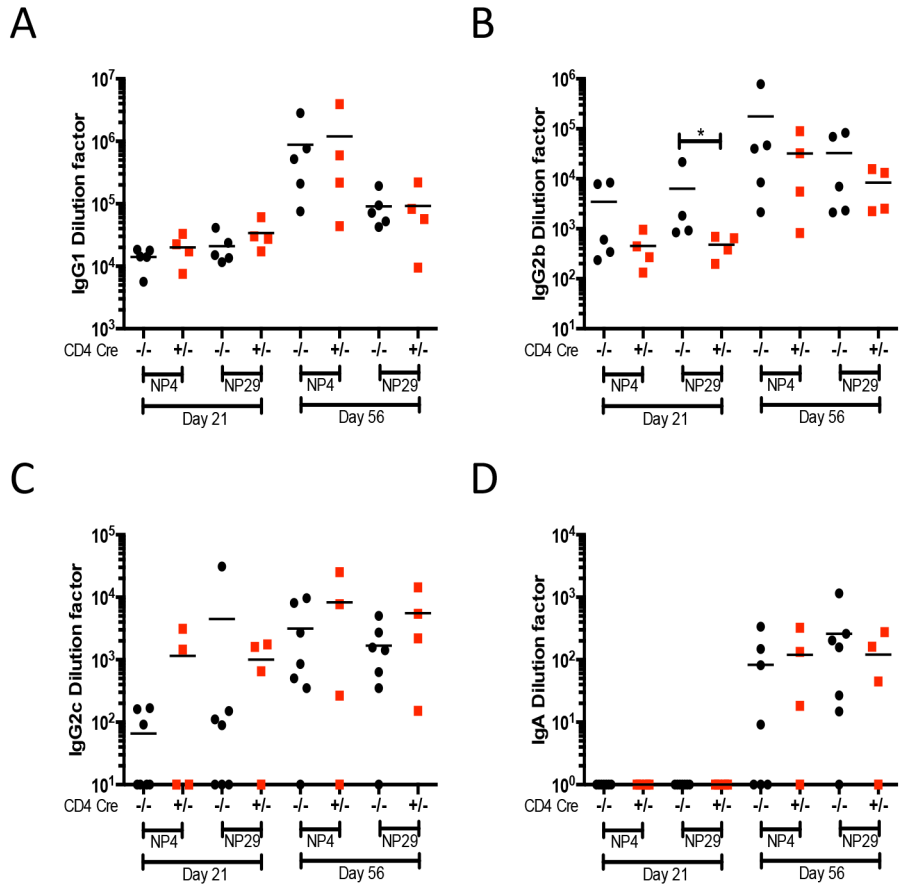

Figure 6-3 *- T cell dependent NP immunisation of T cell specific DR3 KO mice. DR3$^{FL/FL}$ CD4 Cre$^{-/-}$ or DR3$^{FL/FL}$ CD4 Cre$^{+/-}$ mice were immunised subcutaneously on day 0 with 10ng of NP-16-OVA in alum and boosted with 10ng of NP-16-OVA in PBS on day 48. Serum was collected on day 21 and 56 and the level of total or high affinity NP specific antibodies measured by ELISA against either NP-4-BSA or NP-29-BSA respectively. Levels of NP specific IgG1 (**A**), IgG2b (**B**), IgG2c (**C**) and IgA (**D**) were measured. Dilution factor represents the fold dilution of each sample required to give an OD twice the background. * indicates 0.05>P>0.01 using the Mann-Whitney U test. Data representative of 2 independent experiments.*

6.2.4. T independent immunisation of DR3 KO.

Given that lack of DR3 on T cells does not confer a defect in IgA response (Figure 6-3D) the response to Ti-1 (Figure 6-4) and Ti-2 (Figure 6-5) was assessed. Mice were immunised with NP-LPS in PBS on day 0 and boosted day 48 for a Ti-1 response and NP-ACEM-Ficoll for a Ti-2. Mice had an IgA NP specific defect in Ti-1 and a more minor one in Ti-2.

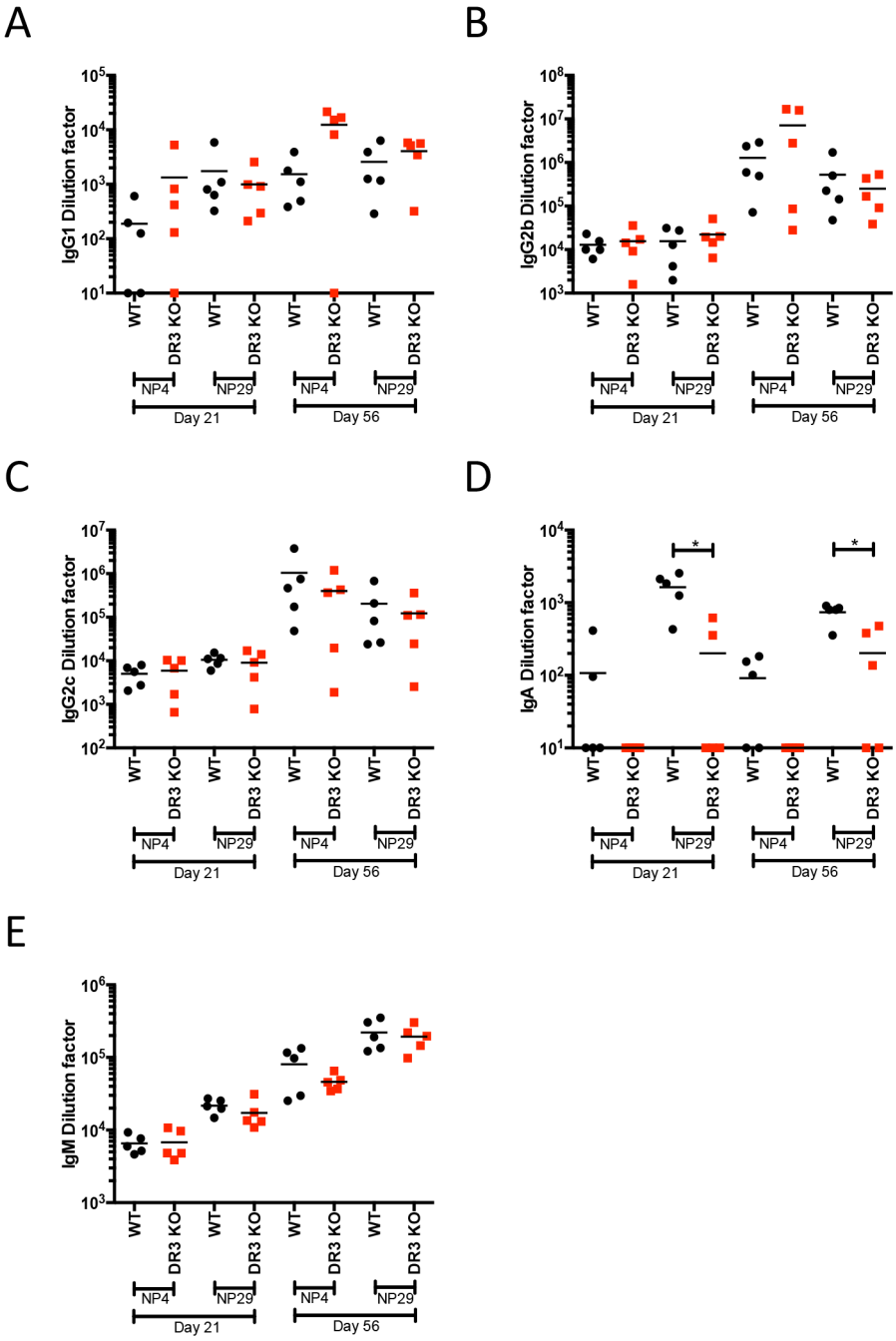

Figure 6-4 *- Type 1 T independent NP immunisation of total DR3 KO mice. WT or DR3 KO mice were immunised via intraperitoneal injection on day 0 and boosted on day 48 with 10ng of NP-0.15-LPS. Serum was collected on day 21 and 56 and the level of total or high affinity NP specific antibodies measured by ELISA against either NP-4-BSA or NP-29-BSA respectively. Levels of NP specific IgG1 (**A**), IgG2b (**B**), IgG2c (**C**), IgA (**D**) and IgM (**E**) were measured. Dilution factor represents the fold dilution of each sample required to give an OD twice the background. * indicates 0.05>P>0.01 using the Mann-Whitney U test.*

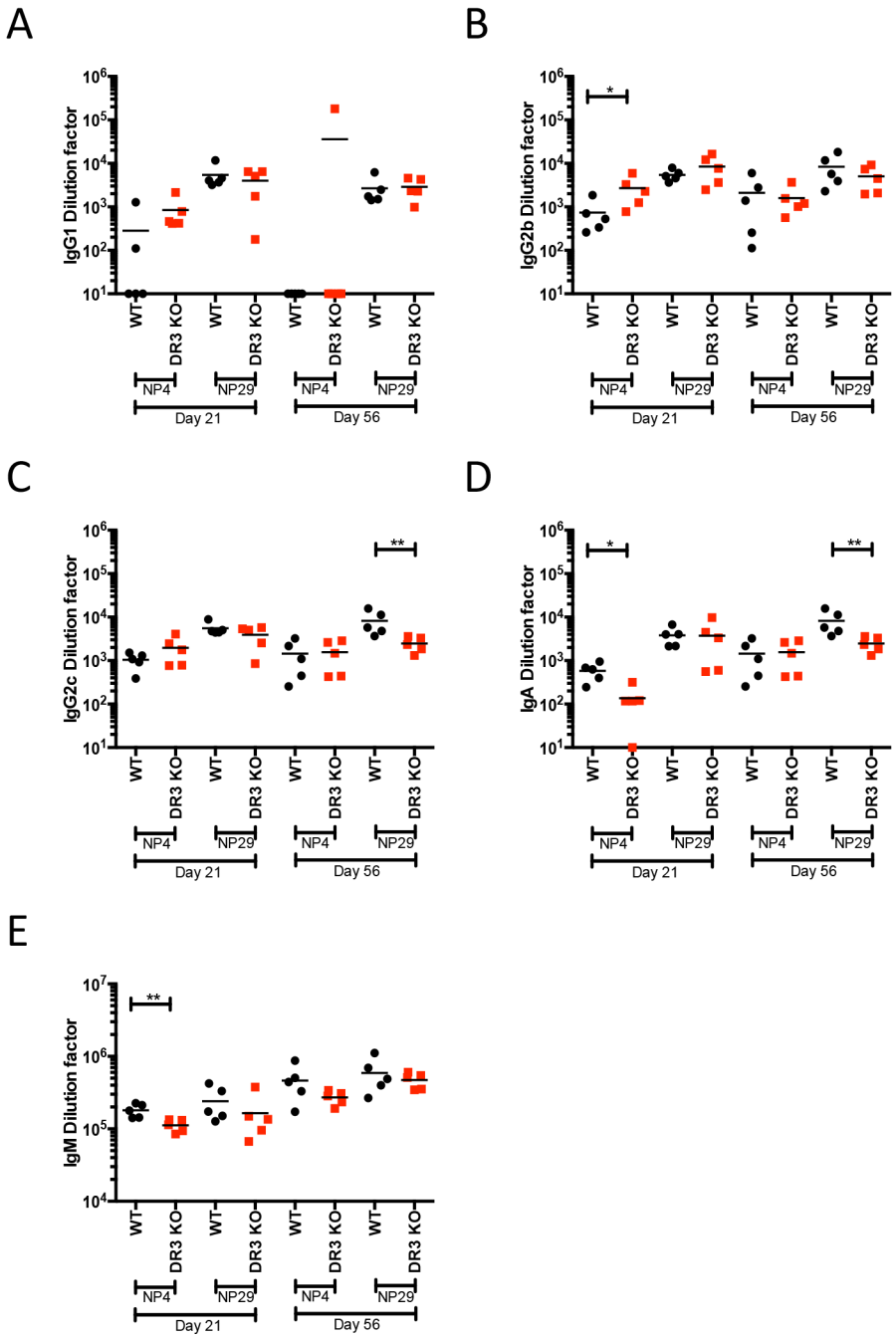

Figure 6-5 *- Type 2 T independent NP immunisation of total DR3 KO mice. WT or DR3 KO mice were immunised via intraperitoneal injection on day 0 and boosted on day 48 with 10ng of NP-49-ACEM-Ficoll. Serum was collected on day 21 and 56 and the level of total or high affinity NP specific antibodies measured by ELISA against either NP-4-BSA or NP-29-BSA respectively. Levels of NP specific IgG1 (**A**), IgG2b (**B**), IgG2c (**C**), IgA (**D**) and IgM (**E**) were measured. Dilution factor represents the fold dilution of each sample required to give an OD twice the background. * indicates 0.05>P>0.01 and ** 0.01>P>0.001 using the Mann-Whitney U test.*

6.2.5. TL1A is a potential novel IgA switch factor in vitro

Given the B cell intrinsic defect in IgA class switching, TL1A was used in an *in vitro* class-switching assay. In this preliminary experiment B cells were activated via CD40 crosslinking in the presence of combinations of IL-4, TGF-β and TL1A. After 3 days the level of surface IgA expression was examined by flow cytometry. TL1A was found to increase the level of surface IgA both with and without the addition of TGF-β (Figure 6-6).

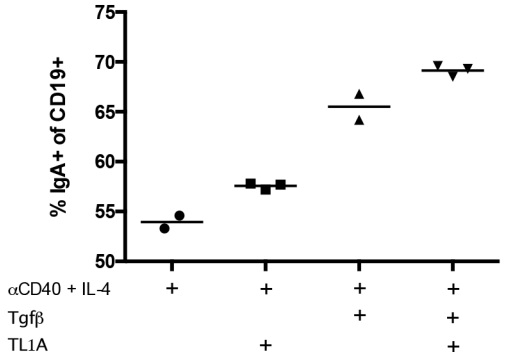

Figure 6-6 *- TL1A induces IgA class switching in vitro. Purified B cells were stimulated for 3 days with the indicated combination of anti CD40 (1ng/ml), IL-4 (2.5ng/ml), TGF-β (1ng/ml) and TL1A (100ng/ml). Level of IgA expression was measured on the surface of the cells by flow cytometry.*

6.3. Discussion

Given the role of multiple members of the TNFSF in antibody responses[93, 270, 294] and the antibody based phenotypes observed in TL1A transgenic mice (Chapters 4 and 5), we sought to examine the role of TL1A in this respect.

Using the Td antigen NP-OVA we demonstrated that there is a defect in IgG2b and IgA antigen specific responses. This defect was not a total defect but rather a partial one; therefore DR3 is not essential for the production of these isotypes. This was backed up by the fact that DR3 KO mice have a normal level of total IgA. Interestingly the defect in both IgA and IgG2b was greatest following the boost. This may suggest a role for TL1A in the generation of isotype specific memory B cells.

Following on from this we demonstrated that the defect observed in antigen specific IgG2b antibodies was T cell intrinsic whereas the defect observed in IgA was unaffected by the loss of DR3 from only the T cell. To definitively prove that the IgA defect was due to signalling via DR3 on the B cell we would need a B cell conditional DR3 KO. Unfortunately at this time this mouse is not available. This mouse could be generated by crossing the floxed DR3 mouse with a CD19 Cre and would be of interest in future studies.

In the absence of a B cell DR3 conditional KO mouse we immunised conventional DR3 KO mice with Ti-1 and Ti-2 antigens. Whilst this does not directly address the lack of DR3 on B cells only, it does examine B cell intrinsic phenotypes. This does not however rule out other possible defects on B cells due to development or indirect effects. When the mice were immunised with either of the Ti antigens the effects on IgG2b were lost. Combined with the T cell DR3 conditional KO data this suggests that effects on this isotype were due to T cell help as part of the GC reaction. In contrast the effect of DR3 on IgA class switching was maintained, with the greatest effect observed in the Ti-1 immunisation. A difference was observed under Ti-2 conditions however this was not as prominent though this may be due to the stronger antibody response observed with NP-ACEM-Ficoll which may negate much of the effect of lacking DR3. Further as LPS was used as the carrier for the Ti-1 antigen, and this is a known stimulator of TL1A production[159], perhaps greater effects for lack of DR3 are to be expected in this setting.

To assess if TL1A could act in isolation on B cells we cultured them under IgA differentiating conditions with the addition of TL1A for 3 days. In this preliminary assay we found that TL1A had a small but obvious effect on the expression of

surface IgA as measured by flow cytometry. Further optimisation of this assay is required to determine if a greater role of TL1A can be observed. As observed in T cells[159] the greatest effect of TL1A costimulation is seen under sub-optimal conditions. It may be that upon titration of the anti CD40 TL1A has a greater effect. Further the effect of TL1A could also be measured by assessing the level of IgA heavy chain transcript present in the cell following stimulation as was shown for APRIL stimulation[294].

These data, along with previous work[236], identify TL1A as a potential novel B cell intrinsic IgA switch factor. The role of TL1A/DR3 signalling in IgA class switching is less than that of APRIL[294] as it is not required for maintenance of total IgA and appears to be only necessary under immunisation settings.

A possible mechanism for the effect conferred by TL1A in immunisation is through synergy with TGF-β. In the differentiation of Th9 cells TL1A was shown to act in a synergistic manner with TGF-β and reduce the threshold for TGF-β promotion of the Th9 subset of helper T cells[133]. TGF-β is also able to promote class switching to IgA [295] and IgG2b[296] and its receptor is required to mount an IgA mucosal response to immunisation[297]. Further, as TGF-β has been shown to inhibit B cell proliferation[298] this may explain the inhibition of proliferation of B cells observed by Cavallini *et al*[129] in response to TL1A. Recent data has demonstrated the suppressive effects of IL-21 on IgG2b but not IgA class switching[299]. Given the production of IL-21 from T cells[300] this may be a potential mechanism to explain the IgG2b defect only in Td responses. It is possible that a lack of TL1A in combination with T cell derived IL-21 is enough to reduce the class switching to IgG2b in Td responses. However in Ti response there may not be enough IL-21 present and lacking the brake on IgG2b class switching may overcome any deleterious effects of absence of TL1A. However, further studies would have to be undertaken to validate these hypotheses.

Chapter 7. The role of DR3 in chronic autoimmunity

7.1. Introduction

As DR3 shows a relatively restricted expression pattern (Table 1-1) it is an attractive therapeutic target. To this end we wished to examine the role of DR3/TL1A in chronic autoimmune models to evaluate this pathway's role and examine if signalling modulation could be a potential therapy. To date all the published work on TL1A and DR3 has examined its role in acute disease models. Here we assess the role of DR3/TL1A signalling in chronic autoimmune pathogenesis.

Systemic Lupus Erythematous (SLE) is a multi-system autoimmune disease. It shows a higher incidence for those of African rather than European descent with a strong female bias, most often presenting in those of child bearing age[301]. Symptoms are diverse and include rash, nephritis, seizure, psychosis, arthritis and thrombocytopenia[302]. SLE has a genetic component however it is not an absolute as monozygotic twins have a 24-69% concordance and first degree relatives 1-3% suggesting multiple genetic and environmental factors[303]. A major symptom of SLE is a high level of autoantibodies in the serum, including but not limited to, anti-dsDNA antibodies[304]. The autoantibodies subsequently bind to their antigen and are deposited in the glomerulus leading to the development of lupus nephritis[302]. There are multiple mouse models that mimic SLE.

A common model of SLE which has been linked with the TNFSF is the LPR mouse. These mice develop many of the symptoms of SLE including increased autoantibody titres, glomerulonephritis, proteinuria, increased double negative T cells and spontaneous autoimmune skin lesions[305]. Interestingly, this phenotype occurs due to an insertion mutation in the TNFSF member Fas resulting in a lack of expression[80]. Other members of the TNFSF play a role in modulating the LPR phenotype. Crossing LPR mice to the TNFR1 KO greatly exacerbated the pathology[306] whereas blocking BAFF and APRIL signalling with an adenoviral TACI-Fc protected the mice[307]. Further recent unpublished work from R. Siegel's laboratory highlighted a role for DR3 in the development of kidney pathology.

As a lupus-like B cell driven model of autoimmunity we utilised a strain of mice where Bcl2 is expressed constitutively under the control of the Vav promoter. As a result Bcl2 is expressed across the haematopoietic lineage [308]. Bcl2 is a transcription

factor that promotes cell survival and has been shown to be a potent oncogene in human follicular lymphoma[309, 310]. Vav-Bcl2 mice present with age dependent splenomegaly, GC hyperplasia, hypermutation of Ig V genes, increased autoantibody titres, hypergammaglobulinemia and an increased proportion of Tregs[311, 312]. When crossed to mice which express a TACI-Ig fusion protein the phenotype is attenuated[313]. To study the effect of the TL1A/DR3 pathway we crossed these mice to both the Mem+Sol TL1A transgenic and the DR3 KO to study both increased and ablated signalling.

To further investigate potential roles of TL1A/DR3 signalling in lupus we used the parent into F1 chronic GVHD model. This model can either be induced by transfer of whole splenocytes from a DBA/2 mouse into the F1 progeny from a cross between C57bl/6 and DBA/2 (referred to here as BDF1 mice) or by transfer of purified CD4+ T cells from a C57bl/6. DBA/2 mice express the Kd MHC haplotype, C57bl/6 mice Kb and BDF1 mice express both. Due to the mismatch of MHC haplotype the donor cells, allo-specific CD4+ T cells, are activated and induce the model through activation of host B cells. This results in the rapid production of auto-antibodies and the development of glomerulonephritis[314]. Members of the TNFSF have also been shown to play a role in the pathogenesis of this model. Transfer of TRAIL KO donor cells resulted in reduced pathology with less IgG deposits in the kidney and reduced serum titres of anti single stranded DNA (ssDNA) from day 28[315]. In addition when TNFR2 KO mice were used as the donor cells under conditions that would normally result in acute GVHD it was observed the mice instead developed chronic lupus like GVHD. The recipient mice had neither depletion of host B cells nor any other sign of acute GVHD. However the mice receiving TNFR2 KO cells showed increases in anti ssDNA. This phenotype was not observed when TNFR1 KO donor cells were used and mimics the effect of TNFR1KO in LPR mice[306, 316]. To investigate the role of DR3 in this system we transferred DR3 KO CD4+ cells. We demonstrated that the DR3 KO cells were able to induce the autoantibody phenotype but were unable to promote glomerulonephritis.

7.2. Results

7.2.1. Vav-Bcl-2 x Mem+Sol TL1A transgenic mice

Given the observed phenotype in the B cell compartment of the TL1A transgenic mice (Chapters 4 and 5) we crossed the Vav-Bcl2 transgenic onto this background. For this we used the Mem+Sol strain from A. Al-Shamkhani's group. This mouse has not been published before however has the same phenotype as the strain published by Meylan *et al*[174] and was produced from a very similar construct. All transgenic mice were maintained as heterozygotes and the mice assessed were littermates, which were born at expected Mendelian frequencies. The mice that were positive for both the TL1A and Bcl2 transgenes are referred to as double mice in this section only. The phenotype of these mice was assessed in both the spleen and serum at 18 weeks of age.

Ectopic expression of TL1A in conjunction with the VavBL-2 transgene had no effect on splenomegaly or the proportion of CD4+ or CD19+ cells within the spleen (Figure 7-1). However TL1A did promote an additive increase in double mice in both Tregs and Tfh as a percentage of the CD4+ T cell compartment(Figure 7-2).

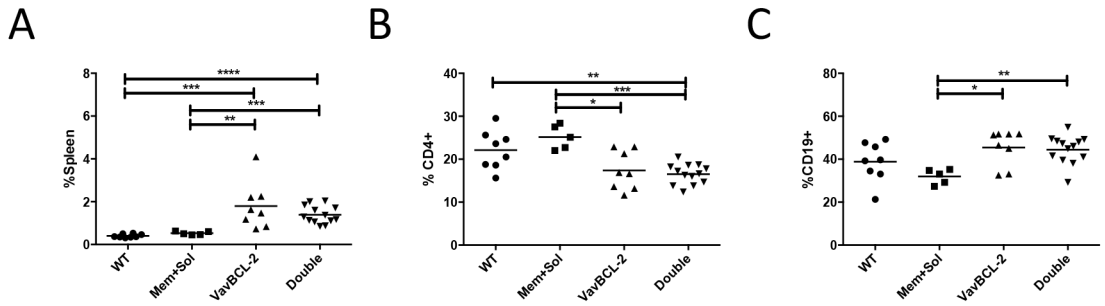

Figure 7-1 *– Splenic components of Mem+Sol TL1A x Vav-BCL2. Mem+Sol TL1A transgenic mice were crossed to the Vav-BCL2 strain to give either WT, Mem+Sol alone, Vav-Bcl2 alone or double transgenic mice and culled at 18 weeks of age. The spleen was weighed and its percentage of the total mass of the mouse calculated (**A**). The spleen was assessed by flow cytometry and the proportion of CD4+ cells (**B**) and CD19+ cells (**C**) of total splenocytes calculated. * indicates 0.05>P>0.01, ** 0.01>P>0.001, *** 0.001>P>0.0001 and **** P<0.0001 using the Mann-Whitney U test.*

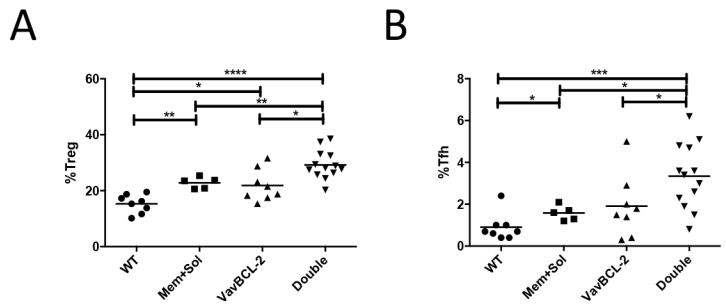

Figure 7-2 *- CD4 T cell subsets in the spleen of Mem+Sol TL1A x Vav-BCL2. The proportion of Treg (**A**, CD4+ FoxP3+) and Tfh (**B**, CD4+ PD1+ CXCR5+) of CD4+ cells was assessed in the spleen of the indicated 18 week old mice by flow cytometry. * indicates 0.05>P>0.01, ** 0.01>P>0.001, *** 0.001>P>0.0001 and **** P<0.0001 using the Mann-Whitney U test.*

Given the prominent B cell phenotype in the Vav-Bcl2 mice[308] we next assessed both the cellular and humoral arms of the B cell compartment. There was a trend towards an increase in the fraction of class switched B cells in the spleen and a significant increase in GC B cells as a result of TL1A expression (Figure 7-3 A and B). In the serum the levels of anti dsDNA IgG2b antibodies were increased in the double over the Vav-Bcl2 alone however this was lower than Mem+Sol (Figure 7-3C). A minor effect, which appears additive, was observed in total Ig levels in the serum (Figure 7-3 D-F).

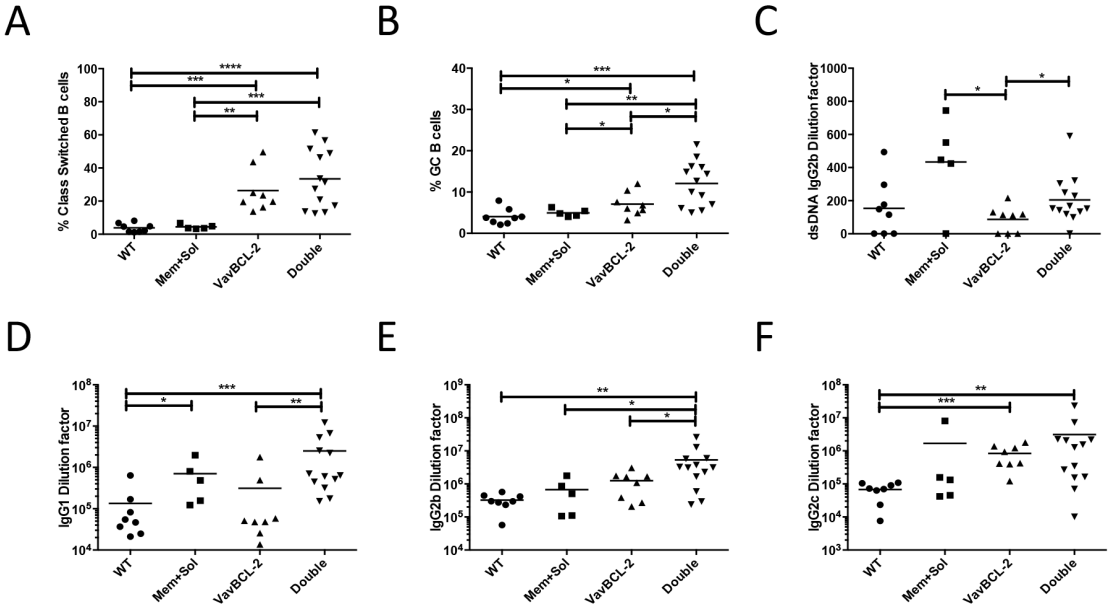

Figure 7-3 *- B cell compartment in the spleen of Mem+Sol TL1A x Vav-BCL2. The proportion of class switched B cells (**A**, CD19+ IgM- IgD-) or GC B cells (**B**, CD19+ PNA+) out of total CD19+ cells was assessed in the spleen of 18 week old mice of*

*the indicated genotypes. At the same time serum was collected and levels of IgG2b anti dsDNA (**C**) and total IgG1(**D**), IgG2b (**E**) and IgG2c (**F**) measured. Dilution factor represents the fold dilution of each sample required to give an OD twice the background. * indicates 0.05>P>0.01, ** 0.01>P>0.001, *** 0.001>P>0.0001 and **** P<0.0001 using the Mann-Whitney U test.*

7.2.2. DR3 KO x Vav-Bcl2 mice

To assess the result of lack of DR3 signalling in the Vav-Bcl2 model we backcrossed the DR3 KO mice onto the Vav-Bcl2 transgenic strain. Given the relatively minor phenotype observed at 18 weeks of age (See Section 7.2.1) we assessed the phenotype in these mice at 30 weeks of age. The mice were born at expected Mendelian frequencies and assessed as littermates. As a result the Vav-Bcl2 mice in this section are heterozygous for DR3. In addition double mice are DR3 KO Vav-Bcl2 heterozygotes.

The lack of DR3 had no significant effect on splenomegaly nor the frequency of Tregs within the CD4 compartment(Figure 7-4 A and B). However the frequencies of Tfh and class switch B cells were reduced along with a trend towards reduction of the GC B cells (Figure 7-4 C-E).

The lack of DR3 in the Vav-Bcl2 mice did not affect levels in the serum of either total Ig, anti nuclear-antibodies (ANA) or anti dsDNA antibodies (Figure 7-5).

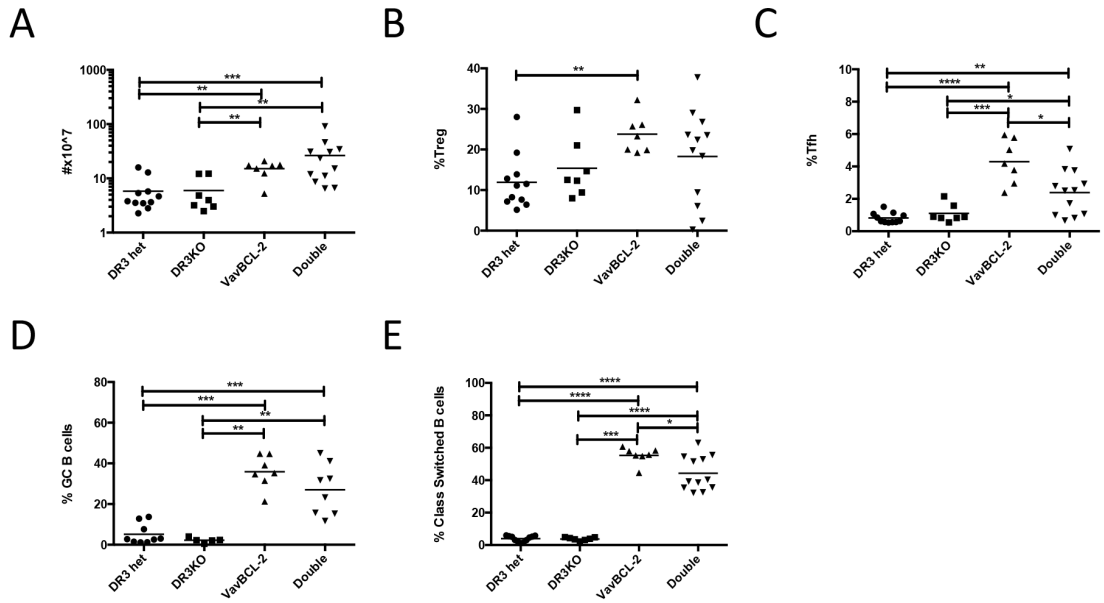

Figure 7-4 *- Splenic composition in DR3KO x Vav-Bcl2. Vav-Bcl2 transgenic mice were backcrossed to the DR3 KO and the four possible genotypes (DR3 -/+, DR3 -/-, DR3 -/+ Vav-BCL-2 +/- and DR3 -/- Vav-BCL-2 +/-[Double]) assessed at 30 weeks of*

*age. Total numbers of splenocytes were counted (A) and cell populations assessed by flow cytometry. Treg (B, CD4+ FoxP3+ of CD4+), Tfh (C, CD4+ CXCR5+ PD1+ of CD4+), GC B cell (D, CD19+ PNA+ GL7+ of CD19+) and class switched B cell (E, CD19+IgM-IgD- of CD19+) fractions of their parent population were calculated. * indicates 0.05>P>0.01, ** 0.01>P>0.001, *** 0.001>P>0.0001 and **** P<0.0001 using the Mann-Whitney U test.*

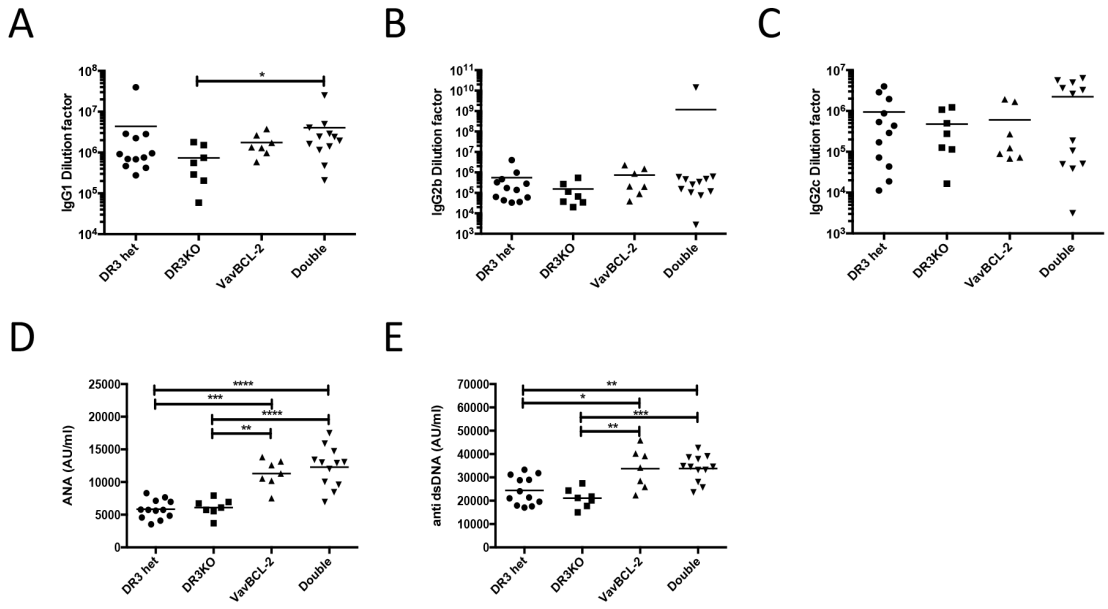

Figure 7-5 *- Immunoglobulin serum composition in DR3KO x Vav-Bcl2. Serum was collected from the indicated genotypes at 30 weeks of age and the levels of total IgG1 (**A**), IgG2b (**B**) and IgG2c (**C**) measured by ELISA. Dilution factor represents the fold dilution of each sample required to give an OD twice the background. Total ANA and anti dsDNA antibody levels were also measured. AU corresponds to standards provided by the manufacturer. * indicates 0.05>P>0.01, ** 0.01>P>0.001, *** 0.001>P>0.0001 and **** P<0.0001 using the Mann-Whitney U test.*

Given the increased auto antibody titres observed (Figure 7-5 D and E) and the link between these and lupus nephritis[302] we assessed the kidneys for gross pathology (Figure 7-6) and IgG and C3 deposits (Figure 7-7). Both deposits and lymphoid infiltrates were increased in the Vav-BCL2 mice however there was no effect as a result of lack of DR3.

A

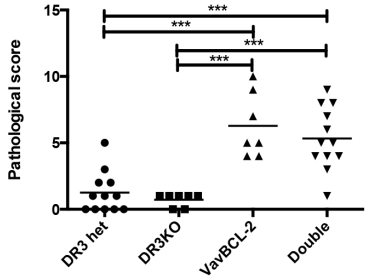

B

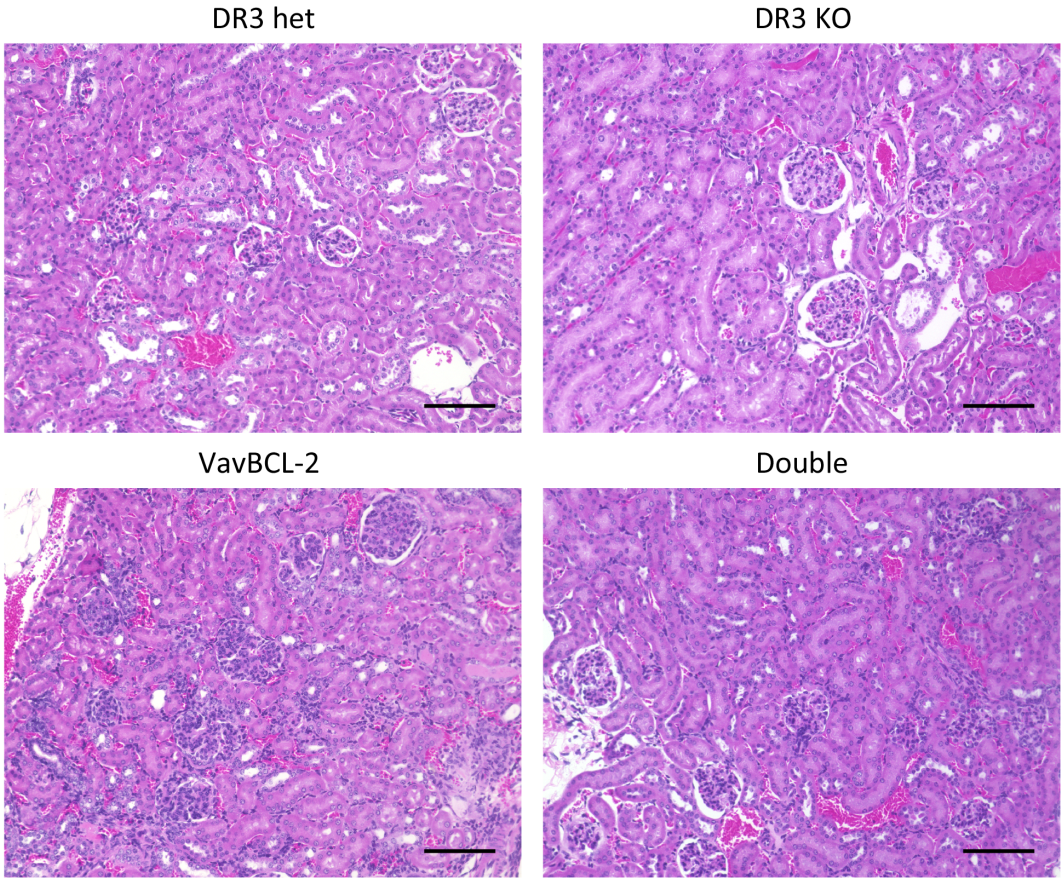

Figure 7-6 *- Kidney pathology in DR3KO x Vav-Bcl2. At 30 weeks of age the kidneys were removed and processed for H and E staining (**B**). Scale bars are equal to 100μm. The kidney slides were scored in a blinded fashion by a veterinary pathologist with a composite score given (**A**).*

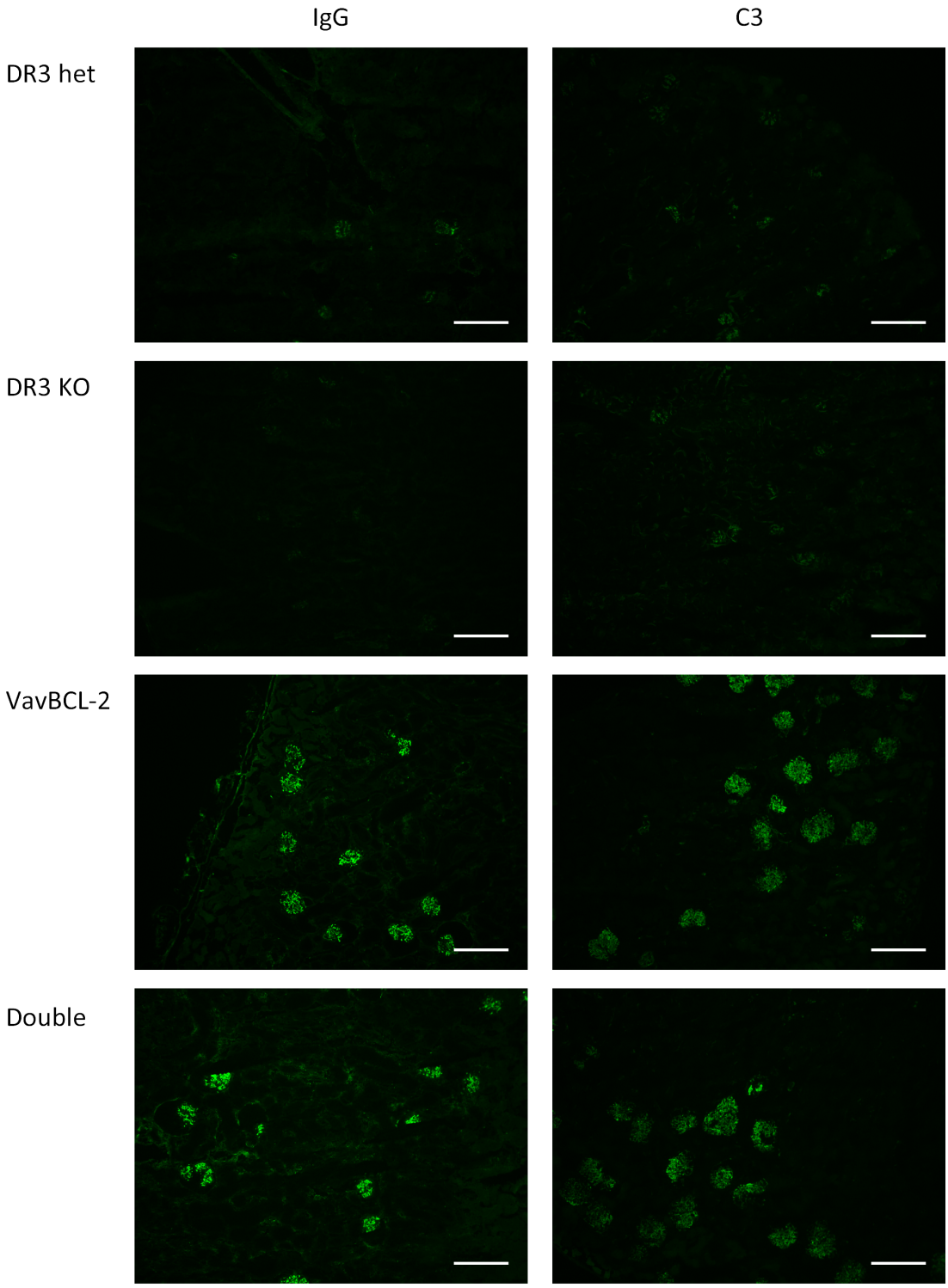

Figure 7-7 *- Glomerular immune deposition in DR3KO x Vav-Bcl2. Frozen sections were produced from the kidneys of the indicated mice at 30 weeks of age and stained for IgG and C3 deposition as indicated. Images were initially focused on the cortex using the nuclear stain DAPI to identify glomeruli (not shown). Scale bars are equal to 200μm. Images are representative of greater than 6 mice per group.*

7.2.3. Parent into F1 model of lupus

To study lupus in an inducible model we employed the chronic GVHD parent into F1 model[314]. This model was induced by the transfer of 1.5-2x10^7 CD4+ T cells from either a WT C57bl/6 or a DR3 KO mouse into BDF1 recipients. Progress was followed for 12 weeks in the blood after which the mice were euthanised and the pathology in the kidneys, spleen and urine analysed.

Transfer of WT or DR3 KO cells resulted in the production of ANA and anti dsDNA antibodies within 7 days with no differences observed between the groups. However graft cells from the DR3 KO were unable to expand as well as WT cells (Figure 7-8 A-C). For comparison, mice that did not receive transferred cells (naïve) are shown.

To demonstrate this was not a defect in proliferation in DR3 KO mice, a mixture of congenically marked WT and DR3 KO cells were transferred into RAG KO hosts. Here no major defect in homeostatic proliferation in either genotype was observed in circulating CD4+ cells or in the spleen after 8 weeks (Figure 7-8).

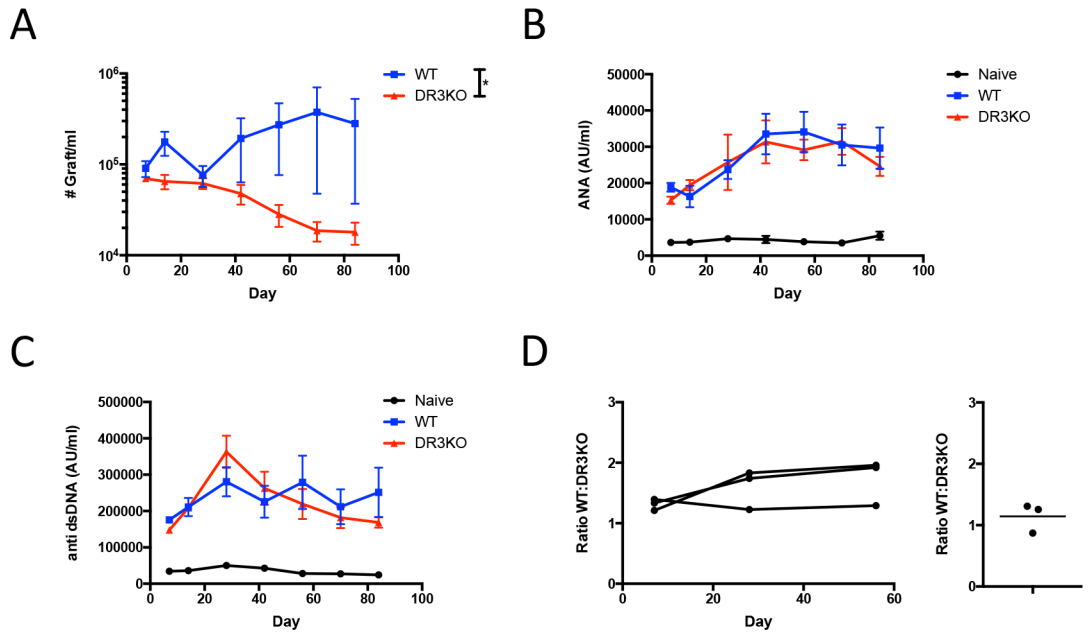

Figure 7-8 *- Development of chronic graft vs host disease in the parent into F1 model. Chronic Graft vs Host disease was induced by the transfer of 1.5-2x10^7 purified CD4+ cells from either a WT or DR3 KO mouse into female BDF1 hosts (5 mice per group). For comparison naïve mice which did not receive any transferred cells were bled at the same time (3 mice in group). The levels of graft expansion (**A**, Kb+ Kd- cells) were followed in peripheral blood over time using flow cytometry. Serum samples were taken at the same time and levels of total ANA (**B**) and anti*

*dsDNA (**C**) antibodies were measured. AU corresponds to standards provided by the manufacturer. * indicates 0.05>P>0.01 using a two way ANOVA for genotype for comparison between WT and DR3 KO only. **D**- As a control for proliferation of WT and DR3 KO CD4+ T cells 5x10^5 purified CD4+ T cells were transferred into RAG 1 KO mice and the ratio of WT:DR3 KO followed in the blood over time (left panel, individual mice) and after 8 weeks in the spleen (right panel). CD45.1 congenic WT mice were used to enable easy tracking of genotype by flow cytometry. Data representative of 2 independent experiments.*

Mice were euthanised 12 weeks post induction of the model and the splenic phenotype examined. Mice developed splenomegaly in response to transfer of cells. The graft expanded in all mice and there was no defect in host cell compartments detected. There were no significant differences between the mice that received WT and DR3 KO CD4+ T cells but there was a trend towards reduced splenomegaly and graft expansion in the DR3 KO (Figure 7-9).

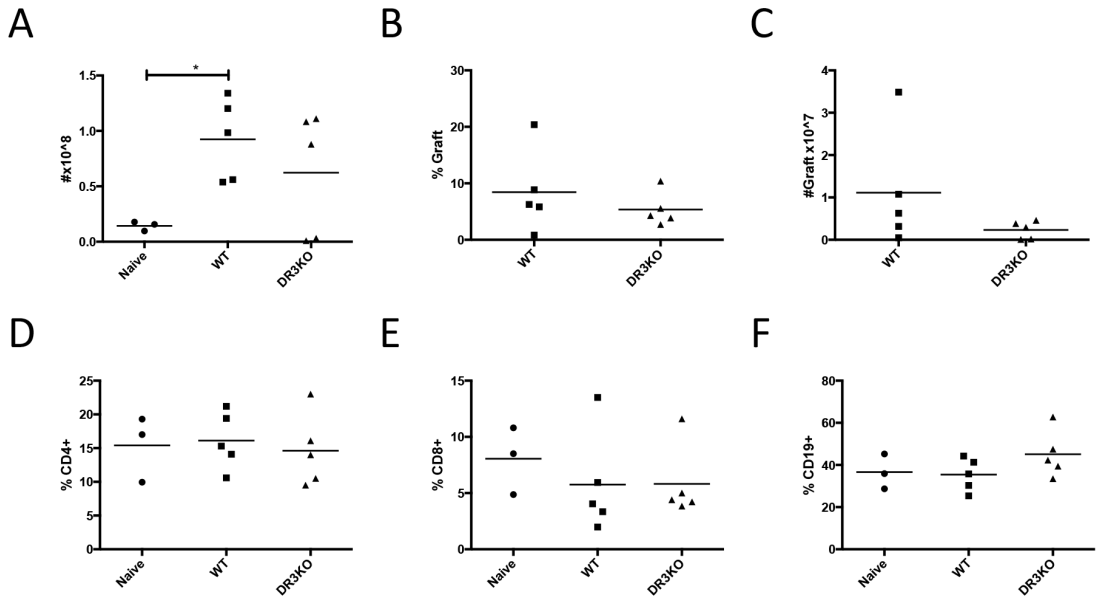

***Figure 7-9** - Splenic phenotype of mice with chronic graft versus host disease. Mice were euthanised 12 weeks post induction of the model and the composition of the spleen examined. Total cell numbers were counted (**A**) and the proportion of graft (**B** and **C**, Kd-Kb+), and host (Kd+Kb+) CD4+ (**D**), CD8+ (**E**) and CD19+ (**F**) cells out of the spleen calculated. * indicates 0.05>P>0.01 using the Mann-Whitney U test. Data representative of 2 independent experiments.*

Within the CD4+ T cell subsets there was a trend towards a decreased graft Tfh cells in mice that received DR3 KO cells (Figure 7-10A). As the graft cells were exposed

chronically to antigen we examined the expression of the exhaustion markers Lag3 and PD1 on CD4+ T cells. The surface expression of these markers was elevated above the level of host CD4+ cells from naïve mice (Figure 7-11). Interestingly activation status (Figure 7-10C) and T cell exhaustion markers (Figure 7-11) were increased on host mice that received transferred cells regardless of genotype.

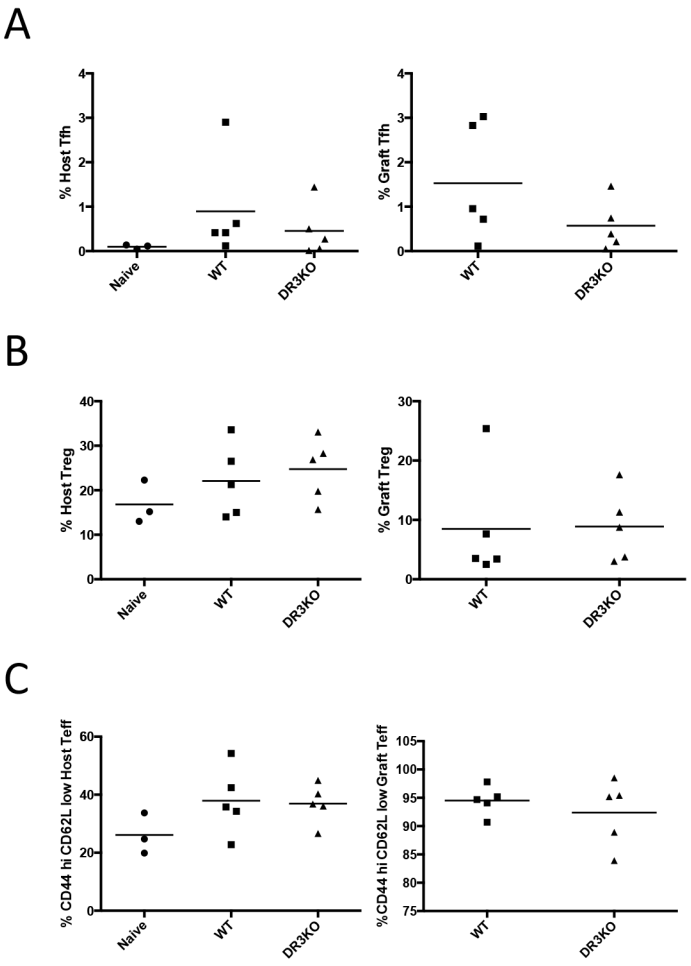

Figure 7-10 *- Splenic T helper cell compartment in mice with chronic graft versus host disease. Splenic CD4+ T cell subtypes of either host (left, Kd+Kb+) or graft (right, Kd-Kb+) were determined by flow cytometry. Tfh (**A**, CD4+ ICOS+ CD40L+ CXCR5+ PD1+), Treg (**B**, CD4+ FoxP3+) and CD44 hi CD62L Teff (**C**, CD4+ FoxP3-) are plotted as a proportion of total CD4+ cells of either host or graft. No P<0.05 were found for pairwise comparisons using the Mann-Whitney U test. Data representative of 2 independent experiments.*

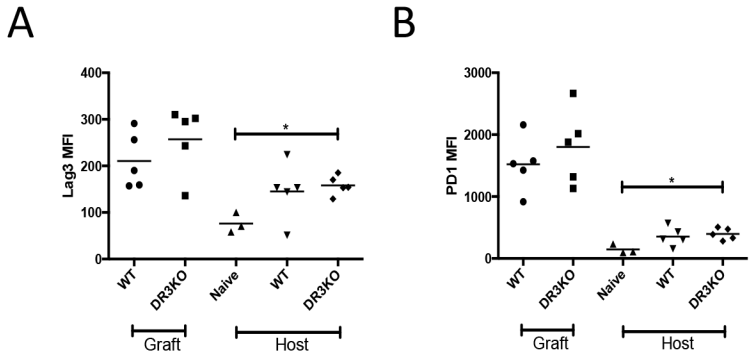

Figure 7-11 *- T cell exhaustion in mice with chronic graft versus host disease. The expression of the T cell exhaustion markers Lag3 (**A**) and PD1 (**B**) was assessed on graft and host CD4+ T cells by flow cytometry with the geometric mean fluorescence reported. * indicates 0.05>P>0.01 using the Mann-Whitney U test. Data representative of 2 independent experiments.*

The method of action of this model is activation of host B cells by graft CD4+ cells through allorecognition[314]. As such we examined the host B cell compartment for perturbations. Within the spleen we found increased class switched B cells and GC B cells however no effect of lack of DR3 signalling was observed. There was a trend towards increased plasma cells in the spleen in the mice that received WT donor cells to a greater extent than those receiving DR3 KO (Figure 7-12).

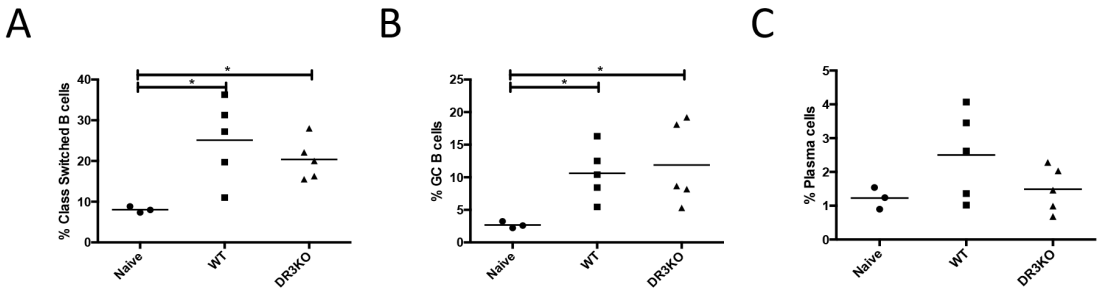

Figure 7-12 *- Splenic B cell compartment in mice with chronic graft versus host disease. The proportion of class switched B cells (**A**, CD19+ IgM- IgD-), GC B cells (**B**, CD19+ PNA+ GL7+) and plasma cells (**C**, CD19+ B220int-hi IgM- CD138+) of B cells. * indicates 0.05>P>0.01 using the Mann-Whitney U test. Data representative of 2 independent experiments.*

We examined the kidneys for signs of glomerulonephritis and general kidney pathology as this was known to develop in this model[314]. A very mild pathology with small lymphoid infiltrates was observed in the mice that received DR3 KO cells. The pathology was generally worse in the mice which received the WT cells with approximately 50% of the mice presenting with large peri-glomerular lymphoid

aggregates and large vacuole like structures filled with proteinaceous deposits (Figure 7-13 A). To examine the kidney function we measured the ratio of albumin to creatinine in the urine on the day of euthanasia. We found that this reflected the level of kidney pathology observed with a high ratio in approximately 50% of the group that received WT cells. Whilst the mice receiving DR3 KO cells were slightly elevated over naïve mice they were considerably lower than those receiving WT cells (Figure 7-13 B). However no difference was observed in IgG or C3 deposition in the glomeruli (Figure 7-14).

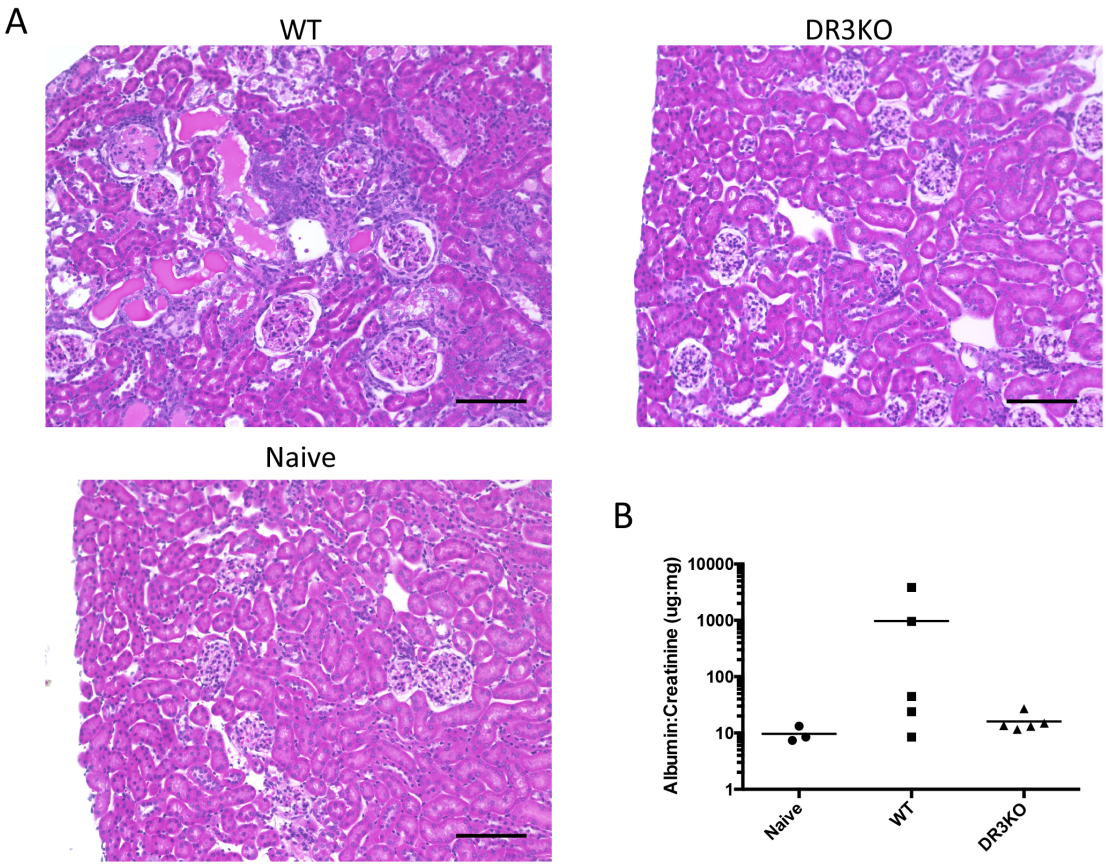

Figure 7-13 *- Kidney pathology in response to chronic graft versus host disease.* ***A*** *Kidneys were processed for H and E and images taken of the cortex. Scale bars are equivalent to 100μm.* ***B*** *The albumin and creatinine levels were measured in urine samples taken at the end of the model by ELISA and the alkaline picrate colorimetric assay respectively. No P<0.05 were found for pairwise comparisons using the Mann-Whitney U test. Data representative of 2 independent experiments.*

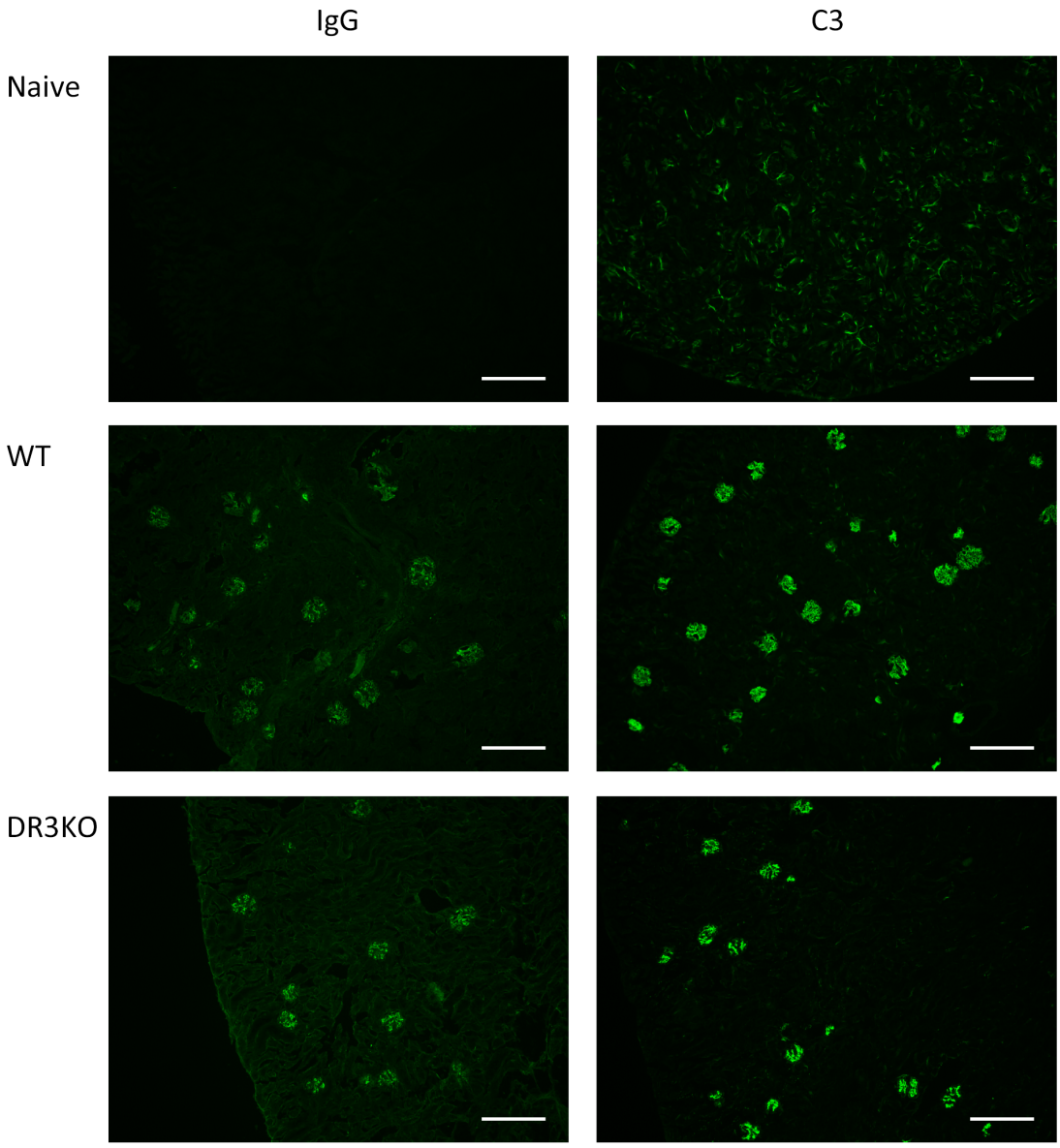

Figure 7-14 *- Glomerular immune deposition. Frozen sections were produced perimortem and stained for IgG and C3 deposition as indicated. Images were initially focused on the cortex using the nuclear stain DAPI staining to identify glomeruli (not shown). Scale bars are equal to 200μm. Images are representative of 3-5 mice per group from 2 independent experiments.*

Given the differences in pathology observed we digested one whole kidney and extracted the cells for flow cytometric analysis. There was an increase in the total number of CD45+ cells in the kidney along with increased activation status of host lymphocytes. Further host CD8+ cells were the main lymphocyte to be increased as a proportion of the CD45+ cells. However there were no major differences in the cell sub-sets examined between the mice that received WT or DR3 KO CD4+ T cells (Figure 7-15).

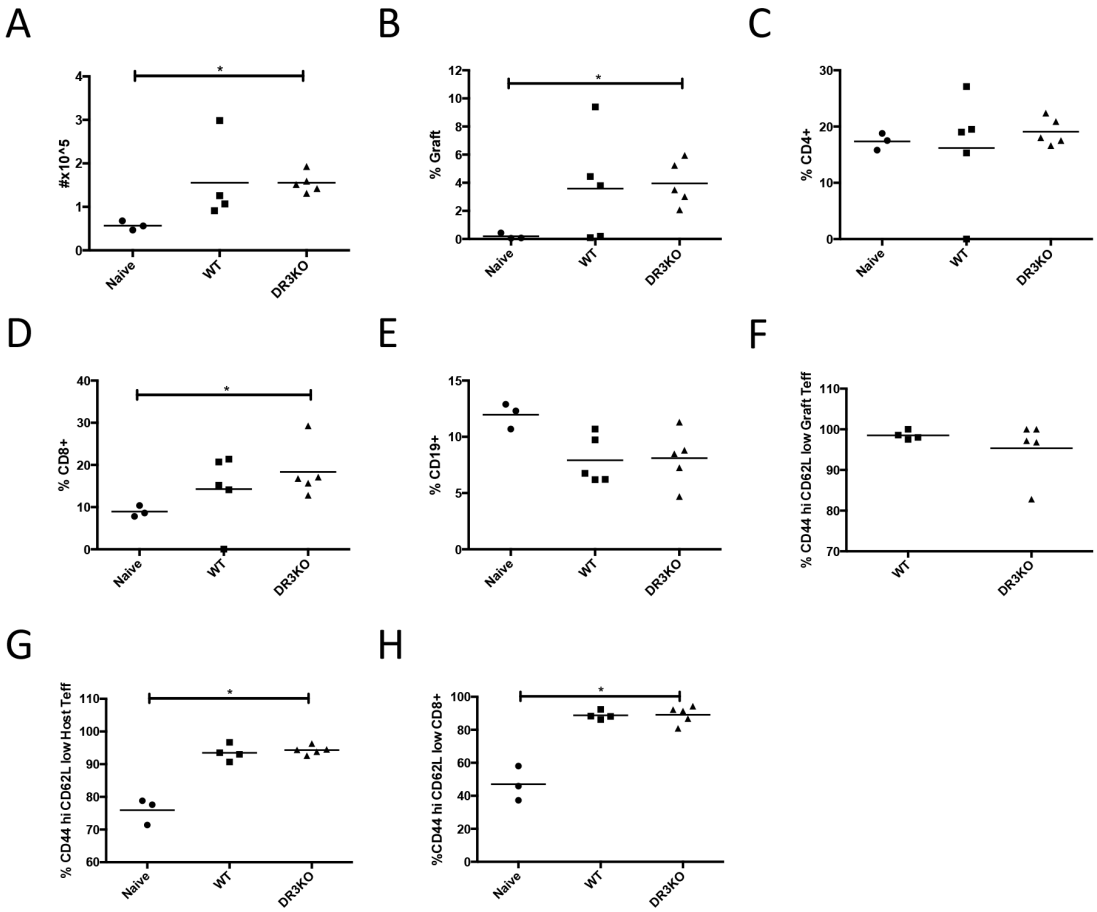

Figure 7-15 *- Cellular composition of the kidney in response to chronic graft vs host disease. Cells were extracted from one whole kidney at the end of the model and assessed by flow cytometry. Total numbers of CD45+ cells in the kidney were enumerated (**A**) and the proportion of graft (**B**, Kd- Kb+), and host (Kd- Kb+) CD4+ (**C**), CD8+ (**D**) and CD19+ (**E**) cells of the total CD45+ calculated. The proportion of CD44hi CD62L low of graft (**F**) and host (**G**) Teff (CD4+ Foxp3-) and CD8+ out of the parent population was measured. * indicates 0.05>P>0.01 using the Mann-Whitney U test. Data representative of 2 independent experiments.*

7.3. Discussion

In this Chapter we have investigated the role of DR3/TL1A signalling in the development of two murine chronic autoimmune models.

The first model examined was the Vav-BCL2 transgenic mouse strain[308] that we crossed to both the Mem+Sol TL1A transgenic and the DR3 KO. By crossing to both these lines we were able to identify common pathways that are promoted by, and potentially reliant on, TL1A/DR3 signalling.

We found that Tregs were expanded in a normal Vav-Bcl2 mouse, as previously reported[312], so it is unsurprising that the addition of TL1A further increases the fraction of Tregs present given a similar expansion of Tregs has been previously reported in multiple TL1A transgenic lines[174, 175]. However there was also a trend towards a decrease in Tregs when Vav-Bcl2 was crossed to the DR3 KO. This suggests that in this system signalling via DR3 may promote Treg generation or differentiation. The area of TL1A control of Tregs is a complicated one. *In vitro* it has been demonstrated that exogenous sTL1A inhibits the differentiation towards iTreg, instead promoting differentiation towards a Th9 status[133, 174]. In contrast DR3 agonistic monoclonal antibodies[137] and recombinant soluble TL1A[176] have been shown to promote increased Treg numbers *in vivo* in an IL-2 dependent manner[159, 175]. The increase observed in Tregs in these mice is most likely due to a combination of the increased proliferation of these cells in a TL1A transgenic, as shown by increased Ki-67 expression[175], in conjunction with the anti apoptotic effect of Bcl2 overexpression[309]. The increased proliferation of the cells is most likely promoted as a result of the ability of TL1A to increase the surface expression of CD25 thus making the cells more sensitive to IL-2 mediated proliferation[317].

Signalling via TL1A and DR3 appears to play a role in the T cell help for B cell responses in the Vav-Bcl2 model. When crossed to the TL1A transgenic line there is an increase in the proportion of Tfh cells within CD4+ cells and there is a corresponding decrease when crossed to the DR3 KO. In addition to this there is an increase in GC B cells and a trend towards increased class switched B cells when crossed to the TL1A transgenic, and a corresponding decrease in both in the DR3 KO cross. These data suggest that the TL1A pathway may promote differentiation towards a Tfh phenotype thereby promoting help for B cell and the GC reaction. It is not possible from these results however to determine if the effect on the B cell phenotype is directly due to TL1A acting on the B cells, given that non class switched

B cells express DR3[129], or a result of modulating the number of Tfh cells. Given that the increase in Tfh and GC B cells observed in the Mem TL1A transgenic mice is lost when crossed to the T cell conditional DR3 KO (Figures 5-3 C and 5-4 A) it is likely that this effect observed in the Vav-BCL2 mice is due to modulation of Tfh numbers. This modulation may be due to increased survival of the cells due to increased NF-κB activation or a direct effect on differentiation. Further the RNASeq data from the Mem and Mem Hi transgenic mice (Table 4-2) shows an increased level of ICOS in the lungs which in turn promotes Tfh differentiation[261, 318]. Further TL1A stimulation has been shown to promote CD154 expression which is vital to the function of Tfh cells[317].

The second model of murine chronic autoimmunity examined in this Chapter is the parent into F1 model of chronic GVHD, which is a murine lupus model. There are two main methods for the promotion of chronic GVHD using the parent into F1 system. The first is to transfer DBA/2 splenocytes into BDF1 mice[314]. Unfortunately the DR3 KO mice are not currently on this background but are rather on the C57bl/6 so this was not possible. Therefore we transferred either WT C57bl/6 or DR3 KO CD4+ T cells which had been negatively selected by magnetic separation thus inducing chronic GVHD[314].

We found that regardless of the type of cell transferred the recipient mice developed high levels of autoantibodies by day 7 which remained high for the duration of the model. Thus demonstrating the ability of the DR3 KO cells to activate host B cells in this model. However DR3 KO graft cells did not expand over the course of the model and there was a trend towards reduced graft in the spleen after 12 weeks as well as in peripheral blood. This is a model dependent phenotype rather than a reduced ability of DR3 KO CD4+ cells to proliferate as we demonstrated that there was no major defect in homeostatic proliferation upon transfer into a RAG KO mouse.

The major phenotypic difference in the chronic GVHD model was the lack of pathology in the kidney upon transfer of DR3 KO cells. Across multiple experiments the incidence of severe kidney pathology and corresponding proteinuria upon transfer of WT cells was approximately 50%. However this was never observed in the transfer of DR3 KO. This effect seemed to correlate with the mice which had the highest levels of graft cells in the peripheral blood and spleen however no defect in kidney resident graft cells or immune deposits were observed. This suggests that higher levels of graft expansion in the periphery are required to induce kidney disease than autoantibodies and the lack of expansion of DR3 KO cells hampers the

pathology of this model. In addition, as the levels of graft cells in the kidney did not correlate with incidence of kidney disease suggesting there is a phenotypic difference in the cells present in the kidney rather than disease being promoted as a result of increased expansion. Lastly whilst this model is only lacking DR3 on the graft cells it is clear from the results that not only host B cells but also host CD4+ and CD8+ cells are active in this model. These data demonstrate that blocking DR3 on the initiator population is sufficient to prevent pathology and progression of the disease. Interestingly the Vav-Bcl2 mice which were crossed to the DR3 KO did not show any amelioration of kidney pathology.

Unpublished work from R. Siegel's lab has been examining the role of DR3 in the LPR lupus model. Strikingly the phenotype in these mice is highly similar to the chronic GVHD model as DR3 KO mice on the MRL/LPR background develop increased autoantibody titres but are protected from kidney pathology at an intercross of the F2 generation.

Two out of the three models imply a role for DR3 in kidney damage. The lack of effect observed in the Vav-BCL2 model of TL1A on the kidney may be due to the severity of the model. Perhaps if development of kidney disease in these mice was assessed longitudinally we may see an effect at an earlier stage. Al-Lamki *et al* have previously demonstrated DR3 expression in kidney tubular epithelial cells and that addition of recombinant TL1A to kidney organ cultures promotes the activation of NF-κB pathway and caspase-3 mediated apoptosis suggesting a potential mechanism of action[149].

Whilst more work is required on this topic these data suggest blockade or inhibition of the TL1A/DR3 pathway may be of use in preventing the pathogenesis and progression of lupus nephritis. Given that the major effect of DR3 in the pathogenesis of these models is seemingly confined to the kidney and that other minor effects only reduce pathology but do not prevent normal function of the immune system (for example GC formation), a potential key advantage of therapeutically targeting TL1A would be treated individuals would seemingly still respond to other immunological challenges. The next step in these experiments would be to attempt to antagonise the DR3/TL1A pathway after the induction of lupus to examine the therapeutic potential of blockade. This could be achieved through multiple methods however use of an antagonistic anti TL1A monoclonal antibody, such as Tan 2-2[185], is most appealing. Due to the long term nature of murine models of chronic autoimmune disease the blockade required would have to be administered regularly. We found

that Tan2-2 is unsuitable for this purpose as the mouse under treatment generates an immune response against this rat Ig and after 3 administrations the treatment is cleared quickly and thus unable to provide effective blockade (data not shown). As such, testing of TL1A blockade as a potential treatment for lupus will require the generation of novel murine therapeutics.

Chapter 8. General discussion

8.1. General comments

Since the initial discovery of TL1A as the ligand for the receptor DR3[43] over 13 years ago much progress has been made in understanding its role in healthy and pathogenic immune responses. However, TL1A biology still holds its secrets, some of which we have attempted to elucidate within this thesis.

Chapter 4 of this thesis explores the potential role of membrane bound and soluble forms of TL1A. This question is of interest as multiple other members of the TNFSF have differential roles dependent upon their state[70, 71, 225, 229]. Early studies which examined the overexpression of TL1A used either T cell or DC promoters [174, 175, 213]. Given that work published prior to the production of these mice suggested that lymphocytes did not produce soluble TL1A but myeloid cells did[164] it was expected that these different transgenic mice would also allow examination of differences in membrane and soluble forms of TL1A. In general the phenotypes of these different transgenic mouse lines were highly similar. Here we demonstrated that indeed WT T cells were unable to cleave TL1A however when TL1A was overexpressed on T cells it was cleaved and found in the serum.

As a result of our findings on differential cleavage of TL1A between T cells and DCs, we progressed to produce a membrane restricted TL1A transgenic mouse. Our work has demonstrated that excessive TL1A is able to promote pathology regardless of its state. This included an IL-13 driven ileitis pathology with goblet cell hyperplasia, elevation of IL-17a in the lungs and an elevation of IL-9 and IL-13 in both the lungs and ileum. In addition we observed an increase in splenic Tregs and Tfh cells as well as an increase in activation of both T and B cells and elevation of total IgE and IgA. However we found that soluble TL1A had a bias towards development of intestinal pathology. Interestingly the pathologies that were promoted by soluble TL1A, as administered via an osmotic pump, were the same phenotypes which were shown in Chapter 5 to be independent of the expression of DR3 on T cells, suggesting that soluble TL1A is more important for modulation of other DR3 expressing cells such as ILC2s[140]. Members of the ILC family are activated in response to inducer cytokines[28] and as such do not rely on cell-cell interactions, unlike T cells, for their activation. As a result they may be able to respond more efficiently to soluble TL1A than other cell types where one could envisage local concentrations of TL1A, due to membrane restriction, being higher. This differential threshold for TL1A activation

could either be due to increased downstream signalling due to amplification or an increased affinity for the ligand. There are two alternative membrane bound DR3 splice variants of which the full length isoform[127], containing 4 CRR, is upregulated upon activation of CD8+ T cells[132]. Unpublished data produced prior to this thesis suggested that the full-length isoform has a higher affinity for soluble recombinant TL1A than the shorter form. If ILCs constitutively expressed the full-length isoform then this may explain their enhanced activation in response to soluble TL1A. Given we are now in the age of "big data" the expression pattern of these isoforms on ILCs, as well as other cell types, could be easily determined through re-analysis of existing RNASeq data. Further, differences in the affinity between the isoforms could be assessed via surface plasmon resonance experiments.

The comparisons between the Mem+Sol and membrane restricted lines, and the *in vitro* and *in vivo* experiments with soluble TL1A demonstrated that both forms of TL1A are capable of signalling. However, as exemplified by the *Salmonella* infection model, the level of soluble TL1A expressed in the transgenic mice is above the level found in response to infection. As such one could assume that under normal immune conditions the cleavage of TL1A could be a mechanism for controlling its signalling. Cleavage would effectively dilute the local concentration of TL1A throughout the serum taking it below its K_D for DR3 thus preventing signalling. However if the cleaved soluble TL1A was unable to escape the local area it could easily increase to a level where pathogenic signalling is possible as may occur in the synovium in patients with RA[200]. Several groups have suggested that targeting TL1A may be a therapeutic option in multiple autoimmune conditions including RA. If TL1A neutralising therapies are to be considered then the relative levels of both membrane bound and soluble TL1A, as well as which form is pathogenic in each disease, must be taken into account. Our data would suggest that, if TL1A were proven to be pathogenic in these diseases, then targeting of both membrane and soluble components would be required to reduce pathology. As such, a high dose of a neutralising therapy may have to be administered locally to ensure the membrane bound form of TL1A is sufficiently blocked rather than the drug being depleted by the pool of soluble TL1A.

DR3 is most similar to the archetypal member of the TNFRSF family, TNFR1[126]. Interestingly TNF is also able to signal as a soluble ligand and as such it may be possible to draw comparisons between the two. Firstly, TNFR1, along with other members of the TNFRSF contain PLAD in CRD1 that enables the receptor to form trimers in the membrane in the absence of ligand[44]. This could reduce the need for

pre-clustering of the ligand on a membrane thus improving the chance of signalling taking place with a soluble ligand. Pre-clustering of DR3 has not been demonstrated however given its high homology with TNFR1[126] this is highly likely and could be confirmed through super resolution microscopy. Secondly, several ligands within the TNFSF are naturally unable to signal in the soluble form unless they are oligomerised into higher order complexes including CD154[319] and OX40L[320]. Here we found that soluble recombinant TL1A that was produced in CHO cells was naturally a trimer and that further oligomerisation of the ligand had no increased effect on signalling. Whilst this has not been shown with natural TL1A this lack of need for oligomerisation greater than a trimer is shared with TNF[321] and this may reflect a receptor intrinsic property of TNFRSF members which are able to signal via soluble ligands. Finally both TNFR1[322] and DR3[122] signal via the adapter protein TRADD. This adapter may require less cross-linking of the receptor to induce downstream signal induction thus enabling productive signalling from soluble ligands.

Arguably the most striking phenotype of TL1A overexpressing mice is the IL-13 mediated small intestinal pathology[174, 175] and as such it is the one that has been assessed in most detail[140]. In Chapter 5 we examined other phenotypes of these various transgenic mice and attempted to determine the cell type that TL1A is acting on in these instances. Here we demonstrated that the development of all observed pathology and cytokines in the small bowel is independent of DR3 expression on T cells, this is in concordance with and further expands upon previous data[140]. We also demonstrated that the T cell activation phenotype in the spleen along with the expansion of Tregs and Tfh cells is a result of direct signalling of TL1A through DR3 on T cells. Further the phenotype which was reported in the lungs in Chapter 4 was also dependent upon T cells however ILCs were required for optimal expansion of T cells and subsequent induction of pathology following transfer into RAG KO hosts. These data, combined with the RNASeq data detailing transcriptional changes induced by TL1A, further our understanding of both cell types and processes in which TL1A may play a role.

The effect of TL1A and DR3 on B cells has not been previously investigated to any great depth. In this thesis we demonstrated that TL1A transgenic mice have an increased proportion of Tfh cells and also GC and class switched B cells. This effect seems to be T cell intrinsic as conditional deletion of DR3 in T cells restores this defect. From this we would propose that TL1A either directly, or as a product of increased activation of T cells, promotes Tfh differentiation and it is this increase in Tfh cells which, in turn, promotes the increase in GC and class switched B cells

rather than direct signalling via DR3 on the B cell. Interestingly we observed a significant increase in total IgA and IgE in the transgenic mice and a trend towards an increase in total IgG2b. However, only the increase in IgE was lost when the T cell DR3 dependent effect was removed. This suggests that IgA class switching may be promoted by TL1A either acting directly on B cells or on an intermediary cell that then promotes this effect. Crossing the TL1A transgenic mice onto a B cell conditional DR3 KO could test this hypothesis. To further investigate the role of TL1A in class switching we immunised DR3 KO mice with both Td and Ti antigens and showed a defect in the IgA response and that this effect was independent of T cell DR3 expression. We also demonstrated that DR3 KO mice had a defect in IgG2b class switching only in the Td response. Further through a preliminary study we found that exogenous soluble TL1A was able to increase the proportion of surface IgA positive B cells following activation with anti CD40. This effect of TL1A is similar to another member of the TNFSF; LT[83]. These data, along with previously published work[236], suggest that activation of TL1A expression would be a potent strategy for increasing efficiency of vaccines where a IgA response is favourable, for example the seasonal influenza vaccine[323]. As previously discussed, this effect of TL1A on class switching may be due to synergy with TGF-β however further investigation is required.

Chapter 7 investigates the role of DR3 in chronic autoimmunity. To date all published models of autoimmunity that have been investigated have been acute in nature. Here we assessed the role of either ectopic TL1A or genomic ablation of DR3 on two lupus like models; Vav-Bcl2 transgenic mice and the parent into F1 chronic GVHD model. The major finding from these experiments was the protection of mice receiving DR3 KO T cells from the development of nephritic diseases in the chronic GVHD model. This protection of the kidneys was not observed in the Vav-Bcl2 model however this might not have been observed due to the severity of the phenotype and the late time point of analysis. This protection is exciting as it raises the potential for DR3 blockade to be used as a therapy in the treatment of lupus to prevent progression to lupus nephritis. A key appeal of this finding would be the minimal effect observed through DR3 blockade on the rest of the immune system in this model thus leaving the patient with a functioning immune system in case of infection or other immune challenge. Whilst DR3 blockade has been used in multiple murine disease models in the past (Table 1-3), in none of these cases, nor in the DR3 KO mice at resting state[216], was any major defect in the general immune system observed. Together these data indicate the potential for blockade of DR3/TL1A signalling as a treatment

in lupus and potentially other autoimmune diseases. Results from this and multiple other studies imply that lymphocytes which have been primed in the absence of DR3 are less fit[145, 159, 185]. This lack of fitness may either present itself as a reduction of lymphocytic infiltration into an organ or a reduction in pathology. This hypothesis could be examined by transferring cells which were stimulated in a primary response in an environment which lacked TL1A into a TL1A sufficient environment and determining if any detrimental effect remained. This could be examined using a combination of a TL1A KO mouse and either the OTI or OTII transgenic T cells strains.

8.2. Concluding remarks

In conclusion, we have investigated several of the many unanswered questions in TL1A biology within this thesis and the generalised key findings from this work are summarised below.

- Both membrane bound and soluble forms of TL1A are active and expressed *in vivo.*
- WT T cells are unable to cleave TL1A however TL1A transgenic T cells are.
- Amino acids 69-93 are required for cleavage of murine TL1A from the surface of cells.
- Membrane-bound-TL1A promotes T cell responses including elevation of cytokines in the lungs and increases in Tregs.
- Soluble TL1A promotes intestinal pathology in a T cell independent manner.
- TL1A promotes IgA class switching *in vitro* and *in vivo* in response to T cell dependent and independent antigens through direct effects on B cells.
- Lack of DR3/TL1A signalling protects from the development of nephritic disease in murine models of lupus.

Appendix I – TL1A transgenic RNASeq analysis graphs

Below are the quality control graphs for the RNAseq analysis of the TL1A transgenic lungs and ileum.

A B

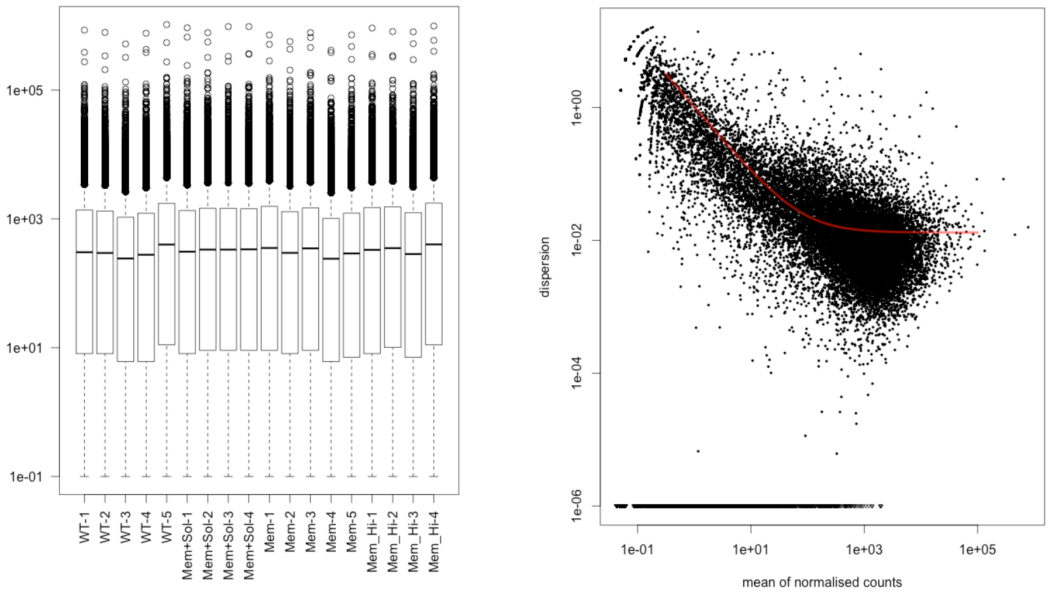

Figure I-1 *- QC plots for RNASeq analysis of TL1A transgenic lungs. RNA was extracted from the post-caval lobe of 12 week old transgenic and WT mice prepared for and sequenced on a HiSeq (Illumina). Differential expression was calculated with DESeq using a generalised liner model comparing each transgenic line to WT in a pairwise manner.* ***A*** *– The raw counts were plotted for each individual sample with the median and quartile range indicated.* ***B*** *The fit of the data to the generalised linear model is assed by plotting the mean of normalised counts for each gene against the dispersion of said gene. The regression curve is indicated in red.*

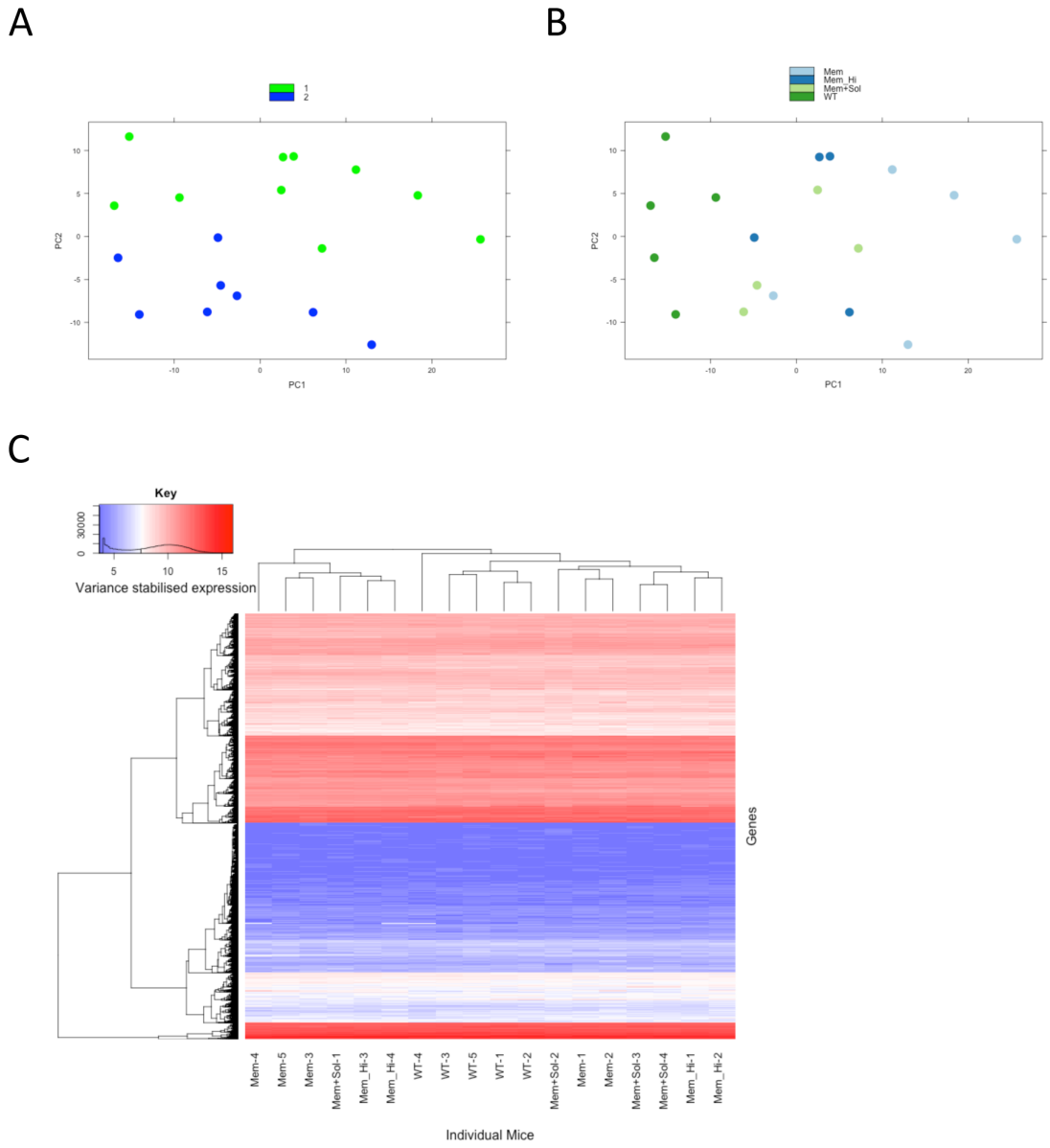

Figure I-2 *- QC plots for RNASeq analysis of TL1A transgenic lungs.* ***A*** *and* ***B*** *– The raw counts were normalised and variance stabilised using DESeq and the clustering of the data assessed by principal component analysis for the first and second component. As the data was collected from two separate runs* ***A*** *highlights the clustering based on run number and* ***B*** *based on genotype.* ***C*** *Heat map depicting the variance stabilised expression data for all genes excluding the Y chromosome for each individual sample. Both the genes and samples are hierarchically clustered.*

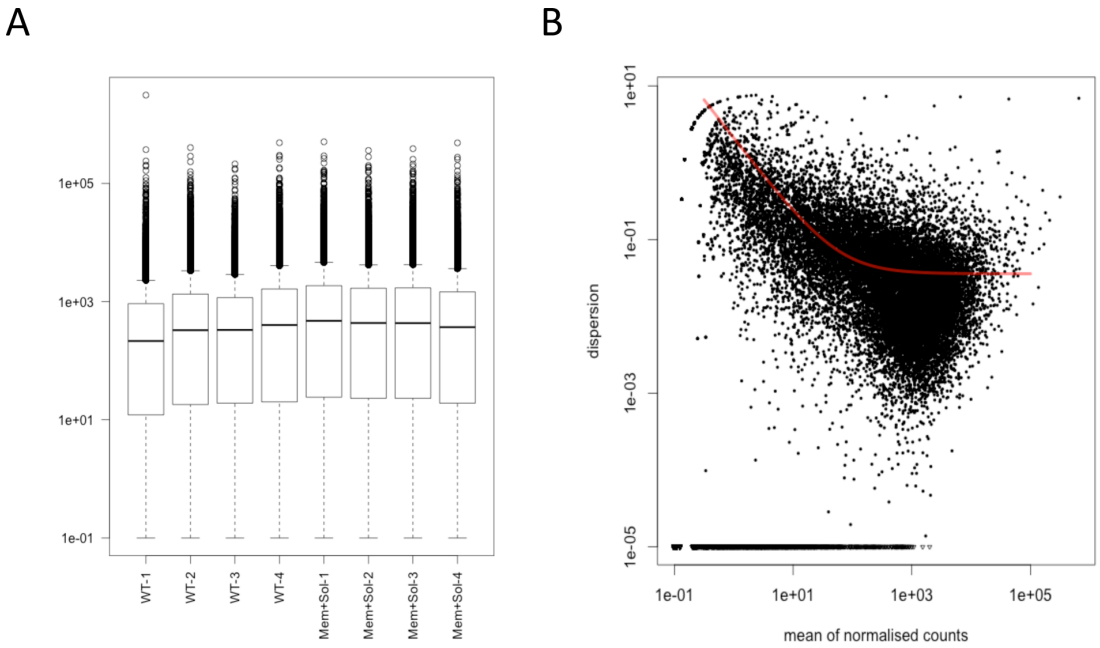

Figure I-3 *- QC plots for RNASeq analysis of TL1A Mem+Sol transgenic Ileum. RNA was extracted from the post-caval lobe of 8 week old Mem+Sol TL1A transgenic and WT mice prepared for and sequenced on a HiSeq (Illumina). Differential expression was calculated with DESeq using a negative binomial distribution comparing transgenic to WT mice.* ***A*** *– The raw counts were plotted for each individual sample with the median and quartile range indicated.* ***B*** *The fit of the data to the model is assed by plotting the mean of normalised counts for each gene against the dispersion of said gene. The regression curve is indicated in red.*

A

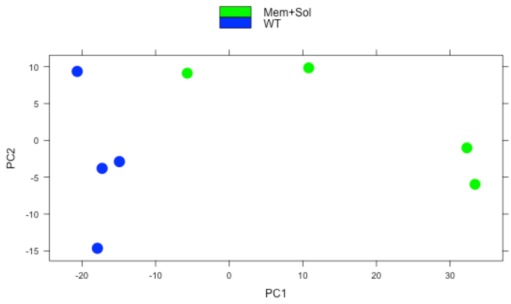

B

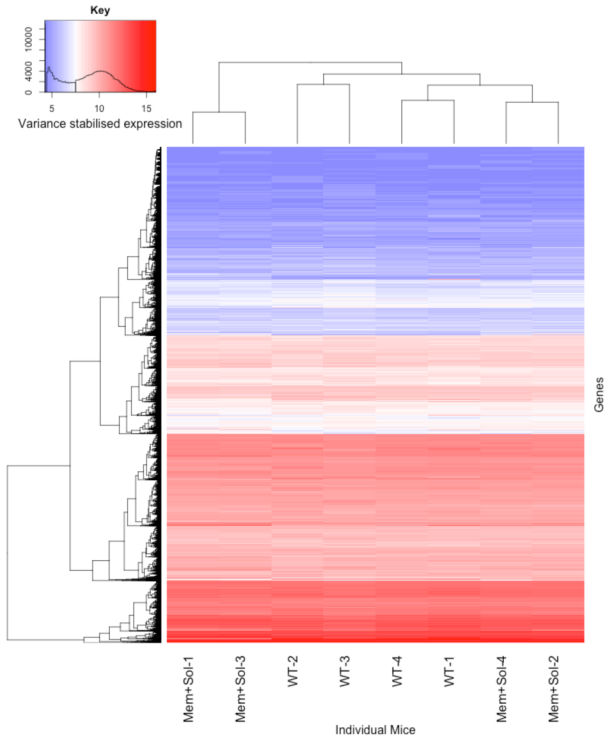

Figure I-4 *- QC plots for RNASeq analysis of TL1A Mem+Sol transgenic Ileum.* ***A*** *– The raw counts were normalised and variance stabilised using DESeq and the clustering of the data assessed by principal component analysis for the first and second component, the clustering based on genotype is indicated.* ***B*** *Heat map depicting the variance stabilised expression data for all genes excluding the Y chromosome for each individual sample. Both the genes and samples are hierarchically clustered.*

A

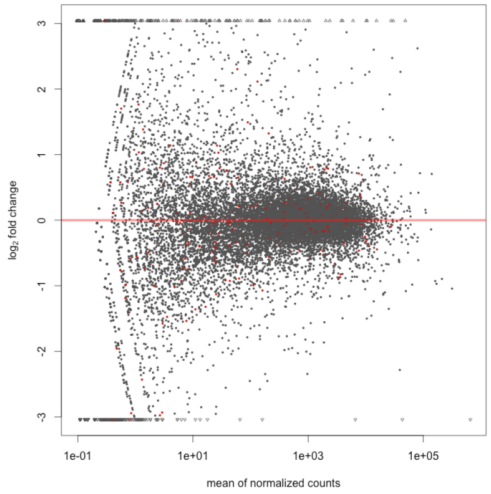

B

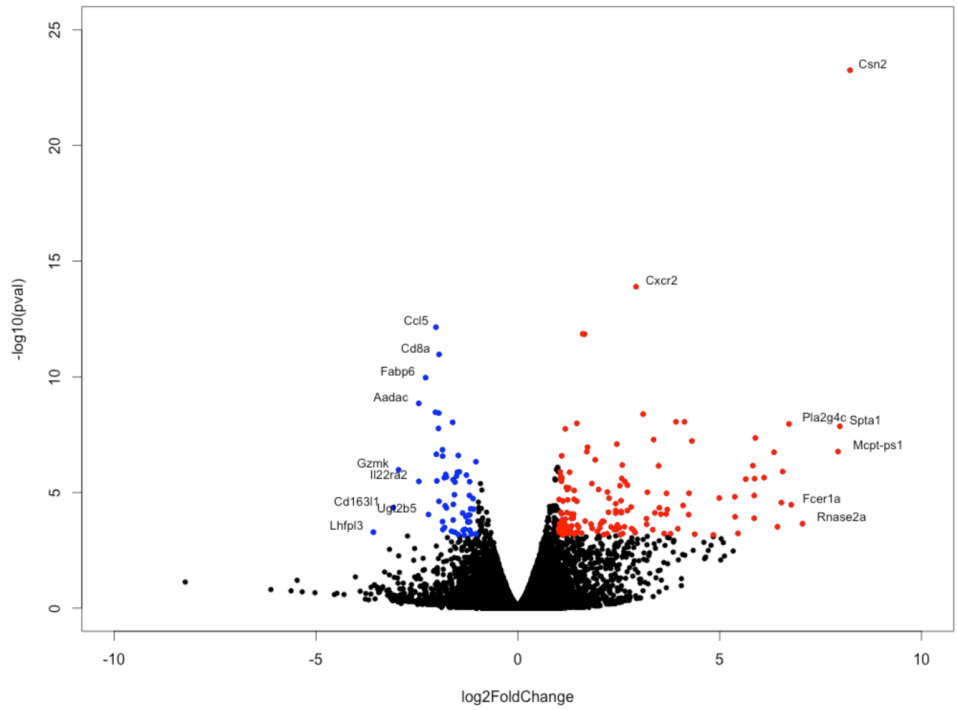

Figure I-5 - RNASeq analysis of TL1A Mem+Sol transgenic Ileum. Differential expression was calculated with DESeq using a negative binomial distribution comparing transgenic to W mice. **A** – MA plot indicated the mean normalised count for each gene against the log2fold change for said gene. Genes with an adjusted P value <0.05 using the Benjamini-Hochberg method are indicated in red. **B** – A volcano plot of the data of log2fold change against –log10 non-adjusted P value. Up regulated genes with a adjusted P value are shown in red and down regulated in blue.

Appendix II – TL1A transgenic lung RNASeq differential expression analysis

The table below details all genes which had an adjusted P value of <0.05 from differential expression analysis of the lungs within RNASeq and were found in the identified groups from figure 4-19.

Decreased			Increased		
All	**Mem+sol only**	**Mem and Mem Hi only**	**All**	**Mem+sol only**	**Mem and Mem Hi only**
Glp1r	Slc7a13	Plcxd3	Clca3	Csn3	Il17a
Itih2	Cd163l1	Sytl5	A230065H16 Rik	Myh4	Capn9
Fgf2	Nr4a3	Samd5	Ubd	Csn2	Gpa33
Ar	Cxcr2	Zan	Ceacam-ps1	Amtn	Slc26a4
Pde3a	Lama1	Cdkl5	Pvalb	Ear6	Saa3
Glb1l3	Nlrp12	Per3	Ccl20	Mcpt8	Fcgbp
D830031N03 Rik	Dhrs9	Dhtkd1	Cd209e	1700112E06 Rik	Ccl17
Shroom4	Bcl6b	Hlf	Igj	Fank1	Cxcl9
Ptar1	Dusp8	Smoc1	St6galnac1	Spp1	Gp2
Tnxb	Sorbs2os	Arl5b	Ccl8	Klhl29	5430421N21 Rik
Col12a1	Gm15910	Sned1	Msx3	2810468N07 Rik	Olfr60
Adamts1	Cd59a	Lrrn3	Foxp3	Fst	Ccl7
Fat4	Tnfrsf10b	Zbtb37	Atcay	Mfsd2a	Gm11413
Lphn3	Fam178b	Esr2	Ctla4	Rab3c	Alox12e
Adcy8	Mex3a	Cyyr1	Plekhs1	Apoc1	Pla2g2d
Scube2	Lrrn2	Lcor	Ccr4	Edn1	Pdcd1
Hmbox1	Sync	Pclo	Prg2	Myrip	Gpr25
Adcyap1r1	Slc1a2	Pcdhac2	Cxcl5	Clec12b	Rln3
Ppp1r12b	Kcnj2	Abca8b	Ccl12	Zfp119b	Cxcl10
Unc5c	Tubb4a	Ptpn4	Tnfsf15	Prmt8	Adra2a
Sema6d	Pcdhga9	Fmo2	Serpina11	Tfap4	Gm8221
Itga1	Arhgap28	Plcb4	Bex6	Ifitm10	Serpina3h
Olfml2a	Col1a1	Prex2	Cd209d	Cth	Acsbg1
Itga8	Col6a3	Dpysl5	Gcnt3	Pmvk	Ackr1
Hivep3	Gm20554	Klhl11	Ccr8	Lpl	B4galnt4
Fndc1	Pcdhgc4	Nbeal1	Ano7	Gdpd1	Gpr15
Bmp5	Apln	Nebl	Tnfrsf9	Fmnl2	Scn2b
Lama2	Zswim5	Slc26a2	Mab21l3	Gjb6	Dscam
Plekha6	Bdkrb2	Gria1	Cd207	Pknox2	Serpina3f
Hipk2	Slitrk6	Ago3	Serpina10	Gm6251	5830411N06 Rik
Pdzd2	Kcnk5	Abca8a	Tnfsf11	Bmf	Serpina3i
Hmcn1	Cntn1	Hgf	Fcrl5	Fbxo32	Dscaml1
Bmp3	Fat2	Zbed6	Tnip3	Amigo2	Icos
Gpr126	6030408B16 Rik	Cyp3a13	Ccl22	Sec14l2	Atp10b
Npnt	Pprc1	Cyp4f15	Aqp3	Gm4956	Arnt2
Pde5a	Nos1ap	Ptprb	Sox8	Atp1b1	Il1rl1
Pde7b	Loxl1	Abca6	Apol7c	Tmem243	Cd4
	Epha2	Lnpep	Serpina3g	Eef1b2	AU040972
	Bysl	Sntb1	Tigit		Alox15

	Tmem181b-ps	Tlr5	Tnfrsf4	Msc
	Chsy3	Zfp369	Podnl1	Apol9b
	Nnt	Atp2b2	Crmp1	Folr4
	Klf4	Tef	Cxcl13	Adamts4
	Cdr2	Zfp641	Batf3	Cd6
	C7	Lrrc8b	Mgl2	Ptprv
	Mrgprf	Angptl2	Nccrp1	Il12rb1
	Slc12a5	Mib1	Cd209c	Fscn1
	Dchs1	Xrn1	Ms4a6d	Gm5547
	Zfp827	Epha1	Klrg1	Mthfd2
	Mrc2	Gpr155	S100a4	Arsi
	Pcdh12	Ptch1	Cd209a	Lta
	Jph2	D630045J12 Rik	Ccr6	Sdf2l1
	Cd300ld	Robo1	Sit1	Nxpe5
	Hspg2	Elk4	Clec10a	Gna15
	Bmper	Col17a1	Gjb1	Stk32c
	Palld	Ccbe1	Sept3	Tspan33
	Col5a1	Sema5a	A430093F15 Rik	Cfp
	Ackr3	Rasal2	Flt3	Ifi30
	Fzd1	Sgip1	Tnfsf8	Cxcr3
	Dusp16	Timp3	Kcne3	Pglyrp1
	Tnfrsf12a	Tek	F2rl2	Csf2
	Fam101a	Gan	Steap4	Dok2
	Cand2	Arhgap32	Fcgr2b	Tesc
	Smtn	Aox3	Chil1	Gfi1
	Pcdhb9	Heg1	Aif1	Gpr65
	Sh3rf3	Bmx	Pkib	Socs1
	Cpm	Ciart	2810417H13 Rik	Fam26f
	Gna14	Nr1d2	Slamf1	Noxo1
	Tgfb2	Gria3	Lrg1	Plbd1
	Zfp521	Nox4	Cd5	Mnda
	Cdh4	Hdac4	Kcnn4	Basp1
	Col4a5	Prickle2	Lpxn	Lag3
	Rnf144a	Ppp1r9a	Bcl2a1b	Lat
	Garnl3	Sema6a	H2-Eb1	Batf
	Tmem8b	Dmd	Sh2d1a	Cfb
	Gpr153	Gm14420	H2-Ab1	Sla
	Spats2l	A430105I19 Rik	Hepacam2	Serpind1
	Snai2	Uggt2	Cd52	Clmp
	Rasgrp3	Sspn	Tmem171	Ptpn7
	Plekhh2	Erg	Ccr2	Glipr1
	Fam212b	Sptbn1	AI662270	Cd3g
	Nes	Prkg1	Rab37	Glipr2
	Filip1l	5330426P16 Rik	H2-Aa	Hmga2-ps1
	Fam20a	Crispld2	Cd74	Ms4a4c
	Ssc5d	Casc4	Evi2a	Sh2b2
	Tmem132c	Dync2h1	Clec4a3	Oas1a
	Tstd2	Tulp4	Tgm1	Marcksl1
	Lama4	Sipa1l2	Cacna1s	Ptpro
	Vgll4	Cdc42bpa	Pim1	Snx20
	Ghr	Utrn	Ly86	Ryr1
	Igsf3	Slc23a2	Tspan32	Ltb4r1
	Mex3d	Plxdc2	H2-DMa	Skap1
	Col1a2	Cacna2d1	Ppfia4	Gpr35

Prkab2	Mpdz	H2-DMb1	Irf5
Jmjd6	Adcy9	Samsn1	Olfm1
Cdh11	Chst11	Nfkbiz	Cyth4
Sparc	1190002N15 Rik	Tnfrsf18	Tnfrsf25
Slc38a2	Scube1	Fgd2	Naaa
Rps6ka2	Tppp	Ms4a6c	Zbp1
2610507I01R ik	Ptprg	Klrb1b	Thy1
Palmd	Slit3	Capg	Tifab
Bcar1	Clic5	Phf11b	Zfp385a
Nav2	Tln2	Lat2	Pdlim4
Olfml3	Zeb1	Itgb7	Relt
Rcan1	Dock9	Emr1	Agap2
Tgfb1i1	Arhgef10	Cd48	Pf4
Agrn	Dip2c	Kcnab2	Fcho1
Stk40	Tmtc1	Epsti1	Pglyrp2
	Rreb1	Casp1	C4b
	Rasgrf2	Cyba	Rnf19b
	Arhgap29	Sh3bgrl3	Ccdc109b
	Pxdn	Crip1	Bcl3
	Ddr2	Rgs10	Asb2
	Usp54	Rnase6	Adap1
		Gng10	Cotl1
		Map4k1	Trpv2
		Sec11c	Phgdh
			Ikzf4
			Spi1
			Hcls1
			Psmb8
			Zap70
			Amz1
			Lcp2
			Pstpip1
			Ciita
			Syngr2
			Rinl
			Nrros
			Slfn2
			Ccdc88b
			Lrrc25
			Lsp1
			Myo1g
			Pycard
			Cd2
			Pld4
			Casp4
			Galnt12
			Selplg
			Cmtm7
			Nfkb2
			Relb
			Prkcd
			Cd53
			Alox5ap
			Fermt3
			AW112010
			Pirb
			Unc93b1
			Plekho1

	Vav1
	Dtx4
	Bri3bp
	Fam105a

Table II-1 *– Differentially regulated genes in TL1A transgenic lungs as defined by groups of common expression.*

Appendix III – TL1A transgenic lung RNASeq gene ontology analysis

The tables below give the results of gene ontology analysis using the gene list given in appendix II. The analysis was carried out using the program GOrilla.

GO Term	Description	FDR q-value
GO:0019933	cAMP-mediated signaling	5.01E-04
GO:0019935	cyclic-nucleotide-mediated signaling	7.67E-04
GO:0043408	regulation of MAPK cascade	2.25E-03
GO:0090100	positive regulation of transmembrane receptor protein serine/threonine kinase signaling pathway	2.48E-03
GO:0045937	positive regulation of phosphate metabolic process	7.04E-03
GO:0010562	positive regulation of phosphorus metabolic process	8.22E-03
GO:0023056	positive regulation of signaling	8.45E-03
GO:2000721	positive regulation of transcription from RNA polymerase II promoter involved in smooth muscle cell differentiation	8.55E-03
GO:1903846	positive regulation of cellular response to transforming growth factor beta stimulus	9.01E-03
GO:0043067	regulation of programmed cell death	9.01E-03
GO:0010941	regulation of cell death	9.02E-03
GO:0007160	cell-matrix adhesion	9.03E-03
GO:0042327	positive regulation of phosphorylation	9.68E-03
GO:0001934	positive regulation of protein phosphorylation	9.70E-03
GO:0030511	positive regulation of transforming growth factor beta receptor signaling pathway	9.91E-03
GO:0048522	positive regulation of cellular process	1.03E-02
GO:0060282	positive regulation of oocyte development	1.41E-02
GO:0090092	regulation of transmembrane receptor protein serine/threonine kinase signaling pathway	1.41E-02
GO:0010647	positive regulation of cell communication	1.47E-02
GO:0001932	regulation of protein phosphorylation	1.48E-02
GO:0051094	positive regulation of developmental process	1.53E-02
GO:0051174	regulation of phosphorus metabolic process	1.59E-02
GO:0031401	positive regulation of protein modification process	1.61E-02
GO:0019220	regulation of phosphate metabolic process	1.61E-02
GO:0007613	memory	1.65E-02
GO:0007275	multicellular organismal development	1.66E-02
GO:0042325	regulation of phosphorylation	1.90E-02
GO:0044707	single-multicellular organism process	2.01E-02
GO:0019932	second-messenger-mediated signaling	2.05E-02
GO:0048518	positive regulation of biological process	2.07E-02
GO:0032501	multicellular organismal process	2.12E-02
GO:0001658	branching involved in ureteric bud morphogenesis	2.19E-02
GO:0043410	positive regulation of MAPK cascade	2.24E-02
GO:0042981	regulation of apoptotic process	2.26E-02

GO:0031589	cell-substrate adhesion	2.28E-02
GO:0045935	positive regulation of nucleobase-containing compound metabolic process	2.32E-02
GO:0050890	cognition	2.45E-02
GO:0044708	single-organism behavior	2.70E-02
GO:1902680	positive regulation of RNA biosynthetic process	2.75E-02
GO:0031328	positive regulation of cellular biosynthetic process	2.76E-02
GO:1903508	positive regulation of nucleic acid-templated transcription	2.77E-02
GO:0045597	positive regulation of cell differentiation	2.78E-02
GO:0051173	positive regulation of nitrogen compound metabolic process	2.81E-02
GO:0031325	positive regulation of cellular metabolic process	2.82E-02
GO:0045893	positive regulation of transcription, DNA-templated	2.84E-02
GO:0048513	organ development	2.91E-02
GO:0009891	positive regulation of biosynthetic process	2.94E-02
GO:0051254	positive regulation of RNA metabolic process	2.97E-02
GO:0009187	cyclic nucleotide metabolic process	3.01E-02
GO:0007166	cell surface receptor signaling pathway	3.03E-02
GO:0048754	branching morphogenesis of an epithelial tube	3.04E-02
GO:0009967	positive regulation of signal transduction	3.05E-02
GO:0060281	regulation of oocyte development	3.36E-02
GO:0007165	signal transduction	3.56E-02
GO:0032270	positive regulation of cellular protein metabolic process	3.63E-02
GO:0031399	regulation of protein modification process	3.69E-02
GO:0010455	positive regulation of cell fate commitment	3.81E-02
GO:0061138	morphogenesis of a branching epithelium	4.53E-02
GO:0010557	positive regulation of macromolecule biosynthetic process	4.93E-02
GO:0010604	positive regulation of macromolecule metabolic process	4.94E-02

Table III-1 *– Gene ontology analysis of decreased lung transcripts in all TL1A transgenic lines compared to WT mice.*

GO Term	Description	FDR q-value
GO:0001568	blood vessel development	6.51E-03
GO:0044767	single-organism developmental process	7.99E-03
GO:0022610	biological adhesion	9.45E-03
GO:0007155	cell adhesion	1.03E-02
GO:0032502	developmental process	1.16E-02
GO:0010632	regulation of epithelial cell migration	1.56E-02
GO:0048856	anatomical structure development	1.74E-02
GO:0010594	regulation of endothelial cell migration	1.79E-02
GO:0009653	anatomical structure morphogenesis	1.85E-02
GO:0051239	regulation of multicellular organismal process	2.01E-02
GO:0022603	regulation of anatomical structure morphogenesis	2.36E-02
GO:0051270	regulation of cellular component movement	3.67E-02
GO:0030199	collagen fibril organization	3.67E-02

GO:0007156	homophilic cell adhesion via plasma membrane adhesion molecules	3.93E-02
GO:0044236	multicellular organismal metabolic process	4.31E-02

Table III-2 *– Gene ontology analysis of decreased lung transcripts in Mem+Sol TL1A transgenic mice and not in Mem or Mem Hi compared to WT mice.*

GO Term	Description	FDR q-value
GO:0051240	positive regulation of multicellular organismal process	1.85E-02
GO:0051239	regulation of multicellular organismal process	4.56E-02
GO:0051130	positive regulation of cellular component organization	4.60E-02

Table III-3 *– Gene ontology analysis of decreased lung transcripts in Mem and Mem Hi TL1A transgenic mice and not in Mem+Sol Hi compared to WT mice.*

GO Term	Description	FDR q-value
GO:0002376	immune system process	1.68E-24
GO:0006955	immune response	3.45E-15
GO:0002682	regulation of immune system process	2.17E-13
GO:0002684	positive regulation of immune system process	6.08E-10
GO:0019886	antigen processing and presentation of exogenous peptide antigen via MHC class II	6.44E-10
GO:0002495	antigen processing and presentation of peptide antigen via MHC class II	7.51E-10
GO:0002504	antigen processing and presentation of peptide or polysaccharide antigen via MHC class II	9.01E-10
GO:0051249	regulation of lymphocyte activation	3.16E-09
GO:0002694	regulation of leukocyte activation	3.33E-09
GO:0050865	regulation of cell activation	1.13E-08
GO:0002478	antigen processing and presentation of exogenous peptide antigen	1.97E-08
GO:0002683	negative regulation of immune system process	7.98E-08
GO:0019884	antigen processing and presentation of exogenous antigen	1.13E-07
GO:0002695	negative regulation of leukocyte activation	1.49E-07
GO:0006952	defense response	1.52E-07
GO:0050863	regulation of T cell activation	2.65E-07
GO:0050866	negative regulation of cell activation	4.10E-07
GO:1903037	regulation of leukocyte cell-cell adhesion	4.20E-07
GO:0034110	regulation of homotypic cell-cell adhesion	6.49E-07
GO:0022407	regulation of cell-cell adhesion	1.45E-06
GO:0070663	regulation of leukocyte proliferation	3.16E-06
GO:0002687	positive regulation of leukocyte migration	4.52E-06
GO:0051250	negative regulation of lymphocyte activation	8.65E-06
GO:0048002	antigen processing and presentation of peptide antigen	1.20E-05
GO:0022409	positive regulation of cell-cell adhesion	2.12E-05
GO:0050670	regulation of lymphocyte proliferation	2.15E-05
GO:0032944	regulation of mononuclear cell proliferation	2.30E-05

GO:0030155	regulation of cell adhesion	2.65E-05
GO:0050870	positive regulation of T cell activation	2.83E-05
GO:0006935	chemotaxis	2.91E-05
GO:0042330	taxis	2.94E-05
GO:0002685	regulation of leukocyte migration	3.08E-05
GO:0034112	positive regulation of homotypic cell-cell adhesion	3.37E-05
GO:1903039	positive regulation of leukocyte cell-cell adhesion	3.47E-05
GO:0051251	positive regulation of lymphocyte activation	4.76E-05
GO:0006954	inflammatory response	4.82E-05
GO:0001817	regulation of cytokine production	9.56E-05
GO:0048583	regulation of response to stimulus	1.06E-04
GO:0019221	cytokine-mediated signaling pathway	1.17E-04
GO:0002688	regulation of leukocyte chemotaxis	1.36E-04
GO:0002696	positive regulation of leukocyte activation	1.39E-04
GO:0019882	antigen processing and presentation	1.55E-04
GO:0050869	negative regulation of B cell activation	1.87E-04
GO:0050867	positive regulation of cell activation	1.95E-04
GO:0048520	positive regulation of behavior	2.95E-04
GO:0045785	positive regulation of cell adhesion	3.15E-04
GO:2000401	regulation of lymphocyte migration	3.71E-04
GO:0032693	negative regulation of interleukin-10 production	3.71E-04
GO:0048584	positive regulation of response to stimulus	4.19E-04
GO:0070664	negative regulation of leukocyte proliferation	4.50E-04
GO:0050920	regulation of chemotaxis	4.55E-04
GO:0050864	regulation of B cell activation	4.67E-04
GO:0070098	chemokine-mediated signaling pathway	4.96E-04
GO:0002690	positive regulation of leukocyte chemotaxis	5.38E-04
GO:0032653	regulation of interleukin-10 production	5.44E-04
GO:0032101	regulation of response to external stimulus	5.60E-04
GO:0050921	positive regulation of chemotaxis	6.12E-04
GO:0016064	immunoglobulin mediated immune response	6.46E-04
GO:0050795	regulation of behavior	8.43E-04
GO:0050776	regulation of immune response	1.00E-03
GO:0002819	regulation of adaptive immune response	1.02E-03
GO:0006950	response to stress	1.32E-03
GO:0019724	B cell mediated immunity	1.34E-03
GO:0001819	positive regulation of cytokine production	1.38E-03
GO:0002274	myeloid leukocyte activation	1.40E-03
GO:0042129	regulation of T cell proliferation	1.40E-03
GO:0050868	negative regulation of T cell activation	1.52E-03
GO:0045321	leukocyte activation	1.62E-03
GO:0002449	lymphocyte mediated immunity	1.63E-03
GO:2000406	positive regulation of T cell migration	1.68E-03
GO:0045619	regulation of lymphocyte differentiation	1.69E-03
GO:0060326	cell chemotaxis	1.80E-03
GO:0031347	regulation of defense response	2.00E-03

GO:1903038	negative regulation of leukocyte cell-cell adhesion	2.02E-03
GO:0002548	monocyte chemotaxis	2.14E-03
GO:0065007	biological regulation	2.15E-03
GO:2000403	positive regulation of lymphocyte migration	2.44E-03
GO:2000404	regulation of T cell migration	2.48E-03
GO:0002460	adaptive immune response based on somatic recombination of immune receptors built from immunoglobulin superfamily domains	2.89E-03
GO:0034111	negative regulation of homotypic cell-cell adhesion	3.16E-03
GO:0032103	positive regulation of response to external stimulus	3.47E-03
GO:0050789	regulation of biological process	4.03E-03
GO:0050672	negative regulation of lymphocyte proliferation	4.07E-03
GO:0045580	regulation of T cell differentiation	4.10E-03
GO:0032945	negative regulation of mononuclear cell proliferation	4.12E-03
GO:0001775	cell activation	4.41E-03
GO:0032879	regulation of localization	4.71E-03
GO:0051085	chaperone mediated protein folding requiring cofactor	4.79E-03
GO:0002250	adaptive immune response	4.80E-03
GO:0045582	positive regulation of T cell differentiation	4.97E-03
GO:0002443	leukocyte mediated immunity	5.03E-03
GO:1902105	regulation of leukocyte differentiation	5.06E-03
GO:0050777	negative regulation of immune response	5.08E-03
GO:0050794	regulation of cellular process	5.09E-03
GO:0042127	regulation of cell proliferation	6.00E-03
GO:0040017	positive regulation of locomotion	6.08E-03
GO:0051707	response to other organism	7.07E-03
GO:0006968	cellular defense response	7.13E-03
GO:0050778	positive regulation of immune response	7.23E-03
GO:0048518	positive regulation of biological process	7.29E-03
GO:0045620	negative regulation of lymphocyte differentiation	7.32E-03
GO:0051084	'de novo' posttranslational protein folding	8.36E-03
GO:0006458	'de novo' protein folding	8.45E-03
GO:0045621	positive regulation of lymphocyte differentiation	8.88E-03
GO:0050707	regulation of cytokine secretion	8.93E-03
GO:1902107	positive regulation of leukocyte differentiation	9.23E-03
GO:0002821	positive regulation of adaptive immune response	1.03E-02
GO:0043207	response to external biotic stimulus	1.11E-02
GO:1901623	regulation of lymphocyte chemotaxis	1.17E-02
GO:0002704	negative regulation of leukocyte mediated immunity	1.18E-02
GO:0022408	negative regulation of cell-cell adhesion	1.18E-02
GO:0040011	locomotion	1.34E-02
GO:0030335	positive regulation of cell migration	1.49E-02
GO:0009607	response to biotic stimulus	1.56E-02
GO:0050896	response to stimulus	1.78E-02
GO:0002697	regulation of immune effector process	1.79E-02
GO:2000147	positive regulation of cell motility	1.80E-02
GO:0007166	cell surface receptor signaling pathway	1.81E-02

GO:0007162	negative regulation of cell adhesion	1.86E-02
GO:0042130	negative regulation of T cell proliferation	2.05E-02
GO:0002703	regulation of leukocyte mediated immunity	2.09E-02
GO:0051272	positive regulation of cellular component movement	2.10E-02
GO:0009617	response to bacterium	2.50E-02
GO:1903708	positive regulation of hemopoiesis	2.79E-02
GO:0051046	regulation of secretion	2.80E-02
GO:0050859	negative regulation of B cell receptor signaling pathway	2.87E-02
GO:0032730	positive regulation of interleukin-1 alpha production	2.89E-02
GO:1900424	regulation of defense response to bacterium	2.91E-02
GO:0002381	immunoglobulin production involved in immunoglobulin mediated immune response	2.93E-02
GO:0072676	lymphocyte migration	2.94E-02
GO:0030888	regulation of B cell proliferation	2.94E-02
GO:1903706	regulation of hemopoiesis	3.38E-02
GO:0050671	positive regulation of lymphocyte proliferation	3.39E-02
GO:0002822	regulation of adaptive immune response based on somatic recombination of immune receptors built from immunoglobulin superfamily domains	3.62E-02
GO:0032946	positive regulation of mononuclear cell proliferation	3.65E-02
GO:0032650	regulation of interleukin-1 alpha production	4.13E-02
GO:0070665	positive regulation of leukocyte proliferation	4.18E-02
GO:0001818	negative regulation of cytokine production	4.23E-02
GO:0051239	regulation of multicellular organismal process	4.59E-02
GO:0097028	dendritic cell differentiation	4.68E-02
GO:0051240	positive regulation of multicellular organismal process	4.76E-02
GO:0048585	negative regulation of response to stimulus	4.86E-02

Table III-4 *– Gene ontology analysis of increased lung transcripts in all TL1A transgenic lines compared to WT mice.*

GO Term	Description	FDR q-value
	No Significant enriched GO terms	

Table III-5 *– Gene ontology analysis of increased lung transcripts in Mem+Sol TL1A transgenic mice and not in Mem or Mem Hi compared to WT mice.*

GO Term	Description	FDR q-value
GO:0002376	immune system process	1.24E-17
GO:0006952	defense response	6.26E-14
GO:0002682	regulation of immune system process	4.80E-12
GO:0006955	immune response	5.32E-12
GO:0002684	positive regulation of immune system process	7.76E-11
GO:0050776	regulation of immune response	1.30E-08
GO:0048584	positive regulation of response to stimulus	1.79E-08
GO:0050778	positive regulation of immune response	1.90E-08

GO:0001775	cell activation	8.09E-08
GO:0006954	inflammatory response	1.30E-07
GO:0002252	immune effector process	1.83E-07
GO:0002253	activation of immune response	3.43E-07
GO:0006950	response to stress	5.19E-07
GO:0001773	myeloid dendritic cell activation	7.09E-06
GO:0002274	myeloid leukocyte activation	8.47E-06
GO:0098542	defense response to other organism	9.47E-06
GO:0045321	leukocyte activation	1.45E-05
GO:0072678	T cell migration	1.47E-05
GO:0001817	regulation of cytokine production	3.38E-05
GO:0048518	positive regulation of biological process	4.15E-05
GO:0019221	cytokine-mediated signaling pathway	4.27E-05
GO:0030155	regulation of cell adhesion	6.16E-05
GO:0051707	response to other organism	7.84E-05
GO:0031349	positive regulation of defense response	8.46E-05
GO:0043011	myeloid dendritic cell differentiation	9.24E-05
GO:0032649	regulation of interferon-gamma production	1.01E-04
GO:0002460	adaptive immune response based on somatic recombination of immune receptors built from immunoglobulin superfamily domains	1.03E-04
GO:0002757	immune response-activating signal transduction	2.03E-04
GO:0045087	innate immune response	2.09E-04
GO:0072676	lymphocyte migration	2.74E-04
GO:0042330	taxis	4.58E-04
GO:0002764	immune response-regulating signaling pathway	4.63E-04
GO:0006935	chemotaxis	4.68E-04
GO:0031347	regulation of defense response	6.29E-04
GO:0048583	regulation of response to stimulus	6.37E-04
GO:0002449	lymphocyte mediated immunity	6.51E-04
GO:0097028	dendritic cell differentiation	6.56E-04
GO:0034097	response to cytokine	8.64E-04
GO:0050896	response to stimulus	1.06E-03
GO:0022407	regulation of cell-cell adhesion	1.15E-03
GO:0050900	leukocyte migration	1.42E-03
GO:0043207	response to external biotic stimulus	1.73E-03
GO:0060326	cell chemotaxis	1.99E-03
GO:0010818	T cell chemotaxis	2.05E-03
GO:0070098	chemokine-mediated signaling pathway	2.27E-03
GO:0050865	regulation of cell activation	2.42E-03
GO:0009607	response to biotic stimulus	2.57E-03
GO:0002443	leukocyte mediated immunity	2.59E-03
GO:0001816	cytokine production	2.93E-03
GO:0045088	regulation of innate immune response	2.99E-03
GO:0034110	regulation of homotypic cell-cell adhesion	3.17E-03
GO:0045089	positive regulation of innate immune response	3.29E-03
GO:0001819	positive regulation of cytokine production	3.37E-03

GO:0051704	multi-organism process	3.49E-03
GO:0002250	adaptive immune response	3.71E-03
GO:0007166	cell surface receptor signaling pathway	3.88E-03
GO:0030099	myeloid cell differentiation	4.19E-03
GO:0002694	regulation of leukocyte activation	4.27E-03
GO:0019724	B cell mediated immunity	4.33E-03
GO:0051249	regulation of lymphocyte activation	4.87E-03
GO:0002521	leukocyte differentiation	5.28E-03
GO:0002429	immune response-activating cell surface receptor signaling pathway	5.70E-03
GO:0019372	lipoxygenase pathway	5.92E-03
GO:0043367	CD4-positive, alpha-beta T cell differentiation	6.52E-03
GO:0030595	leukocyte chemotaxis	7.10E-03
GO:0051239	regulation of multicellular organismal process	7.13E-03
GO:0050863	regulation of T cell activation	7.69E-03
GO:0070593	dendrite self-avoidance	9.31E-03
GO:0002268	follicular dendritic cell differentiation	9.44E-03
GO:0002266	follicular dendritic cell activation	9.58E-03
GO:0035710	CD4-positive, alpha-beta T cell activation	9.59E-03
GO:0045346	regulation of MHC class II biosynthetic process	9.93E-03
GO:1903037	regulation of leukocyte cell-cell adhesion	9.94E-03
GO:0007159	leukocyte cell-cell adhesion	1.13E-02
GO:0002768	immune response-regulating cell surface receptor signaling pathway	1.14E-02
GO:0043950	positive regulation of cAMP-mediated signaling	1.26E-02
GO:0032729	positive regulation of interferon-gamma production	1.31E-02
GO:0032101	regulation of response to external stimulus	1.36E-02
GO:0007155	cell adhesion	1.43E-02
GO:0050789	regulation of biological process	1.46E-02
GO:0030098	lymphocyte differentiation	1.49E-02
GO:0022610	biological adhesion	1.57E-02
GO:0009615	response to virus	1.57E-02
GO:0046649	lymphocyte activation	1.61E-02
GO:0042742	defense response to bacterium	1.63E-02
GO:0030217	T cell differentiation	2.00E-02
GO:0048522	positive regulation of cellular process	2.05E-02
GO:0050851	antigen receptor-mediated signaling pathway	2.07E-02
GO:0016337	single organismal cell-cell adhesion	2.12E-02
GO:0045347	negative regulation of MHC class II biosynthetic process	2.17E-02
GO:0048247	lymphocyte chemotaxis	2.18E-02
GO:0065007	biological regulation	2.25E-02
GO:0046632	alpha-beta T cell differentiation	2.30E-02
GO:1903034	regulation of response to wounding	2.35E-02
GO:0051607	defense response to virus	2.65E-02
GO:0098609	cell-cell adhesion	2.81E-02
GO:0040011	locomotion	2.84E-02
GO:0032103	positive regulation of response to external stimulus	2.88E-02

GO:0048523	negative regulation of cellular process	2.89E-02
GO:0042093	T-helper cell differentiation	2.90E-02
GO:0009617	response to bacterium	2.90E-02
GO:0002294	CD4-positive, alpha-beta T cell differentiation involved in immune response	2.92E-02
GO:0050727	regulation of inflammatory response	2.96E-02
GO:0098602	single organism cell adhesion	3.10E-02
GO:0050852	T cell receptor signaling pathway	3.27E-02
GO:0022409	positive regulation of cell-cell adhesion	3.37E-02
GO:0002573	myeloid leukocyte differentiation	3.39E-02
GO:0044116	growth of symbiont involved in interaction with host	3.45E-02
GO:0044117	growth of symbiont in host	3.48E-02
GO:0044110	growth involved in symbiotic interaction	3.51E-02
GO:0016064	immunoglobulin mediated immune response	3.52E-02
GO:0001818	negative regulation of cytokine production	3.53E-02
GO:0032827	negative regulation of natural killer cell differentiation involved in immune response	3.54E-02
GO:0002293	alpha-beta T cell differentiation involved in immune response	3.55E-02
GO:0032826	regulation of natural killer cell differentiation involved in immune response	3.57E-02
GO:0032824	negative regulation of natural killer cell differentiation	3.61E-02
GO:0030814	regulation of cAMP metabolic process	3.61E-02
GO:0042221	response to chemical	3.61E-02
GO:0045064	T-helper 2 cell differentiation	3.64E-02
GO:0002287	alpha-beta T cell activation involved in immune response	3.95E-02
GO:0010033	response to organic substance	3.97E-02
GO:0045785	positive regulation of cell adhesion	4.50E-02
GO:1901739	regulation of myoblast fusion	4.51E-02
GO:0046631	alpha-beta T cell activation	4.51E-02
GO:0009967	positive regulation of signal transduction	4.53E-02
GO:0043949	regulation of cAMP-mediated signaling	4.55E-02
GO:0006909	phagocytosis	4.55E-02
GO:0050870	positive regulation of T cell activation	4.94E-02
GO:0032747	positive regulation of interleukin-23 production	4.94E-02
GO:0030816	positive regulation of cAMP metabolic process	4.98E-02
GO:0045918	negative regulation of cytolysis	4.98E-02

Table III-6 *– Gene ontology analysis of increased lung transcripts in Mem+Sol TL1A transgenic mice and not in Mem or Mem Hi compared to WT mice.*

References

1. Kondo, M., I.L. Weissman, and K. Akashi, *Identification of clonogenic common lymphoid progenitors in mouse bone marrow.* Cell, 1997. **91**(5): p. 661-72.
2. Van De Wiele, C.J., et al., *Thymocytes between the beta-selection and positive selection checkpoints are nonresponsive to IL-7 as assessed by STAT-5 phosphorylation.* J Immunol, 2004. **172**(7): p. 4235-44.
3. Klein, L., et al., *Positive and negative selection of the T cell repertoire: what thymocytes see (and don't see).* Nat Rev Immunol, 2014. **14**(6): p. 377-91.
4. Aifantis, I., E. Raetz, and S. Buonamici, *Molecular pathogenesis of T-cell leukaemia and lymphoma.* Nat Rev Immunol, 2008. **8**(5): p. 380-90.
5. Xu, X., et al., *Maturation and emigration of single-positive thymocytes.* Clin Dev Immunol, 2013. **2013**: p. 282870.
6. Smith-Garvin, J.E., G.A. Koretzky, and M.S. Jordan, *T cell activation.* Annu Rev Immunol, 2009. **27**: p. 591-619.
7. Bonelli, M., et al., *Helper T cell plasticity: impact of extrinsic and intrinsic signals on transcriptomes and epigenomes.* Curr Top Microbiol Immunol, 2014. **381**: p. 279-326.
8. Shahinian, A., et al., *Differential T cell costimulatory requirements in CD28-deficient mice.* Science, 1993. **261**(5121): p. 609-12.
9. Pages, F., et al., *Binding of phosphatidylinositol-3-OH kinase to CD28 is required for T-cell signalling.* Nature, 1994. **369**(6478): p. 327-9.
10. Narayan, P., et al., *CARMA1 is required for Akt-mediated NF-kappaB activation in T cells.* Mol Cell Biol, 2006. **26**(6): p. 2327-36.
11. Tivol, E.A., et al., *Loss of CTLA-4 leads to massive lymphoproliferation and fatal multiorgan tissue destruction, revealing a critical negative regulatory role of CTLA-4.* Immunity, 1995. **3**(5): p. 541-7.
12. Lee, K.M., et al., *Molecular basis of T cell inactivation by CTLA-4.* Science, 1998. **282**(5397): p. 2263-6.
13. Schneider, H., et al., *CTLA-4 disrupts ZAP70 microcluster formation with reduced T cell/APC dwell times and calcium mobilization.* Eur J Immunol, 2008. **38**(1): p. 40-7.
14. Calvo, C.R., D. Amsen, and A.M. Kruisbeek, *Cytotoxic T lymphocyte antigen 4 (CTLA-4) interferes with extracellular signal-regulated kinase (ERK) and Jun NH2-terminal kinase (JNK) activation, but does not affect phosphorylation of T cell receptor zeta and ZAP70.* J Exp Med, 1997. **186**(10): p. 1645-53.
15. Wakamatsu, E., D. Mathis, and C. Benoist, *Convergent and divergent effects of costimulatory molecules in conventional and regulatory CD4+ T cells.* Proc Natl Acad Sci U S A, 2013. **110**(3): p. 1023-8.
16. Onishi, Y., et al., *Foxp3+ natural regulatory T cells preferentially form aggregates on dendritic cells in vitro and actively inhibit their maturation.* Proc Natl Acad Sci U S A, 2008. **105**(29): p. 10113-8.
17. Qureshi, O.S., et al., *Trans-endocytosis of CD80 and CD86: a molecular basis for the cell-extrinsic function of CTLA-4.* Science, 2011. **332**(6029): p. 600-3.
18. Tokoyoda, K., et al., *Cellular niches controlling B lymphocyte behavior within bone marrow during development.* Immunity, 2004. **20**(6): p. 707-18.
19. Galler, G.R., et al., *Surface mu heavy chain signals down-regulation of the V(D)J-recombinase machinery in the absence of surrogate light chain components.* J Exp Med, 2004. **199**(11): p. 1523-32.
20. Melchers, F., *Checkpoints that control B cell development.* J Clin Invest, 2015. **125**(6): p. 2203-10.

21. Parker, M.J., et al., *The pre-B-cell receptor induces silencing of VpreB and lambda5 transcription.* EMBO J, 2005. **24**(22): p. 3895-905.
22. Allende, M.L., et al., *S1P1 receptor directs the release of immature B cells from bone marrow into blood.* J Exp Med, 2010. **207**(5): p. 1113-24.
23. Tiegs, S.L., D.M. Russell, and D. Nemazee, *Receptor editing in self-reactive bone marrow B cells.* J Exp Med, 1993. **177**(4): p. 1009-20.
24. Kraus, M., et al., *Survival of resting mature B lymphocytes depends on BCR signaling via the Igalpha/beta heterodimer.* Cell, 2004. **117**(6): p. 787-800.
25. Bojarczuk, K., et al., *B-cell receptor signaling in the pathogenesis of lymphoid malignancies.* Blood Cells Mol Dis, 2015. **55**(3): p. 255-65.
26. Ying, H., et al., *Syk mediates BCR- and CD40-signaling integration during B cell activation.* Immunobiology, 2011. **216**(5): p. 566-70.
27. Kiessling, R., et al., *"Natural" killer cells in the mouse. II. Cytotoxic cells with specificity for mouse Moloney leukemia cells. Characteristics of the killer cell.* Eur J Immunol, 1975. **5**(2): p. 117-21.
28. Spits, H., et al., *Innate lymphoid cells--a proposal for uniform nomenclature.* Nat Rev Immunol, 2013. **13**(2): p. 145-9.
29. Sonnenberg, G.F. and D. Artis, *Innate lymphoid cells in the initiation, regulation and resolution of inflammation.* Nat Med, 2015. **21**(7): p. 698-708.
30. Klose, C.S., et al., *Differentiation of type 1 ILCs from a common progenitor to all helper-like innate lymphoid cell lineages.* Cell, 2014. **157**(2): p. 340-56.
31. Fuchs, A., et al., *Intraepithelial type 1 innate lymphoid cells are a unique subset of IL-12- and IL-15-responsive IFN-gamma-producing cells.* Immunity, 2013. **38**(4): p. 769-81.
32. Mjosberg, J.M., et al., *Human IL-25- and IL-33-responsive type 2 innate lymphoid cells are defined by expression of CRTH2 and CD161.* Nat Immunol, 2011. **12**(11): p. 1055-62.
33. Neill, D.R., et al., *Nuocytes represent a new innate effector leukocyte that mediates type-2 immunity.* Nature, 2010. **464**(7293): p. 1367-70.
34. Moro, K., et al., *Innate production of T(H)2 cytokines by adipose tissue-associated c-Kit(+)Sca-1(+) lymphoid cells.* Nature, 2010. **463**(7280): p. 540-4.
35. Zhao, A., et al., *Critical role of IL-25 in nematode infection-induced alterations in intestinal function.* J Immunol, 2010. **185**(11): p. 6921-9.
36. Buonocore, S., et al., *Innate lymphoid cells drive interleukin-23-dependent innate intestinal pathology.* Nature, 2010. **464**(7293): p. 1371-5.
37. Sawa, S., et al., *Lineage relationship analysis of RORgammat+ innate lymphoid cells.* Science, 2010. **330**(6004): p. 665-9.
38. Cella, M., et al., *A human natural killer cell subset provides an innate source of IL-22 for mucosal immunity.* Nature, 2009. **457**(7230): p. 722-5.
39. Zheng, Y., et al., *Interleukin-22 mediates early host defense against attaching and effacing bacterial pathogens.* Nat Med, 2008. **14**(3): p. 282-9.
40. Croft, M., *The role of TNF superfamily members in T-cell function and diseases.* Nat Rev Immunol, 2009. **9**(4): p. 271-85.
41. Pitti, R.M., et al., *Genomic amplification of a decoy receptor for Fas ligand in lung and colon cancer.* Nature, 1998. **396**(6712): p. 699-703.
42. Bodmer, J.L., P. Schneider, and J. Tschopp, *The molecular architecture of the TNF superfamily.* Trends Biochem Sci, 2002. **27**(1): p. 19-26.
43. Migone, T.S., et al., *TL1A is a TNF-like ligand for DR3 and TR6/DcR3 and functions as a T cell costimulator.* Immunity, 2002. **16**(3): p. 479-92.
44. Chan, F.K., et al., *A domain in TNF receptors that mediates ligand-independent receptor assembly and signaling.* Science, 2000. **288**(5475): p. 2351-4.
45. Siegel, R.M., et al., *Fas preassociation required for apoptosis signaling and dominant inhibition by pathogenic mutations.* Science, 2000. **288**(5475): p. 2354-7.

46. Hymowitz, S.G., et al., *Triggering cell death: the crystal structure of Apo2L/TRAIL in a complex with death receptor 5.* Mol Cell, 1999. **4**(4): p. 563-71.
47. Bossen, C., et al., *Interactions of tumor necrosis factor (TNF) and TNF receptor family members in the mouse and human.* J Biol Chem, 2006. **281**(20): p. 13964-71.
48. Hashimoto, T., D. Schlessinger, and C.Y. Cui, *Troy binding to lymphotoxin-alpha activates NF kappa B mediated transcription.* Cell Cycle, 2008. **7**(1): p. 106-11.
49. Schneider, P., et al., *Identification of a new murine tumor necrosis factor receptor locus that contains two novel murine receptors for tumor necrosis factor-related apoptosis-inducing ligand (TRAIL).* J Biol Chem, 2003. **278**(7): p. 5444-54.
50. Hu, Y., et al., *A DR6/p75(NTR) complex is responsible for beta-amyloid-induced cortical neuron death.* Cell Death Dis, 2013. **4**: p. e579.
51. Pattarawarapan, M. and K. Burgess, *Molecular basis of neurotrophin-receptor interactions.* J Med Chem, 2003. **46**(25): p. 5277-91.
52. Hehlgans, T. and K. Pfeffer, *The intriguing biology of the tumour necrosis factor/tumour necrosis factor receptor superfamily: players, rules and the games.* Immunology, 2005. **115**(1): p. 1-20.
53. Yamamoto, H., T. Kishimoto, and S. Minamoto, *NF-kappaB activation in CD27 signaling: involvement of TNF receptor-associated factors in its signaling and identification of functional region of CD27.* J Immunol, 1998. **161**(9): p. 4753-9.
54. Ishida, T.K., et al., *TRAF5, a novel tumor necrosis factor receptor-associated factor family protein, mediates CD40 signaling.* Proc Natl Acad Sci U S A, 1996. **93**(18): p. 9437-42.
55. Rothe, M., et al., *A novel family of putative signal transducers associated with the cytoplasmic domain of the 75 kDa tumor necrosis factor receptor.* Cell, 1994. **78**(4): p. 681-92.
56. Wajant, H., F. Henkler, and P. Scheurich, *The TNF-receptor-associated factor family: scaffold molecules for cytokine receptors, kinases and their regulators.* Cell Signal, 2001. **13**(6): p. 389-400.
57. McWhirter, S.M., et al., *Crystallographic analysis of CD40 recognition and signaling by human TRAF2.* Proc Natl Acad Sci U S A, 1999. **96**(15): p. 8408-13.
58. Wen, L., et al., *TL1A-induced NF-kappaB activation and c-IAP2 production prevent DR3-mediated apoptosis in TF-1 cells.* J Biol Chem, 2003. **278**(40): p. 39251-8.
59. Park, Y.C., et al., *Structural basis for self-association and receptor recognition of human TRAF2.* Nature, 1999. **398**(6727): p. 533-8.
60. Yin, Q., et al., *E2 interaction and dimerization in the crystal structure of TRAF6.* Nat Struct Mol Biol, 2009. **16**(6): p. 658-66.
61. Wu, C.J., et al., *Sensing of Lys 63-linked polyubiquitination by NEMO is a key event in NF-kappaB activation [corrected].* Nat Cell Biol, 2006. **8**(4): p. 398-406.
62. Chung, J.Y., et al., *All TRAFs are not created equal: common and distinct molecular mechanisms of TRAF-mediated signal transduction.* J Cell Sci, 2002. **115**(Pt 4): p. 679-88.
63. Kischkel, F.C., et al., *Cytotoxicity-dependent APO-1 (Fas/CD95)-associated proteins form a death-inducing signaling complex (DISC) with the receptor.* EMBO J, 1995. **14**(22): p. 5579-88.
64. Muzio, M., et al., *An induced proximity model for caspase-8 activation.* J Biol Chem, 1998. **273**(5): p. 2926-30.

65. Yu, K.Y., et al., *A newly identified member of tumor necrosis factor receptor superfamily (TR6) suppresses LIGHT-mediated apoptosis.* J Biol Chem, 1999. **274**(20): p. 13733-6.
66. MacFarlane, M., et al., *Identification and molecular cloning of two novel receptors for the cytotoxic ligand TRAIL.* J Biol Chem, 1997. **272**(41): p. 25417-20.
67. Marsters, S.A., et al., *A novel receptor for Apo2L/TRAIL contains a truncated death domain.* Curr Biol, 1997. **7**(12): p. 1003-6.
68. You, R.I., et al., *Apoptosis of dendritic cells induced by decoy receptor 3 (DcR3).* Blood, 2008. **111**(3): p. 1480-8.
69. Moss, M.L., et al., *Cloning of a disintegrin metalloproteinase that processes precursor tumour-necrosis factor-alpha.* Nature, 1997. **385**(6618): p. 733-6.
70. Kriegler, M., et al., *A novel form of TNF/cachectin is a cell surface cytotoxic transmembrane protein: ramifications for the complex physiology of TNF.* Cell, 1988. **53**(1): p. 45-53.
71. Alexopoulou, L., et al., *Transmembrane TNF protects mutant mice against intracellular bacterial infections, chronic inflammation and autoimmunity.* Eur J Immunol, 2006. **36**(10): p. 2768-80.
72. Ohta, T., *Gene Families: Multigene Families and Superfamilies.* eLS, 2008.
73. Rogers, P.R., et al., *OX40 promotes Bcl-xL and Bcl-2 expression and is essential for long-term survival of CD4 T cells.* Immunity, 2001. **15**(3): p. 445-55.
74. Hendriks, J., et al., *CD27 is required for generation and long-term maintenance of T cell immunity.* Nat Immunol, 2000. **1**(5): p. 433-40.
75. Arens, R., et al., *Constitutive CD27/CD70 interaction induces expansion of effector-type T cells and results in IFNgamma-mediated B cell depletion.* Immunity, 2001. **15**(5): p. 801-12.
76. Feau, S., et al., *The CD4(+) T-cell help signal is transmitted from APC to CD8(+) T-cells via CD27-CD70 interactions.* Nat Commun, 2012. **3**: p. 948.
77. Peter, M.E., et al., *The role of CD95 and CD95 ligand in cancer.* Cell Death Differ, 2015. **22**(5): p. 885-6.
78. Shah, S., et al., *Autoimmune lymphoproliferative syndrome: an update and review of the literature.* Curr Allergy Asthma Rep, 2014. **14**(9): p. 462.
79. Bleesing, J.J., S.E. Straus, and T.A. Fleisher, *Autoimmune lymphoproliferative syndrome. A human disorder of abnormal lymphocyte survival.* Pediatr Clin North Am, 2000. **47**(6): p. 1291-310.
80. Chu, J.L., et al., *The defect in Fas mRNA expression in MRL/lpr mice is associated with insertion of the retrotransposon, ETn.* J Exp Med, 1993. **178**(2): p. 723-30.
81. Griffith, T.S., et al., *Fas ligand-induced apoptosis as a mechanism of immune privilege.* Science, 1995. **270**(5239): p. 1189-92.
82. Albarbar, B., C. Dunnill, and N.T. Georgopoulos, *Regulation of cell fate by lymphotoxin (LT) receptor signalling: Functional differences and similarities of the LT system to other TNF superfamily (TNFSF) members.* Cytokine Growth Factor Rev, 2015.
83. Kruglov, A.A., et al., *Nonredundant function of soluble LTalpha3 produced by innate lymphoid cells in intestinal homeostasis.* Science, 2013. **342**(6163): p. 1243-6.
84. Mauri, D.N., et al., *LIGHT, a new member of the TNF superfamily, and lymphotoxin alpha are ligands for herpesvirus entry mediator.* Immunity, 1998. **8**(1): p. 21-30.
85. Ware, C.F., et al., *Expression of surface lymphotoxin and tumor necrosis factor on activated T, B, and natural killer cells.* J Immunol, 1992. **149**(12): p. 3881-8.

86. Williams-Abbott, L., et al., *The lymphotoxin-alpha (LTalpha) subunit is essential for the assembly, but not for the receptor specificity, of the membrane-anchored LTalpha1beta2 heterotrimeric ligand.* J Biol Chem, 1997. **272**(31): p. 19451-6.
87. Stopfer, P., D.N. Mannel, and T. Hehlgans, *Lymphotoxin-beta receptor activation by activated T cells induces cytokine release from mouse bone marrow-derived mast cells.* J Immunol, 2004. **172**(12): p. 7459-65.
88. Force, W.R., et al., *Mouse lymphotoxin-beta receptor. Molecular genetics, ligand binding, and expression.* J Immunol, 1995. **155**(11): p. 5280-8.
89. Browning, J.L., et al., *Characterization of lymphotoxin-alpha beta complexes on the surface of mouse lymphocytes.* J Immunol, 1997. **159**(7): p. 3288-98.
90. Mackay, F., et al., *Lymphotoxin but not tumor necrosis factor functions to maintain splenic architecture and humoral responsiveness in adult mice.* Eur J Immunol, 1997. **27**(8): p. 2033-42.
91. Fava, R.A., et al., *A role for the lymphotoxin/LIGHT axis in the pathogenesis of murine collagen-induced arthritis.* J Immunol, 2003. **171**(1): p. 115-26.
92. De Togni, P., et al., *Abnormal development of peripheral lymphoid organs in mice deficient in lymphotoxin.* Science, 1994. **264**(5159): p. 703-7.
93. Banks, T.A., et al., *Lymphotoxin-alpha-deficient mice. Effects on secondary lymphoid organ development and humoral immune responsiveness.* J Immunol, 1995. **155**(4): p. 1685-93.
94. Cupedo, T., et al., *Human fetal lymphoid tissue-inducer cells are interleukin 17-producing precursors to RORC+ CD127+ natural killer-like cells.* Nat Immunol, 2009. **10**(1): p. 66-74.
95. Vondenhoff, M.F., et al., *LTbetaR signaling induces cytokine expression and up-regulates lymphangiogenic factors in lymph node anlagen.* J Immunol, 2009. **182**(9): p. 5439-45.
96. Armitage, R.J., et al., *Molecular and biological characterization of a murine ligand for CD40.* Nature, 1992. **357**(6373): p. 80-2.
97. Grammer, A.C., et al., *The CD40 ligand expressed by human B cells costimulates B cell responses.* J Immunol, 1995. **154**(10): p. 4996-5010.
98. Pinchuk, L.M., et al., *Functional CD40 ligand expressed by human blood dendritic cells is up-regulated by CD40 ligation.* J Immunol, 1996. **157**(10): p. 4363-70.
99. Henn, V., et al., *CD40 ligand on activated platelets triggers an inflammatory reaction of endothelial cells.* Nature, 1998. **391**(6667): p. 591-4.
100. Maliszewski, C.R., et al., *Recombinant CD40 ligand stimulation of murine B cell growth and differentiation: cooperative effects of cytokines.* Eur J Immunol, 1993. **23**(5): p. 1044-9.
101. Higuchi, T., et al., *Cutting Edge: Ectopic expression of CD40 ligand on B cells induces lupus-like autoimmune disease.* J Immunol, 2002. **168**(1): p. 9-12.
102. Aruffo, A., et al., *The CD40 ligand, gp39, is defective in activated T cells from patients with X-linked hyper-IgM syndrome.* Cell, 1993. **72**(2): p. 291-300.
103. Schoenberger, S.P., et al., *T-cell help for cytotoxic T lymphocytes is mediated by CD40-CD40L interactions.* Nature, 1998. **393**(6684): p. 480-3.
104. Caux, C., et al., *Activation of human dendritic cells through CD40 cross-linking.* J Exp Med, 1994. **180**(4): p. 1263-72.
105. Rothwarf, D.M., et al., *IKK-gamma is an essential regulatory subunit of the IkappaB kinase complex.* Nature, 1998. **395**(6699): p. 297-300.
106. Deng, L., et al., *Activation of the IkappaB kinase complex by TRAF6 requires a dimeric ubiquitin-conjugating enzyme complex and a unique polyubiquitin chain.* Cell, 2000. **103**(2): p. 351-61.
107. Mahoney, D.J., et al., *Both cIAP1 and cIAP2 regulate TNFalpha-mediated NF-kappaB activation.* Proc Natl Acad Sci U S A, 2008. **105**(33): p. 11778-83.

108. Rushe, M., et al., *Structure of a NEMO/IKK-associating domain reveals architecture of the interaction site.* Structure, 2008. **16**(5): p. 798-808.
109. Huxford, T., et al., *The crystal structure of the IkappaBalpha/NF-kappaB complex reveals mechanisms of NF-kappaB inactivation.* Cell, 1998. **95**(6): p. 759-70.
110. Malek, S., et al., *IkappaBbeta, but not IkappaBalpha, functions as a classical cytoplasmic inhibitor of NF-kappaB dimers by masking both NF-kappaB nuclear localization sequences in resting cells.* J Biol Chem, 2001. **276**(48): p. 45225-35.
111. Ghosh, G., et al., *Structure of NF-kappa B p50 homodimer bound to a kappa B site.* Nature, 1995. **373**(6512): p. 303-10.
112. Ghosh, S. and D. Baltimore, *Activation in vitro of NF-kappa B by phosphorylation of its inhibitor I kappa B.* Nature, 1990. **344**(6267): p. 678-82.
113. Napetschnig, J. and H. Wu, *Molecular basis of NF-kappaB signaling.* Annu Rev Biophys, 2013. **42**: p. 443-68.
114. Rooney, J.W., T. Hoey, and L.H. Glimcher, *Coordinate and cooperative roles for NF-AT and AP-1 in the regulation of the murine IL-4 gene.* Immunity, 1995. **2**(5): p. 473-83.
115. Angel, P. and M. Karin, *The role of Jun, Fos and the AP-1 complex in cell-proliferation and transformation.* Biochim Biophys Acta, 1991. **1072**(2-3): p. 129-57.
116. Steinmuller, L., et al., *Regulation and composition of activator protein 1 (AP-1) transcription factors controlling collagenase and c-Jun promoter activities.* Biochem J, 2001. **360**(Pt 3): p. 599-607.
117. Liu, Z.G., et al., *Dissection of TNF receptor 1 effector functions: JNK activation is not linked to apoptosis while NF-kappaB activation prevents cell death.* Cell, 1996. **87**(3): p. 565-76.
118. Bai, C., et al., *Overexpression of M68/DcR3 in human gastrointestinal tract tumors independent of gene amplification and its location in a four-gene cluster.* Proc Natl Acad Sci U S A, 2000. **97**(3): p. 1230-5.
119. Yujiri, T., et al., *MEK kinase 1 gene disruption alters cell migration and c-Jun NH2-terminal kinase regulation but does not cause a measurable defect in NF-kappa B activation.* Proc Natl Acad Sci U S A, 2000. **97**(13): p. 7272-7.
120. Yang, D., et al., *Targeted disruption of the MKK4 gene causes embryonic death, inhibition of c-Jun NH2-terminal kinase activation, and defects in AP-1 transcriptional activity.* Proc Natl Acad Sci U S A, 1997. **94**(7): p. 3004-9.
121. Screaton, G.R., et al., *LARD: a new lymphoid-specific death domain containing receptor regulated by alternative pre-mRNA splicing.* Proc Natl Acad Sci U S A, 1997. **94**(9): p. 4615-9.
122. Kitson, J., et al., *A death-domain-containing receptor that mediates apoptosis.* Nature, 1996. **384**(6607): p. 372-5.
123. Chinnaiyan, A.M., et al., *Signal transduction by DR3, a death domain-containing receptor related to TNFR-1 and CD95.* Science, 1996. **274**(5289): p. 990-2.
124. Bodmer, J.L., et al., *TRAMP, a novel apoptosis-mediating receptor with sequence homology to tumor necrosis factor receptor 1 and Fas(Apo-1/CD95).* Immunity, 1997. **6**(1): p. 79-88.
125. Marsters, S.A., et al., *Apo-3, a new member of the tumor necrosis factor receptor family, contains a death domain and activates apoptosis and NF-kappa B.* Curr Biol, 1996. **6**(12): p. 1669-76.
126. Borysenko, C.W., W.F. Furey, and H.C. Blair, *Comparative modeling of TNFRSF25 (DR3) predicts receptor destabilization by a mutation linked to rheumatoid arthritis.* Biochem Biophys Res Commun, 2005. **328**(3): p. 794-9.

127. Wang, E.C., et al., *Genomic structure, expression, and chromosome mapping of the mouse homologue for the WSL-1 (DR3, Apo3, TRAMP, LARD, TR3, TNFRSF12) gene.* Immunogenetics, 2001. **53**(1): p. 59-63.
128. Banner, D.W., et al., *Crystal structure of the soluble human 55 kd TNF receptor-human TNF beta complex: implications for TNF receptor activation.* Cell, 1993. **73**(3): p. 431-45.
129. Cavallini, C., et al., *The TNF-family cytokine TL1A inhibits proliferation of human activated B cells.* PLoS One, 2013. **8**(4): p. e60136.
130. Wang, X., et al., *TNF-like ligand 1A (TL1A) gene knockout leads to ameliorated collagen-induced arthritis in mice: implication of TL1A in humoral immune responses.* J Immunol, 2013. **191**(11): p. 5420-9.
131. Pappu, B.P., et al., *TL1A-DR3 interaction regulates Th17 cell function and Th17-mediated autoimmune disease.* J Exp Med, 2008. **205**(5): p. 1049-62.
132. Twohig, J.P., et al., *The death receptor 3/TL1A pathway is essential for efficient development of antiviral CD4(+) and CD8(+) T-cell immunity.* FASEB J, 2012. **26**(8): p. 3575-86.
133. Richard, A.C., et al., *The TNF-family ligand TL1A and its receptor DR3 promote T cell-mediated allergic immunopathology by enhancing differentiation and pathogenicity of IL-9-producing T cells.* J Immunol, 2015. **194**(8): p. 3567-82.
134. Slebioda, T.J., et al., *Triggering of TNFRSF25 promotes CD8(+) T-cell responses and anti-tumor immunity.* Eur J Immunol, 2011.
135. Cohavy, O., et al., *Cd161 Defines Effector T Cells That Express Light and Respond to Tl1a-Dr3 Signaling.* Eur J Microbiol Immunol (Bp), 2011. **1**(1): p. 70-79.
136. Taraban, V.Y., J.R. Ferdinand, and A. Al-Shamkhani, *Expression of TNFRSF25 on conventional T cells and Tregs.* J Clin Invest, 2011. **121**(2): p. 463-4; author reply 465.
137. Schreiber, T.H., et al., *Therapeutic Treg expansion in mice by TNFRSF25 prevents allergic lung inflammation.* J Clin Invest, 2010. **120**(10): p. 3629-40.
138. Fang, L., et al., *Essential role of TNF receptor superfamily 25 (TNFRSF25) in the development of allergic lung inflammation.* J Exp Med, 2008. **205**(5): p. 1037-48.
139. Papadakis, K.A., et al., *TL1A synergizes with IL-12 and IL-18 to enhance IFN-gamma production in human T cells and NK cells.* J Immunol, 2004. **172**(11): p. 7002-7.
140. Meylan, F., et al., *The TNF-family cytokine TL1A promotes allergic immunopathology through group 2 innate lymphoid cells.* Mucosal Immunol, 2014. **7**(4): p. 958-68.
141. Yu, X., et al., *TNF superfamily member TL1A elicits type 2 innate lymphoid cells at mucosal barriers.* Mucosal Immunol, 2014. **7**(3): p. 730-40.
142. Hedl, M. and C. Abraham, *A TNFSF15 disease-risk polymorphism increases pattern-recognition receptor-induced signaling through caspase-8-induced IL-1.* Proc Natl Acad Sci U S A, 2014. **111**(37): p. 13451-6.
143. Al-Lamki, R.S., et al., *Expression of silencer of death domains and death-receptor-3 in normal human kidney and in rejecting renal transplants.* Am J Pathol, 2003. **163**(2): p. 401-11.
144. Twohig, J.P., et al., *Age-dependent maintenance of motor control and corticostriatal innervation by death receptor 3.* J Neurosci, 2010. **30**(10): p. 3782-92.
145. Richard, A.C., et al., *The TNF-family cytokine TL1A: from lymphocyte costimulator to disease co-conspirator.* J Leukoc Biol, 2015.
146. Thoma, B., et al., *Identification of a 60-kD tumor necrosis factor (TNF) receptor as the major signal transducing component in TNF responses.* J Exp Med, 1990. **172**(4): p. 1019-23.

147. Brockhaus, M., et al., *Identification of two types of tumor necrosis factor receptors on human cell lines by monoclonal antibodies.* Proc Natl Acad Sci U S A, 1990. **87**(8): p. 3127-31.
148. Slebioda, T.J., et al., *Triggering of TNFRSF25 promotes CD8(+) T-cell responses and anti-tumor immunity.* Eur J Immunol, 2011. **41**(9): p. 2606-11.
149. Al-Lamki, R.S., et al., *TL1A both promotes and protects from renal inflammation and injury.* J Am Soc Nephrol, 2008. **19**(5): p. 953-60.
150. Warzocha, K., et al., *A new death receptor 3 isoform: expression in human lymphoid cell lines and non-Hodgkin's lymphomas.* Biochem Biophys Res Commun, 1998. **242**(2): p. 376-9.
151. Marsters, S.A., et al., *Identification of a ligand for the death-domain-containing receptor Apo3.* Curr Biol, 1998. **8**(9): p. 525-8.
152. Zhai, Y., et al., *VEGI, a novel cytokine of the tumor necrosis factor family, is an angiogenesis inhibitor that suppresses the growth of colon carcinomas in vivo.* FASEB J, 1999. **13**(1): p. 181-9.
153. Yue, T.L., et al., *TL1, a novel tumor necrosis factor-like cytokine, induces apoptosis in endothelial cells. Involvement of activation of stress protein kinases (stress-activated protein kinase and p38 mitogen-activated protein kinase) and caspase-3-like protease.* J Biol Chem, 1999. **274**(3): p. 1479-86.
154. Jin, T., et al., *X-ray crystal structure of TNF ligand family member TL1A at 2.1A.* Biochem Biophys Res Commun, 2007. **364**(1): p. 1-6.
155. Takimoto, T., et al., *Molecular cloning and functional characterizations of chicken TL1A.* Dev Comp Immunol, 2005. **29**(10): p. 895-905.
156. Takimoto, T., et al., *Role of chicken TL1A on inflammatory responses and partial characterization of its receptor.* J Immunol, 2008. **180**(12): p. 8327-32.
157. Gonsky, R., R.L. Deem, and S.R. Targan, *Multiple activating and repressive cis-promoter regions regulate TNFSF15 expression in human primary mononuclear cells.* Cytokine, 2013. **63**(1): p. 36-42.
158. Prehn, J.L., et al., *The T cell costimulator TL1A is induced by FcgammaR signaling in human monocytes and dendritic cells.* J Immunol, 2007. **178**(7): p. 4033-8.
159. Meylan, F., et al., *The TNF-family receptor DR3 is essential for diverse T cell-mediated inflammatory diseases.* Immunity, 2008. **29**(1): p. 79-89.
160. Buchan, S.L., et al., *Death receptor 3 is essential for generating optimal protective CD4(+) T-cell immunity against Salmonella.* Eur J Immunol, 2012. **42**(3): p. 580-8.
161. Longman, R.S., et al., *CX(3)CR1(+) mononuclear phagocytes support colitis-associated innate lymphoid cell production of IL-22.* J Exp Med, 2014. **211**(8): p. 1571-83.
162. Shih, D.Q., et al., *Microbial induction of inflammatory bowel disease associated gene TL1A (TNFSF15) in antigen presenting cells.* Eur J Immunol, 2009. **39**(11): p. 3239-50.
163. Bamias, G., et al., *Expression, localization, and functional activity of TL1A, a novel Th1-polarizing cytokine in inflammatory bowel disease.* J Immunol, 2003. **171**(9): p. 4868-74.
164. Cassatella, M., et al., *Soluble TNF-Like Cytokine (TL1A) Production by Immune Complexes Stimulated Monocytes in Rheumatoid Arthritis.* The Journal of Immunology, 2007. **178**(11): p. 7325.
165. Biener-Ramanujan, E., et al., *Functional signaling of membrane-bound TL1A induces IFN-gamma expression.* FEBS Lett, 2010. **584**(11): p. 2376-80.
166. Zhan, C., et al., *Decoy strategies: the structure of TL1A:DcR3 complex.* Structure, 2011. **19**(2): p. 162-71.
167. Takahama, Y., et al., *The prognostic significance of overexpression of the decoy receptor for Fas ligand (DcR3) in patients with gastric carcinomas.* Gastric Cancer, 2002. **5**(2): p. 61-8.

168. Liu, C., et al., *Progranulin-derived Atsttrin directly binds to TNFRSF25 (DR3) and inhibits TNF-like ligand 1A (TL1A) activity.* PLoS One, 2014. **9**(3): p. e92743.
169. Tang, W., et al., *The growth factor progranulin binds to TNF receptors and is therapeutic against inflammatory arthritis in mice.* Science, 2011. **332**(6028): p. 478-84.
170. Jian, J., et al., *Progranulin directly binds to the CRD2 and CRD3 of TNFR extracellular domains.* FEBS Lett, 2013. **587**(21): p. 3428-36.
171. Gout, S., et al., *Death receptor-3, a new E-Selectin counter-receptor that confers migration and survival advantages to colon carcinoma cells by triggering p38 and ERK MAPK activation.* Cancer Res, 2006. **66**(18): p. 9117-24.
172. Pobezinskaya, Y.L., et al., *The adaptor protein TRADD is essential for TNF-like ligand 1A/death receptor 3 signaling.* J Immunol, 2011. **186**(9): p. 5212-6.
173. Chu, Z.L., et al., *Suppression of tumor necrosis factor-induced cell death by inhibitor of apoptosis c-IAP2 is under NF-kappaB control.* Proc Natl Acad Sci U S A, 1997. **94**(19): p. 10057-62.
174. Meylan, F., et al., *The TNF-family cytokine TL1A drives IL-13-dependent small intestinal inflammation.* Mucosal Immunol, 2011. **4**(2): p. 172-85.
175. Taraban, V.Y., et al., *Sustained TL1A expression modulates effector and regulatory T-cell responses and drives intestinal goblet cell hyperplasia.* Mucosal Immunol, 2011. **4**(2): p. 186-96.
176. Khan, S.Q., et al., *Cloning, expression, and functional characterization of TL1A-Ig.* J Immunol, 2013. **190**(4): p. 1540-50.
177. Meylan, F., A.C. Richard, and R.M. Siegel, *TL1A and DR3, a TNF family ligand-receptor pair that promotes lymphocyte costimulation, mucosal hyperplasia, and autoimmune inflammation.* Immunol Rev, 2011. **244**(1): p. 188-96.
178. Jones, G.W., et al., *Naive and activated T cells display differential responsiveness to TL1A that affects Th17 generation, maintenance, and proliferation.* FASEB J, 2011. **25**(1): p. 409-19.
179. Chang, H.C., et al., *The transcription factor PU.1 is required for the development of IL-9-producing T cells and allergic inflammation.* Nature Immunology, 2010. **11**(6): p. 527-34.
180. Veldhoen, M., et al., *Transforming growth factor-beta 'reprograms' the differentiation of T helper 2 cells and promotes an interleukin 9-producing subset.* Nat Immunol, 2008. **9**(12): p. 1341-6.
181. Ahn, Y.O., et al., *Human group3 innate lymphoid cells express DR3 and respond to TL1A with enhanced IL-22 production and IL-2-dependent proliferation.* Eur J Immunol, 2015. **45**(8): p. 2335-42.
182. McLaren, J.E., et al., *The TNF-like protein 1A-death receptor 3 pathway promotes macrophage foam cell formation in vitro.* J Immunol, 2010. **184**(10): p. 5827-34.
183. Takedatsu, H., et al., *TL1A (TNFSF15) regulates the development of chronic colitis by modulating both T-helper 1 and T-helper 17 activation.* Gastroenterology, 2008. **135**(2): p. 552-67.
184. Oliphant, C.J., et al., *MHCII-mediated dialog between group 2 innate lymphoid cells and CD4(+) T cells potentiates type 2 immunity and promotes parasitic helminth expulsion.* Immunity, 2014. **41**(2): p. 283-95.
185. Bull, M.J., et al., *The Death Receptor 3-TNF-like protein 1A pathway drives adverse bone pathology in inflammatory arthritis.* J Exp Med, 2008. **205**(11): p. 2457-64.
186. Yamazaki, K., et al., *Single nucleotide polymorphisms in TNFSF15 confer susceptibility to Crohn's disease.* Hum Mol Genet, 2005. **14**(22): p. 3499-506.

187. Picornell, Y., et al., *TNFSF15 is an ethnic-specific IBD gene.* Inflamm Bowel Dis, 2007. **13**(11): p. 1333-8.
188. Asgharpour, A., J. Cheng, and S.J. Bickston, *Adalimumab treatment in Crohn's disease: an overview of long-term efficacy and safety in light of the EXTEND trial.* Clin Exp Gastroenterol, 2013. **6**: p. 153-160.
189. Shih, D.Q. and S.R. Targan, *Insights into IBD Pathogenesis.* Curr Gastroenterol Rep, 2009. **11**(6): p. 473-80.
190. Jostins, L., et al., *Host-microbe interactions have shaped the genetic architecture of inflammatory bowel disease.* Nature, 2012. **491**(7422): p. 119-24.
191. Peter, I., et al., *Evaluation of 22 genetic variants with Crohn's disease risk in the Ashkenazi Jewish population: a case-control study.* BMC Med Genet, 2011. **12**: p. 63.
192. Kenny, E.E., et al., *A genome-wide scan of Ashkenazi Jewish Crohn's disease suggests novel susceptibility loci.* PLoS Genet, 2012. **8**(3): p. e1002559.
193. Slebioda, T.J., et al., *TL1A as a potential local inducer of IL17A Expression in colon mucosa of inflammatory bowel disease patients.* Scand J Immunol, 2015.
194. Kontoyiannis, D., et al., *Impaired on/off regulation of TNF biosynthesis in mice lacking TNF AU-rich elements: implications for joint and gut-associated immunopathologies.* Immunity, 1999. **10**(3): p. 387-98.
195. Rivera-Nieves, J., et al., *Emergence of perianal fistulizing disease in the SAMP1/YitFc mouse, a spontaneous model of chronic ileitis.* Gastroenterology, 2003. **124**(4): p. 972-82.
196. Bamias, G., et al., *Role of TL1A and its receptor DR3 in two models of chronic murine ileitis.* Proc Natl Acad Sci U S A, 2006.
197. Scott, D.L., *Prognostic factors in early rheumatoid arthritis.* Rheumatology (Oxford), 2000. **39 Suppl 1**: p. 24-9.
198. Osawa, K., et al., *Death receptor 3 (DR3) gene duplication in a chromosome region 1p36.3: gene duplication is more prevalent in rheumatoid arthritis.* Genes Immun, 2004. **5**(6): p. 439-43.
199. Zhang, J., et al., *Role of TL1A in the pathogenesis of rheumatoid arthritis.* J Immunol, 2009. **183**(8): p. 5350-7.
200. Sun, X., et al., *Elevated serum and synovial fluid TNF-like ligand 1A (TL1A) is associated with autoantibody production in patients with rheumatoid arthritis.* Scand J Rheumatol, 2013. **42**(2): p. 97-101.
201. Bamias, G., et al., *Circulating levels of TNF-like cytokine 1A (TL1A) and its decoy receptor 3 (DcR3) in rheumatoid arthritis.* Clin Immunol, 2008. **129**(2): p. 249-55.
202. Xiu, Z., et al., *Serum and synovial fluid levels of tumor necrosis factor-like ligand 1A and decoy receptor 3 in rheumatoid arthritis.* Cytokine, 2015. **72**(2): p. 185-9.
203. Park, J.S., et al., *TWEAK Promotes Osteoclastogenesis in Rheumatoid Arthritis.* Am J Pathol, 2013. **183**(3): p. 857-67.
204. Cho, Y.G., et al., *Type II collagen autoimmunity in a mouse model of human rheumatoid arthritis.* Autoimmun Rev, 2007. **7**(1): p. 65-70.
205. Gavett, S.H., et al., *Depletion of murine CD4+ T lymphocytes prevents antigen-induced airway hyperreactivity and pulmonary eosinophilia.* Am J Respir Cell Mol Biol, 1994. **10**(6): p. 587-93.
206. Akbari, O., et al., *Essential role of NKT cells producing IL-4 and IL-13 in the development of allergen-induced airway hyperreactivity.* Nat Med, 2003. **9**(5): p. 582-8.
207. Zhang, F.R., et al., *Genomewide association study of leprosy.* N Engl J Med, 2009. **361**(27): p. 2609-18.

208. Zhang, F., et al., *Identification of two new loci at IL23R and RAB32 that influence susceptibility to leprosy.* Nat Genet, 2011. **43**(12): p. 1247-51.
209. Grant, A.V., et al., *Crohn's disease susceptibility genes are associated with leprosy in the Vietnamese population.* J Infect Dis, 2012. **206**(11): p. 1763-7.
210. Wong, S.H., et al., *Genomewide association study of leprosy.* N Engl J Med, 2010. **362**(15): p. 1446-7; author reply 1447-8.
211. Aiba, Y., et al., *Systemic and local expression levels of TNF-like ligand 1A and its decoy receptor 3 are increased in primary biliary cirrhosis.* Liver Int, 2014. **34**(5): p. 679-88.
212. Nakamura, M., et al., *Genome-wide association study identifies TNFSF15 and POU2AF1 as susceptibility loci for primary biliary cirrhosis in the Japanese population.* Am J Hum Genet, 2012. **91**(4): p. 721-8.
213. Shih, D.Q., et al., *Constitutive TL1A (TNFSF15) expression on lymphoid or myeloid cells leads to mild intestinal inflammation and fibrosis.* PLoS ONE, 2011. **6**(1): p. e16090.
214. Maynard, C.L., et al., *Reciprocal interactions of the intestinal microbiota and immune system.* Nature, 2012. **489**(7415): p. 231-41.
215. Livak, K.J. and T.D. Schmittgen, *Analysis of relative gene expression data using real-time quantitative PCR and the 2(-Delta Delta C(T)) Method.* Methods, 2001. **25**(4): p. 402-8.
216. Wang, E.C., et al., *DR3 regulates negative selection during thymocyte development.* Mol Cell Biol, 2001. **21**(10): p. 3451-61.
217. Radley, J.M. and G. Scurfield, *Effects of 5-fluorouracil on mouse bone marrow.* Br J Haematol, 1979. **43**(3): p. 341-51.
218. Trapnell, C., L. Pachter, and S.L. Salzberg, *TopHat: discovering splice junctions with RNA-Seq.* Bioinformatics, 2009. **25**(9): p. 1105-11.
219. Li, H., et al., *The Sequence Alignment/Map format and SAMtools.* Bioinformatics, 2009. **25**(16): p. 2078-9.
220. Liao, Y., G.K. Smyth, and W. Shi, *The Subread aligner: fast, accurate and scalable read mapping by seed-and-vote.* Nucleic Acids Res, 2013. **41**(10): p. e108.
221. Anders, S. and W. Huber, *Differential expression analysis for sequence count data.* Genome Biol, 2010. **11**(10): p. R106.
222. Eden, E., et al., *GOrilla: a tool for discovery and visualization of enriched GO terms in ranked gene lists.* BMC Bioinformatics, 2009. **10**: p. 48.
223. Song, J., et al., *PROSPER: an integrated feature-based tool for predicting protease substrate cleavage sites.* PLoS One, 2012. **7**(11): p. e50300.
224. Grell, M., et al., *The transmembrane form of tumor necrosis factor is the prime activating ligand of the 80 kDa tumor necrosis factor receptor.* Cell, 1995. **83**(5): p. 793-802.
225. Ruuls, S.R., et al., *Membrane-bound TNF supports secondary lymphoid organ structure but is subservient to secreted TNF in driving autoimmune inflammation.* Immunity, 2001. **15**(4): p. 533-43.
226. Pasparakis, M., et al., *Immune and inflammatory responses in TNF alpha-deficient mice: a critical requirement for TNF alpha in the formation of primary B cell follicles, follicular dendritic cell networks and germinal centers, and in the maturation of the humoral immune response.* J Exp Med, 1996. **184**(4): p. 1397-411.
227. Olleros, M.L., et al., *Membrane-bound TNF induces protective immune responses to M. bovis BCG infection: regulation of memTNF and TNF receptors comparing two memTNF molecules.* PLoS One, 2012. **7**(5): p. e31469.
228. Kayagaki, N., et al., *Metalloproteinase-mediated release of human Fas ligand.* J Exp Med, 1995. **182**(6): p. 1777-83.

229. O'Reilly, L.A., et al., *Membrane-bound Fas ligand only is essential for Fas-induced apoptosis.* Nature, 2009. **461**(7264): p. 659-63.
230. Hohlbaum, A.M., S. Moe, and A. Marshak-Rothstein, *Opposing effects of transmembrane and soluble Fas ligand expression on inflammation and tumor cell survival.* J Exp Med, 2000. **191**(7): p. 1209-20.
231. Solorzano, C.C., et al., *A matrix metalloproteinase inhibitor prevents processing of tumor necrosis factor alpha (TNF alpha) and abrogates endotoxin-induced lethality.* Shock, 1997. **7**(6): p. 427-31.
232. Engels, B., et al., *Retroviral vectors for high-level transgene expression in T lymphocytes.* Hum Gene Ther, 2003. **14**(12): p. 1155-68.
233. Ramalingam, T.R., et al., *Unique functions of the type II interleukin 4 receptor identified in mice lacking the interleukin 13 receptor alpha1 chain.* Nat Immunol, 2008. **9**(1): p. 25-33.
234. Townley, R.G. and M. Horiba, *Airway hyperresponsiveness: a story of mice and men and cytokines.* Clin Rev Allergy Immunol, 2003. **24**(1): p. 85-110.
235. Punnonen, J., et al., *Interleukin 13 induces interleukin 4-independent IgG4 and IgE synthesis and CD23 expression by human B cells.* Proc Natl Acad Sci U S A, 1993. **90**(8): p. 3730-4.
236. Kayamuro, H., et al., *TNF superfamily member, TL1A, is a potential mucosal vaccine adjuvant.* Biochem Biophys Res Commun, 2009. **384**(3): p. 296-300.
237. Gentil, K., et al., *Eotaxin-1 is involved in parasite clearance during chronic filarial infection.* Parasite Immunol, 2014. **36**(2): p. 60-77.
238. Rieger, M.A., et al., *Hematopoietic cytokines can instruct lineage choice.* Science, 2009. **325**(5937): p. 217-8.
239. Bhattacharya, P., et al., *GM-CSF: An immune modulatory cytokine that can suppress autoimmunity.* Cytokine, 2015.
240. Suratt, B.T., et al., *Role of the CXCR4/SDF-1 chemokine axis in circulating neutrophil homeostasis.* Blood, 2004. **104**(2): p. 565-71.
241. Mohapatra, A., et al., *Group 2 innate lymphoid cells utilize the IRF4-IL-9 module to coordinate epithelial cell maintenance of lung homeostasis.* Mucosal Immunol, 2015.
242. Van der Vieren, M., et al., *A novel leukointegrin, alpha d beta 2, binds preferentially to ICAM-3.* Immunity, 1995. **3**(6): p. 683-90.
243. Hurtado, A., et al., *Anti-CD11d monoclonal antibody treatment for rat spinal cord compression injury.* Exp Neurol, 2012. **233**(2): p. 606-11.
244. Mabon, P.J., L.C. Weaver, and G.A. Dekaban, *Inhibition of monocyte/macrophage migration to a spinal cord injury site by an antibody to the integrin alphaD: a potential new anti-inflammatory treatment.* Exp Neurol, 2000. **166**(1): p. 52-64.
245. Gonzalez-Dominguez, E., et al., *CD163L1 and CLEC5A discriminate subsets of human resident and inflammatory macrophages in vivo.* J Leukoc Biol, 2015.
246. Heng, T.S., M.W. Painter, and C. Immunological Genome Project, *The Immunological Genome Project: networks of gene expression in immune cells.* Nat Immunol, 2008. **9**(10): p. 1091-4.
247. Uliana, V., et al., *Alport syndrome and leiomyomatosis: the first deletion extending beyond COL4A6 intron 2.* Pediatr Nephrol, 2011. **26**(5): p. 717-24.
248. Kumamoto, Y., et al., *CD301b(+) dermal dendritic cells drive T helper 2 cell-mediated immunity.* Immunity, 2013. **39**(4): p. 733-43.
249. Claudio, J.O., et al., *HACS1 encodes a novel SH3-SAM adaptor protein differentially expressed in normal and malignant hematopoietic cells.* Oncogene, 2001. **20**(38): p. 5373-7.
250. Zhu, Y.X., et al., *The SH3-SAM adaptor HACS1 is up-regulated in B cell activation signaling cascades.* J Exp Med, 2004. **200**(6): p. 737-47.

251. Wang, D., et al., *Enhanced adaptive immunity in mice lacking the immunoinhibitory adaptor Hacs1.* FASEB J, 2010. **24**(3): p. 947-56.
252. Colombo, F., et al., *A 5'-region polymorphism modulates promoter activity of the tumor suppressor gene MFSD2A.* Mol Cancer, 2011. **10**: p. 81.
253. Spinola, M., et al., *MFSD2A is a novel lung tumor suppressor gene modulating cell cycle and matrix attachment.* Mol Cancer, 2010. **9**: p. 62.
254. Ben-Zvi, A., et al., *Mfsd2a is critical for the formation and function of the blood-brain barrier.* Nature, 2014. **509**(7501): p. 507-11.
255. Farrell, H.M., Jr., et al., *Nomenclature of the proteins of cows' milk--sixth revision.* J Dairy Sci, 2004. **87**(6): p. 1641-74.
256. Mottet, C., H.H. Uhlig, and F. Powrie, *Cutting edge: cure of colitis by CD4+CD25+ regulatory T cells.* J Immunol, 2003. **170**(8): p. 3939-43.
257. Eken, A., et al., *IL-23R+ innate lymphoid cells induce colitis via interleukin-22-dependent mechanism.* Mucosal Immunol, 2014. **7**(1): p. 143-54.
258. Zenewicz, L.A., et al., *Innate and adaptive interleukin-22 protects mice from inflammatory bowel disease.* Immunity, 2008. **29**(6): p. 947-57.
259. Fort, M.M., M.W. Leach, and D.M. Rennick, *A role for NK cells as regulators of CD4+ T cells in a transfer model of colitis.* J Immunol, 1998. **161**(7): p. 3256-61.
260. Yamaji, O., et al., *The development of colitogenic CD4(+) T cells is regulated by IL-7 in collaboration with NK cell function in a murine model of colitis.* J Immunol, 2012. **188**(6): p. 2524-36.
261. Choi, Y.S., et al., *ICOS receptor instructs T follicular helper cell versus effector cell differentiation via induction of the transcriptional repressor Bcl6.* Immunity, 2011. **34**(6): p. 932-46.
262. Baumjohann, D., T. Okada, and K.M. Ansel, *Cutting Edge: Distinct waves of BCL6 expression during T follicular helper cell development.* J Immunol, 2011. **187**(5): p. 2089-92.
263. Hardtke, S., L. Ohl, and R. Forster, *Balanced expression of CXCR5 and CCR7 on follicular T helper cells determines their transient positioning to lymph node follicles and is essential for efficient B-cell help.* Blood, 2005. **106**(6): p. 1924-31.
264. Luther, S.A., et al., *Differing activities of homeostatic chemokines CCL19, CCL21, and CXCL12 in lymphocyte and dendritic cell recruitment and lymphoid neogenesis.* J Immunol, 2002. **169**(1): p. 424-33.
265. Veerman, K.M., et al., *Interaction of the selectin ligand PSGL-1 with chemokines CCL21 and CCL19 facilitates efficient homing of T cells to secondary lymphoid organs.* Nat Immunol, 2007. **8**(5): p. 532-9.
266. Poholek, A.C., et al., *In vivo regulation of Bcl6 and T follicular helper cell development.* J Immunol, 2010. **185**(1): p. 313-26.
267. Dong, C., U.A. Temann, and R.A. Flavell, *Cutting edge: critical role of inducible costimulator in germinal center reactions.* J Immunol, 2001. **166**(6): p. 3659-62.
268. Qi, H., et al., *SAP-controlled T-B cell interactions underlie germinal centre formation.* Nature, 2008. **455**(7214): p. 764-9.
269. Good-Jacobson, K.L., et al., *PD-1 regulates germinal center B cell survival and the formation and affinity of long-lived plasma cells.* Nat Immunol, 2010. **11**(6): p. 535-42.
270. Cunningham, A.F., et al., *Loss of CD154 impairs the Th2 extrafollicular plasma cell response but not early T cell proliferation and interleukin-4 induction.* Immunology, 2004. **113**(2): p. 187-93.
271. Chtanova, T., et al., *T follicular helper cells express a distinctive transcriptional profile, reflecting their role as non-Th1/Th2 effector cells that provide help for B cells.* J Immunol, 2004. **173**(1): p. 68-78.

272. Nurieva, R.I., et al., *Bcl6 mediates the development of T follicular helper cells.* Science, 2009. **325**(5943): p. 1001-5.
273. Yu, D., et al., *The transcriptional repressor Bcl-6 directs T follicular helper cell lineage commitment.* Immunity, 2009. **31**(3): p. 457-68.
274. Foy, T.M., et al., *gp39-CD40 interactions are essential for germinal center formation and the development of B cell memory.* J Exp Med, 1994. **180**(1): p. 157-63.
275. Ettinger, R., et al., *IL-21 induces differentiation of human naive and memory B cells into antibody-secreting plasma cells.* J Immunol, 2005. **175**(12): p. 7867-79.
276. Suzuki, K., et al., *Visualizing B cell capture of cognate antigen from follicular dendritic cells.* J Exp Med, 2009. **206**(7): p. 1485-93.
277. Gitlin, A.D., Z. Shulman, and M.C. Nussenzweig, *Clonal selection in the germinal centre by regulated proliferation and hypermutation.* Nature, 2014. **509**(7502): p. 637-40.
278. Toellner, K.M., et al., *Low-level hypermutation in T cell-independent germinal centers compared with high mutation rates associated with T cell-dependent germinal centers.* J Exp Med, 2002. **195**(3): p. 383-9.
279. Victora, G.D., et al., *Germinal center dynamics revealed by multiphoton microscopy with a photoactivatable fluorescent reporter.* Cell, 2010. **143**(4): p. 592-605.
280. Khan, W.N., et al., *Defective B cell development and function in Btk-deficient mice.* Immunity, 1995. **3**(3): p. 283-99.
281. Satterthwaite, A.B. and O.N. Witte, *The role of Bruton's tyrosine kinase in B-cell development and function: a genetic perspective.* Immunol Rev, 2000. **175**: p. 120-7.
282. Mosier, D.E., J.J. Mond, and E.A. Goldings, *The ontogeny of thymic independent antibody responses in vitro in normal mice and mice with an X-linked B cell defect.* J Immunol, 1977. **119**(6): p. 1874-8.
283. Pone, E.J., et al., *BCR-signalling synergizes with TLR-signalling for induction of AID and immunoglobulin class-switching through the non-canonical NF-kappaB pathway.* Nat Commun, 2012. **3**: p. 767.
284. Mond, J.J., A. Lees, and C.M. Snapper, *T cell-independent antigens type 2.* Annu Rev Immunol, 1995. **13**: p. 655-92.
285. von Bulow, G.U., J.M. van Deursen, and R.J. Bram, *Regulation of the T-independent humoral response by TACI.* Immunity, 2001. **14**(5): p. 573-82.
286. Groom, J.R., et al., *BAFF and MyD88 signals promote a lupuslike disease independent of T cells.* J Exp Med, 2007. **204**(8): p. 1959-71.
287. Giordano, D., et al., *Nitric oxide regulates BAFF expression and T cell-independent antibody responses.* J Immunol, 2014. **193**(3): p. 1110-20.
288. Macpherson, A.J., Y. Koller, and K.D. McCoy, *The bilateral responsiveness between intestinal microbes and IgA.* Trends Immunol, 2015. **36**(8): p. 460-70.
289. Gommerman, J.L., O.L. Rojas, and J.H. Fritz, *Re-thinking the functions of IgA(+) plasma cells.* Gut Microbes, 2014. **5**(5): p. 652-62.
290. Jacob, C.M., et al., *Autoimmunity in IgA deficiency: revisiting the role of IgA as a silent housekeeper.* J Clin Immunol, 2008. **28 Suppl 1**: p. S56-61.
291. Mbawuike, I.N., et al., *Mucosal immunity to influenza without IgA: an IgA knockout mouse model.* J Immunol, 1999. **162**(5): p. 2530-7.
292. Harriman, G.R., et al., *Targeted deletion of the IgA constant region in mice leads to IgA deficiency with alterations in expression of other Ig isotypes.* J Immunol, 1999. **162**(5): p. 2521-9.
293. Schena, F.P., *A retrospective analysis of the natural history of primary IgA nephropathy worldwide.* Am J Med, 1990. **89**(2): p. 209-15.
294. Castigli, E., et al., *Impaired IgA class switching in APRIL-deficient mice.* Proc Natl Acad Sci U S A, 2004. **101**(11): p. 3903-8.

295. Coffman, R.L., D.A. Lebman, and B. Shrader, *Transforming growth factor beta specifically enhances IgA production by lipopolysaccharide-stimulated murine B lymphocytes.* J Exp Med, 1989. **170**(3): p. 1039-44.
296. McIntyre, T.M., et al., *Transforming growth factor beta 1 selectivity stimulates immunoglobulin G2b secretion by lipopolysaccharide-activated murine B cells.* J Exp Med, 1993. **177**(4): p. 1031-7.
297. Borsutzky, S., et al., *TGF-beta receptor signaling is critical for mucosal IgA responses.* J Immunol, 2004. **173**(5): p. 3305-9.
298. Richards, S.M., et al., *Prolactin is an antagonist of TGF-beta activity and promotes proliferation of murine B cell hybridomas.* Cell Immunol, 1998. **184**(2): p. 85-91.
299. Seo, G.Y., J. Youn, and P.H. Kim, *IL-21 ensures TGF-beta 1-induced IgA isotype expression in mouse Peyer's patches.* J Leukoc Biol, 2009. **85**(5): p. 744-50.
300. Parrish-Novak, J., et al., *Interleukin 21 and its receptor are involved in NK cell expansion and regulation of lymphocyte function.* Nature, 2000. **408**(6808): p. 57-63.
301. Johnson, A.E., et al., *The prevalence and incidence of systemic lupus erythematosus in Birmingham, England. Relationship to ethnicity and country of birth.* Arthritis Rheum, 1995. **38**(4): p. 551-8.
302. Rahman, A. and D.A. Isenberg, *Systemic lupus erythematosus.* N Engl J Med, 2008. **358**(9): p. 929-39.
303. Sullivan, K.E., *Genetics of systemic lupus erythematosus. Clinical implications.* Rheum Dis Clin North Am, 2000. **26**(2): p. 229-56, v-vi.
304. ter Borg, E.J., et al., *Measurement of increases in anti-double-stranded DNA antibody levels as a predictor of disease exacerbation in systemic lupus erythematosus. A long-term, prospective study.* Arthritis Rheum, 1990. **33**(5): p. 634-43.
305. Andrews, B.S., et al., *Spontaneous murine lupus-like syndromes. Clinical and immunopathological manifestations in several strains.* J Exp Med, 1978. **148**(5): p. 1198-215.
306. Zhou, T., et al., *Greatly accelerated lymphadenopathy and autoimmune disease in lpr mice lacking tumor necrosis factor receptor I.* J Immunol, 1996. **156**(8): p. 2661-5.
307. Liu, W., et al., *Control of spontaneous B lymphocyte autoimmunity with adenovirus-encoded soluble TACI.* Arthritis Rheum, 2004. **50**(6): p. 1884-96.
308. Ogilvy, S., et al., *Constitutive Bcl-2 expression throughout the hematopoietic compartment affects multiple lineages and enhances progenitor cell survival.* Proc Natl Acad Sci U S A, 1999. **96**(26): p. 14943-8.
309. Vaux, D.L., S. Cory, and J.M. Adams, *Bcl-2 gene promotes haemopoietic cell survival and cooperates with c-myc to immortalize pre-B cells.* Nature, 1988. **335**(6189): p. 440-2.
310. Ladanyi, M. and S. Wang, *Detection of rearrangements of the BCL2 major breakpoint region in follicular lymphomas. Correlation of polymerase chain reaction results with Southern blot analysis.* Diagn Mol Pathol, 1992. **1**(1): p. 31-5.
311. Egle, A., et al., *VavP-Bcl2 transgenic mice develop follicular lymphoma preceded by germinal center hyperplasia.* Blood, 2004. **103**(6): p. 2276-83.
312. Tischner, D., et al., *Defective cell death signalling along the Bcl-2 regulated apoptosis pathway compromises Treg cell development and limits their functionality in mice.* J Autoimmun, 2012. **38**(1): p. 59-69.
313. Woess, C., et al., *Combined loss of the BH3-only proteins Bim and Bmf restores B-cell development and function in TACI-Ig transgenic mice.* Cell Death Differ, 2015. **22**(9): p. 1477-88.

314. Via, C.S., *Advances in lupus stemming from the parent-into-F1 model.* Trends Immunol, 2010. **31**(6): p. 236-45.
315. Rus, V., et al., *T cell TRAIL promotes murine lupus by sustaining effector CD4 Th cell numbers and by inhibiting CD8 CTL activity.* J Immunol, 2007. **178**(6): p. 3962-72.
316. Soloviova, K., et al., *In vivo maturation of allo-specific CD8 CTL and prevention of lupus-like graft-versus-host disease is critically dependent on T cell signaling through the TNF p75 receptor but not the TNF p55 receptor.* J Immunol, 2013. **190**(9): p. 4562-72.
317. Reichwald, K., T.Z. Jorgensen, and S. Skov, *TL1A increases expression of CD25, LFA-1, CD134 and CD154, and induces IL-22 and GM-CSF production from effector CD4 T-cells.* PLoS One, 2014. **9**(8): p. e105627.
318. Barrett, J.C., et al., *Genome-wide association defines more than 30 distinct susceptibility loci for Crohn's disease.* Nat Genet, 2008. **40**(8): p. 955-62.
319. Haswell, L.E., M.J. Glennie, and A. Al-Shamkhani, *Analysis of the oligomeric requirement for signaling by CD40 using soluble multimeric forms of its ligand, CD154.* Eur J Immunol, 2001. **31**(10): p. 3094-100.
320. Muller, N., et al., *Activity of soluble OX40 ligand is enhanced by oligomerization and cell surface immobilization.* FEBS J, 2008. **275**(9): p. 2296-304.
321. Smith, R.A. and C. Baglioni, *The active form of tumor necrosis factor is a trimer.* J Biol Chem, 1987. **262**(15): p. 6951-4.
322. Hsu, H., J. Xiong, and D.V. Goeddel, *The TNF receptor 1-associated protein TRADD signals cell death and NF-kappa B activation.* Cell, 1995. **81**(4): p. 495-504.
323. Hasegawa, H., E. van Reit, and H. Kida, *Mucosal immunization and adjuvants.* Curr Top Microbiol Immunol, 2015. **386**: p. 371-80.